

Development of novel nanomedicines based on antimicrobial peptides for the treatment of multidrug-resistant Gram-negative pneumonia



Hessel van der Weide

hessel 7½

Development of novel nanomedicines based
on antimicrobial peptides for the treatment of
multidrug-resistant Gram-negative pneumonia

Hessel van der Weide

Colophon

Printing of this thesis was kindly supported by the Netherlands Society of Medical Microbiology (NVMM) and the Royal Netherlands Society for Microbiology (KNVM).



ISBN: 978-94-6416-002-4

Cover: Hessel van der Weide, Ridderprint BV

Layout: Hessel van der Weide, Ridderprint BV

Print: Ridderprint BV | www.ridderprint.nl |  **RIDDERPRINT**

Copyright © 2020, Hessel van der Weide, Barcelona, Spain.

All rights reserved. No part of this thesis may be reproduced, stored in a retrieval system or transmitted in any form or by any means without prior permission of the author.

Development of Novel Nanomedicines based on Antimicrobial Peptides for the Treatment of Multidrug-Resistant Gram-Negative Pneumonia

Ontwikkeling van nieuwe nanogeneesmiddelen gebaseerd
op antimicrobiële peptiden ter behandeling van
multidrug-resistente Gram-negatieve longinfectie

Proefschrift

ter verkrijging van de graad van doctor aan de
Erasmus Universiteit Rotterdam
op gezag van de rector magnificus
Prof. dr. R.C.M.E. Engels
en volgens besluit van het College voor Promoties.

De openbare verdediging zal plaatsvinden op
woensdag 30 september 2020 om 09:30

door

Hessel van der Weide

geboren te Groningen.

Promotiecommissie

Promotor: Prof. dr. A. Verbon

Overige leden: Prof. dr. H.W. Frijlink

Prof. dr. A.G. Vulto

Prof. dr. H.F.L. Wertheim

Copromotoren: Dr. J.P. Hays

Dr. I.A.J.M. Bakker-Woudenberg

Table of contents

Section I	Background	9
<hr/>		
Chapter 1	General introduction	11
Chapter 2	Antibiotic-nanomedicines: facing the challenge of effective treatment of antibiotic-resistant respiratory tract infections <i>Future Microbiology, 2018</i>	31
Chapter 3	Aims and outline	53
Section II	<i>In vitro</i> investigations	59
<hr/>		
Chapter 4	Antimicrobial activity of two novel antimicrobial peptides AA139 and SET-M33 against clinically and genotypically diverse <i>Klebsiella pneumoniae</i> isolates with differing antibiotic resistance profiles <i>International Journal of Antimicrobial Agents, 2019</i>	61
Chapter 5	Investigations into the killing activity of an antimicrobial peptide active against extensively antibiotic-resistant <i>Klebsiella pneumoniae</i> and <i>Pseudomonas aeruginosa</i> <i>Biochimica et Biophysica Acta – Biomembranes, 2017</i>	89

Section III	<i>In vivo</i> investigations	119
<hr/>		
Chapter 6	Successful high-dosage monotherapy of tigecycline in a multidrug-resistant <i>Klebsiella pneumoniae</i> pneumonia-septicemia model in rats <i>Antibiotics, 2020</i>	121
Chapter 7	<i>In vitro</i> and <i>in vivo</i> bacterial killing activity of novel antimicrobial peptide SET-M33-nanomedicines against multidrug-resistant <i>Klebsiella pneumoniae</i>	151
Chapter 8	Therapeutic efficacy of novel antimicrobial peptide AA139-nanomedicines in a multidrug-resistant <i>Klebsiella pneumoniae</i> pneumonia-septicemia model in rats <i>Antimicrobial Agents and Chemotherapy, 2020</i>	173
<hr/>		
Section IV	Final assessment	205
<hr/>		
Chapter 9	Summarizing discussion and future perspectives	207
Chapter 10	Glossary	229
Chapter 11	Nederlandse samenvatting	235
<hr/>		
Section V	Appendices	245
<hr/>		
	Dankwoord	246
	Curriculum Vitae	254
	List of publications	255
	PhD portfolio	256

Chapter 1 General introduction

Chapter 2 Antibiotic-nanomedicines: facing the challenge of effective treatment of antibiotic-resistant respiratory tract infections

Chapter 3 Aims and outline

Chapter 1 is a general introduction which covers the discovery and characteristics of Gram-negative bacteria and their ability to cause pneumonia; the current state of multidrug resistance in Gram-negative bacteria; the healthcare threat posed by multidrug-resistant Gram-negative pneumonia, and the urgency of developing novel therapeutic approaches (focused on antimicrobial peptides and direct drug delivery) to treat multidrug-resistant Gram-negative pneumonia.

Chapter 2 is a review of the current state of antibiotic-nanomedicines research aimed at the treatment of antibiotic-resistant respiratory tract infections, including multidrug-resistant Gram-negative pneumonia. It provides an overview of the current state of research, the development of different nanocarriers, and the potential value and clinical status of inhalable antibiotic-nanomedicines.

Chapter 3 is a brief outline of the research presented in the current thesis and the research questions it aims to answer.



Section

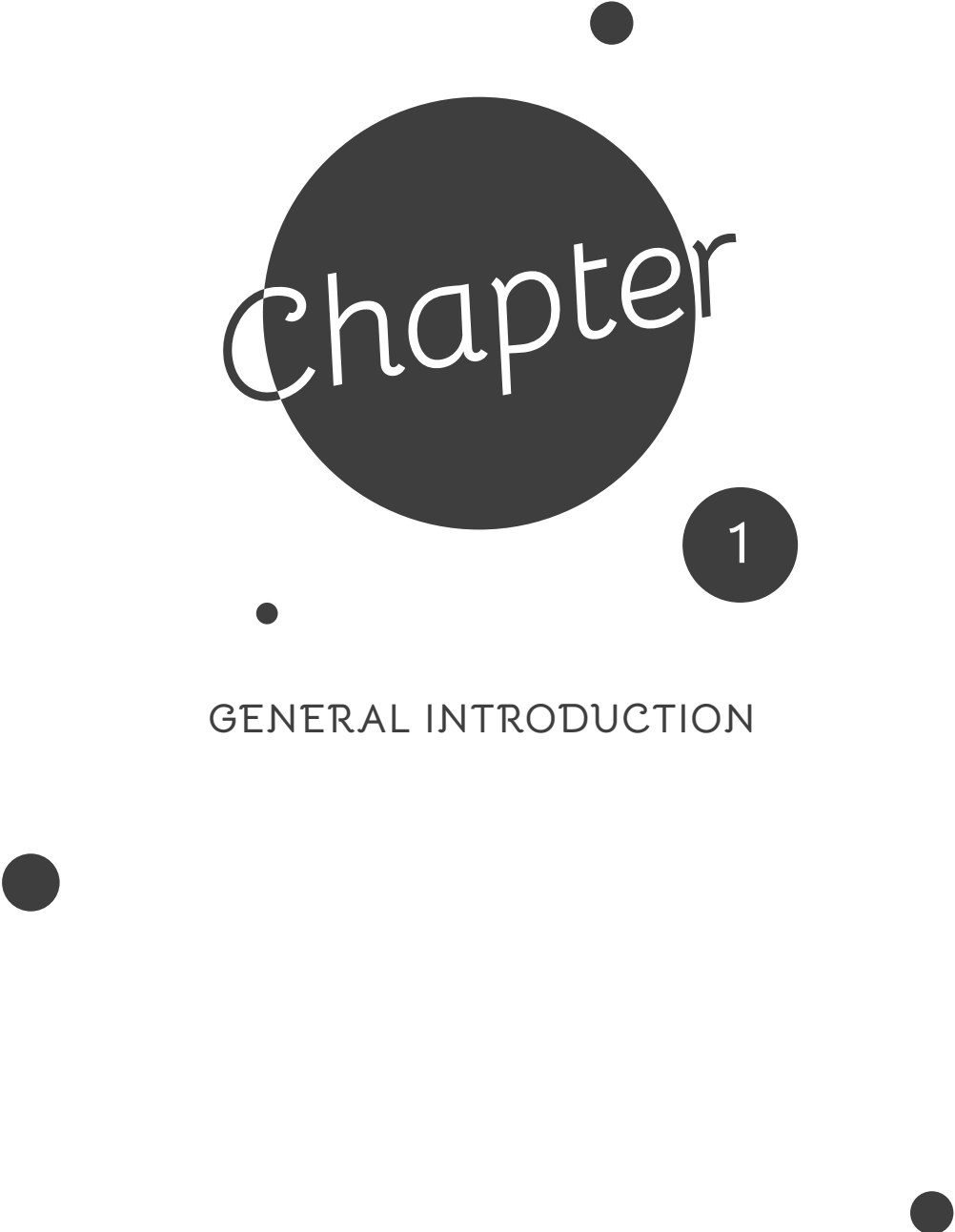


I



BACKGROUND





Chapter

1

GENERAL INTRODUCTION

Gram-negative pneumonia

Pneumonia is an inflammatory condition of the lungs, usually caused by infection with microorganisms such as bacteria. The first observation of bacteria in the airways of patients who had died from pneumonia was made by Edwin Klebs in 1875¹. However, the significance of bacteria as the etiological cause of pneumonia was not recognized until Carl Friedländer reported their presence in nearly all cases of pneumonia he had examined in 1883². This observation of bacteria in infected lung tissue was aided by the use of a new staining technique developed by Hans Christian Gram, which facilitated the visibility of bacteria in histological sections and hence their association with clinical disease³. Gram's staining technique was refined over the following decades, and after more than one hundred years, still remains one of the basic techniques utilized in the microbial diagnostic laboratory^{4,5}. It serves as the basis for one of the major classifications of bacteria: the differentiation between Gram-negative bacteria and Gram-positive bacteria by the composition and characteristics of their cell envelope⁶. Gram-positive bacteria (staining blue-purple) possess a thick peptidoglycan cell-wall covering their cell membrane, whereas Gram-negative bacteria (staining pink-red) possess a thin peptidoglycan cell-wall in between their cell membrane and a highly immunogenic outer membrane mainly composed of lipopolysaccharide (LPS) and phospholipids (Figure 1)⁷.

The structural differences in bacterial cell envelopes have major repercussions for the pathophysiology and treatment of infections caused by Gram-negative or Gram-positive bacteria. First, the outer membrane of Gram-negative bacteria is a major factor in disease spread and severity⁸. As an example, the lipid A portion of LPS is a potent endotoxin, and the spread of a Gram-negative infection to the circulatory system of a patient may lead to overstimulation of lipid A receptors of the immune system^{9,10}. The resulting inflammatory reaction can lead to 'septic shock', a life-threatening medical condition that requires immediate medical intervention¹¹.

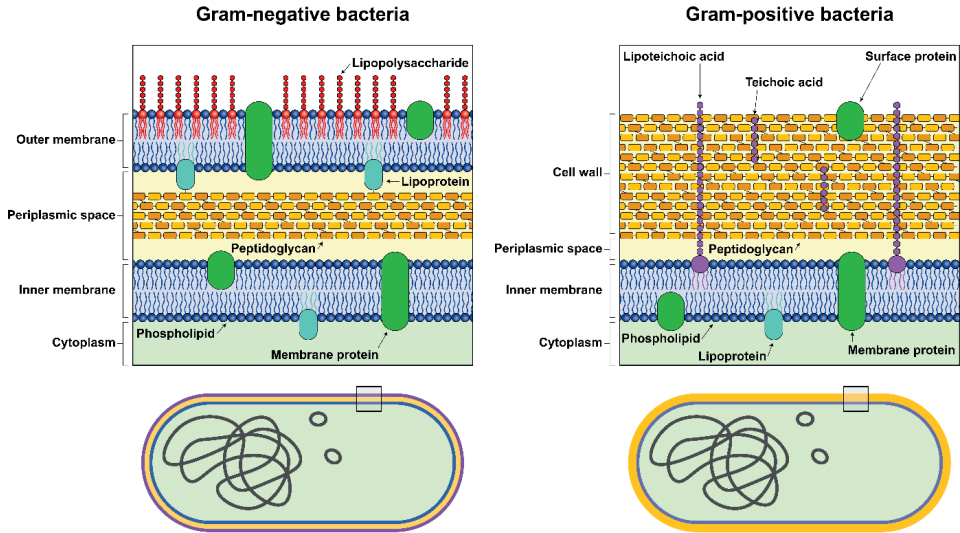


Figure 1. Diagram of the cell envelope structure of Gram-negative bacteria and Gram-positive bacteria.

Further, the outer membrane of Gram-negative bacteria provides intrinsic protection from various antibiotics, detergents, and innate immune components, and is involved in many mechanisms of antibiotic resistance¹². This is aided by many differing outer membrane proteins with a variety of functions (Figure 2)¹³, including so-called porins (which allow the influx of most nutrients while restricting the influx of certain antibiotics)¹⁴ and efflux pumps (which pump waste products and certain antibiotics out of the bacterial cell)¹⁵.

Gram-negative bacteria include several major human commensals and (opportunistic) pathogens, such as *Klebsiella pneumoniae*, the bacillus first discovered by Carl Friedländer when he first demonstrated a link between bacteria and pneumonia²⁴. Even today, diseases caused by Gram-negative bacteria continue to be a major global healthcare burden more than a century after their first discovery. These bacteria are the primary causative pathogens in ~30% of healthcare-associated infections, rising to ~70% in cases of healthcare-associated pneumonia^{16,17}. Pneumonia is associated with high mortality rates and lengthy hospital stays¹⁸ and over 230,000 deaths and €10 billion in

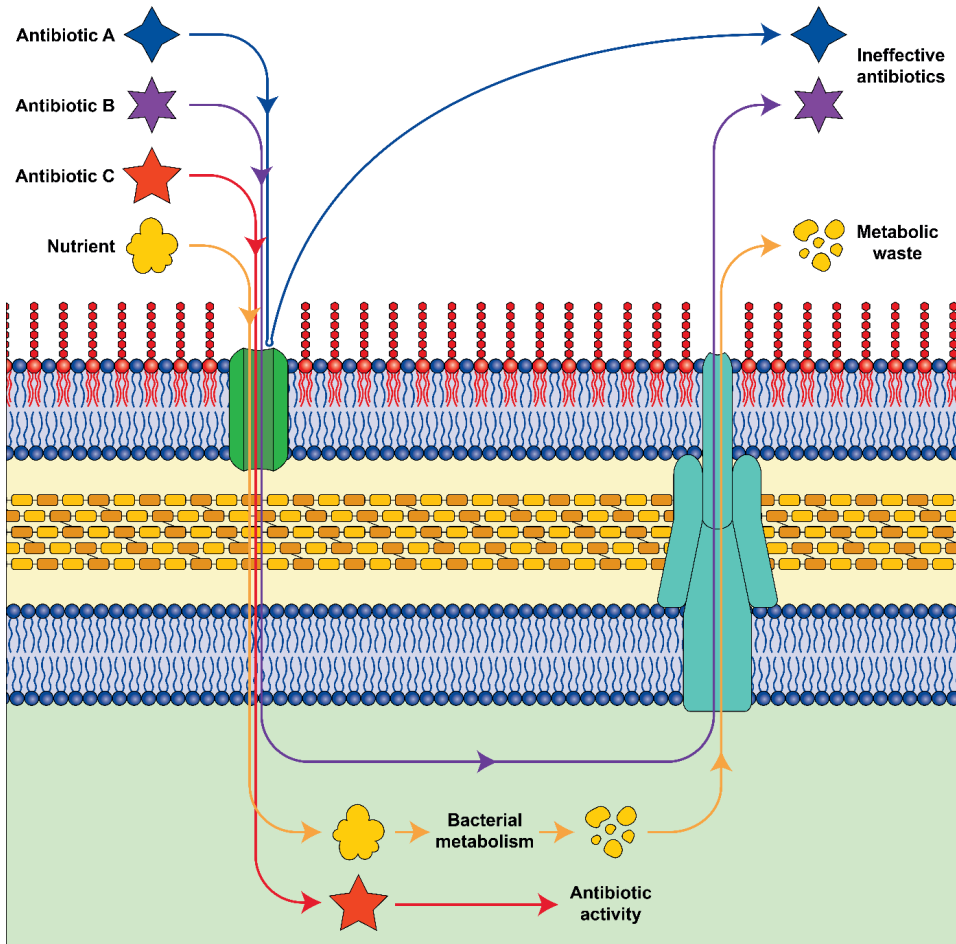


Figure 2. Diagram of the function of porins and efflux pumps in the outer membrane of the Gram-negative bacterial cell envelope and the role they play in antibiotic resistance. Antibiotic A is a representation of antibiotics which cannot pass through porins in the outer membrane. Antibiotic B is a representation of antibiotics which pass through porins in the outer membrane, but are transported out of the bacterial cell by efflux pumps. Antibiotic C is a representation of antibiotics which pass through porins in the outer membrane and are not transported by efflux pumps, thereby able to enact their antibiotic activity. Nutrients are capable of passing through porins in the outer membrane, and once metabolized, the resulting metabolic waste products are transported out of the bacterial cell by efflux pumps.

economic costs across the European Union (EU) every year^{19,20}. The healthcare burden of pneumonia is projected to further increase in the coming decades due to aging populations as well as the emergence and spread of multidrug resistance in Gram-negative bacteria, which is currently rendering many existing antibiotic therapies ineffective²¹.

Antimicrobial resistance

Gram-negative bacteria continue to demonstrate their ability to adapt to many different types of antibiotics. Already, ~50% of invasive Gram-negative bacterial isolates cultured in Europe are resistant to at least one antibiotic (Figure 3)²². The spread of multidrug resistance has rendered a growing list of antibiotics ineffective in the treatment of Gram-negative infections²³, raising concerns about an oncoming post-antibiotic era in which pan-resistant bacterial infections will be common and there are little to no treatment options available for clinicians²⁴.

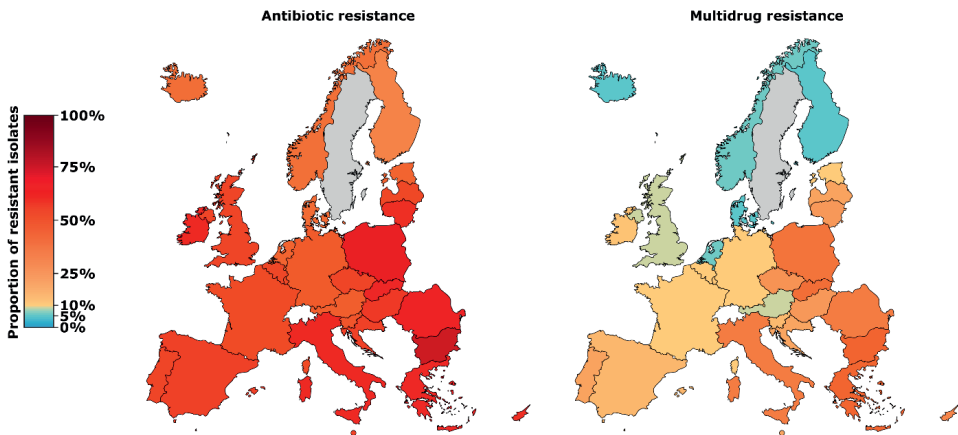


Figure 3. Antibiotic resistance and multidrug resistance among Gram-negative *Enterobacteriaceae* in the EU/EEA in 2017. Shown are the proportions of antibiotic-resistant (resistant to ≥ 1 antibiotic families) and multidrug-resistant (resistant to ≥ 3 antibiotic families) isolates of *K. pneumoniae* and *E. coli* found in each individual country in 2017. The data from EARS-Net were kindly supplied by the European Centre for Disease Control (ECDC)²⁵.

Antibiotic resistance can arise via three different mechanisms (Figure 4)²⁶. First, bacteria can be intrinsically resistant to antibiotics due to natural characteristics which make them resistant to the activity of specific antibiotics²⁷. In this respect, Gram-negative bacteria are intrinsically resistant to many antibiotics due to the impermeability of their outer membrane²⁸ and the presence of active efflux pumps²⁹. For instance, the outer membrane of Gram-negative bacteria is impermeable to large glycopeptide antibiotics like vancomycin (a potent antibiotic for Gram-positive bacteria) due to their molecular size¹². Second, bacteria can become antibiotic-resistant through adaptive mutations after exposure to antibiotics³⁰. For example, exposure to fluoroquinolone antibiotics such as ciprofloxacin can select for bacteria with mutations in the quinolone resistance determining region (QRDR) of the bacterial deoxyribonucleic acid (DNA) gyrase gene³¹. Third, bacteria can acquire antibiotic resistance from other bacteria via the horizontal gene transfer of antibiotic resistance genes present on mobile genetic elements (MGEs)³². The most common MGEs involved in antibiotic resistance are plasmids: extra-chromosomal, circular pieces of DNA that can exist in large numbers inside a single bacterial cell³³. Plasmid-mediated antibiotic resistance by the Gram-negative bacterial family *Enterobacteriaceae* is particularly problematic, as it allows emerging forms of antibiotic resistance to rapidly spread through bacterial populations with the potential to cause disease – a process that can occur on a global level in the modern world^{34,35}.

Of all current forms of antibiotic resistance, the carriage and expression of extended-spectrum β -lactamases (ESBLs) are among the most important acquired antibiotic resistance determinants worldwide and are especially prevalent in *Escherichia coli* and *K. pneumoniae*, both of which belong to the Gram-negative *Enterobacteriaceae*³⁶. ESBLs confer resistance to widely used broad-spectrum β -lactam antibiotics, but ESBL-producing isolates are often found to be also resistant to several different types of antibiotics – making such isolates multidrug-resistant³⁷. In the treatment of such cases, carbapenem antibiotics are the drug of choice, but recent years have seen a growing prevalence of Gram-negative bacteria producing carbapenem inactivating enzymes (carbapenemases), including the *K. pneumoniae* carbapenemase (KPC)³⁸ and

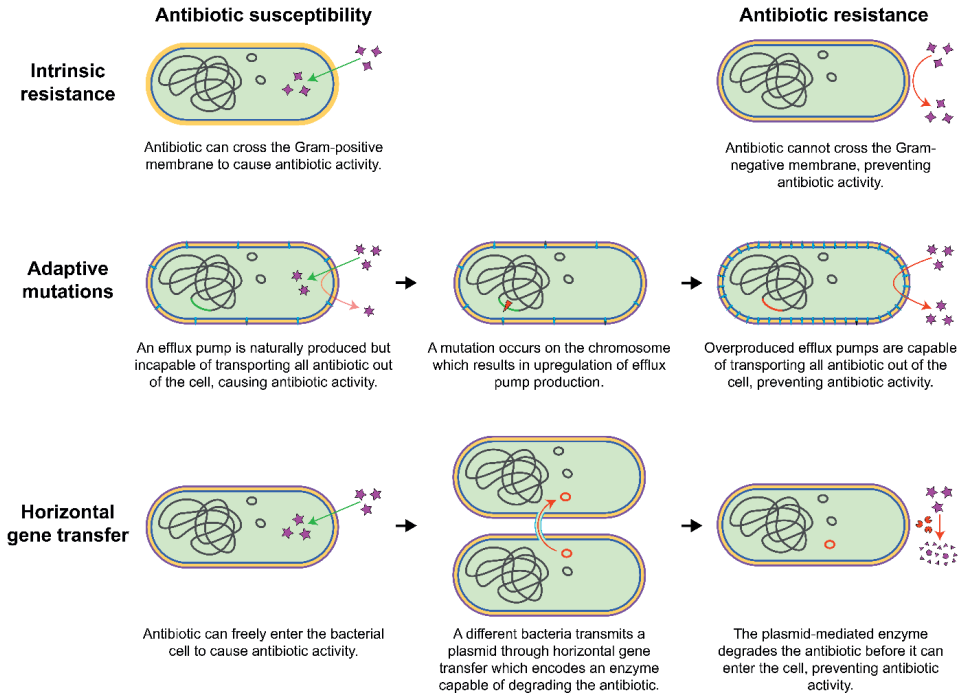


Figure 4. Diagram with different examples of mechanisms of resistance. Intrinsic resistance is represented by an antibiotic which is able to permeate the Gram-positive membrane but not the Gram-negative membrane. Adaptive mutation is represented by the upregulation of an intrinsic efflux pump which allows Gram-negative bacteria to keep specific antibiotics out of the cell. Horizontal gene transfer is represented by a plasmid-mediated enzyme which degrades specific antibiotics.

New Delhi metallo- β -lactamase (NDM)³⁵. The continuing spread of such multidrug-resistant bacteria has forced clinicians to use ‘drugs of last resort’ such as colistin and tigecycline³⁹. Inevitably, the increasing use of these last resort antibiotics has already led to the emergence of bacteria resistant to colistin⁴⁰ or tigecycline⁴¹.

A particularly worrying concurrent development is that fewer new antibiotics are reaching clinical development, which has resulted in a lack of antibiotics that are effective against multidrug-resistant Gram-negative bacteria^{42,43}. In fact, most currently available antibiotic compounds were discovered in the 1960’s and 1970’s by screening microorganisms (usually fungi) for naturally produced antibiotic compounds e.g.

penicillins, macrolides, tetracyclines and aminoglycosides^{44,45}. In later decades, synthetic chemistry approaches have been employed to generate new types of antibiotics, for example the carbapenems, though both of these approaches have failed to generate any new classes of antibiotics in recent decades⁴³. Indeed, as of March 2019, no novel classes of antibiotics have entered clinical development for the treatment of Gram-negative pneumonia⁴⁶.

There are several reasons why the current research and development (R&D) portfolios of large pharmaceutical corporations do not include the development of new antibiotics, but it is mainly due to the fact that antibiotic discovery is not sufficiently profitable when compared to the development of drugs for other disease areas, most notably drugs for the long-term treatment of chronic conditions⁴⁷. The consequence of this R&D policy is that relatively few new candidate antibiotics are being developed for clinical application^{44,48}. Global authorities such as the EU and the United Nations (UN) as well as the World Health Organization (WHO) are aware of this problem and are trying to solve the worldwide endemic of antibiotic resistance by focusing on several key 'One Health' action areas⁴⁹⁻⁵¹. These key areas include increased epidemiological reporting of antibiotic resistance, the implementation of guidelines for effective infection prevention policies, reducing the use of antibiotics as growth promoters in food animals, the development of novel rapid diagnostics, and the development of new antibiotics which are active against multidrug-resistant bacteria.

In addition to the activities of these global authorities, small companies and academic scientists have recently focused on the development of novel methods for antibiotic discovery⁵², as well as the improvement and development of previously discovered classes of antibiotics that have seen little clinical application for the treatment of multidrug-resistant Gram-negative infections. One example of a previously discovered, yet underutilized, class of antibiotics are the antimicrobial peptides (AMPs)^{53,54}. It is the discovery of new classes of antibiotics and/or the development of underutilized classes of antibiotics (like AMPs) which are most likely to be successful in the worldwide fight against antibiotic-resistant bacteria.

Antimicrobial peptides

AMPs are a diverse family of naturally occurring antimicrobial oligopeptides with varying numbers of amino acids⁵⁵. AMPs are produced by living organisms as a defensive mechanism towards micro-organisms and are therefore also referred to as host defense peptides⁵⁶. AMPs were discovered in 1939 by René Dubos when he isolated an antimicrobial agent from *Bacillus brevis*, which was found to be composed of two AMPs: gramicidin and tyrocidine⁵⁷. Since that initial discovery, over 3000 different AMPs have been described⁵⁸. Although AMPs have been known since the 1940's, this family of antibiotics has seen only limited use for the treatment of Gram-negative pneumonia, largely due to a number of hurdles that have limited their clinical use, including toxic side-effects⁵⁹, short biological half-life due to degradation by proteases^{59,60}, and limited efficacy against Gram-negative bacteria⁶¹. In fact, only a limited number of AMPs have seen 'real-world' application, the most clinically relevant being colistin⁶¹.

Colistin is one of the polymyxins, a class of cationic polypeptide antibiotics used for the treatment of Gram-negative bacterial infections. The precise mechanism by which polymyxins exert their antibiotic activity remains contentious. The main model of 'self-promoted uptake' postulates that the cationic polymyxin molecules first bind and inhibit LPS on the outer membrane, which is then followed by an insertion of the polymyxin molecule into the cell envelope which results in outer membrane permeabilization and disruption of the cytoplasmic membrane, leading to bacterial cell death (Figure 5)⁶². Additional mechanisms also contribute to the antibiotic activity of polymyxins, such as the inhibition of the bacterial respiratory chain⁶³. Colistin has been available for clinical use since 1959, but was largely discontinued due to reports of potential toxic side effects in the 1980's. The global increase of multidrug-resistant infections and diminishing supply of effective antibiotics available has caused a resurgence of colistin as a drug of last resort for the treatment of multidrug-resistant Gram-negative infections⁶⁴, which inevitably has also led to the concurrent emergence and spread of colistin resistance⁶⁵. Acquired colistin resistance utilizes various molecular mechanisms, including LPS modifications or expression of outer membrane proteins and efflux pumps⁶⁶. The first

report of a plasmid conferring mobilized colistin resistance (MCR) was published in 2015⁴⁰. Since then, different variants of plasmidal colistin resistance have been identified and isolated from patients across the world, rendering this drug of last resort potentially ineffective⁶⁷.

Other AMPs may remain a viable alternative in the treatment of colistin-resistant Gram-negative infections depending on the absence of colistin cross-resistance – a phenomenon which occurs when resistance to one antibiotic results in additional

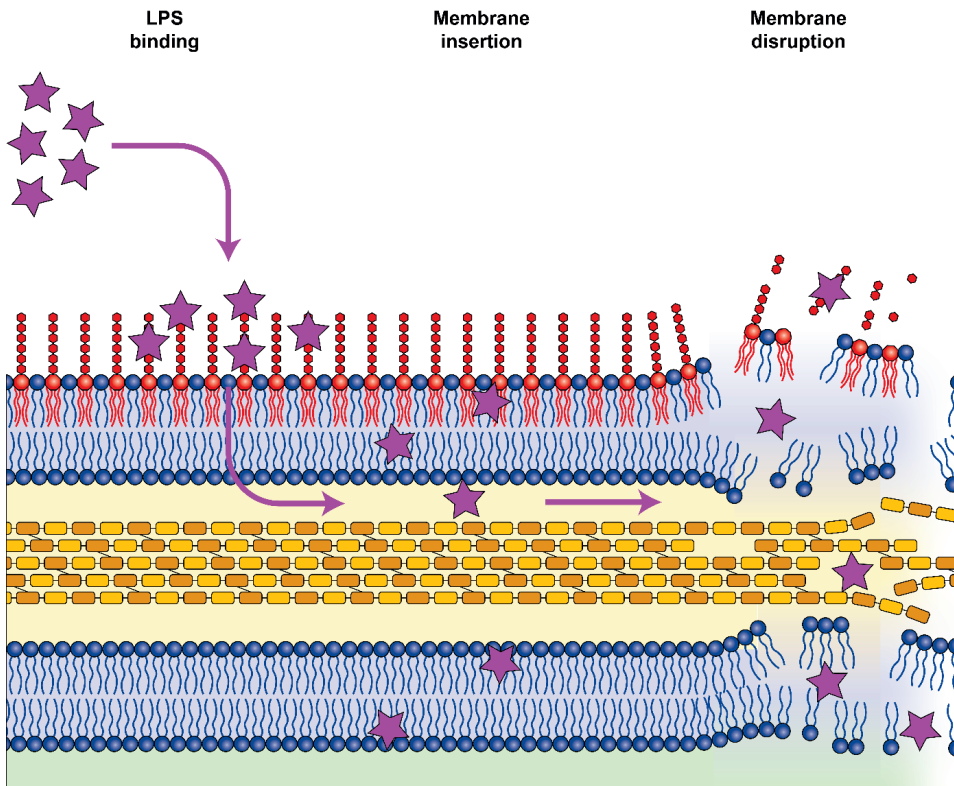


Figure 5. Diagram of the 'self-promoted uptake' mechanism of antibiotic action employed by colistin and cationic antimicrobial peptides. In the first step, the cationic antibiotic binds to the LPS on the outer membrane of Gram-negative bacteria. In the second step, the cationic antibiotic inserts itself within the membranes of the cell envelope. In the third step, the cationic antibiotic causes permeabilization and disruption of the cell envelope.

resistance to related antibiotics. Studies have shown that AMPs differ in their potential for cross-resistance with colistin, which is most likely due to differences between the mechanisms of antimicrobial activity of different AMPs⁶⁸⁻⁷⁰. Like colistin, most AMPs are cationic and share the same ‘self-promoted uptake’ mechanism of bacterial killing (Figure 5)⁷¹. However, while most cationic AMPs have this membrane-disrupting mechanism of action in common, many have different additional mechanisms of antimicrobial activity including membrane protein targeting, intracellular activity, and immunomodulation⁷²⁻⁷⁴. As mentioned above, biological hurdles exist to the implementation of AMPs into clinical practice, even those AMPs potentially useful for the treatment of multidrug-resistant Gram-negative bacterial infections (including colistin-resistant infections). To ameliorate those issues, novel therapeutic approaches need to be considered in the development of AMPs as effective antibiotic treatments.

Novel therapeutic approaches

The regular approach to the treatment of bacterial pneumonia in primary care occurs via the prescription of a course of oral antibiotics, whereas in secondary and tertiary care, more powerful antibiotics are usually prescribed and administered via the intravenous route^{75,76}. However, although the parenteral (intravenous) application of antibiotics allows for high systemic bioavailability, this route of administration may not always achieve the minimum inhibitory concentration (MIC) of antibiotic necessary to inhibit or kill bacteria at the actual site of infection. Furthermore, the systemic (whole body) application of antibiotics to patients can cause unwanted toxic side-effects due to the antibiotic reaching tissues that are not infected⁷⁷⁻⁸⁰ and/or patients becoming allergic to the prescribed antibiotic⁸¹. Another serious side-effect of systemic antibiotics is the enhanced selection of antibiotic-resistant subpopulations of bacteria from the patient’s own endogenous microbiota (all of the microorganisms that live in and on our bodies), so-called collateral damage⁸². Such resistant subpopulations, selected from the endogenous microbiota, may cause multidrug-resistant invasive infections which prove

very hard to treat in critically ill patients. Therefore, there is room for therapeutic improvement beyond the traditional intravenous administration of antibiotics⁸³.

Along with the development of new antibiotic agents (such as AMPs), current research is also focused on the development of novel and improved antibiotic therapeutic approaches. Such novel therapeutic approaches may allow for an amelioration of the disadvantages associated with treatment strategies involving current antibiotics, potentially allowing all kinds of antibiotics to be used more effectively to combat multidrug-resistant infections. They may also help reduce or overcome the development of antibiotic-resistant subpopulations as a consequence of antibiotic therapy. The combination of developing or improving antibiotic agents, in parallel with the development of such novel therapeutic approaches, has the potential to be a major development in the fight against multidrug-resistant bacterial infections⁸⁴.

One such promising novel therapeutic approach is the use of nanotechnology for coupling antibiotics with nanocarriers⁸⁵. Nanocarriers are nanomaterials used as a mode of transporting another substance⁸⁶. In this way, nanotechnological products such as nanomedicines can be generated, which can transport therapeutic agents to the appropriate tissues and cells in the body. Attaching antibiotics to nanocarriers to create antibiotic-nanomedicines allows for improved antibiotic treatment without an increase in risk to the patient⁸⁷.

Another novel therapeutic approach to effectively treat a patient suffering from an infection is the improved administration of antibiotics. Indeed, the direct delivery of antibiotics to the site of infection would represent a therapeutic improvement⁸⁸, facilitating increased antibiotic concentrations at the site of infection^{89,90} and helping to reduce any toxic side effects and/or collateral damage associated with the systemic administration of antibiotics^{91,92}. For pneumonia, the site of infection is the lung and over the last decade there has been an increasing interest into developing and exploiting inhalable treatments that deliver antibiotics directly to the lungs⁹³. The accurate delivery of antibiotics directly to the pulmonary site of infection via inhalation (in patients) and endotracheal aerosolization (in experimental animals) allows the antibiotics to reach

higher local concentrations. Inhalation of nanomedicines may further result in prolonged biological half-life of the antibiotic due to protection from degradation by local proteases resulting in improved therapeutic efficacy^{93,94}.

The combined approach of the direct delivery of inhalable antibiotic-nanomedicines will be further outlined in **Chapter 2**⁹⁵.

References

1. Klebs E. Beiträge zur Kenntniss der pathogenen Schistomyceten. *Archiv für experimentelle Pathologie und Pharmakologie*. 1875;3(5-6):305-24.
2. Friedländer C. Die mikrokokken der pneumonie 1883.
3. Gram C. Ueber die isolirte Färbung der Schizomyceten in Schnitt- und Trockenpräparaten. *Fortschritte der Medicin*. 1884;2:185-9.
4. Austrian R. The Gram stain and the etiology of lobar pneumonia, an historical note. *Bacteriological Reviews*. 1960;24(3):261.
5. Fournier P-E, Drancourt M, Colson P, Rolain J-M, La Scola B, Raoult D. Modern clinical microbiology: new challenges and solutions. *Nature Reviews Microbiology*. 2013;11(8):574.
6. Beveridge TJ. Use of the Gram stain in microbiology. *Biotechnic & Histochemistry*. 2001;76(3):111-8.
7. Nikaido H, Nakae T. The outer membrane of Gram-negative bacteria. *Advances in Microbial Physiology*. 20: Elsevier; 1980. p. 163-250.
8. Dirienzo JM, Nakamura K, Inouye M. The outer membrane proteins of Gram-negative bacteria: biosynthesis, assembly, and functions. *Annual Review of Biochemistry*. 1978;47(1):481-532.
9. Preston A, Mandrell RE, Gibson BW, Apicella MA. The lipooligosaccharides of pathogenic gram-negative bacteria. *Critical Reviews in Microbiology*. 1996;22(3):139-80.
10. Lu Y-C, Yeh W-C, Ohashi PS. LPS/TLR4 signal transduction pathway. *Cytokine*. 2008;42(2):145-51.
11. Opal SM, Scannon PJ, Vincent J-L, White M, Carroll SF, Palardy JE, et al. Relationship between plasma levels of lipopolysaccharide (LPS) and LPS-binding protein in patients with severe sepsis and septic shock. *The Journal of Infectious Diseases*. 1999;180(5):1584-9.
12. Nikaido H. Outer membrane barrier as a mechanism of antimicrobial resistance. *Antimicrobial Agents and Chemotherapy*. 1989;33(11):1831.
13. Koebnik R, Locher KP, Van Gelder P. Structure and function of bacterial outer membrane proteins: barrels in a nutshell. *Molecular Microbiology*. 2000;37(2):239-53.
14. Galdiero S, Falanga A, Cantisani M, Tarallo R, Elena Della Pepa M, D'Orlando V, et al. Microbe-host interactions: structure and role of Gram-negative bacterial porins. *Current Protein and Peptide Science*. 2012;13(8):843-54.
15. Nikaido H. Multidrug efflux pumps of gram-negative bacteria. *Journal of Bacteriology*. 1996;178(20):5853.
16. Sader HS, Farrell DJ, Flamm RK, Jones RN. Antimicrobial susceptibility of Gram-negative organisms isolated from patients hospitalised with pneumonia in US and European hospitals: results from the SENTRY Antimicrobial Surveillance Program, 2009–2012. *International Journal of Antimicrobial Agents*. 2014;43(4):328-34.
17. Cilloniz C, Martin-Loeches I, Garcia-Vidal C, San Jose A, Torres A. Microbial etiology of pneumonia: epidemiology, diagnosis and resistance patterns. *International Journal of Molecular Sciences*. 2016;17(12):2120.
18. Ibrahim EH, Ward S, Sherman G, Kollef MH. A comparative analysis of patients with early-onset vs late-onset nosocomial pneumonia in the ICU setting. *Chest*. 2000;117(5):1434-42.
19. Marshall DC, Goodson RJ, Xu Y, Komorowski M, Shalhoub J, Maruthappu M, et al. Trends in mortality from pneumonia in the Europe union: a temporal analysis of the European detailed mortality database between 2001 and 2014. *Respiratory Research*. 2018;19(1):81.
20. Welte T, Torres A, Nathwani D. Clinical and economic burden of community-acquired pneumonia among adults in Europe. *Thorax*. 2012;67(1):71-9.
21. Bassetti M, Welte T, Wunderink RG. Treatment of Gram-negative pneumonia in the critical care setting: is the beta-lactam antibiotic backbone broken beyond repair? *Critical Care*. 2015;20(1):19.

22. ECDC. Antimicrobial Resistance Surveillance in Europe 2017. Annual Report of the European Antimicrobial Resistance Surveillance Network (EARS-Net). ECDC Stockholm, Sweden; 2017.
23. O'Neill J. Antimicrobial resistance: tackling a crisis for the health and wealth of nations. *The Review on Antimicrobial Resistance*. 2014;20.
24. Ventola CL. The antibiotic resistance crisis: part 1: causes and threats. *Pharmacy and Therapeutics*. 2015;40(4):277.
25. ECDC. Antimicrobial Resistance Surveillance in Europe 2017. Annual Report of the European Antimicrobial Resistance Surveillance Network (EARS-Net). ECDC Stockholm, Sweden; 2019.
26. Blair JM, Webber MA, Baylay AJ, Ogbolu DO, Piddock LJ. Molecular mechanisms of antibiotic resistance. *Nature Reviews Microbiology*. 2015;13(1):42.
27. Cox G, Wright GD. Intrinsic antibiotic resistance: mechanisms, origins, challenges and solutions. *International Journal of Medical Microbiology*. 2013;303(6-7):287-92.
28. Delcour AH. Outer membrane permeability and antibiotic resistance. *Biochimica et Biophysica Acta (BBA)-Proteins and Proteomics*. 2009;1794(5):808-16.
29. Nikaido H. Antibiotic resistance caused by Gram-negative multidrug efflux pumps. *Clinical Infectious Diseases*. 1998;27(Supplement_1):S32-S41.
30. Martinez J, Baquero F. Mutation frequencies and antibiotic resistance. *Antimicrobial Agents and Chemotherapy*. 2000;44(7):1771-7.
31. Weigel LM, Steward CD, Tenover FC. *gyrA* Mutations Associated with Fluoroquinolone Resistance in Eight Species of Enterobacteriaceae. *Antimicrobial Agents and Chemotherapy*. 1998;42(10):2661-7.
32. Stokes HW, Gillings MR. Gene flow, mobile genetic elements and the recruitment of antibiotic resistance genes into Gram-negative pathogens. *FEMS Microbiology Reviews*. 2011;35(5):790-819.
33. Bennett P. Plasmid encoded antibiotic resistance: acquisition and transfer of antibiotic resistance genes in bacteria. *British Journal of Pharmacology*. 2008;153(S1):S347-S57.
34. Schultsz C, Geerlings S. Plasmid-mediated resistance in Enterobacteriaceae. *Drugs*. 2012;72(1):1-16.
35. Johnson AP, Woodford N. Global spread of antibiotic resistance: the example of New Delhi metallo- β -lactamase (NDM)-mediated carbapenem resistance. *Journal of Medical Microbiology*. 2013;62(4):499-513.
36. Girlich D, Poirel L, Nordmann P. CTX-M expression and selection of ertapenem resistance in *Klebsiella pneumoniae* and *Escherichia coli*. *Antimicrobial Agents and Chemotherapy*. 2009;53(2):832-4.
37. Tumbarello M, Sanguinetti M, Montuori E, Trecarichi EM, Posteraro B, Fiori B, et al. Predictors of mortality in patients with bloodstream infections caused by extended-spectrum- β -lactamase-producing Enterobacteriaceae: importance of inadequate initial antimicrobial treatment. *Antimicrobial Agents and Chemotherapy*. 2007;51(6):1987-94.
38. Tzouveleki LS, Markogiannakis A, Psychogiou M, Tassios PT, Daikos GL. Carbapenemases in *Klebsiella pneumoniae* and other Enterobacteriaceae: an evolving crisis of global dimensions. *Clinical Microbiology Reviews*. 2012;25(4):682-707.
39. McKenna M. Antibiotic resistance: the last resort. *Nature News*. 2013;499(7459):394.
40. Liu Y-Y, Wang Y, Walsh TR, Yi L-X, Zhang R, Spencer J, et al. Emergence of plasmid-mediated colistin resistance mechanism MCR-1 in animals and human beings in China: a microbiological and molecular biological study. *The Lancet Infectious Diseases*. 2016;16(2):161-8.
41. Sun Y, Cai Y, Liu X, Bai N, Liang B, Wang R. The emergence of clinical resistance to tigecycline. *International Journal of Antimicrobial Agents*. 2013;41(2):110-6.
42. Butler MS, Blaskovich MA, Cooper MA. Antibiotics in the clinical pipeline at the end of 2015. *The Journal of Antibiotics*. 2017;70(1):3.
43. Lewis K. Platforms for antibiotic discovery. *Nature Reviews Drug Discovery*. 2013;12(5):371-87.
44. Lewis K. Antibiotics: Recover the lost art of drug discovery. *Nature*. 2012;485(7399):439-40.

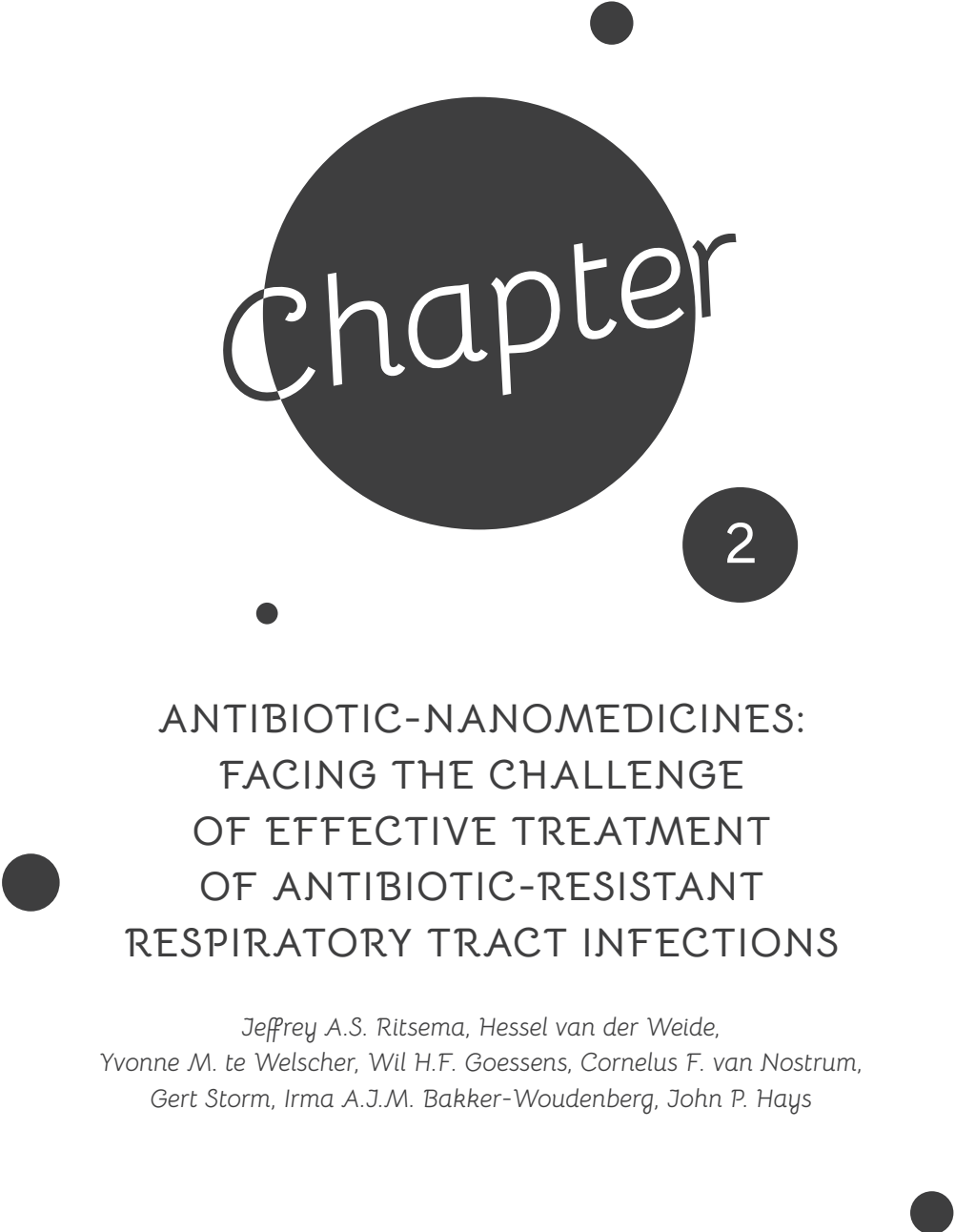
45. Aminov RI. A brief history of the antibiotic era: lessons learned and challenges for the future. *Frontiers in Microbiology*. 2010;1.
46. Pew Charitable Trusts. Antibiotics Currently in Global Clinical Development; 2019. Available from: <https://www.pewtrusts.org/es/research-and-analysis/data-visualizations/2014/antibiotics-currently-in-clinical-development>.
47. Projan SJ. Why is big Pharma getting out of antibacterial drug discovery? *Current Opinion in Microbiology*. 2003;6(5):427-30.
48. Davies J, Davies D. Origins and evolution of antibiotic resistance. *Microbiology and Molecular Biology Reviews*. 2010;74(3):417-33.
49. Council of the European Union. Council conclusions on the impact of antimicrobial resistance in the human health sector and in the veterinary sector – a “One Health” perspective. C 211/2 2012 [
50. United Nations. Draft political declaration of the high-level meeting of the General Assembly on antimicrobial resistance. 16-16108(E) 2016 [
51. Shallcross LJ, Davies SC. The World Health Assembly resolution on antimicrobial resistance. *Journal of Antimicrobial Chemotherapy*. 2014;69(11):2883-5.
52. Ling LL, Schneider T, Peoples AJ, Spoering AL, Engels I, Conlon BP, et al. A new antibiotic kills pathogens without detectable resistance. *Nature*. 2015;517(7535):455.
53. Gordon YJ, Romanowski EG, McDermott AM. A review of antimicrobial peptides and their therapeutic potential as anti-infective drugs. *Current Eye Research*. 2005;30(7):505-15.
54. Novak R, Shlaes DM. The pleuromutilin antibiotics: a new class for human use. *Current Opinion in Investigational Drugs*. 2010;11(2):182-91.
55. Epand RM, Vogel HJ. Diversity of antimicrobial peptides and their mechanisms of action. *Biochimica et Biophysica Acta (BBA)-Biomembranes*. 1999;1462(1-2):11-28.
56. Hancock RE, Sahl H-G. Antimicrobial and host-defense peptides as new anti-infective therapeutic strategies. *Nature Biotechnology*. 2006;24(12):1551.
57. DUBOS RJ, Hotchkiss R. Origin, Nature and Properties of Gramicidin and Tyrocidine. *Trams & Studies of College of Physicians of Philadelphia*. 1942;10(1):11-9.
58. Wang G, Li X, Wang Z. APD3: the antimicrobial peptide database as a tool for research and education. *Nucleic Acids Research*. 2015;44(D1):D1087-D93.
59. Marr AK, Gooderham WJ, Hancock RE. Antibacterial peptides for therapeutic use: obstacles and realistic outlook. *Current Opinion in Pharmacology*. 2006;6(5):468-72.
60. Pini A, Falciani C, Bracci L. Branched peptides as therapeutics. *Current Protein and Peptide Science*. 2008;9(5):468-77.
61. Fox JL. Antimicrobial peptides stage a comeback. *Nature Publishing Group*; 2013.
62. Velkov T, Roberts KD, Nation RL, Thompson PE, Li J. Pharmacology of polymyxins: new insights into an ‘old’ class of antibiotics. *Future Microbiology*. 2013;8(6):711-24.
63. Deris ZZ, Akter J, Sivanesan S, Roberts KD, Thompson PE, Nation RL, et al. A secondary mode of action of polymyxins against Gram-negative bacteria involves the inhibition of NADH-quinone oxidoreductase activity. *The Journal of Antibiotics*. 2014;67(2):147.
64. Falagas ME, Kasiakou SK, Saravolatz LD. Colistin: the revival of polymyxins for the management of multidrug-resistant gram-negative bacterial infections. *Clinical Infectious Diseases*. 2005;40(9):1333-41.
65. Wang R, Dorp L, Shaw LP, Bradley P, Wang Q, Wang X, et al. The global distribution and spread of the mobilized colistin resistance gene *mcr-1*. *Nature Communications*. 2018;9(1):1179.
66. Olaitan AO, Morand S, Rolain J-M. Mechanisms of polymyxin resistance: acquired and intrinsic resistance in bacteria. *Frontiers in Microbiology*. 2014;5:643.
67. Kluytmans J. Plasmid-encoded colistin resistance: *mcr*-one, two, three and counting. *Eurosurveillance*. 2017;22(31).
68. Napier BA, Burd EM, Satola SW, Cagle SM, Ray SM, McGann P, et al. Clinical use of colistin induces cross-resistance to host antimicrobials in *Acinetobacter baumannii*. *mBio*. 2013;4(3):e00021-13.

69. Pránting M, Andersson DI. Mechanisms and physiological effects of protamine resistance in *Salmonella enterica* serovar Typhimurium LT2. *Journal of Antimicrobial Chemotherapy*. 2010;65(5):876-87.
70. Hashemi MM, Rovig J, Weber S, Hilton B, Forouzan MM, Savage PB. Susceptibility of colistin-resistant, Gram-negative bacteria to antimicrobial peptides and ceragenins. *Antimicrobial Agents and Chemotherapy*. 2017;61(8):e00292-17.
71. Bechinger B, Lohner K. Detergent-like actions of linear amphipathic cationic antimicrobial peptides. *Biochimica et Biophysica Acta (BBA)-Biomembranes*. 2006;1758(9):1529-39.
72. Bechinger B, Gorr S-U. Antimicrobial peptides: Mechanisms of action and resistance. *Journal of Dental Research*. 2017;96(3):254-60.
73. Lai Y, Gallo RL. AMPed up immunity: how antimicrobial peptides have multiple roles in immune defense. *Trends in Immunology*. 2009;30(3):131-41.
74. Trimble MJ, Mlynářčík P, Kolář M, Hancock RE. Polymyxin: alternative mechanisms of action and resistance. *Cold Spring Harbor Perspectives in Medicine*. 2016;6(10):a025288.
75. MacGregor RR, Graziani AL. Oral administration of antibiotics: a rational alternative to the parenteral route. *Clinical Infectious Diseases*. 1997;24(3):457-67.
76. McMullan BJ, Andresen D, Blyth CC, Avent ML, Bowen AC, Britton PN, et al. Antibiotic duration and timing of the switch from intravenous to oral route for bacterial infections in children: systematic review and guidelines. *The Lancet Infectious Diseases*. 2016;16(8):e139-e52.
77. Falagas ME, Kasiakou SK. Toxicity of polymyxins: a systematic review of the evidence from old and recent studies. *Critical Care*. 2006;10(1):R27.
78. Kaewpoowat Q, Ostrosky-Zeichner L. Tigecycline: a critical safety review. *Expert Opinion on Drug Safety*. 2015;14(2):335-42.
79. Prayle A, Watson A, Fortnum H, Smyth A. Side effects of aminoglycosides on the kidney, ear and balance in cystic fibrosis. *Thorax*. 2010;65(7):654-8.
80. Grill MF, Maganti RK. Neurotoxic effects associated with antibiotic use: management considerations. *British Journal of Clinical Pharmacology*. 2011;72(3):381-93.
81. Blanca M, Romano A, Torres M, Fernandez J, Mayorga C, Rodriguez J, et al. Update on the evaluation of hypersensitivity reactions to betalactams. *Allergy*. 2009;64(2):183-93.
82. Paterson DL. "Collateral damage" from cephalosporin or quinolone antibiotic therapy. *Clinical Infectious Diseases*. 2004;38(Supplement 4):S341-S5.
83. Hauser AR, Mecsas J, Moir DT. Beyond antibiotics: new therapeutic approaches for bacterial infections. *Clinical Infectious Diseases*. 2016;63(1):89-95.
84. Stanton TB. A call for antibiotic alternatives research. *Trends in Microbiology*. 2013;21(3):111-3.
85. Huh AJ, Kwon YJ. "Nanoantibiotics": a new paradigm for treating infectious diseases using nanomaterials in the antibiotics resistant era. *Journal of Controlled Release*. 2011;156(2):128-45.
86. Shen S, Wu Y, Liu Y, Wu D. High drug-loading nanomedicines: progress, current status, and prospects. *International Journal of Nanomedicine*. 2017;12:4085-109.
87. Zazo H, Colino CI, Lanao JM. Current applications of nanoparticles in infectious diseases. *Journal of Controlled Release*. 2016;224:86-102.
88. Wenzler E, Fraidenburg DR, Scardina T, Danziger LH. Inhaled antibiotics for Gram-negative respiratory infections. *Clinical Microbiology Reviews*. 2016;29(3):581-632.
89. Yang W, Peters JI, Williams III RO. Inhaled nanoparticles—a current review. *International Journal of Pharmaceutics*. 2008;356(1-2):239-47.
90. Patton JS, Byron PR. Inhaling medicines: delivering drugs to the body through the lungs. *Nature Reviews Drug Discovery*. 2007;6(1):67.
91. Sung JC, Pulliam BL, Edwards DA. Nanoparticles for drug delivery to the lungs. *Trends in Biotechnology*. 2007;25(12):563-70.
92. Bailey MM, Berkland CJ. Nanoparticle formulations in pulmonary drug delivery. *Medicinal Research Reviews*. 2009;29(1):196-212.

93. Yang W, Peters JI, Williams RO. Inhaled nanoparticles—a current review. *International Journal of Pharmaceutics*. 2008;356(1):239-47.
94. Patton JS, Byron PR. Inhaling medicines: delivering drugs to the body through the lungs. *Nature Reviews Drug Discovery*. 2007;6(1):67-74.
95. Ritsema JA, van der Weide H, Te Welscher YM, Goessens WH, Van Nostrum CF, Storm G, et al. Antibiotic-nanomedicines: facing the challenge of effective treatment of antibiotic-resistant respiratory tract infections. *Future Microbiology*. 2018;13(15):1683-92.

Abstract

Respiratory tract infections are one of the most frequent infections worldwide, with an increasing number being associated with (multiple) antibiotic-resistant pathogens. Improved treatment requires the development of new therapeutic strategies, including the possible development of antibiotic-nanomedicines. Antibiotic-nanomedicines comprise antibiotic molecules coupled to nanocarriers via surface adsorption, surface attachment, entrapment or conjugation, and can be administered via aerosolization. The efficacy and tolerability of this approach has been shown in clinical studies, with amikacin liposome inhalation suspension being the first inhalatory antibiotic-nanomedicine approved by the United States Food and Drug Administration (FDA). In this special report, we summarize and discuss the potential value and the clinical status of antibiotic-nanomedicines for the treatment of (antibiotic-resistant) respiratory tract infections.



Chapter

2

ANTIBIOTIC-NANOMEDICINES: FACING THE CHALLENGE OF EFFECTIVE TREATMENT OF ANTIBIOTIC-RESISTANT RESPIRATORY TRACT INFECTIONS

*Jeffrey A.S. Ritsema, Hessel van der Weide,
Yvonne M. te Welscher, Wil H.F. Goessens, Cornelus F. van Nostrum,
Gert Storm, Irma A.J.M. Bakker-Woudenberg, John P. Hays*

Respiratory tract infections (RTIs) present a significant burden on global healthcare and have been estimated as the underlying cause of 6% of disability-adjusted life years in 2015¹. In primary care, many RTIs are often self-limiting viral infections and are usually not fatal unless a secondary bacterial infection occurs^{2,3}. However, in secondary and tertiary care, bacterial RTIs predominate over viral infections, with bacterial infections being much more likely to lead to significant morbidity and/or mortality in affected patients⁴. The effective antimicrobial treatment of bacterial infections is a crucial component in reducing the disease burden of RTIs and may be a life-saving action in many cases⁵. However, pathogenic bacteria continue to demonstrate their ability to adapt to many different types of antimicrobial compounds. As a result, global antibiotic resistance continues to increase, while the pool of effective antimicrobial compounds is simultaneously drying up. There are several reasons why the current research and development (R&D) portfolios of pharmaceutical companies are insufficient. Importantly, antibiotic discovery is not sufficiently successful as compared to developing drugs for other disease areas. The consequence is that relatively few new candidate antibiotics have reached the market^{6,7}. Global authorities such as the European Union (EU) and the United Nations (UN) as well as the World Health Organization (WHO) are aware of this problem and invest in trying to solve the worldwide endemic of antibiotic resistance by focusing on several key 'One Health' action areas⁸⁻¹⁰. These key areas include increased epidemiological reporting of antibiotic resistance, the implementation of guidelines for effective infection prevention policies, reducing the use of antibiotics as growth promoters in food animals, the development of novel rapid diagnostics, and the development of new antibiotics which are active against extensively resistant microorganisms.

Novel antimicrobial compounds

Most currently available antimicrobial compounds were initially discovered by screening microorganisms (usually fungi) for naturally produced antimicrobial compounds e.g. penicillins, macrolides, tetracyclines and aminoglycosides^{7,11}. Additionally, synthetic

chemistry approaches have been utilized to generate new types of antibiotics, for example the carbapenems. However, both of these approaches have failed to generate any new classes of antibiotics in recent years¹². As of September 2018, only one novel class of antibiotics has entered clinical development, namely gepotidacin for the treatment of RTIs¹³. Further, two known, but undervalued, classes of antibiotics that have previously seen little therapeutic application are also being developed for the treatment of RTIs; namely antimicrobial peptides and pleuromutilins^{14,15}. It is the discovery and development of these new/undervalued classes of antibiotics (rather than the continual adaptation of already existing classes of antibiotics) which is most likely to be successful in the worldwide fight against antibiotic resistant bacterial pathogens.

New treatment strategies

The treatment of RTIs in primary care occurs via the prescription of a course of oral antibiotics, whereas in secondary and tertiary care, more powerful antibiotics are usually prescribed and administered via the intravenous route^{16,17}. However, although the parenteral (intravenous) application of antibiotics allows for high systemic bioavailability, this route of administration may not always achieve the necessary minimum inhibitory antibiotic concentration at the site of infection. Furthermore, the systemic application of antibiotics can cause unwanted toxic side-effects due to the antibiotic reaching tissues other than the infected¹⁸⁻²¹. Another serious side-effect of systemic antibiotics is the enhanced selection of antibiotic-resistant bacteria residing in the endogenous microbiota, so-called collateral damage²². Such resistant subpopulations, selected from the endogenous microbiota, may cause invasive infections which prove very hard to treat in critically ill patients. Therefore, in addition to the development of novel antibiotics, new treatment strategies are also being investigated including the administration of β -lactams combined with β -lactamase inhibitors, bacteriophage-based treatment, and the synthesis of hybrid antibiotics²³⁻²⁶. Another promising approach is the use of antibiotic-nanomedicines, as outlined in this Special Report.

Role of aerosolized antibiotics

To effectively treat a patient suffering from an infection, it is important to deliver antibiotic molecules to the actual site of the infection such that the minimum inhibitory concentration (MIC) is achieved while causing minimal side-effects and collateral damage to the patient's own microbiota. For RTIs, the site of infection is the lung and over the last decade there has been an increasing interest to exploit pulmonary delivery of antibiotics²⁷. The accurate delivery of antibiotics directly to the pulmonary site of infection would allow the antibiotics to reach higher local concentrations, thereby increasing their effective antimicrobial activity^{27,28}. This local delivery approach also avoids 'first-pass' metabolism and may help reduce any toxic side-effects associated with systemic administration^{29,30}. However, although antibiotics have been non-invasively administered to patients via aerosols – in solid or liquid particles ranging in size from 0.01–100 microns in diameter – the majority of aerosolized antibiotics often show suboptimal therapeutic efficacy due to their short lung half-life and low therapeutic availability at the intrapulmonary site of infection³¹. The short half-life and too limited therapeutic activity of aerosolized antibiotics is primarily due to mucociliary-related pulmonary clearance mechanisms present in the host³². Exogenous particles and chemicals are typically trapped within the mucus layer in the lungs with cilia facilitating coordinated movement of these particles to the pharynx, where these are coughed out or swallowed. Deposited particles are also susceptible to alveolar macrophage clearance, as alveolar macrophages engulf, transport and thereby clear particles from the alveolar epithelium. The large surface area, epithelial permeability and high vascularization of the lung also facilitate the rapid absorption of antibiotics into the bloodstream (away from the lung) via passive diffusion or passage through tight junctions³². Additionally, many antibiotics possess hydrolytically susceptible chemical bonds (e.g., esters and amides), causing degradation (and subsequent loss of biological activity) via enzymes secreted by the lung.

Nanocarrier formulations

The protection of antibiotics from clearance, enzymatic/chemical degradation and rapid adsorption, as well as the reliable deposition and residence of aerosolized drug doses at predetermined locations in the lung, can prove challenging³³⁻³⁵. Incorporation of antibiotics in so-called ‘nanocarriers’ can potentially overcome these hurdles. In this respect, many different nanocarrier formulations have been developed for antibiotic encapsulation or coupling.

Nanocarriers are particles ranging in size from 10–1000 nm³⁶ and are used in a wide variety of medicines, where the active pharmaceutical ingredient is either adsorbed, covalently attached to the surface, entrapped or conjugated into the matrix of the nanocarrier (Figure 1)³⁷. Nanocarriers may in general be classified based on the type of material from which the matrix is made i.e., organic nanocarriers or inorganic nanocarriers.

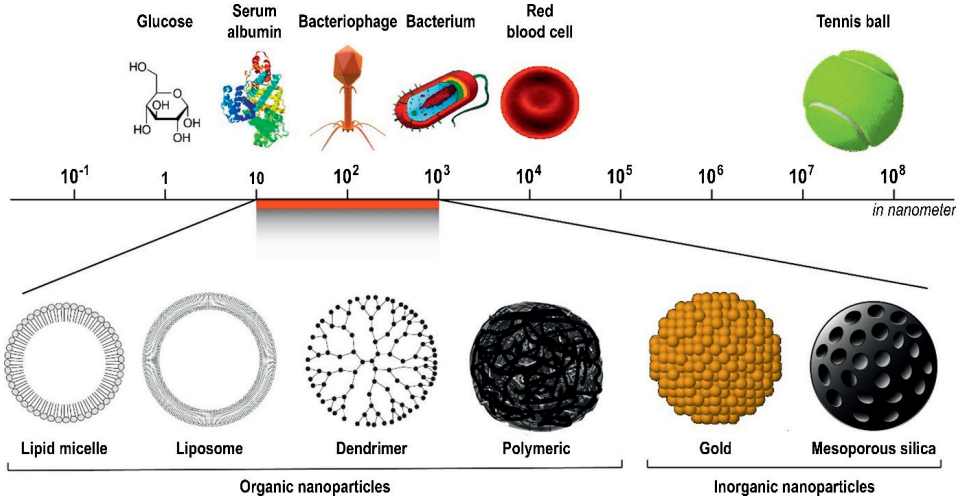


Figure 1. Pictorial representation of different types of nanoparticles and their size in comparison to various biological and physical objects. Nanocarriers can be classified into two essential groups: Organic nanoparticles (e.g. lipid micelles, liposomes, dendrimers, polymeric nanoparticles) and inorganic nanoparticles (e.g. gold and mesoporous silica nanoparticles as examples).

Organic nanocarriers, especially liposomes³⁷, are the most widely studied nanoparticulate delivery systems³⁸. Liposomes are self-assembling spherical nanostructures consisting of one or more lipid bilayers, formed via the intrinsic interfacial properties imparted by the constituent phospholipids. Other widely studied organic drug delivery systems include polymeric nanocarriers, which can be highly stable due to their high structural integrity afforded by the rigidity of the polymer matrix. Poly(lactic-*co*-glycolic acid) (PLGA), chitosan, dextran, alginates, polyvinyl alcohol (PVA), and polyethylene glycol (PEG) are examples of components of polymeric nanocarriers that are currently being extensively studied as drug delivery systems, owing to their minimal toxicity, biodegradability and biocompatibility³⁹. In recent years, other nanocarrier-based drug delivery systems have also been described, including polymeric or lipid micelles, solid-lipid nanoparticles, dendrimers, polymersomes, nanogels, et cetera⁴⁰.

Focusing on RTIs and nanomedicine delivery to the lung, a wide variety of nanocarriers could potentially be utilized⁴¹. The aerodynamic diameter, shape and surface properties of the aerosol are the primary factors, with the architecture of the respiratory tract and biological clearance mechanisms as key determinants of lung deposition pattern and retention of aerosols. For instance, when targeting the lower airways, aerosols with an aerodynamic diameter of 1–5 μm are believed to deposit there most efficiently⁴². In practice, this means that micron-sized powder of agglomerated particles or liquid dispersions are currently mainly used for the pulmonary delivery of nanomedicines^{43,44}.

Advantages of pulmonary administration of antibiotic-nanomedicines

For RTI, aerogenic administration of antibiotic-nanomedicines possess several advantages over free inhaled antibiotics^{32,45-48}.

Increased target localization and efficacy at lower drug dose

To improve lung bioavailability, Pandey *et al.* administered poly(DL-lactide-*co*-glycolide) (PLG) nanoparticles containing rifampicin, isoniazid and pyrazinamide via the

pulmonary route to *Mycobacterium tuberculosis*-infected guinea pigs⁴⁹. The inhaled nanomedicines (as an aerosol) exhibited increased lung retention at therapeutic levels and improved dosage schedule (i.e. reduced dosing frequency as an aerosol) compared with the free drug given via oral or intravenous route. After a single nebulization of drug-loaded PLG nanoparticles, all three antibiotics were detected at therapeutic drug levels up to 11 days in lung homogenates, while oral or aerosol-administered free antibiotic at the same dose were not detectable after 24 hours. Complete killing of *M. tuberculosis* in the lungs of infected guinea pigs was realized after nebulization of 5 doses of drug-loaded PLG nanoparticles at 10-day intervals, whereas 46 similar daily doses of orally administered drugs were required in order to provide similar therapeutic efficacy⁴⁹.

Protection against enzymatic/chemical degradation or unwanted interactions with other molecules

Nanocarriers can physically protect sensitive molecules from rapid degradation and reduce unwanted interactions with non-relevant host biomolecules. For example, nano-sized drug delivery systems can be coated with PEG resulting in decreased uptake and degradation by cells of the mononuclear phagocyte system – a strategy to increase the blood circulation time after intravenous administration⁵⁰⁻⁵².

Nacucchio *et al.* showed that encapsulation of the β -lactam antibiotic piperacillin by phosphatidylcholine-cholesterol (PC:Chol) liposomes protected the drug from hydrolysis by Staphylococcal β -lactamase. This resulted in enhanced antibacterial activity of liposomal piperacillin against Staphylococcal growth in biofilms in the presence of exogenous β -lactamase⁵³. Meers *et al.* showed that encapsulation of amikacin in dipalmitoylphosphatidylcholine-cholesterol (DPPC:Chol) liposomes is beneficial in the treatment of chronic *Pseudomonas aeruginosa* biofilm infections via improvement of biofilm access and/or reducing undesirable interactions with biofilm matrix components. Measurement of amikacin release and efficacy in the rat lung, as measured by fluorescence polarization immunoassay and viable bacterial count, showed that inhaled liposomal amikacin was released in a slow, sustained mode in normal rat

lungs and was superior in antimicrobial activity compared to inhaled free amikacin in infected lungs in a 14 day *P. aeruginosa* infection model. Further, the use of a filter assay and epifluorescence / confocal scanning laser microscopy showed that fluorescently labeled DPPC:Chol liposomes could significantly penetrate the *P. aeruginosa* biofilm⁵⁴. Magabe *et al.* compared the antibacterial activity of liposomal gentamicin versus free gentamicin against gentamicin-resistant strains of *P. aeruginosa*⁵⁵. Gentamicin encapsulated in DPPC:Chol, 1,2-dimyristoyl-*sn*-glycero-3-phosphocholine-cholesterol (DMPC:Chol), or dipalmitoylphosphatidylcholine-cholesterol (DSPC:Chol) liposomes exhibited a higher antimicrobial activity compared to free gentamicin. This effect was attributed to either enhanced diffusion of the liposome-encapsulated antibiotic across the bacterial cell envelope and/or to protection of the antibiotic from enzymatic degradation as a result of liposomal encapsulation.

Protection from pulmonary clearance mechanisms

The inclusion of mucoadhesives (e.g. cationic groups) via surface modification of nanocarriers has been suggested to improve the pulmonary delivery of drugs via an increased lung retention time. In the case of chitosan-modified PLGA nanospheres (approximately 650 nm) loaded with elcatonin (an anti-parathyroid agent), the elimination rate constant was approximately one-third compared to that of unmodified chitosan nanospheres, resulting in enhanced and prolonged pharmacological action compared to unmodified chitosan nanospheres⁵⁶.

Other studies have suggested that the retention of particles that adhere to airway mucus is limited due to mucus clearance mechanisms and that nanocarriers that do not adhere, or rapidly penetrate the mucus, allow uniform and long-lasting drug delivery to the airways following inhalation. Schneider *et al.* demonstrated in *in vitro* experiments that particles as large as 200 nm are able to rapidly penetrate the respiratory mucus of patients with cystic fibrosis (CF) if the particles are densely coated with PEG. On the other hand, mucoadhesive particles were unable to rapidly penetrate respiratory mucus regardless of the particle size⁵⁷. When tested *in vivo*, the mucoadhesive particles were more rapidly eliminated from the lumen of the lung of mice, while the penetrating

nanocarriers were uniformly distributed throughout the mucus layer and exhibited improved retention time. This resulted in improved therapeutic efficacy compared to both carrier-free drug or a drug delivered via a mucoadhesive nanocarrier system.

Enhanced internalization by target cells

In the context of the treatment of intracellular infections, one major challenge is the difficulty of antibiotic access to the protective environment within cells. For example, *Mycobacteria* spp. latently reside in the phagocytic intracellular compartments of macrophages. Kisich *et al.* investigated the effects of moxifloxacin encapsulated in poly(butylcyanoacrylate) (PBCA) nanoparticles against *M. tuberculosis* residing in macrophages⁵⁸. Drug-loaded PBCA nanoparticles showed increased antibacterial activity via 10-fold reduction of the MIC. In macrophages exposed to moxifloxacin PBCA nanoparticles, the intracellular accumulation of moxifloxacin was increased three-fold compared to exposure to free drug. Also, the intracellular retention time of moxifloxacin increased from 4 hours to 24 hours.

Controlled antibiotic release

The use of different types of antibiotic-nanomedicines can enable the controlled release of antibiotics into the lung. For example, antibiotic-nanomedicines may allow the triggered release of an antibiotic at low pH conditions, such as is found in the inflamed lung environment, or may be positively charged to improve their affinity for negatively charged bacterial surfaces and biofilms at the site of infection^{59,60}. Additionally, antibiotics with time-dependent activity may benefit from the use of sustained-release nanomedicines⁶¹, resulting in optimal antimicrobial activity over time, while minimizing the chance of unwanted side-effects due to uncontrolled and massive release of antibiotic within a short period of time.

Finally, the inhalation of insoluble non-degradable or slowly-degradable particles may lead to serious inflammatory responses and oxidative stress, resulting in irritation, cellular injury, edema, phagocytosis impairment, and breakdown by host defense mechanisms^{34,35}. However, the toxicity of nanoparticles is mainly determined by the materials that they are composed of and their surface characteristics. Therefore,

extensive *in vitro* and *in vivo* testing is performed as part of the development process of nanoparticle-based drug-carrier systems. This means that the materials and inhalation strategies established for a particular antibiotic nanomedicine formulation are carefully selected (e.g. the use of biodegradable or biocompatible materials), in order to minimize the possibility of adverse reactions when inhaled by patients.

Clinical status

The use of nanocarriers and the potential value of direct delivery of aerosolized nanocarrier-bound antibiotics to the lung has been shown in patients with inhaled liposomal formulations of ciprofloxacin (Lipoquin™) and a mixed formulation of non-encapsulated and liposomal ciprofloxacin (Pulmaquin™). These formulations have been evaluated in Phase III clinical trials in CF patients and non-CF patients with RTIs.

Initially, two Phase IIA clinical trials of liposomal ciprofloxacin formulations demonstrated that two-week and four-week once-daily administration of Lipoquin™ in CF patients and non-CF bronchiectasis patients was safe and capable of reducing the *P. aeruginosa* bacterial load in sputum⁶². Although the results obtained using Lipoquin™ were encouraging, extra experiments using Pulmaquin™ were performed in order to determine if additional clinical benefit might be gained using a rapid antibiotic release (peak concentration) strategy when compared to using free antibiotic. In Phase I studies, Pulmaquin™ showed significantly higher maximum plasma concentrations of ciprofloxacin when compared to Lipoquin™ due to the presence the non-encapsulated antibiotic in the Pulmaquin™ formulation. The ciprofloxacin concentrations in plasma over time were more than two-fold lower following administration of Pulmaquin™ or Lipoquin™ compared to plasma levels of approved doses of oral or intravenous ciprofloxacin. This suggested that after administration of liposomal ciprofloxacin the potential risk of systemic side-effects, even upon repeated dosing with such ciprofloxacin-nanoparticles, was significantly reduced. In Phase IIb clinical trials, named ORBIT-1 and ORBIT-2 (directed against non-CF bronchiectasis patients suffering from *P. aeruginosa* infection), both Lipoquin™ and Pulmaquin™ were

investigated for their ability to provide the optimum dose of ciprofloxacin with minimal side-effect. Pulmaquin showed superior pulmonary safety profile with rapid and persistent reduction of bacterial load in sputum.

Based on these results, Pulmaquin™ was selected and evaluated by Aradigm Corporation in a Phase III clinical trial in non-CF bronchiectasis patients (ARD-3150-1201), ORBIT-3 (NCT01515007) and ORBIT-4 (NCT02104245), which was followed by a 28-day open label extension study⁶³. The Aradigm Corporation announced that analyses of combined data from both studies demonstrated a statistically significant reduction in *P. aeruginosa* load in the lungs at the end of the first on-treatment period. There was also a statistically significant reduction (27%) in pulmonary exacerbation over a 48-week double-blind treatment period between the Pulmaquin™ group and the placebo group. The median time to first moderate or severe pulmonary exacerbations – those exacerbations that require interventions with antibiotics or hospitalization – were statistically improved in the Pulmaquin™ treated group (198 days) versus placebo group (302 days). Additionally, Pulmaquin™ was safe and well tolerated in both studies. Therefore, in the first quarter of 2018, Aradigm Corporation submitted a marketing authorization request to the European Medicines Agency (EMA) for Linhaliq™ (formerly Pulmaquin™) as a treatment for non-CF bronchiectasis patients with a chronic *P. aeruginosa* lung infection.

Another antibiotic-nanomedicine i.e. liposomal amikacin has been studied in Phase II clinical trials (NCT00558844, NCT00777296, NCT01315236) comparing inhalatory liposomal Amikacin (Arikayce™/Arikace™/ALIST™) to placebo in once-daily and multidrug regimens. In CF patients with *P. aeruginosa* infection, once-daily, Arikayce™ was shown to improve lung function and improve patient-reported respiratory clinical symptoms over a 28 day period of treatment⁶⁴. Additionally, a statistically significant reduction in *P. aeruginosa* density in sputum (>1 log) was observed compared to baseline measurements. In patients with antibiotic-resistant nontuberculous mycobacteria (NTM) infections, negative bacterial cultures were obtained by day 84 in 11/45 patients, whereas this was achieved in 3/45 patients receiving standard treatment⁶⁵. Inmed Inc. also completed a European and Canadian registrational Phase III studies of Arikayce™

in CF patients – the CLEAR-108 (NCT01315678) and CLEAR-110 (NCT01316276) projects⁶⁶. Overall, once daily Arikayce™ was non-inferior to inhalation treatment with tobramycin solution when taken twice daily in patients with CF and chronic bronchopulmonary *P. aeruginosa* infections. Furthermore, inhaled Arikayce™ was generally safe and well tolerated. Insmed Inc. also investigated Amikacin Liposome Inhalation Suspension (ALISTM) in a Phase 3 clinical trial (INS-312, NCT02628600), which was established to investigate the treatment of adult patients with refractory NTM infections caused by *Mycobacterium avium* complex (MAC)⁶⁷. The study demonstrated that ALISTM when added to guideline-based therapy, eliminated the infection in 29% of patients, compared to 9% of patients treated using guideline-based therapy. Based on these results, in the first quarter of 2018, Insmed Inc. announced United States Food and Drug Administration (FDA) acceptance for a New Drug Application (NDA) for ALISTM for treating NTM lung infections caused by MAC. The FDA granted accelerated approval on the fourth quarter for the amikacin liposomes inhalation suspension (Arikayce™/ALISTM) for the treatment of lung disease caused by MAC in adult patients, left with a few or no treatment options⁶⁸.

The EMA (EU) and FDA (USA) have also granted the orphan drug designation fusogenic liposomes loaded with tobramycin (Tobramycin Fluidosomes™, Axentis Pharma), for CF patient-associated RTIs^{69,70}. Although the results of clinical trials using Fluidosomes™ are not available, *in vitro* studies have described the antimicrobial activity of the Fluidosomes™ versus free tobramycin using biofilm infection models of *P. aeruginosa*, *Stenotrophomonas maltophilia* and *Burkholderia cepacia*. These studies showed an increased antimicrobial effect (>17-50x) of Fluidosomes™ compared to free tobramycin in all biofilm models tested^{71,72}. Also *in vivo* studies using Fluidosomes™ have shown increased bactericidal activity against infections caused by antibiotic-susceptible or resistant *P. aeruginosa* strains^{73,74}.

Conclusions and future perspectives

The worrying failure of conventional antibiotics in the treatment of infected patients is attributable to the worldwide emergence of antibiotic-resistant bacteria, and therefore the development and testing of new or undervalued antibiotics, or new antibiotic treatment modalities is urgently needed. Furthermore, toxic side-effects associated with prolonged oral and parenteral delivery of high dose antibiotics to patients, and a lack of a targeting mechanism to guide antibiotics to the focus of infection, may lead to treatment with sub-therapeutic levels of antibiotic and therefore inadequate killing of the infectious pathogens. The current lack of novel effective antibiotics, implies that the development of efficient delivery modalities, such as the use of inhaled, customized antibiotic-nanomedicines containing existing and/or novel antibiotics, could result in improved treatment of pulmonary infections. In this respect, the sheer variety and versatility of nanocarriers available provide many opportunities for the development of antibiotic-nanomedicines, including the possibility of targeting the antibiotics to both extracellular and intracellular pathogens in infected tissues, or to pathogens embedded within protective niches of the lung, within sputum or within pulmonary biofilms. That said, only one antibiotic-nanomedicine has entered the market as of this time, mainly due to several hurdles limiting their implementation. Some of these hurdles include factors relating to manufacturing processes (scaling-up production, good manufacturing practice etc.), the unique environment of the lung (e.g. overcoming host defense mechanisms) and the different delivery needs in case of treatment of acute versus chronic infections (creation of rapid versus slow antibiotic release profiles, respectively). At a time when existing antibiotics are becoming ineffective and few new antibiotics are in the developmental pipeline, the potential advantages (i.e. reduction of patient morbidity and mortality) that could be gained by using antibiotic-nanomedicine therapies should be seriously valued.

Executive Summary

Respiratory tract infections (RTIs) and antibiotic treatment

- Increasing worldwide antibiotic resistance means that the successful treatment of RTIs is often challenging.
- One major critical factor involved in promoting the spread of antibiotic resistance is sub-optimal antibiotic dosing and inferior pharmacokinetic profiles (associated with antibiotic administration via oral and parenteral routes).
- Antibiotic therapy may also be associated with host tissue toxicity and damage to the host's protective microbiota.

New strategies to provide effective treatment against bacterial RTIs

- Novel antimicrobial compounds could be utilized to treat antibiotic-resistant RTIs, but there is currently a lack of novel antibiotics available for clinical use.
- The effective administration of antibiotics to the site of infection in patients with RTIs could be facilitated by the local delivery of (existing and/or novel) antibiotics via antibiotics incorporated in nanocarriers (antibiotic-nanomedicines).
- Antibiotic-nanomedicines could be optimized for targeted deposition of (mixtures of) antibiotics at the infection focus in RTIs, thereby increasing the efficacy of antibiotic therapy.

Increased efficacy associated with the use of antibiotic-nanomedicines for bacterial RTIs

- Antibiotic-nanomedicines can increase the antibiotic concentration at the site of infection and therefore can help to reduce the emergence of antibiotic resistance.
- Toxic side-effects and collateral damage by antibiotics to the host's bacterial flora can also be minimized.
- Custom antibiotic-nanomedicines for tailored antibiotic release kinetics can be developed.
- Protection of the antibiotic from host-related pulmonary clearance mechanisms, enzymatic/chemical degradation or detrimental interactions with host biomolecules.

The potential value of direct delivery of aerosolized antibiotic-nanomedicines to the lung has been shown in patients

- Inhaled liposomal formulations of ciprofloxacin (Lipoquin™ and Pulmaquin™/Linhaliq™) and amikacin (Arikayce™/Arikace/Alis™) have been evaluated for their effectiveness and safety in Phase III clinical trials.
- The FDA granted accelerated approval for the amikacin liposomes inhalation suspension (Arikayce™) for the treatment of lung disease caused by *Mycobacterium avium* complex in adult patients, left with a few or no treatment options.

Conclusions

- The development and testing of antibiotic-nanomedicines for the targeted delivery of antibiotics has the potential to be a powerful tool for the treatment of (antibiotic-resistant) bacterial RTIs.
- Antibiotic-nanomedicines can address critical challenges associated with conventional antibacterial therapies and administration routes.
- A better mechanistic understanding of the complex delivery pathways of inhaled antibiotic-nanomedicines is required in order to be able to further improve lung deposition and maximize therapeutic efficacy.

Funding

Erasmus University Medical Center Rotterdam (Erasmus MC) and Utrecht University received funding from the European Union's Seventh Programme for Research, Technological Development and Demonstration under grant agreement No. 604434 PneumoNP. In addition, Utrecht University was supported by the European Union's Seventh Framework Programme for Research, Technological Development and Demonstration under grant agreement No. 604237 NAREB.

Competing interests

The authors have no other relevant affiliations or financial involvement with any organization or entity with a financial interest in or financial conflict with the subject matter or materials discussed in the manuscript apart from those disclosed. No writing assistance was utilized in the production of this manuscript.

References

1. Global Health Estimates 2015: Burden of disease by Cause, Age, Sex, by Country and by Region, 2000-2015. [press release]. 2016.
2. Vos T, Barber RM, Bell B, Bertozzi-Villa A, Biryukov S, Bolliger I, et al. Global, regional, and national incidence, prevalence, and years lived with disability for 301 acute and chronic diseases and injuries in 188 countries, 1990-2013: a systematic analysis for the Global Burden of Disease Study 2013. *The Lancet*. 2015;386(9995):743.
3. Fahey T, Stocks N, Thomas T. Systematic review of the treatment of upper respiratory tract infection. *Archives of Disease in Childhood*. 1998;79(3):225-30.
4. McCullers JA. Insights into the interaction between influenza virus and pneumococcus. *Clinical Microbiology Reviews*. 2006;19(3):571-82.
5. Md PFW, Md KBK, Md JFM. When to consider the use of antibiotics in the treatment of 2009 H1N1 influenza-associated pneumonia. *The New England Journal of Medicine*. 2009;361(24):e112.
6. Davies J, Davies D. Origins and evolution of antibiotic resistance. *Microbiology and Molecular Biology Reviews*. 2010;74(3):417-33.
7. Lewis K. Antibiotics: Recover the lost art of drug discovery. *Nature*. 2012;485(7399):439-40.
8. Council of the European Union. Council conclusions on the impact of antimicrobial resistance in the human health sector and in the veterinary sector – a “One Health” perspective. C 211/2 2012 [
9. United Nations. Draft political declaration of the high-level meeting of the General Assembly on antimicrobial resistance. 16-16108(E) 2016 [
10. Shallcross LJ, Davies SC. The World Health Assembly resolution on antimicrobial resistance. *Journal of Antimicrobial Chemotherapy*. 2014;69(11):2883-5.
11. Aminov RI. A brief history of the antibiotic era: lessons learned and challenges for the future. *Frontiers in Microbiology*. 2010;1.

12. Lewis K. Platforms for antibiotic discovery. *Nature Reviews Drug Discovery*. 2013;12(5):371-87.
13. Pew Charitable Trusts. Antibiotics Currently in Global Clinical Development 2018. Available from: <https://www.pewtrusts.org/es/research-and-analysis/data-visualizations/2014/antibiotics-currently-in-clinical-development>.
14. Gordon YJ, Romanowski EG, McDermott AM. A review of antimicrobial peptides and their therapeutic potential as anti-infective drugs. *Current Eye Research*. 2005;30(7):505-15.
15. Novak R, Shlaes DM. The pleuromutilin antibiotics: a new class for human use. *Current Opinion in Investigational Drugs*. 2010;11(2):182-91.
16. MacGregor RR, Graziani AL. Oral administration of antibiotics: a rational alternative to the parenteral route. *Clinical Infectious Diseases*. 1997;24(3):457-67.
17. McMullan BJ, Andresen D, Blyth CC, Avent ML, Bowen AC, Britton PN, et al. Antibiotic duration and timing of the switch from intravenous to oral route for bacterial infections in children: systematic review and guidelines. *The Lancet Infectious Diseases*. 2016;16(8):e139-e52.
18. Falagas ME, Kasiakou SK. Toxicity of polymyxins: a systematic review of the evidence from old and recent studies. *Critical Care*. 2006;10(1):R27.
19. Kaewpoowat Q, Ostrosky-Zeichner L. Tigecycline: a critical safety review. *Expert Opinion on Drug Safety*. 2015;14(2):335-42.
20. Prayle A, Watson A, Fortnum H, Smyth A. Side effects of aminoglycosides on the kidney, ear and balance in cystic fibrosis. *Thorax*. 2010;65(7):654-8.
21. Grill MF, Maganti RK. Neurotoxic effects associated with antibiotic use: management considerations. *British Journal of Clinical Pharmacology*. 2011;72(3):381-93.
22. Paterson DL. "Collateral damage" from cephalosporin or quinolone antibiotic therapy. *Clinical Infectious Diseases*. 2004;38(Supplement 4):S341-S5.
23. Parkes AL, Yule IA. Hybrid antibiotics—clinical progress and novel designs. *Expert Opinion on Drug Discovery*. 2016;11(7):665-80.
24. Hanlon GW. Bacteriophages: an appraisal of their role in the treatment of bacterial infections. *International Journal of Antimicrobial Agents*. 2007;30(2):118-28.
25. Drawz SM, Bonomo RA. Three decades of β -lactamase inhibitors. *Clinical Microbiology Reviews*. 2010;23(1):160-201.
26. Zhanel GG, Chung P, Adam H, Zelenitsky S, Denisuik A, Schweizer F, et al. Ceftolozane/tazobactam: a novel cephalosporin/ β -lactamase inhibitor combination with activity against multidrug-resistant gram-negative bacilli. *Drugs*. 2014;74(1):31-51.
27. Yang W, Peters JI, Williams RO. Inhaled nanoparticles—a current review. *International Journal of Pharmaceutics*. 2008;356(1):239-47.
28. Patton JS, Byron PR. Inhaling medicines: delivering drugs to the body through the lungs. *Nature Reviews Drug Discovery*. 2007;6(1):67-74.
29. Sung JC, Pulliam BL, Edwards DA. Nanoparticles for drug delivery to the lungs. *Trends in Biotechnology*. 2007;25(12):563-70.
30. Bailey MM, Berkland CJ. Nanoparticle formulations in pulmonary drug delivery. *Medicinal Research Reviews*. 2009;29(1):196-212.
31. Patton JS, Brain JD, Davies LA, Fiegel J, Gumbleton M, Kim KJ, et al. The particle has landed—characterizing the fate of inhaled pharmaceuticals. *Journal of Aerosol Medicine and Pulmonary Drug Delivery*. 2010;23 Suppl 2:S71-87.
32. El-Sherbiny I, Elbaz N, H. Yacoub M. Inhaled nano- and microparticles for drug delivery, 2015.
33. Byron PR. Drug delivery devices: issues in drug development. *Proceedings of the American Thoracic Society*. 2004;1(4):321-8.
34. Abdelaziz HM, Gaber M, Abd-Elwakil MM, Mabrouk MT, Elgohary MM, Kamel NM, et al. Inhalable particulate drug delivery systems for lung cancer therapy: Nanoparticles, microparticles, nanocomposites and nanoaggregates. *Journal of Controlled Release*. 2018;269:374-92.

35. Haque S, Whittaker MR, McIntosh MP, Pouton CW, Kaminskas LM. Disposition and safety of inhaled biodegradable nanomedicines: Opportunities and challenges. *Nanomedicine: Nanotechnology, Biology and Medicine*. 2016;12(6):1703-24.
36. Duncan R, Gaspar R. Nanomedicine(s) under the Microscope. *Molecular Pharmaceutics*. 2011;8(6):2101-41.
37. Shen S, Wu Y, Liu Y, Wu D. High drug-loading nanomedicines: progress, current status, and prospects. *International Journal of Nanomedicine*. 2017;12:4085-109.
38. Lammers T, Kiessling F, Hennink WE, Storm G. Drug targeting to tumors: Principles, pitfalls and (pre-) clinical progress. *Journal of Controlled Release*. 2012;161(2):175-87.
39. Soppimath KS, Aminabhavi TM, Kulkarni AR, Rudzinski WE. Biodegradable polymeric nanoparticles as drug delivery devices. *Journal of Controlled Release*. 2001;70(1):1-20.
40. Bei D, Meng J, Youan BB. Engineering nanomedicines for improved melanoma therapy: progress and promises. *Nanomedicine*. 2010;5(9):1385-99.
41. Mansour HM, Rhee Y-S, Wu X. Nanomedicine in pulmonary delivery. *International Journal of Nanomedicine*. 2009;4:299-319.
42. Heyder J, Gebhart J, Rudolf G, Schiller CF, Stahlhofen W. Deposition of particles in the human respiratory tract in the size range 0.005–15 µm. *Journal of Aerosol Science*. 1986;17(5):811-25.
43. Adam B, Jorrit W, Moritz B-B, Mingshi Y. Nanoembedded Microparticles for Stabilization and Delivery of Drug-Loaded Nanoparticles. *Current Pharmaceutical Design*. 2015;21(40):5829-44.
44. Mangal S, Gao W, Li T, Zhou Q. Pulmonary delivery of nanoparticle chemotherapy for the treatment of lung cancers: challenges and opportunities. *Acta Pharmacologica Sinica*. 2017;38:782.
45. Huh AJ, Kwon YJ. "Nanoantibiotics": a new paradigm for treating infectious diseases using nanomaterials in the antibiotics resistant era. *Journal of Controlled Release : official journal of the Controlled Release Society*. 2011;156(2):128-45.
46. Costa-Gouveia J, Aínsa JA, Brodin P, Lucía A. How can nanoparticles contribute to antituberculous therapy? *Drug Discovery Today*. 2017;22(3):600-7.
47. Moreno-Sastre M, Pastor M, Salomon CJ, Esquisabel A, Pedraz JL. Pulmonary drug delivery: a review on nanocarriers for antibacterial chemotherapy. *The Journal of Antimicrobial Chemotherapy*. 2015;70(11):2945-55.
48. Bobo D, Robinson KJ, Islam J, Thurecht KJ, Corrie SR. Nanoparticle-Based Medicines: A Review of FDA-Approved Materials and Clinical Trials to Date. *Pharmaceutical Research*. 2016;33(10):2373-87.
49. Pandey R, Sharma A, Zahoor A, Sharma S, Khuller GK, Prasad B. Poly (dl-lactide-co-glycolide) nanoparticle-based inhalable sustained drug delivery system for experimental tuberculosis. *Journal of Antimicrobial Chemotherapy*. 2003;52(6):981-6.
50. Shan X, Liu C, Yuan Y, Xu F, Tao X, Sheng Y, et al. In vitro macrophage uptake and in vivo biodistribution of long-circulation nanoparticles with poly(ethylene-glycol)-modified PLA (BAB type) triblock copolymer. *Colloids and Surfaces B, Biointerfaces*. 2009;72(2):303-11.
51. Allen TM, Hansen C. Pharmacokinetics of stealth versus conventional liposomes: effect of dose. *Biochimica et Biophysica Acta (BBA)*. 1991;1068(2):133-41.
52. Bhattarai N, Bhattarai SR, Khil MS, Lee DR, Kim HY. Aqueous solution properties of amphiphilic triblock copolymer poly(p-dioxanone-co-l-lactide)-block-poly(ethylene glycol). *European Polymer Journal*. 2003;39(8):1603-8.
53. Nacucchio MC, Bellora MJ, Sordelli DO, D'Aquino M. Enhanced liposome-mediated activity of piperacillin against staphylococci. *Antimicrobial Agents and Chemotherapy*. 1985;27(1):137-9.
54. Meers P, Neville M, Malinin V, Scotto AW, Sardaryan G, Kurumunda R, et al. Biofilm penetration, triggered release and in vivo activity of inhaled liposomal amikacin in chronic *Pseudomonas aeruginosa* lung infections. *Journal of Antimicrobial Chemotherapy*. 2008;61(4):859-68.
55. Mugabe C, Azghani AO, Omri A. Liposome-mediated gentamicin delivery: development and activity against resistant strains of *Pseudomonas aeruginosa* isolated from cystic fibrosis patients. *Journal of Antimicrobial Chemotherapy*. 2005;55(2):269-71.

56. Yamamoto H, Kuno Y, Sugimoto S, Takeuchi H, Kawashima Y. Surface-modified PLGA nanosphere with chitosan improved pulmonary delivery of calcitonin by mucoadhesion and opening of the intercellular tight junctions. *Journal of Controlled Release : official journal of the Controlled Release Society*. 2005;102(2):373-81.
57. Schneider CS, Xu Q, Boylan NJ, Chisholm J, Tang BC, Schuster BS, et al. Nanoparticles that do not adhere to mucus provide uniform and long-lasting drug delivery to airways following inhalation. *Science Advances*. 2017;3(4).
58. Kisich KO, Gelperina S, Higgins MP, Wilson S, Shipulo E, Oganessian E, et al. Encapsulation of moxifloxacin within poly(butyl cyanoacrylate) nanoparticles enhances efficacy against intracellular *Mycobacterium tuberculosis*. *International Journal of Pharmaceutics*. 2007;345(1-2):154-62.
59. Paliwal SR, Paliwal R, Vyas SP. A review of mechanistic insight and application of pH-sensitive liposomes in drug delivery. *Drug Delivery*. 2015;22(3):231-42.
60. Sercombe L, Veerati T, Moheimani F, Wu SY, Sood AK, Hua S. Advances and challenges of liposome assisted drug delivery. *Frontiers in Pharmacology*. 2015;6.
61. Levison ME, Levison JH. Pharmacokinetics and pharmacodynamics of antibacterial agents. *Infectious Disease Clinics of North America*. 2009;23(4):791-815.
62. Cipolla D, Blanchard J, Gonda I. Development of Liposomal Ciprofloxacin to Treat Lung Infections. *Pharmaceutics*. 2016;8(1):6.
63. Aradigm. Aradigm Announces Top-Line Results from Two Phase 3 Studies Evaluating Pulmaquin for the Chronic Treatment of Non-Cystic Fibrosis Bronchiectasis Patients with Lung Infections with *Pseudomonas aeruginosa* (<https://aradigm.gcs-web.com/news-releases/news-release-details/aradigm-announces-top-line-results-two-phase-3-studies>). 2016.
64. Clancy JP, Dupont L, Konstan MW, Billings J, Fustik S, Goss CH, et al. Phase II studies of nebulised Orikace in CF patients with *Pseudomonas aeruginosa* infection. *Thorax*. 2013;68(9):818-25.
65. Olivier KN, Griffith DE, Eagle G, II JPM, Micioni L, Liu K, et al. Randomized Trial of Liposomal Amikacin for Inhalation in Nontuberculous Mycobacterial Lung Disease. *American Journal of Respiratory and Critical Care Medicine*. 2017;195(6):814-23.
66. Michael Konstan IF, Tacjana Pressler, John Paul Clancy, Dorota Sands, Predrag Minic, Marco Cipolli, Ivanka Galeva, Amparo Solé, Rebecca Monroe, John P. McGinnis II, Gina Eagle, Diana Bilton. Long-Term Study of Liposomal Amikacin for Inhalation in Patients With Cystic Fibrosis and Chronic *Pseudomonas aeruginosa* Infection. 29th Annual North American Cystic Fibrosis Conference (NACFC),; Phoenix, Arizona. 2015.
67. INSMED. Insmmed Announces Additional Data from ALIS (Amikacin Liposome Inhalation Suspension) Phase 3 Clinical Program for Adult Patients with Treatment Refractory NTM Lung Disease Caused by MAC and Reports Progress with Commercial Preparations <http://investor.insmed.com/releasedetail.cfm?releaseid=10532372018>.
68. FDA. FDA approves a new antibacterial drug to treat a serious lung disease using a novel pathway to spur innovation, 2018.
69. AxentisPharmaAG. 2018. Available from: <http://www.axentispharma.com/>.
70. FDA. Cumulative List of all Products that have received Orphan Designation: FDA; 2009 [
71. Beaulac C, Sachelletti S, Lagace J. In Vitro Bactericidal Evaluation of a Low Phase Transition Temperature Liposomal Tobramycin Formulation as a Dry Powder Preparation Against Gram Negative and Gram Positive Bacteria. *Journal of Liposome Research*. 1999;9(3):301-12.
72. Beaulac C, Sachelletti S, Lagace J. In-vitro bactericidal efficacy of sub-MIC concentrations of liposome-encapsulated antibiotic against gram-negative and gram-positive bacteria. *The Journal of Antimicrobial Chemotherapy*. 1998;41(1):35-41.
73. Beaulac C, Clement-Major S, Hawari J, Lagace J. Eradication of mucoid *Pseudomonas aeruginosa* with fluid liposome-encapsulated tobramycin in an animal model of chronic pulmonary infection. *Antimicrobial Agents and Chemotherapy*. 1996;40(3):665-9.

74. Omri A, Beulac C, Bouhajib M, Montplaisir S, Sharkawi M, Lagace J. Pulmonary retention of free and liposome-encapsulated tobramycin after intratracheal administration in uninfected rats and rats infected with *Pseudomonas aeruginosa*. *Antimicrobial Agents and Chemotherapy*. 1994;38(5):1090-5.



Chapter

3

AIMS AND OUTLINE

The main focus of the research presented in this thesis was to develop novel nanomedicines based on new antimicrobial peptides (AMPs), and to investigate their bacterial killing activity against multidrug-resistant Gram-negative bacteria *in vitro* and *in vivo*. *In vivo* experiments included the measurement of therapeutic efficacy when the nanomedicines were administered directly to the lungs of rats in a rat model of multidrug-resistant Gram-negative pneumonia-septicemia. The research described in this thesis was part of the collaborative research project “Nanotherapeutics to treat bacterial infectious diseases” (PneumoNP) which was financially supported by the European Union’s Seventh Programme for Research, Technological Development and Demonstration under grant agreement No. 604434 PneumoNP.

The aim of the **PneumoNP project** was to develop a theragnostic system for the treatment of multidrug-resistant Gram-negative bacterial infections of the lung, with a focus on *Klebsiella pneumoniae* as a causative organism. Alongside the development of a new diagnostic kit, PneumoNP partners were involved in the pre-clinical development of novel inhalable antibiotic-nanomedicines based on two new AMPs (AA139 and SET-M33). These two new AMPs were entrapped in several different nanocarriers (polymeric nanoparticles, liposomes, or lipid-core micelles), with an extensive pre-clinical development pipeline being established in order to prepare the various nanomedicine formulations and to select the most effective nanomedicines (Figure 1). Other research performed by PneumoNP partners, which is not described in the present thesis, included chemical stability measurements and reproducibility testing of the nanocarriers, as well as cytotoxicity and genotoxicity assays using nanomedicines, and finally, the development of a novel aerosol delivery system.

The chapters in **Section II** cover the *in vitro* investigations of the antimicrobial activity of the novel AMPs tested against different clinically relevant multidrug-resistant Gram-negative bacterial isolates. The data was used as a starting point in the development and testing of PneumoNP AMP-nanomedicines. In **Chapter 4** we tested the antimicrobial activity of two novel AMPs, SET-M33 and AA139, against a collection of genotypically diverse *K. pneumoniae* isolates recovered from individual patients and a variety of different clinical samples.

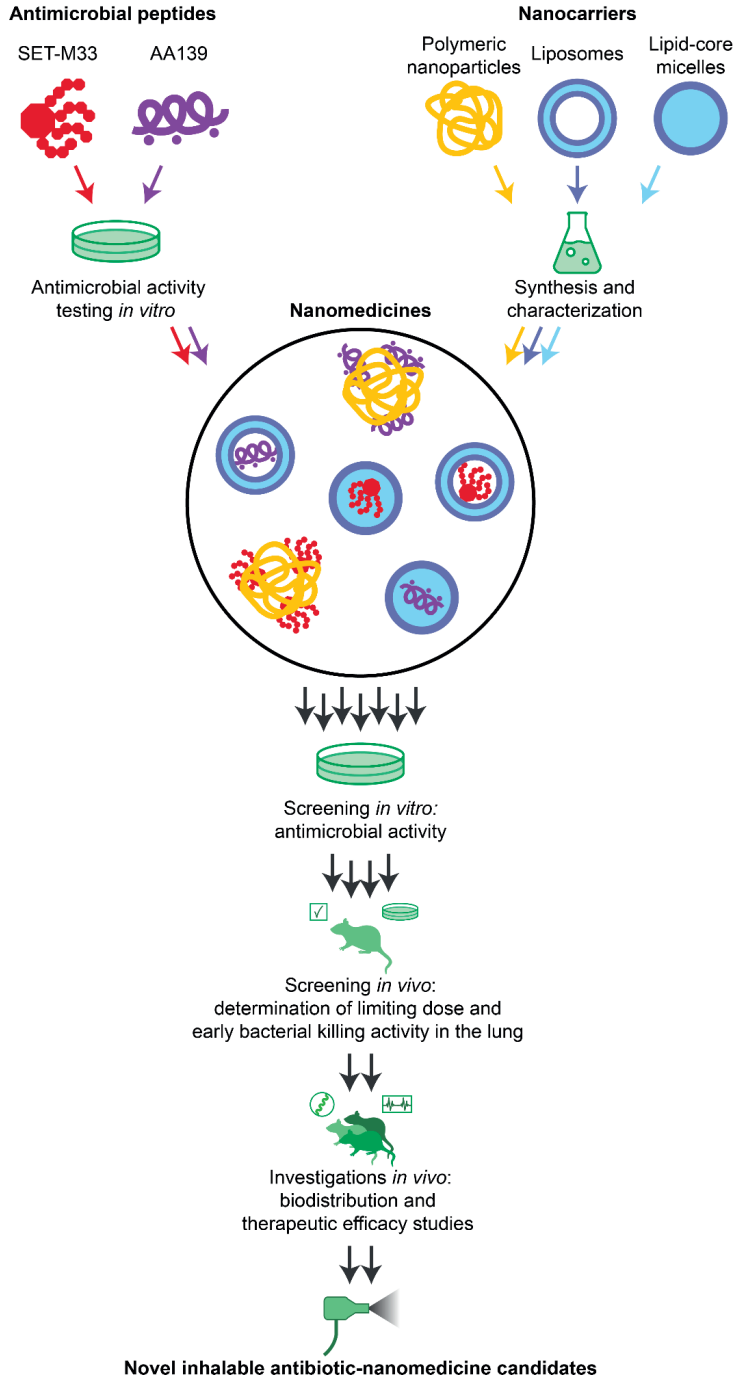


Figure 1. Diagram of the research in the PneumoNP pre-clinical development pipeline to develop novel AMP-nanomedicine candidates which is included in this thesis.

The collection of isolates showed differing antibiotic resistance profiles, including colistin-resistant isolates, and was examined for susceptibility to SET-M33 and AA139 (and colistin as comparator drug) in different assays. These assays included: bacteriostatic activity after 18 hours antibiotic exposure (minimum inhibitory concentration, MIC); concentration- and time-dependent bactericidal activity (time-kill kinetics, TKK); and susceptibility (determined by MIC) before and after 24 hours exposure to SET-M33 or AA139. **Chapter 5** describes a more in-depth investigation into the precise bactericidal mode of action of SET-M33 against isogenic colistin-susceptible and colistin-resistant *K. pneumoniae* and *Pseudomonas aeruginosa* strains using a TKK assay, electron microscopy, nuclear magnetic resonance (NMR) structure analysis, and a hemolytic activity assay.

The chapters in Section III detail the *in vivo* investigations of our selected AMP-nanomedicines administered via endotracheal aerosolization. The testing of novel treatment modalities in animal experiments is an essential and prerequisite link between pre-clinical *in vitro* studies and clinical trials in patients. In **Chapter 6**, we first set out to establish and characterize a new rat model of acute lobar pneumonia leading to fatal septicemia caused by multidrug-resistant (ESBL-producing or KPC-producing) *K. pneumoniae* which could be used to investigate our nanomedicines *in vivo*. We validated this rat model using a high-dose treatment regimen of the ‘drug of last resort’ tigecycline, with the carbapenem antibiotic meropenem as comparator drug.

Chapter 7 and Chapter 8 cover the *in vivo* investigation of the SET-M33-nanomedicines and AA139-nanomedicines compared to free SET-M33 and free AA139, respectively. In all our *in vivo* experiments, the nanomedicines were administered to rats via endotracheal aerosolization (as a means of direct delivery to the lungs). We used single-dose administration of the nanomedicines to determine the limiting dose as either maximum tolerated dose (MTD) or maximum feasible dose (MFD) in uninfected rats and to screen for the early bacterial killing activity in the lungs of infected rats. Based on the results of these studies, the most promising AA139-nanomedicines were selected for continued investigations. **Chapter 8** further elaborates on these studies using AA139-nanomedicines via extensive biodistribution studies in

uninfected rats using single-dose administration of radioactively labelled AA139-nanomedicines. Finally, therapeutic efficacy studies were performed in infected rats using once-daily administration of AA139-nanomedicines over a period of 10 days.

Chapter 4 Antimicrobial activity of two novel antimicrobial peptides AAI39 and SET-M33 against clinically and genotypically diverse *Klebsiella pneumoniae* isolates with differing antibiotic resistance profiles

Chapter 5 Investigations into the killing activity of an antimicrobial peptide active against extensively antibiotic-resistant *Klebsiella pneumoniae* and *Pseudomonas aeruginosa*

The chapters in **Section II** cover the *in vitro* investigations of the antimicrobial activity of novel AMPs against different clinically relevant multidrug-resistant Gram-negative isolates as a starting point of the development pipeline towards effective AMP-nanomedicines.

Chapter 4 describes the antimicrobial activity of two novel AMPs, AAI39 and SET-M33, against a collection of genotypically diverse *Klebsiella pneumoniae* isolates recovered from a variety of different clinical samples of individual patients. The isolates showed differing antibiotic resistance profiles, including colistin resistance, and was examined by determination of bacteriostatic activity (minimum inhibitory concentration, MIC); concentration- and time-dependent bactericidal activity (time-kill kinetics, TKK); and susceptibility (determined by MIC) before and after exposure to AMPs.

Chapter 5 describes a more in-depth investigation into the precise bactericidal mode of action of SET-M33 against isogenic colistin-susceptible and colistin-resistant *K. pneumoniae* and *Pseudomonas aeruginosa* strains using TKK assays, electron microscopy, nuclear magnetic resonance (NMR) structure analysis, and hemolytic activity assay.



Section



IN VITRO INVESTIGATIONS

Abstract

Colistin is an antimicrobial peptide (AMP) used as a drug of last resort, although plasmidial resistance (MCR) has been reported. AAI39 and SET-M33 are novel AMPs currently in development for the treatment of multidrug-resistant Gram-negative infections. As many AMPs have a similar mode of action as colistin, which can potentially lead to cross-resistance, the antimicrobial activity of AAI39 and SET-M33 was investigated against a collection of 50 clinically and genotypically diverse *Klebsiella pneumoniae* isolates with differing antibiotic resistance profiles, including colistin-resistant strains. The collection was genotypically characterized and susceptibility to clinically relevant antibiotics was determined. Susceptibility to AAI39 and SET-M33 did not deviate among the collection, despite differences in underlying mechanisms of resistance or susceptibility to colistin. For 3 colistin-susceptible and 3 colistin-resistant strains with distinct multidrug-resistant profiles, and an additional MCR-producing strain, the bactericidal activity of AAI39, SET-M33, and colistin during 24 hours exposure was examined. After the 24 hours exposure to AAI39, SET-M33, or colistin, the 7 strains were tested for changes in susceptibility towards the respective AMPs. AAI39 and SET-M33 showed a concentration-dependent bactericidal effect irrespective of the susceptibility of the bacteria to colistin. Exposure to low concentrations of colistin resulted in the development of colistin resistance in colistin-susceptible strains, whereas susceptibility to AAI39 and SET-M33 after exposure to the respective AMPs was maintained. The two novel AMPs remained effective against colistin-resistant strains and may be promising novel drugs for the treatment of clinically and genotypically diverse multidrug-resistant *K. pneumoniae* infections, including infections associated with colistin-resistant bacteria.



Chapter

4

ANTIMICROBIAL ACTIVITY OF TWO NOVEL ANTIMICROBIAL PEPTIDES AA139 AND SET-M33 AGAINST CLINICALLY AND GENOTYPICALLY DIVERSE KLEBSIELLA PNEUMONIAE ISOLATES WITH DIFFERING ANTIBIOTIC RESISTANCE PROFILES

*Hessel van der Weide, Denise M.C. Vermeulen-de Jongh,
Aart van der Meijden, Stefan A. Boers, Deborah Kreft,
Marian T. ten Kate, Chiara Falciani, Alessandro Pini, Magnus Strandh,
Irma A.J.M. Bakker-Woudenberg, John P. Hays, Wil H.F. Goessens*

Introduction

The spread of multidrug-resistance has rendered a growing list of antibiotics ineffective in the treatment of antibiotic-resistant bacterial infections, while the past decades have seen a dearth in the discovery and development of new antibiotics¹. This has caused concerns about an oncoming post-antibiotic era, in which pan-resistant bacterial infections will be common in the clinical setting and there are little to no treatment options left available to clinicians². Already, this post-antibiotic era is being heralded by clinical reports of pan-resistant bacterial infections³.

Due to the increase of antibiotic-resistant infections, colistin has resurfaced as a drug of last resort in the clinic for the treatment of multidrug-resistant infections⁴. This polypeptide antibiotic has been available for clinical use since 1959, but was largely abandoned due to issues with potential toxic side effects. The diminishing supply of effective antibiotics available for the treatment of multidrug-resistant infections has caused a renewal in investigations on the potential of colistin in the clinical setting⁵.

Unfortunately, the renewed use of colistin has led to the emergence and spread of colistin resistance⁶. The first report of a plasmid conferring mobilized colistin resistance (MCR) was published in 2015⁷. Since then, different variants of plasmidal colistin resistance have been identified and isolated from patients across the world, rendering even this drug of last resort potentially ineffective⁸.

Antimicrobial peptides (AMPs) are a family of naturally occurring antimicrobial compounds that were discovered in the first half of the 20th century, of which colistin is the most well-known example in the clinical setting⁹. In nature, AMPs are produced by all living organisms as a defensive mechanism towards micro-organisms, and thus far over 3000 different AMPs have been described in the Antimicrobial Peptide Database (<http://aps.unmc.edu/AP/main.php>)^{10,11}.

Most AMPs, including colistin, are cationic and share a broad-spectrum mechanism of antimicrobial killing which is non-specific but highly efficient¹². This cationic mechanism works through disruption of the bacterial cytoplasmic membrane by

interaction of the cationic peptide with anionic bacterial membrane lipids, which leads to the arrest of bacterial growth and cell death. While most cationic AMPs have this membrane-disrupting mechanism of action in common, many have additional mechanisms of antimicrobial activity including membrane protein targeting, intracellular activity, and immunomodulation¹³⁻¹⁵. Studies have shown that AMPs differ in their potential for cross-resistance with colistin, which may be the result of differences between their additional mechanisms of antimicrobial activity¹⁶⁻¹⁸. Importantly, AMPs that do not share cross-resistance with colistin may remain a viable alternative in the treatment of colistin-resistant infections.

In the present study, the antimicrobial activity of two novel cationic AMPs AA139 and SET-M33 was investigated using a collection of 50 clinically and genotypically diverse *Klebsiella pneumoniae* isolates with differing antibiotic resistance profiles. AA139 originates from Arenicin-3, an AMP isolated from the marine lugworm *Arenicola marina* with a 21-residue amphipathic β -hairpin structure, and was developed from Arenicin-3 based on decreases in plasma protein binding properties, cytotoxicity, and hemolytic activity^{19,20}. AA139 has shown potent *in vitro* antimicrobial activity against multidrug-resistant Gram-negative bacteria and has shown promising *in vivo* results in a number of animal models of infectious disease^{20,21}. Studies into its mode of action have suggested a dual mode of action through direct binding of AA139 to membrane phospholipids followed by interruption of phospholipid transportation pathways, resulting in membrane dysregulation resulting in bacterial cell death^{19,22}.

SET-M33 is a synthetic tetrabranched peptide linked by a lysine core, providing high resistance to proteolytic degradation²³. SET-M33 has likewise shown potent antimicrobial activity against Gram-negative bacteria and promising *in vivo* results in a number of animal models of infectious disease²⁴. Investigations into its mode of action have suggested that SET-M33 directly binds the bacterial lipopolysaccharide (LPS) and adopts an α -helix conformation in the membrane phospholipid bilayer, leading to membrane disruption resulting in bacterial cell death^{25,26}. Further studies have indicated additional mechanisms which may contribute to the use of SET-M33 in treating

infectious diseases, namely through immunomodulatory and anti-inflammatory activity²⁷, synergistic activity with other antibiotic families²⁸, and anti-biofilm activity²⁵.

In this manuscript, the authors investigate the potential usefulness of AA139 and SET-M33 against clinically and genotypically diverse *K. pneumoniae* isolates with differing antibiotic resistance profiles, including colistin-resistant isolates.

Materials and methods

Bacterial isolates

A collection of 50 *K. pneumoniae* isolates was utilized in this study. The isolates were cultured from various clinical specimens: blood, wound, mouth, throat, tracheal aspirate, rectum, catheter, urine, and perineum. The collection contains isolates representing five different antibiotic resistance profiles, consisting of 10 isolates per profile: Wildtype, extended-spectrum β -lactamase (ESBL)-producing, *K. pneumoniae* carbapenemase (KPC)-producing, oxacillinase β -lactamase (OXA)-48-like-producing, and New Delhi metallo- β -lactamase (NDM)-producing. Among the ESBL-producing isolates was one isolate positive for mobilized colistin resistance (MCR). The majority of the clinical samples had been collected between 2008 and 2015 from patients admitted at the Erasmus University Medical Center Rotterdam (Erasmus MC), the Netherlands. A KPC-producing isolate was obtained from a clinical sample from Greece, and 6 NDM-producing isolates were obtained from clinical samples from Bangladesh.

Genotypic characterization

Polymerase chain reaction (PCR) assays were used to verify the presence of the following resistance genes in the *K. pneumoniae* collection: cefotaxime-M β -lactamase (CTX-M) groups 1, 2, 8, 9, 25²⁹; temoniera β -lactamase (TEM)³⁰; sulfhydryl reagent variable β -lactamase (SHV)³¹; OXA-1-like³²; OXA-48-like³³; KPC³⁴; NDM-1³⁵; and MCR-1⁷. Multilocus sequence typing (MLST) was used to investigate genetic relatedness: partial deoxyribonucleic acid (DNA) sequences of housekeeping genes

were generated using a published high-throughput MLST (HiMLST) strategy that had been adapted for *K. pneumoniae* isolates³⁶. The results were compared to the publicly available *K. pneumoniae* MLST profiles at <https://bigsd.b.pasteur.fr>. Pulsed-field gel electrophoresis (PFGE) was performed to further assess the genetic relation between the isolates³⁷.

Antimicrobial agents

Ceftazidime hydrate, cefotaxime sodium salt, meropenem trihydrate, tigecycline, and colistin sulfate salt were purchased from Sigma-Aldrich Chemie BV (Zwijndrecht, the Netherlands). AA139 in Ringer's acetate solution was obtained from Adenium Biotech ApS (Copenhagen, Denmark). Dry-frozen L-isomeric SET-M33-acetate³⁸ was obtained from Setlance srl (Siena, Italy).

Antimicrobial susceptibility

The minimum inhibitory concentrations (MICs) of the *K. pneumoniae* collection to clinically relevant antibiotics were determined using the broth microdilution method following European Committee on Antimicrobial Susceptibility Testing (EUCAST) guidelines³⁹. Two-fold antibiotic concentration ranges were used; ceftazidime (0.0625–512 mg/L), cefotaxime (0.0625–512 mg/L), meropenem (0.0156–128 mg/L), tigecycline (0.0625–64 mg/L), AA139 (0.0625–64 mg/L), SET-M33 (0.0625–64 mg/L), colistin (0.0625–64 mg/L). Antimicrobial susceptibility of the collection was also determined using the VITEK®2 system and AST-N344 Gram-Negative Susceptibility Cards (bioMérieux Benelux BV, Zaltbommel, The Netherlands).

Selection of multidrug-resistant isolates

A panel of 6 *K. pneumoniae* isolates was selected from the collection for the investigation of concentration- and time-dependent bactericidal activity and potential changes in susceptibility to AA139, SET-M33 and colistin. This panel of 6 isolates comprised one colistin-susceptible and one colistin-resistant strain from each of the three most extensively antibiotic-resistant profiles (KPC-producing, OXA-48-like-producing, NDM-producing). Selection of isolates was based on genotypic diversity and divergent

susceptibilities to clinically relevant antibiotics, representing distinct groups of clinically relevant multidrug-resistance. The MCR-producing isolate was investigated using the same methods as the selected panel.

Concentration- and time-dependent bactericidal activity of AMPs

Time-kill kinetics (TKK) assays were performed as described previously⁴⁰ in triplicate for each of the 7 *K. pneumoniae* isolates. Four-fold increasing concentrations were used from 0.25–64 mg/L for all AMPs. At sampling time-points, suspensions were centrifuged at $12,500 \times g$ for 5 minutes to avoid antibiotic carry-over, serially 10-fold diluted, and sub-cultured on Mueller Hinton II (MH-II) agar plates. The plates were incubated at 37 °C during 20 hours for colony-forming units (CFU) counting.

Change in susceptibility towards AMPs after exposure

The 7 *K. pneumoniae* isolates exposed to AMPs for 24 hours during the TKK assays were tested for changes in their susceptibility towards the respective AMPs by MIC determination³⁹. For colistin-resistant isolates, a concentration range of 0.5–512 mg/L colistin was used to be able to detect further increases in MIC.

Results

Characterization of *K. pneumoniae* collection

The clinical origins of the 50 isolates in the *K. pneumoniae* collection are shown in Supplementary Table S1. A variety of genetic lineages was observed within the collection when HiMLST data was compared to global *K. pneumoniae* MLST genotypes, although some isolates clustered together more than others (Figure 1). PFGE data showed little overlap between the genetic profiles of the 50 isolates, with 40 clusters and singletons at 95% similarity (Supplementary Figure S1).

PCR data showed that all 50 isolates were positive for the SHV resistance gene as expected for *K. pneumoniae* (Supplementary Table S2). Wildtype isolates did not contain additional β -lactamase genes, except for one TEM-positive isolate. ESBL-producing

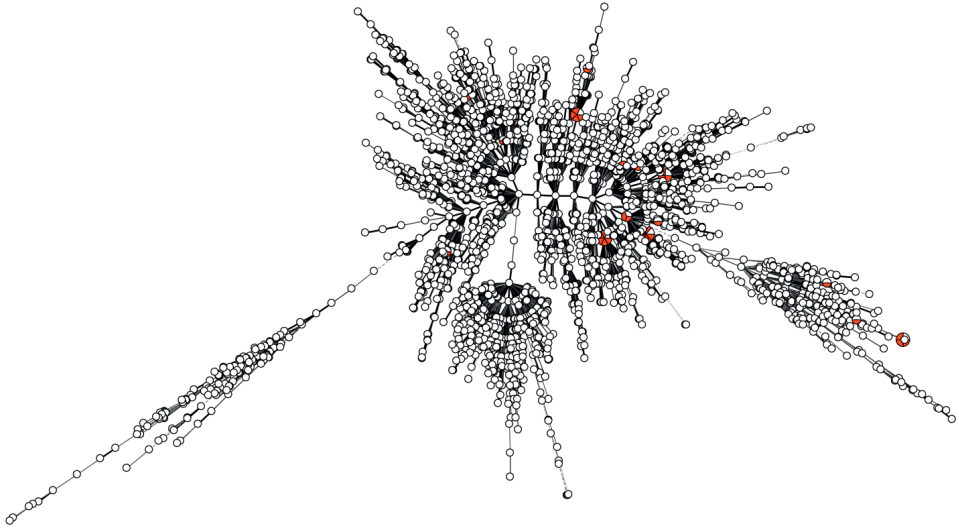


Figure 1. Minimum spanning tree with logarithmic scaling of MLST data of the collection of 50 *K. pneumoniae* isolates shown in comparison to a global *K. pneumoniae* collection of the Pasteur Institute, Paris, France. Red; Erasmus MC collection. White; Pasteur Institute collection available at <http://bigsd.b.pasteur.fr> accessed at 20 June 2018.

isolates were all positive for CTX-M groups 1 or 9, and many were also positive for TEM (70%) or OXA-1 (40%). The MCR resistance gene was detected in one ESBL-producing isolate. KPC, OXA-48-like, and NDM resistance genes were restricted to their respective antibiotic resistance profiles, i.e. KPC-producing, OXA-48-like-producing, and NDM-producing isolates. The other plasmid-mediated resistance genes were spread between these 3 multidrug-resistance profiles in no obvious pattern.

Antimicrobial susceptibility of *K. pneumoniae* collection

The antimicrobial susceptibility of the *K. pneumoniae* collection against clinically relevant antibiotics (ceftazidime, cefotaxime, meropenem, tigecycline, colistin) as well as against two novel AMPs (AA139, SET-M33) was compared based on antibiotic resistance profiles (Table 1).

Wildtype isolates were found to be phenotypically susceptible to all antibiotics tested, including the TEM-positive isolate. ESBL-producing and KPC-producing isolates were

Table 1. MIC values (mg/L) of *K. pneumoniae* groups differing in antibiotic resistance profile

Antibiotic resistance profile	Wildtype	ESBL	KPC	OXA-48-like	NDM
Number of isolates	10	10	10	10	10
Ceftazidime	0.5 0.25 – 1	64 2 – 128	512 128 – >512	256 0.5 – 512	>512 >512 – >512
Cefotaxime	0.09 <0.06 – 1	512 128 – >512	512 128 – >512	512 2 – >512	>512 512 – >512
Meropenem	0.06 0.03 – 0.5	0.06 0.03 – 0.13	32 16 – 128	2 1 – >128	96 16 – >128
Tigecycline	2 1 – 2	2 1 – 16	4 2 – 8	2 1 – 8	8 2 – 16
AA139	4 4 – 4	4 4 – 4	4 2 – 16	4 4 – 8	4 2 – 8
SET-M33	8 8 – 16	8 4 – 16	16 4 – 16	16 8 – 32	8 8 – 16
Colistin	1 0.5 – 2	0.5 0.5 – 16	1.5 0.5 – 64	1 0.5 – >64	3 0.5 – 32

MIC assays were performed in triplicate for each isolate, shown are the median values and range. MIC values are interpreted as susceptible, intermediate (italic), or resistant (bold) according to EUCAST guidelines. Interpretation has not been performed for the novel antimicrobial peptides AA139 and SET-M33.

all resistant to ceftazidime and cefotaxime. ESBL-producing isolates remained susceptible to meropenem, while KPC-producing isolates were resistant to meropenem. OXA-48-like-producing isolates showed considerable variation in susceptibility towards ceftazidime, cefotaxime, and meropenem, with no obvious pattern. 80% of NDM-producing isolates were resistant to all antibiotics tested. Tigecycline-resistant and colistin-resistant isolates were found among all antibiotic resistance profiles, except among Wildtype isolates. Antimicrobial susceptibility towards AA139 and SET-M33 never exceeded a two-fold change, irrespective of the antibiotic resistance profile.

The *K. pneumoniae* collection was then divided into colistin-susceptible and colistin-resistant isolates based on colistin MIC values, and the antimicrobial susceptibility of

Table 2. MIC values (mg/L) of *K. pneumoniae* groups differing in colistin susceptibility

Antibiotic resistance profile	Colistin-susceptible	Colistin-resistant
Number of isolates	37	13
Ceftazidime	128 0.25 - >512	>512 1 - >512
Cefotaxime	512 <0.06 - >512	512 2 - >512
Meropenem	0.5 0.03 - 128	64 0.13 - >128
Tigecycline	2 1 - 16	4 2 - 16
AA139	4 2 - 8	4 2 - 16
SET-M33	8 4 - 16	16 8 - 32
Colistin	0.5 0.5 - 2	32 4 - >64

MIC assays were performed in triplicate for each isolate, shown are the median values and range. MIC values are interpreted as susceptible, intermediate (italic), or resistant (bold) according to the EUCAST guidelines. Interpretation has not been performed for the novel antimicrobial peptides AA139 and SET-M33.

these two groupings was reanalyzed (Table 2). The groupings showed differences in susceptibility to meropenem, colistin, and tigecycline, with the colistin-susceptible isolates being susceptible and the colistin-resistant isolates being resistant to these antibiotics. The antimicrobial susceptibility to AA139 and SET-M33 did not exceed a two-fold change between the two groups.

VITEK® MICs for the *K. pneumoniae* collection based on antibiotic resistance profiles are shown in Supplementary Table S3. The VITEK® MICs matched the pattern of MICs found using the broth microdilution assay.

Concentration- and time-dependent bactericidal activity of AMPs

The MIC results for the selected panel of 3 colistin-susceptible and 3 colistin-resistant *K. pneumoniae* isolates from the three most extensively antibiotic-resistant profiles (KPC-producing, OXA-48-like-producing, NDM-producing) against the AMPs tested are shown in Table 3. The bactericidal activity of the AMPs was investigated for this panel of 6 isolates using TKK assays (Figure 2).

Regarding colistin-susceptible isolates, more than 99.9% of bacteria were killed after 2 hours of exposure to ≥ 4 mg/L AA139, ≥ 4 mg/L SET-M33, or ≥ 0.25 mg/L colistin. After initial bacterial killing, bacterial re-growth up to the level of non-exposed bacteria occurred after 24 hours exposure to ≤ 1 mg/L AA139, ≤ 4 mg/L SET-M33, or ≤ 4 mg/L colistin.

Regarding colistin-resistant isolates, more than 99.9% of bacteria were killed after 2 hours of exposure to ≥ 16 mg/L AA139, ≥ 16 mg/L SET-M33, or ≥ 64 mg/L colistin. After initial bacterial killing, bacterial re-growth up to the level of non-exposed bacteria occurred after 24 hours exposure to ≤ 4 mg/L AA139, ≤ 4 mg/L SET-M33, or ≤ 16 mg/L colistin.

Table 3. MIC values (mg/L) of selection of multidrug-resistant *K. pneumoniae* isolates

Selection	Isolate name	Antibiotic resistance profile	AA139	SET-M33	Colistin
Colistin-susceptible	<i>K. pneumoniae</i> ESBL 1059	KPC	4	8	0.5
	<i>K. pneumoniae</i> R-DYK 4861	OXA-48-like	4	8	1
	<i>K. pneumoniae</i> B-DYK 9557	NDM	4	16	0.5
Colistin-resistant	<i>K. pneumoniae</i> R-DYK 3427	KPC	8	16	64
	<i>K. pneumoniae</i> R-DYK 7926	OXA-48-like	4	16	32
	<i>K. pneumoniae</i> ESBL 635	NDM	4	8	16
MRC-producing	<i>K. pneumoniae</i> R-DYK 11347	ESBL	4	8	16

MIC assays were performed in triplicate for each isolate, shown are the median values. MIC values for colistin are interpreted as susceptible or resistant (bold) according to EUCAST guidelines. Interpretation has not been performed for the novel antimicrobial peptides AA139 and SET-M33.

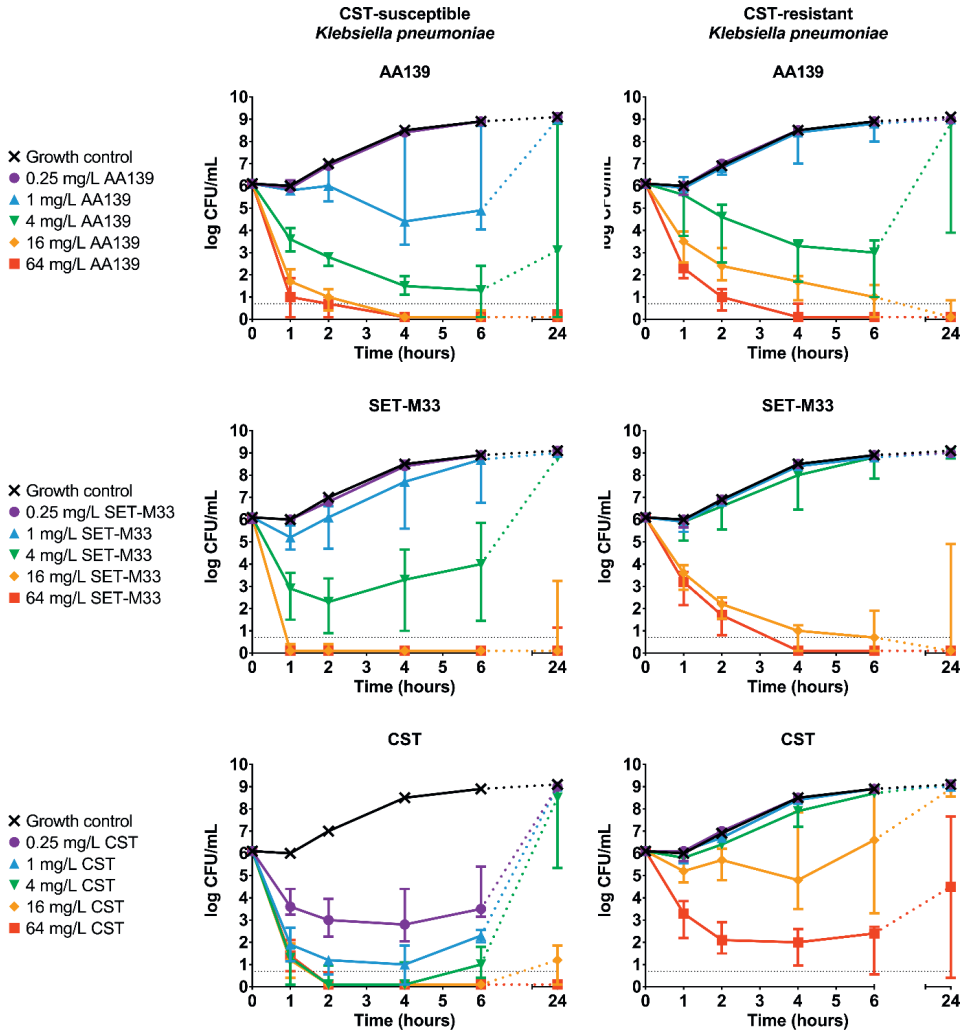


Figure 2. Concentration- and time-dependent bactericidal activity of AA139, SET-M33 and colistin (CST) against 3 colistin-susceptible and 3 colistin-resistant *K. pneumoniae* KPC, OXA-48-like and NDM isolates. Shown here are the median and interquartile range for 3 colistin-susceptible or 3 colistin-resistant *K. pneumoniae*; experiments were performed in triplicate for all 6 isolates. The dashed grey line indicates the lower limit of quantification (Log 0.7 CFU/mL).

Change in susceptibility towards AMPs after exposure

After 24 hours of exposure to AA139, SET-M33 or colistin in TKK assays, the susceptibility to the respective antibiotic of exposure was determined for the 3 colistin-susceptible and 3 colistin-resistant *K. pneumoniae* isolates (Table 4).

Regarding colistin-susceptible isolates, susceptibility towards AA139 remained unchanged except after exposure to AA139 at its MIC, which led to a 4-fold MIC increase. Susceptibility towards SET-M33 showed some minor changes, but never exceeded a 2-fold increase in MIC after exposure to SET-M33. Exposure to colistin led to the development of colistin resistance, even at low concentrations of colistin.

Regarding colistin-resistant isolates, susceptibility towards AA139 remained unchanged except after exposure to AA139 at its MIC, which led to a 4-fold MIC increase. Susceptibility towards SET-M33 remained unchanged except after exposure of SET-M33 at its MIC, which led to a 2-fold increase in MIC. Exposure to high concentrations of colistin led to a further increase in the MIC values for colistin.

Table 4. Change in susceptibility to AMPs of *K. pneumoniae* isolates

AMP concentration (mg/L)	MIC (mg/L) after 24 hours exposure to AMP					
	Colistin-susceptible isolates			Colistin-resistant isolates		
	AA139	SET-M33	Colistin	AA139	SET-M33	Colistin
0	4	8	1	4	16	64
0.25	4	8	16	4	16	32
1	4	8	32	4	16	32
4	16	16	32	16	16	64
16	nd	Nd	nd	nd	32	128
64	nd	Nd	nd	nd	nd	256

MIC assays were performed in triplicate for each isolate. Shown are the median MIC values of 3 isolates pooled together. MIC values for colistin are interpreted as susceptible or resistant (bold) according to EUCAST guidelines. Interpretation has not been performed for the novel AMPs AA139 and SET-M33. nd, not determined (no regrowth in the original TKK experiment).

AMP antimicrobial activity towards an MCR-producing isolate

MIC results of an MCR-producing *K. pneumoniae* isolate towards AMPs can be found in Table 3. The TKK results for the MCR-producing isolate are shown in Figure 3.

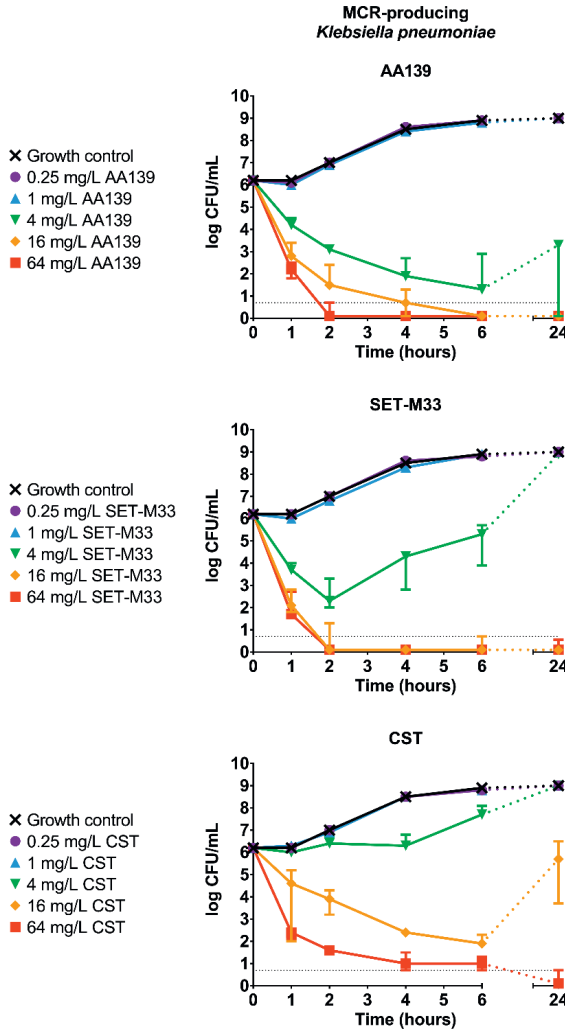


Figure 3. Concentration- and time-dependent bactericidal activity of AA139, SET-M33 and colistin (CST) against a MCR-producing *K. pneumoniae* ESBL isolate. Shown here are the median and range from triplicate experiments. The dashed grey line indicates the lower limit of quantification (Log 0.7 CFU/mL).

Bacterial killing at $\geq 99.9\%$ was observed after 2 hours of exposure to ≥ 4 mg/L AA139, ≥ 4 mg/L SET-M33, or ≥ 64 mg/L colistin. After initial bacterial killing, bacterial regrowth up to the level of non-exposed bacteria occurred after 24 hours exposure to ≤ 1 mg/L AA139, ≤ 4 mg/L SET-M33, or ≤ 4 mg/L colistin.

As shown in Table 5, after 24 hours exposure to AA139, SET-M33 or colistin in the TKK assay, the change in MIC of SET-M33 for the MCR-producing isolate never exceeded a 2-fold increase, and there was no change in the susceptibility of the isolate to colistin or AA139.

Discussion

AA139 and SET-M33 are two promising novel AMPs currently in development as potential antibiotics for the treatment of Gram-negative multidrug-resistant infections. To examine the clinical relevance of AA139 and SET-M33, a collection of 50 *K. pneumoniae* isolates from clinical samples was established representing 5 distinct antibiotic resistance profiles: Wildtype, ESBL-producing, KPC-producing, OXA-48-like-producing and NDM-producing. These isolates were clinically diverse and

Table 5. Change in susceptibility to AMPs of MCR-producing *K. pneumoniae* isolate

AMP concentration (mg/L)	MIC (mg/L)		
	after 24 hours exposure to AMP		
	AA139	SET-M33	Colistin
0	4	8	1
0.25	4	8	16
1	4	8	32
4	16	16	32
16	nd	Nd	nd
64	nd	Nd	nd

MIC assays were performed in triplicate, shown are the median values. MIC values for colistin are interpreted as susceptible or resistant (bold) according to EUCAST guidelines. Interpretation has not been performed for the novel AMPs AA139 and SET-M33. nd, not determined (no regrowth in the original TKK experiment).

genotypically distinct at the global (MLST) and individual level (PFGE). The antimicrobial susceptibility against clinically relevant antibiotics and the presence of plasmid-mediated antibiotic resistance genes was determined for all 50 *K. pneumoniae* isolates.

The susceptibility to AMPs AA139 and SET-M33 of all 50 isolates remained in the same order of magnitude regardless of antibiotic resistance profile or susceptibility of the isolates to colistin. This implies that the underlying mechanism(s) of resistance in these isolates did not affect the susceptibility of the strains to AA139 and SET-M33. Given that the growing emergence and spread of colistin resistance in the past few years^{6,7} has been coupled to the potential of colistin cross-resistance¹⁶⁻¹⁸, it is necessary to test whether novel AMPs such as AA139 and SET-M33 possess antimicrobial activity against colistin-resistant isolates. These results suggest that AA139 and SET-M33 have potential in the treatment of multidrug-resistant infections, including those associated with colistin-resistant isolates.

In TKK assays using colistin-susceptible isolates, AA139, SET-M33, and colistin showed concentration-dependent bactericidal activity, with colistin showing activity at lower concentrations than AA139 or SET-M33 within the first 6 hours of exposure. Despite these differences in initial bactericidal activity, regrowth of the colistin-susceptible bacteria after 24 hours of exposure to levels similar to non-colistin exposed bacteria was observed at similar concentrations for AA139, SET-M33, and colistin. The activity of colistin was reduced against colistin-resistant isolates when compared to colistin-susceptible isolates, with a 99.9% CFU/mL reduction and no regrowth of colistin-resistant bacteria only being observed at the highest colistin concentration used (64 mg/L). The novel AMPs showed a milder decrease in bactericidal activity compared to colistin, with a 99.9% CFU/mL reduction and no re-growth of colistin-resistant bacteria observed at concentrations of >16 mg/L for AA139 and SET-M33. This reinforces our earlier study on SET-M33²⁶, which found that the antimicrobial activity of SET-M33 was similarly mildly diminished in colistin-resistant mutants of *K. pneumoniae* and *Pseudomonas aeruginosa* when compared to the decrease in antimicrobial

activity of colistin. Here we demonstrated that this is the case for a selection of clinically and genotypically diverse *K. pneumoniae* isolates for both AA139 and SET-M33.

After 24 hours antibiotic exposure in the TKK assays, the isolates were tested for changes in susceptibility that could suggest adaptation to a resistant phenotype. Colistin-susceptible isolates became colistin-resistant after 24 hours exposure to low concentrations of colistin, up to a 64-fold increase in MIC. Conversely, changes in susceptibility of colistin-susceptible isolates towards AA139 or SET-M33 after 24 hours were only observed after exposure to the respective AMPs at their own MIC, but never exceeded a 4-fold increase in MIC. In isolates which were already colistin-resistant, a further decrease in susceptibility to colistin up to 4-fold decrease was observed after exposure to colistin. Conversely, susceptibility of colistin-resistant isolates to AA139 remained unchanged except for a 4-fold increase in MIC after exposure to AA139 at its own MIC, and susceptibility to SET-M33 never decreased more than 2-fold after exposure to SET-M33. This finding matches our earlier study²⁶ where we showed that colistin-resistance was easily selected in *K. pneumoniae* and *P. aeruginosa* isolates after 24 hours exposure to colistin, while 24 hours exposure to SET-M33 did not lead to significant changes in susceptibility to SET-M33 in these isolates. Another study likewise suggested that SET-M33 has a lower propensity for resistance selection compared to colistin²⁴.

Finally, antimicrobial activity and susceptibility changes were also examined for an MCR-producing isolate in order to investigate a difference between a plasmid-mediated colistin-resistant strain and a chromosomal colistin-resistant strain. The bactericidal activity of AA139 and SET-M33 against this strain was similar compared to colistin-susceptible isolates, and no significant changes in susceptibility were observed after 24 hours exposure. This suggests that plasmid-mediated colistin-resistance does not confer cross-resistance towards AA139 or SET-M33, and that treatment with either of these AMPs will not readily select AMP resistant mutants.

The findings of this study suggest that there is only limited cross-resistance between the two novel AMPs and colistin for clinical *K. pneumoniae* isolates, and that the two novel

AMPs have a lower propensity to select for resistant mutants compared to colistin. Future studies will be needed to show that this is the same in other Gram-negative bacterial species. In spite of the shared cationic mechanism of action between these compounds¹², cross-resistance may be limited due to differences between their additional mechanisms of antimicrobial activity, which studies have suggested for AA139^{19,22}, SET-M33^{24,26,27,41}, and colistin¹⁵. These different additional mechanisms of antimicrobial activity may also explain the apparent difference between the two novel AMPs and colistin in their propensity to select for resistant mutants. AA139 and SET-M33 may be of interest for future studies on the mechanisms of antimicrobial activity and resistance for AMPs.

An interesting point for discussion with respect to AMPs is that the MICs values of AA139 and SET-M33 are substantially higher than the MIC values of colistin when compared in weight per volume, and that colistin showed bactericidal activity within the first 6 hours of exposure at lower concentrations than AA139 or SET-M33 when compared in weight per volume. However, it should be noted that the molecular weights of AA139 and SET-M33 are substantially higher compared to colistin, and when the MIC values are calculated based on their respective molarities, the MIC values for AA139 and SET-M33 are very similar to those of colistin²³. Ultimately, the usefulness of any given antibiotic for the clinic depends on its therapeutic window of effect, and the MIC is only an indicator of the minimum effective dose. Other pre-clinical investigations which provide further insight into the therapeutic window of effect have been performed for both of the novel AMPs.

The *in vivo* efficacy of AA139 has been investigated in mice disease models of a peritonitis/bacteremia neutropenic *Escherichia coli* infection, a neutropenic thigh *E. coli* infection, as well as a urinary tract *E. coli* infection⁴²⁻⁴⁴. These studies demonstrated *in vivo* efficacy of AA139 against Gram-negative bacteria at similar concentrations as the effective concentrations found in the present study, with low toxicity and safety issues reported²¹.

SET-M33 demonstrated *in vitro* hemolytic activity²⁶ and *ex vivo* cytotoxic activity³⁸ only at concentrations well above the effective concentrations found in the current study. *In vivo* toxicity studies on SET-M33 in mice showed no to mild toxic signs of acute toxicity, depending on the route of administration, at the effective concentrations found in the present study^{24,38}. The *in vivo* efficacy of SET-M33 has been tested in various mouse models of disease; lethal intraperitoneal infection models caused by *E. coli* or *P. aeruginosa*²³, a lethal sepsis model caused by *E. coli*³⁸, and three neutropenic models of sepsis, lung infection, and skin infection caused by *P. aeruginosa*²⁴. Notably, when colistin was administered at similar concentrations in terms of weight per volume as SET-M33, it resulted in far more severe toxic side effects including death whereas no toxic side effects were reported for SET-M33²⁴.

Conclusions

AA139 and SET-M33 are two novel AMPs currently in development for clinical application which showed consistent antimicrobial activity towards clinically and genotypically diverse *K. pneumoniae* isolates with differing antibiotic resistance profiles. Both AA139 and SET-M33 remained effective against colistin-resistant isolates, including an isolate carrying plasmid-mediated colistin resistance. Exposure of *K. pneumoniae* isolates to the two novel AMPs did not lead to significant change in susceptibility. These findings suggest that AA139 and SET-M33 are promising novel antibiotics for the treatment of multidrug-resistant *K. pneumoniae* infections, even when the bacteria have developed colistin resistance following previous treatment with colistin. An important conclusion is that in comparative studies with high molecular weight antibiotics and low molecular weight antibiotics, it may be more insightful to express antibiotic concentrations in terms of molarity rather than weight per volume.

Acknowledgements

HiMLST analysis was performed at the Streeklaboratorium voor de Volksgezondheid Kennemerland, Haarlem, the Netherlands. Analysis of blood plasma was performed by the Clinical Pharmacological and Toxicological Laboratory at the Erasmus University Medical Center, Rotterdam, The Netherlands.

Funding

This work was financially supported by the European Union's Seventh Program for Research, Technological Development and Demonstration under grant agreement No. 604434 PncumoNP.

Competing interests

This study was performed in collaboration with Adenium Biotech ApS and Setlance srl, who are respectively the patent holders of AA139 and SET-M33.

References

1. O'Neill J. Antimicrobial resistance: tackling a crisis for the health and wealth of nations. *The Review on Antimicrobial Resistance*. 2014;20.
2. Ventola CL. The antibiotic resistance crisis: part 1: causes and threats. *Pharmacy and Therapeutics*. 2015;40(4):277.
3. Bathoorn E, Tsioutis C, da Silva Voorham J, Scoulica E, Ioannidou E, Zhou K, et al. Emergence of pan-resistance in KPC-2 carbapenemase-producing *Klebsiella pneumoniae* in Crete, Greece: a close call. *Journal of Antimicrobial Chemotherapy*. 2016;71(5):1207-12.
4. Falagas ME, Kasiakou SK, Saravolatz LD. Colistin: the revival of polymyxins for the management of multidrug-resistant gram-negative bacterial infections. *Clinical Infectious Diseases*. 2005;40(9):1333-41.
5. Nation RL, Li J. Colistin in the 21st century. *Current Opinion in Infectious Diseases*. 2009;22(6):535.
6. Wang R, Dorp L, Shaw LP, Bradley P, Wang Q, Wang X, et al. The global distribution and spread of the mobilized colistin resistance gene *mcr-1*. *Nature Communications*. 2018;9(1):1179.
7. Liu Y-Y, Wang Y, Walsh TR, Yi L-X, Zhang R, Spencer J, et al. Emergence of plasmid-mediated colistin resistance mechanism MCR-1 in animals and human beings in China: a microbiological and molecular biological study. *The Lancet Infectious Diseases*. 2016;16(2):161-8.
8. Kluytmans J. Plasmid-encoded colistin resistance: *mcr*-one, two, three and counting. *Eurosurveillance*. 2017;22(31).
9. Fox JL. Antimicrobial peptides stage a comeback. *Nature Publishing Group*; 2013.
10. Hancock RE, Sahl H-G. Antimicrobial and host-defense peptides as new anti-infective therapeutic strategies. *Nature Biotechnology*. 2006;24(12):1551.

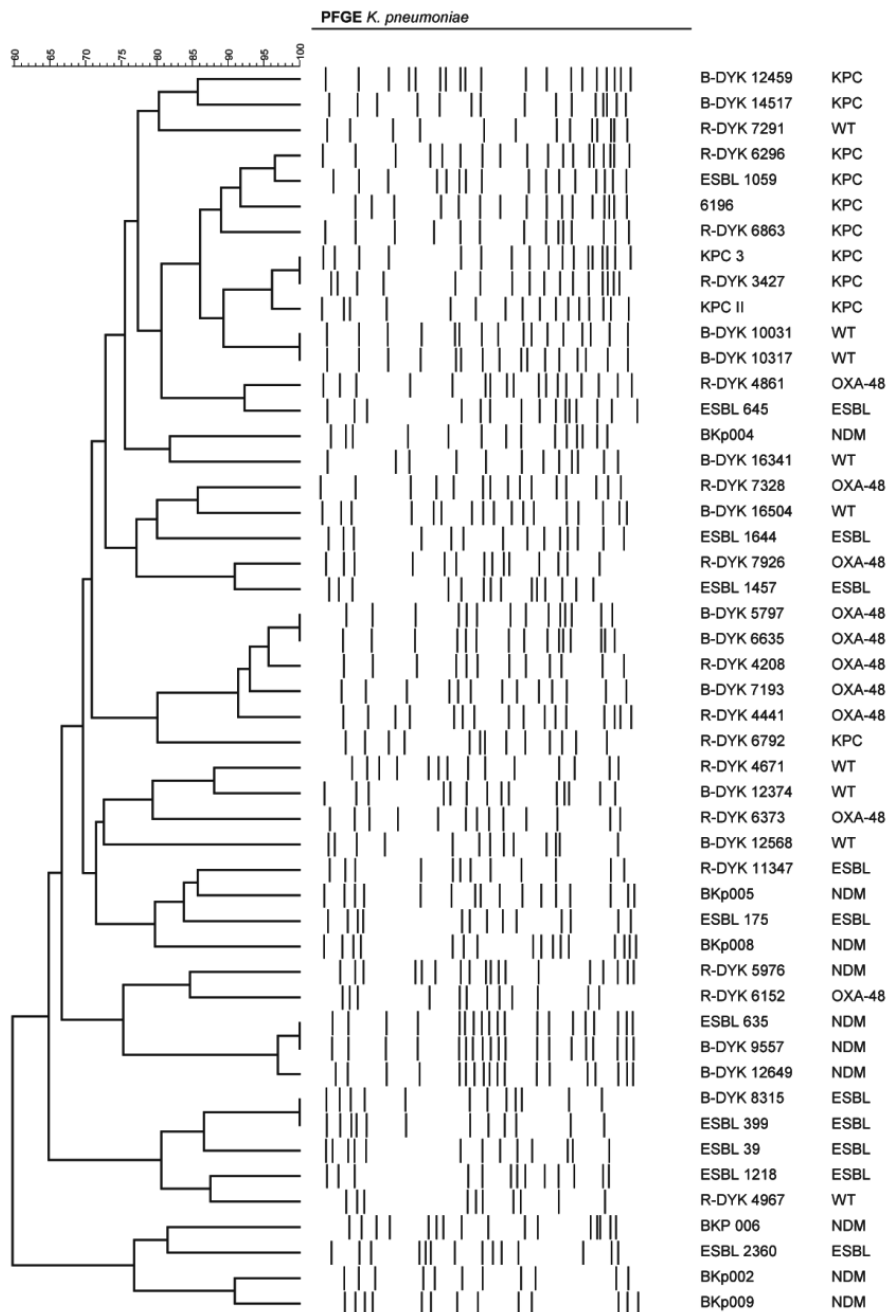
11. Wang G, Li X, Wang Z. APD3: the antimicrobial peptide database as a tool for research and education. *Nucleic Acids Research*. 2015;44(D1):D1087-D93.
12. Bechinger B, Lohner K. Detergent-like actions of linear amphipathic cationic antimicrobial peptides. *Biochimica et Biophysica Acta (BBA)-Biomembranes*. 2006;1758(9):1529-39.
13. Bechinger B, Gorr S-U. Antimicrobial peptides: Mechanisms of action and resistance. *Journal of Dental Research*. 2017;96(3):254-60.
14. Lai Y, Gallo RL. AMPed up immunity: how antimicrobial peptides have multiple roles in immune defense. *Trends in Immunology*. 2009;30(3):131-41.
15. Trimble MJ, Mlynářčík P, Kolář M, Hancock RE. Polymyxin: alternative mechanisms of action and resistance. *Cold Spring Harbor Perspectives in Medicine*. 2016;6(10):a025288.
16. Napier BA, Burd EM, Satola SW, Cagle SM, Ray SM, McGann P, et al. Clinical use of colistin induces cross-resistance to host antimicrobials in *Acinetobacter baumannii*. *mBio*. 2013;4(3):e00021-13.
17. Pránting M, Andersson DI. Mechanisms and physiological effects of protamine resistance in *Salmonella enterica* serovar Typhimurium LT2. *Journal of Antimicrobial Chemotherapy*. 2010;65(5):876-87.
18. Hashemi MM, Rovig J, Weber S, Hilton B, Forouzan MM, Savage PB. Susceptibility of colistin-resistant, Gram-negative bacteria to antimicrobial peptides and ceragenins. *Antimicrobial Agents and Chemotherapy*. 2017;61(8):e00292-17.
19. Huang JX, Neve S, Elliot AG, Cain AK, Boinett CJ, Zuegg J, et al. Novel Arenicin-3 peptide antibiotics with broad-spectrum activity against MDR Gram-negative bacterial act via dual mode of actions. 54th International Conference of Antimicrobial Agents and Chemotherapy (ICAAC) and Infectious Diseases Society of America (IDSA) Joint Meeting: <https://adeniumBiotech.com/publications/>; 2014.
20. Neve S, Lociuo S, Morrissey I, Hawser S, Nordkild P. The arenicin-3 derived clinical candidate AA139 shows potent activity against Gram-negative pathogens, Poster F-261. 54th ICAAC Meeting; 5-9 September 2014; Washington, DC2014.
21. Lociuo S. Oral presentation: Arenicin antimicrobial peptides (novel AMPs with a novel mode of action). 54th International Conference of Antimicrobial Agents and Chemotherapy (ICAAC) and Infectious Diseases Society of America (IDSA) Joint Meeting: <https://adeniumBiotech.com/publications/>; 2014.
22. Cain AK, Boinett CJ, Barquist L, Neve S, Huang JX, Elliot AG, et al. Transposon directed insertion-site sequencing (TraDIS) to elucidate the mode of action of the antimicrobial Arenicin-3 (Arn-3). 54th International Conference of Antimicrobial Agents and Chemotherapy (ICAAC) and Infectious Diseases Society of America (IDSA) Joint Meeting: <https://adeniumBiotech.com/publications/>; 2014.
23. Pini A, Falciani C, Mantengoli E, Bindi S, Brunetti J, Iozzi S, et al. A novel tetrabranching antimicrobial peptide that neutralizes bacterial lipopolysaccharide and prevents septic shock in vivo. *The FASEB Journal*. 2010;24(4):1015-22.
24. Brunetti J, Falciani C, Roscia G, Pollini S, Bindi S, Scali S, et al. In vitro and in vivo efficacy, toxicity, bio-distribution and resistance selection of a novel antibacterial drug candidate. *Scientific Reports*. 2016;6:26077.
25. Falciani C, Iozzi L, Pollini S, Luca V, Carnicelli V, Brunetti J, et al. Isomerization of an antimicrobial peptide broadens antimicrobial spectrum to gram-positive bacterial pathogens. *PLOS ONE*. 2012;7(10):e46259.
26. van der Weide H, Brunetti J, Pini A, Bracci L, Ambrosini C, Lupetti P, et al. Investigations into the killing activity of an antimicrobial peptide active against extensively antibiotic-resistant *K. pneumoniae* and *P. aeruginosa*. *Biochimica et Biophysica Acta (BBA)-Biomembranes*. 2017;1859(10):1796-804.
27. Brunetti J, Roscia G, Lampronti I, Gambari R, Quercini L, Falciani C, et al. Immunomodulatory and anti-inflammatory activity in vitro and in vivo of a novel antimicrobial candidate. *Journal of Biological Chemistry*. 2016;jbc. M116. 750257.

28. Pollini S, Brunetti J, Sennati S, Rossolini GM, Bracci L, Pini A, et al. Synergistic activity profile of an antimicrobial peptide against multidrug-resistant and extensively drug-resistant strains of Gram-negative bacterial pathogens. *Journal of Peptide Science*. 2017;23(4):329-33.
29. Woodford N, Fagan EJ, Ellington MJ. Multiplex PCR for rapid detection of genes encoding CTX-M extended-spectrum β -lactamases. *Journal of Antimicrobial Chemotherapy*. 2005;57(1):154-5.
30. Mabilat C, Goussard S. PCR detection and identification of genes for extended-spectrum β -lactamases. *Diagnostic Molecular Microbiology: Principles and Applications: American Society for Microbiology*; 1993. p. 553-9.
31. Nüesch-Inderbinen MT, Hächler H, Kayser FH. Detection of genes coding for extended-spectrum SHV beta-lactamases in clinical isolates by a molecular genetic method, and comparison with the E test. *European Journal of Clinical Microbiology & Infectious Diseases*. 1996;15(5):398-402.
32. Karisik E, Ellington MJ, Pike R, Warren RE, Livermore DM, Woodford N. Molecular characterization of plasmids encoding CTX-M-15 β -lactamases from *Escherichia coli* strains in the United Kingdom. *Journal of Antimicrobial Chemotherapy*. 2006;58(3):665-8.
33. Dallenne C, Da Costa A, Decré D, Favier C, Arlet G. Development of a set of multiplex PCR assays for the detection of genes encoding important β -lactamases in Enterobacteriaceae. *Journal of Antimicrobial Chemotherapy*. 2010;65(3):490-5.
34. Bradford PA, Bratu S, Urban C, Visalli M, Mariano N, Landman D, et al. Emergence of carbapenem-resistant *Klebsiella* species possessing the class A carbapenem-hydrolyzing KPC-2 and inhibitor-resistant TEM-30 β -lactamases in New York City. *Clinical Infectious Diseases*. 2004;39(1):55-60.
35. Islam MA, Talukdar PK, Hoque A, Huq M, Nabi A, Ahmed D, et al. Emergence of multidrug-resistant NDM-1-producing Gram-negative bacteria in Bangladesh. *European Journal of Clinical Microbiology & Infectious Diseases*. 2012;31(10):2593-600.
36. Souverein D, Boers SA, Veenendaal D, Euser SM, Kluytmans J, Den Boer JW. Polyclonal Spread and Outbreaks with ESBL Positive Gentamicin Resistant *Klebsiella* spp. in the Region Kennemerland, The Netherlands. *PLOS ONE*. 2014;9(6):e101212.
37. Gruteke P, Goessens W, Van Gils J, Peerbooms P, Lemmens-den Toom N, van Santen-Verheuvél M, et al. Patterns of resistance associated with integrons, the extended-spectrum β -lactamase SHV-5 gene, and a multidrug efflux pump of *Klebsiella pneumoniae* causing a nosocomial outbreak. *Journal of Clinical Microbiology*. 2003;41(3):1161-6.
38. Pini A, Lozzi L, Bernini A, Brunetti J, Falciani C, Scali S, et al. Efficacy and toxicity of the antimicrobial peptide M33 produced with different counter-ions. *Amino Acids*. 2012;43(1):467-73.
39. The European Committee on Antimicrobial Susceptibility. Breakpoint tables for interpretation of MICs and zone diameters, Version 4.0. EUCAST; 2014.
40. de Steenwinkel JEM, de Knecht GJ, ten Kate MT, van Belkum A, Verbrugh HA, Kremer K, et al. Time-kill kinetics of anti-tuberculosis drugs, and emergence of resistance, in relation to metabolic activity of *Mycobacterium tuberculosis*. *Journal of Antimicrobial Chemotherapy*. 2010;65(12):2582-9.
41. Pini A, Giuliani A, Falciani C, Fabbrini M, Pileri S, Lelli B, et al. Characterization of the branched antimicrobial peptide M6 by analyzing its mechanism of action and in vivo toxicity. *Journal of Peptide Science*. 2007;13(6):393-9.
42. Lociuo S, Neve S, Lundberg CV, Andersen JM, Nordkild P. Clinical candidate AA139 - Efficacy in two neutropenic bacteraemia/peritonitis models caused by *E. coli* strains with different MIC values. 54th International Conference of Antimicrobial Agents and Chemotherapy (ICAAC) and Infectious Diseases Society of America (IDSA) Joint Meeting: <https://adeniumBiotech.com/publications/>; 2014.
43. Lociuo S, Neve S, Lundberg CV, Andersen JM, Nordkild P. Clinical candidate AA139 - Efficacy in a neutropenic thigh model caused by *E. coli* AID#172. 54th International Conference of Antimicrobial Agents and Chemotherapy (ICAAC) and Infectious Diseases Society of America (IDSA) Joint Meeting: <https://adeniumBiotech.com/publications/>; 2014.

44. Neve S, Lociuro S, Lundberg CV, Nordkild P. Clinical candidate AA139 - Efficacy against ESBL producing *E. coli* in the murine urinary tract infection model. 54th International Conference of Antimicrobial Agents and Chemotherapy (ICAAC) and Infectious Diseases Society of America (IDSA) Joint Meeting: <https://adeniumBiotech.com/publications/>; 2014.

Supplementary Table S1. Origin of collection of 50 *K. pneumoniae* isolates

Antibiotic resistance profile	Isolate name	Year of isolation	Country of origin	Specimen type
Wildtype	B-DYK 12747	2012	The Netherlands	Blood
	B-DYK 10317	2012	The Netherlands	Blood
	B-DYK 12568	2012	The Netherlands	Blood
	B-DYK 16504	2013	The Netherlands	Blood
	B-DYK 16341	2013	The Netherlands	Blood
	R-DYK 7291	2013	The Netherlands	Rectum
	B-DYK 12374	2012	The Netherlands	Catheter
	R-DYK 4671	2011	The Netherlands	Mouth
	R-DYK 4967	2012	The Netherlands	Throat
B-DYK 10031	2012	The Netherlands	Tracheal aspirate	
ESBL	B-DYK 8315	2012	The Netherlands	Blood
	ESBL 1218	2013	The Netherlands	Blood
	ESBL 1644	2013	The Netherlands	Blood
	ESBL 1457	2013	The Netherlands	Blood
	ESBL 645	2012	The Netherlands	Blood
	ESBL 39	2011	The Netherlands	Urine
	ESBL 399	2011	The Netherlands	Rectum
	ESBL 175	2011	The Netherlands	Perineum
	R-DYK 11347	2015	The Netherlands	Rectum
ESBL 2360	2014	The Netherlands	Throat	
KPC	B-DYK 12459	2012	The Netherlands	Blood
	R-DYK 6863	2013	The Netherlands	Throat
	R-DYK 6792	2013	The Netherlands	Perineum
	R-DYK 6296	2013	The Netherlands	Urine
	B-DYK 14517	2013	The Netherlands	Rectum
	ESBL 1059	2013	The Netherlands	Rectum
	6196	n/a	Greece	n/a
	R-DYK 3427	2010	The Netherlands	Urine
	KPC 3	n/a	The Netherlands	n/a
KPC 11	n/a	The Netherlands	n/a	
OXA-48-like	R-DYK 7328	2013	The Netherlands	Rectum
	R-DYK 4441	2011	The Netherlands	Rectum
	R-DYK 6152	2012	The Netherlands	Throat
	R-DYK 6373	2013	The Netherlands	Urine
	R-DYK 4861	2012	The Netherlands	Perineum
	R-DYK 7926	2013	The Netherlands	Rectum
	B-DYK 6635	2011	The Netherlands	Rectum
	B-DYK 5797	2011	The Netherlands	Urine
	B-DYK 7193	2011	The Netherlands	Rectum
	R-DYK 4208	2011	The Netherlands	Rectum
NDM	B-DYK 9557	2012	The Netherlands	Blood
	ESBL 635	2012	The Netherlands	Rectum
	B-DYK 12649	2012	The Netherlands	Wound
	R-DYK 5976	2012	The Netherlands	Rectum
	BKp002	2010	Bangladesh	Urine
	BKp004	2008	Bangladesh	Urine
	BKp005	2008	Bangladesh	Urine
	BKp006	2008	Bangladesh	Tracheal aspirate
	BKp008	2010	Bangladesh	Tracheal aspirate
BKp009	2010	Bangladesh	Urine	



Supplementary Figure S1. PFGE data of 49 isolates from the collection of 50 *K. pneumoniae* isolates. One isolate was untypable and was not included. A phylogenetic tree was constructed based on the relatedness of the isolates according to PFGE results. Clusters were based on >95% similarity.

Supplementary Table S2. PCR data of the collection of 50 *K. pneumoniae* isolates

Antibiotic resistance profile	Wildtype	ESBL	KPC	OXA-48-like	NDM
Number of isolates	10	10	10	10	10
1	nd	8	1	6	10
2	nd	nd	nd	nd	nd
CTX-M 8	nd	nd	nd	nd	nd
9	nd	2	1	nd	nd
25	nd	nd	nd	nd	nd
TEM	1	7	10	7	9
SHV	10	10	10	10	10
1	nd	4	1	6	8
OXA 48	nd	nd	nd	10	nd
KPC	nd	nd	10	nd	nd
NDM-1	nd	nd	nd	nd	10
MCR-1	nd	1	nd	nd	nd

The distribution of plasmid-mediated resistance genes within the collection of 50 *K. pneumoniae* isolates based on their antibiotic resistance profile as determined using PCR assays. nd, not detected.

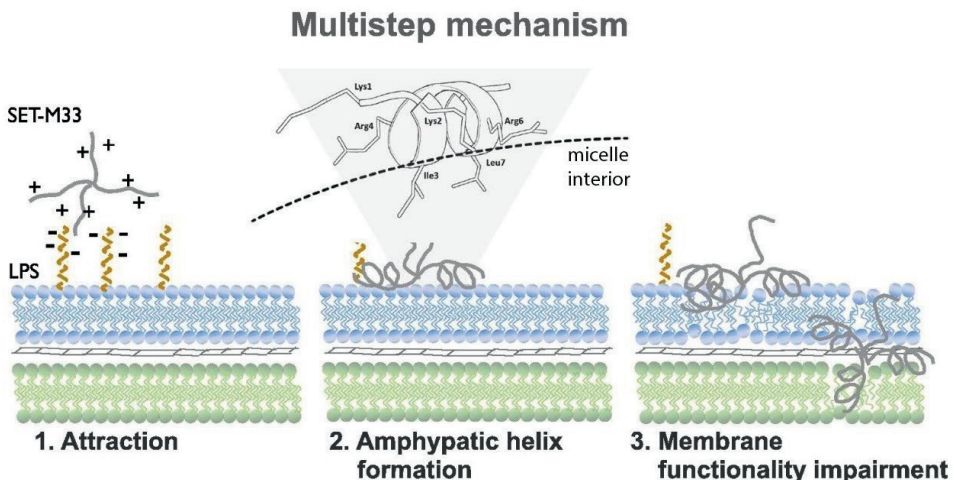
Supplementary Table S3. VITEK® 2 MIC data of the collection of 50 *K. pneumoniae* isolates

Antibiotic resistance profile	Wildtype	ESBL	KPC	OXA-48-like	NDM
Number of isolates	10	10	10	10	10
Ampicillin	16	≥32	≥32	≥32	≥32
Amoxicillin/Clavulanic Acid	≤2	12	≥32	≥32	≥32
Piperacillin/Tazobactam	≤4	6	≥128	≥128	≥128
Cefuroxime	≤1	≥64	≥64	≥64	≥64
Cefuroxime Axetil	≤1	≥64	≥64	≥64	≥64
Cefoxitin	≤4	≤4	≥64	8	≥64
Cefotaxime	≤1	≥64	20	≥64	≥64
Ceftazidime	≤1	16	≥64	≥64	≥64
Cefepime	≤1	2	48	16	≥64
Imipenem	≤0.25	≤0.25	≥16	2	≥16
Meropenem	≤0.25	≤0.25	≥16	1	≥16
Gentamicin	≤1	≥16	4	≥16	≥16
Tobramycin	≤1	8	≥16	≥16	≥16
Ciprofloxacin	≤0.25	0.5	≥4	≥4	≥4
Norfloxacin	≤0.5	2	≥16	≥16	≥16
Trimethoprim	≤0.5	≥16	≥16	≥16	≥16
Trimethoprim/sulfamethoxazole	≤1	≥16	≥16	≥16	≥16

MICs (mg/L) were determined using the automated VITEK® 2 antimicrobial identification system for the collection of 50 *K. pneumoniae* isolates, shown are the median values for each antibiotic resistance profile. The collection was grouped based on their antibiotic resistance profile. Interpretation of antimicrobial susceptibility was defined by the VITEK® antimicrobial identification system as susceptible, intermediate (italic), or resistant (bold) according to EUCAST guidelines. Trimethoprim/sulfamethoxazole was expressed as the trimethoprim concentration.

Abstract

SET-M33 is a multimeric antimicrobial peptide active against Gram-negative bacteria *in vitro* and *in vivo*. Insights into its killing mechanism could elucidate correlations with selectivity. SET-M33 showed concentration-dependent bactericidal activity against colistin-susceptible and resistant isolates of *Klebsiella pneumoniae* and *Pseudomonas aeruginosa*. Scanning and transmission microscopy studies showed that SET-M33 generated cell blisters, blebs, membrane stacks and deep craters in *K. pneumoniae* and *P. aeruginosa* cells. Nuclear magnetic resonance (NMR) analysis and circular dichroism (CD) spectra in the presence of sodium dodecyl sulfate (SDS) micelles showed a transition from an unstructured state to a stable α -helix, driving the peptide to arrange itself on the surface of micelles. SET-M33 kills Gram-negative bacteria after an initial interaction with bacterial lipopolysaccharide. The molecule becomes then embedded in the outer membrane surface, thereby impairing cell function. This activity of SET-M33, in contrast to other similar antimicrobial peptides such as colistin, does not generate resistant mutants after 24 hours of exposure, non-specific interactions or toxicity against eukaryotic cell membranes, suggesting that SET-M33 is a promising new option for the treatment of Gram-negative antibiotic-resistant infections.





Chapter

5



INVESTIGATIONS INTO THE KILLING ACTIVITY OF AN ANTIMICROBIAL PEPTIDE ACTIVE AGAINST EXTENSIVELY ANTIBIOTIC-RESISTANT KLEBSIELLA PNEUMONIAE AND PSEUDOMONAS AERUGINOSA

*Hessel van der Weide, Jlenia Brunetti, Alessandro Pini, Luisa Bracci,
Chiara Ambrosini, Pietro Lupetti, Eugenio Paccagnini, Mariangela Gentile,
Andrea Bernini, Neri Niccolai, Denise M.C. Vermeulen-de Jongh,
Irma A.J.M. Bakker-Woudenberg, Wil H.F. Goessens,
John P. Hays, Chiara Falciani*



Introduction

Extensive use of broad-spectrum antibiotics has led to the development and spread of extensively antibiotic-resistant strains of bacteria, making antimicrobial resistance a global problem. Antibiotic-resistant bacteria kill 25,000 people in the European Union (EU) every year. Infections such as urinary tract infections¹, pneumonia² and septicemia³ are increasingly associated with multidrug-resistant Gram-negative bacteria in all regions of the world⁴. These antibiotic-resistant bacteria generally cause infections associated with increased risk of poor clinical outcome and mortality compared to non-resistant strains of the same bacteria⁵. The World Health Organization (WHO) warns that antimicrobial resistance is an increasingly serious threat to global public health and calls for action across all government sectors and society⁶ to avoid a dreaded 'post-antibiotic' era.

A recent rekindling of antibiotic research has shown that the antimicrobial peptide (AMP) class of antibiotics is particularly promising for use against infections caused by multidrug-resistant microorganisms⁷⁻⁹. AMPs are an important component of the natural defenses of most living organisms, and more than 2500 AMPs have been registered in the Antimicrobial Peptide Database (<https://aps.unmc.edu/AP/main.php>)¹⁰. However, despite their desirable characteristics, antimicrobial peptides have had limited pharmaceutical development due to their toxicity, instability and manufacturing costs, and therefore only a few AMPs have actually been approved for clinical use^{11,12}.

The most common mechanism of antimicrobial killing by antimicrobial peptides is disruption of the cytoplasmic membrane, for example by pore formation, which is rather non-specific but highly efficient¹³⁻¹⁵. Alternative mechanisms of action include peptide translocation into the cytoplasm where the antibiotic interferes with bacterial metabolic processes, such as protein synthesis or deoxyribonucleic acid (DNA) replication, while other peptides are known to interact directly with specific membrane components¹⁶⁻¹⁸. In particular, cationic AMPs have been demonstrated to induce anionic lipid clustering which appears to arrest bacterial growth or trigger cell death^{19,20}.

SET-M33 is an antimicrobial peptide that has been extensively studied in recent years²¹⁻²⁵. It is a cationic non-natural peptide built in a branched form (Figure 1) that makes it more resistant to degradation in biological fluids²⁶. SET-M33 has shown efficacy against a number of Gram-negative multidrug- and extensively drug-resistant clinical

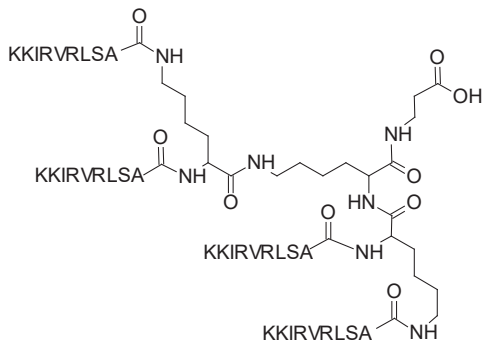


Figure 1. Structure of SET-M33.

isolates^{21,24}. It has also shown acceptable toxicity in human cells and in mice²², as well as anti-inflammatory activity²³. Nevertheless, its mechanism of action has not yet been researched in depth. In this study we used different techniques to study the mechanism of action of SET-M33 against two Gram-negative bacterial species, *Klebsiella pneumoniae* and *Pseudomonas aeruginosa*: 1) bacterial killing kinetics over time to see concentration-dependency and onset of resistance; 2) electron microscopy imaging of treated bacteria to visualize membrane disturbance; 3) hemolytic activity to assess eukaryotic cell toxicity and 4) nuclear magnetic resonance (NMR) and circular dichroism (CD) to study the structure of the peptides in the presence of micelles and their ability to stabilize in a facial amphiphilic helix.

Materials and methods

Peptide synthesis

All peptides were prepared by solid-phase synthesis through standard Fmoc chemistry using a Syro multiple peptide synthesizer (MultiSynTech, Witten, Germany). Side chain protecting groups were 2,2,4,6,7-pentamethyldihydrobenzofuran-5-sulfonyl for R, t-butoxycarbonyl for K, and t-butyl for S (Iris Biotech GmbH, Marktredwitz, Germany). The final products were cleaved from the solid support, de-protected by treatment with trifluoroacetic acid (TFA) containing triisopropylsilane and water (95/2.5/2.5), and precipitated with diethyl ether. Final peptide purity and identity was

confirmed by matrix-assisted laser desorption/ionization (MALDI) mass spectrometry (MS) on a Bruker Daltonics Ultraflex III MALDI time-of-flight (MALDI-TOF) mass spectrometer and by reverse-phase high-performance liquid chromatography (RP-HPLC) on a Phenomenex Jupiter® C18 analytical column (300 Å, 250 × 4.6 mm).

Q-33 (linear peptide, QKKIRVRLSA) was produced on TentaGel® S RAM resin (Iris Biotech GmbH, Marktredwitz, Germany). The crude peptide, released as amide, was purified by reverse-phase chromatography on a Phenomenex Jupiter® C18 column (300 Å, 250 × 10 mm), in a linear gradient, using 0.1% TFA/water as eluent A and acetonitrile as eluent B (from 99% to 50% of eluent A in 30 minutes). The compound QKKIRVRLSA–NH₂ was characterized: MALDI MS: 1198.97 [M+H]⁺; RP-HPLC: t_R = 19.62 minutes, purity >99%.

SET-M33 (tetrabranch peptide, (KKIRVRLSA)₄K₂KβA) was synthesized on a Fmoc4-Lys2-Lys-β-Ala Wang resin (Iris Biotech GmbH, Marktredwitz, Germany). The crude peptide, released as carboxylic acid, was purified by reverse-phase chromatography on a Phenomenex Jupiter® C18 analytical column (300 Å, 250 × 10 mm) in a linear gradient, using 0.1% TFA/water as eluent A and acetonitrile as eluent B (from 82% to 75% of eluent A in 60 minutes). The purified peptide was obtained as a trifluoroacetate salt and exchanged to acetate using a quaternary ammonium resin (AG1–X8, 100–200 mesh, 1.2 mEq/mL capacity). The resin-to-peptide ratio was 2000:1, resin and peptide were stirred for 1 hour, the resin was then filtered off, washed extensively, and the peptide was recovered and freeze-dried. The compound (KKIRVRLSA)₄K₂KβA–OH was characterized: MALDI MS: 4682.48 [M+H]⁺; RP-HPLC: t_R = 21.10 minutes, purity >99%. SET-M33 solubility; water, ≥20 mg/mL; saline, ≥20 mg/mL; phosphate-buffered saline (PBS), ≥15 mg/mL.

Selection of colistin-resistant mutants of *K. pneumoniae* R-DYK 4861 and *P. aeruginosa* B-162

K. pneumoniae R-DYK 4861 and *P. aeruginosa* B-162 were both extensively antibiotic-resistant clinical isolates and colistin-susceptible. Colistin-resistant mutants of both strains were obtained by step-wise serial passages of bacterial strains²⁷ in BBL™ Mueller

Hinton II (MH-II) broth (Becton, Dickinson Benelux NV, Erembodegem, Belgium) containing colistin concentrations in the range 2–64 mg/L (colistin sulfate, Sigma-Aldrich Chemie BV, Zwijndrecht, the Netherlands). This involved sub-culturing 100 µL of overnight culture of the bacteria (grown in MH-II broth) into MH-II broth containing 2 mg/L colistin and incubating overnight at 35°C. In subsequent steps 100 µL of overnight culture was sub-cultured into MH-II broth containing two-fold increases in the concentration of colistin until the highest colistin concentration of 64 mg/L was achieved. Finally, 100 µL volumes were sub-cultured onto solid MH-II medium (Becton, Dickinson Benelux NV, Erembodegem, Belgium). Colistin-resistant colonies were then characterized phenotypically using VITEK® 2.

Phenotypic characterization of bacterial isolates

Phenotypic characterization of *K. pneumoniae* B-DYK 4861 and *P. aeruginosa* B-162 isolates and their colistin-resistant mutants was performed by determining their susceptibility for a panel of 18 different antibiotics from the main classes of antibiotics using the VITEK® 2 antimicrobial identification system (BioMérieux Benelux BV, Zaltbommel, The Netherlands) and AST-N140 cards (Vitek AMS). Interpretation of antimicrobial susceptibility was based on European Committee on Antimicrobial Susceptibility Testing (EUCAST) 2014 guidelines (Supplementary Table S1)²⁸.

Antimicrobial susceptibility of bacterial isolates: minimum inhibitory concentration (MIC)

Antimicrobial susceptibility was assessed by determining the MIC of SET-M33 and colistin using the broth microdilution technique according to 2014 EUCAST guidelines. The MIC assay measures visible inhibition of bacterial growth after 24 hours exposure of bacteria to antibiotic in MH-II broth. The two-fold antibiotic concentration range used for SET-M33 and colistin was 0.063–64 mg/L.

Concentration- and time-dependent bactericidal activity of SET-M33 and colistin: time-kill kinetics (TKK)

The concentration- and time-dependent killing capacity of SET-M33 was determined

using TKK assays, as previously described²⁹. Briefly, stationary-phase MH-II broth cultures of *K. pneumoniae* R-DYK 4861 and *P. aeruginosa* B-162 were diluted in 25 mL MH-II broth until a density of approximately 7×10^5 colony-forming units (CFU)/mL was achieved. Bacterial cultures were exposed to antimicrobial antibiotics at 2-fold increasing concentrations for 24 hours at 37 °C under shaking conditions at 96 rpm at 37 °C. Next, 1 mL samples were taken at 0, 1, 2, 4, 6, and 24 hours of antibiotic exposure and centrifuged at $12500 \times g$ for 5 minutes to pellet the cells, which were then resuspended in sterile PBS. Agar plates were incubated for 24 hours (*K. pneumoniae*) or 48 hours (*P. aeruginosa*) at 37 °C in order to determine the number of CFU. The lower limit of quantification in this assay was 5 CFU/mL (log 0.7). For colistin-susceptible bacterial isolates, the two-fold antibiotic concentration range was 0.125–64 mg/L for SET-M33 and colistin alike. For colistin-resistant isolates, the two-fold antibiotic concentration range was 0.125–64 mg/L for SET-M33 and 1–512 mg/L for colistin. Flasks showing re-growth of bacteria after 24 hours antibiotic exposure were examined for changes in antibiotic susceptibility using the antibiotic MIC assay described above, but with an antibiotic concentration range of 0.5–512 mg/L for the colistin-resistant isolates.

Sample preparation for electron microscopy

P. aeruginosa PAO1 and *K. pneumoniae* American Type Culture Collection (ATCC) 13833 cells in logarithmic phase were resuspended at 2×10^8 CFU/mL in PBS and incubated with 1.5 μ M SET-M33 at room temperature for 15, 30, and 60 minutes. The mixture was then centrifuged for 5 minutes at 10,000 rpm.

Scanning electron microscopy (SEM)

Centrifuged bacteria were resuspended in 500 μ L PBS and a drop of liquid cell suspension was placed on untreated glass coverslip for five minutes. The coverslip was then fixed for immersion in 2.5% glutaraldehyde solution in phosphate buffer 0.1 M pH 7.2 (PB) for 2 hours at 4 °C, washed in PB, post-fixed in 1% OsO₄ in PB for 30 minutes at 4 °C, dehydrated in an ascending alcohol series, and dried in a Balzers CPD 030 CO₂ critical point dryer. The coverslip was then mounted on an aluminum

stub, coated with 20 nm gold in a Balzers MED010 sputtering device, and observed in a Philips XL20 scanning electron microscope with an electron accelerating voltage of 20 kV.

Transmission electron microscopy (TEM)

Centrifuged bacteria were fixed in 2.5% glutaraldehyde solution in PB for 2 hours at 4 °C, washed in PB, post-fixed in 1% O_3O_4 in PB for 30 minutes at 4 °C, dehydrated in an ascending alcohol series, incubated twice in propylene oxide and finally infiltrated and embedded in epon/araldite resin that was polymerized at 60 °C for 48 hours. Ultrathin sections (60 nm thick) were cut from samples on a Reichert-Jung Ultracut E ultramicrotome, mounted on 200-mesh copper grids, stained with uranyl acetate and lead citrate and observed in a FEI Technai™ G2 SPIRIT transmission electron microscope using an electron accelerating voltage of 100 kV under standard operating conditions.

Nuclear magnetic resonance (NMR)

All NMR samples were prepared by dissolving lyophilized peptides in 500 μ l H_2O/D_2O (95:5) to a final concentration of 1.0 mM, with the exception of SET-M33, which was dissolved to a final concentration of 0.25 mM. Since the resonance of N-terminus amide would be missed in aqueous media due to chemical exchange, the peptide sequence of the Q-33 peptide, bearing a leading glutamine [33-34], was used instead, allowing us to gain structural information on the Lys1 residue. Samples with micelles were prepared using 100 mM fully deuterated sodium dodecyl sulfate (SDS-d25; Cambridge Isotopes). Paramagnetic spectra were recorded with 2.5 mM gadolinium-(III)-diethylenetriaminepentaacetic acid-bisamide (Gd(III)DTPA-BMA). All spectra were acquired on a Bruker DRX Avance™ spectrometer operating at 14.1 Tesla at a temperature of 298 K. Two-dimensional spectra were recorded by accumulating 32 free induction decays (FIDs) for 512 experiments, digitalizing over 2048 points. Spectral width was set at 6000 Hz and repetition delay at 3 seconds. The mixing time for total correlation spectroscopy (TOCSY) and nuclear Overhauser effect (NOE) spectroscopy (NOESY) spectra was set at 45/75 milliseconds and 100/200/300

milliseconds, respectively. All spectra were processed to a final size of 2048 by 1024 points. Peak assignment and integration were carried out with Sparky 3 software³⁰ while calibration of NOE peak volumes, distance calculation and restrained torsion angle dynamics for structure calculation were performed using Dyana software³¹.

Circular dichroism (CD)

CD spectra were recorded at 25 °C with a Jasco 815 spectropolarimeter using quartz cells having a path length of 0.1 cm. SET-M33 (100 μM) or Q-33 (100 μM) were dissolved in pure water or 30 mM sodium dodecyl sulfate (SDS). The results were processed with the application Spectra Manager II™ Suite.

Hemolytic activity

The ability of SET-M33 peptide to induce hemolysis of human red blood cells was assessed. Whole blood in ethylenediaminetetraacetic acid (EDTA)-coated tubes was centrifuged at $1100 \times g$ for 10 minutes. Red blood cells diluted 1:100 in PBS were incubated for 24 hours at 37 °C in PBS with two-fold serial dilution of all peptides from 4 mg/L to 1.8 g/L. The absorbance of the supernatants was determined in a 96-well plate at 490 nm using a microplate reader. Data for 100% hemolysis were obtained by adding 0.1% Triton X-100 in water. The negative control was PBS. The hemolysis rate of each peptide was calculated with the following equation:

$$\text{Hemolysis (\%)} = \frac{A_{\text{peptide}} - A_{\text{PBS}}}{A_{\text{triton}} - A_{\text{PBS}}} \times 100\% ; \text{ where } A = \text{absorbance.}$$

Fast protein liquid chromatography (FPLC)-gel filtration

Lipopolysaccharide (LPS) from *P. aeruginosa* (ATCC 27316, Sigma Aldrich) and SET-M33 was gel-filtered on a Superdex® 75 10/300 GL FPLC column using an ÄKTA purifier (GE Healthcare) in PBS pH 7.4. 100 μL 2 mg/mL SET-M33 or 13 mg/mL LPS or 13 mg/mL LPS + 2 mg/mL SET-M33 was injected on a Superdex® 75 10/300 GL FPLC column with a flow rate of 0.75 mL/min and absorbance was measured at 220 and 260 nm.

Results and discussion

The *K. pneumoniae* and *P. aeruginosa* isolates used in the following experiments were resistant to a wide range of β -lactam antibiotics (penicillins, cephalosporins and carbapenems) including the 4th generation cephalosporin cefepime, aminoglycosides (gentamycin and tobramycin) and fluoroquinolones (ciprofloxacin and norfloxacin). Interpretation of antimicrobial susceptibility was based on EUCAST 2014 guidelines²⁸.

Susceptibility of bacterial isolates to SET-M33 and colistin: minimum inhibitory concentration (MIC)

The susceptibility of the colistin-susceptible *K. pneumoniae* B-DYK 4861 and *P. aeruginosa* B-162 isolates and their colistin-resistant mutants to SET-M33 and colistin in terms of MIC are shown in Table 1. Colistin resistance did not affect SET-M33 susceptibility in these two strains, confirming our previous data on seven different colistin-resistant *K. pneumoniae* strains²¹. SET-M33 showed a MIC of 8 mg/L for *K. pneumoniae* ATCC 13833 and *P. aeruginosa* PAO1.

Table 1. MICs of SET-M33 and colistin for bacterial isolates in triplicate

Bacterial isolate		Colistin-susceptible	Colistin-resistant	Colistin-susceptible	Colistin-resistant
		<i>K. pneumoniae</i> R-DYK 4861	<i>K. pneumoniae</i> R-DYK 4861	<i>P. aeruginosa</i> B-162	<i>P. aeruginosa</i> B-162
SET-M33	mg/L	16 16 – 16	16 16 – 32	16 8 – 16	16 8 – 16
	μ M	2.7 2.7 – 2.7	2.7 2.7 – 5.5	2.7 1.4 – 2.7	2.7 1.4 – 2.7
Colistin	mg/L	0.50 0.25 – 0.50	>512 >512 – >512	2 2 – 2	512 128 – 512
	μ M	0.22 0.11 – 0.22	>222 >222 – >222	0.87 0.87 – 0.87	222 55 – 222

Shown are the median values and range. MIC values for colistin are interpreted as susceptible or resistant (bold) according to EUCAST guidelines. Interpretation has not been performed for SET-M33.

SET-M33 and colistin activity against colistin-susceptible and colistin-resistant *K. pneumoniae* B-DYK 4861 and *P. aeruginosa* B-162: time-kill kinetics (TKK)

The major killing effect of an antibiotic against an organism depends on the exposure time or concentration of the drug at the active target site. In the present study we investigated extensively drug-resistant *K. pneumoniae* and *P. aeruginosa* populations, taking the effects of exposure time and concentration into account.

Colistin-susceptible and colistin-resistant *K. pneumoniae* isolates were killed by $\geq 99.9\%$ after 2 hours of exposure to ≥ 4 mg/L and ≥ 8 mg/L SET-M33, respectively (Figure 2A and 2B). This was followed by bacterial re-growth up to the level of non-exposed bacteria after 24 hours exposure to ≤ 4 mg/L and ≤ 16 mg/L, respectively. Colistin killed $\geq 99.9\%$ of the colistin-susceptible *K. pneumoniae* isolate after 2 hours of exposure to ≥ 0.5 mg/L (Figure 2C) and bacterial re-growth after 24 hours exposure was observed up to ≤ 32 mg/L. In the colistin-resistant isolate, colistin concentration-dependent killing was observed in the first hour of exposure but $\geq 99.9\%$ killing was not achieved after 2 hours of exposure (Figure 2D).

For *P. aeruginosa*, $\geq 99.9\%$ killing was achieved in colistin-susceptible and colistin-resistant isolates after 2 hours of exposure to ≥ 8 mg/L SET-M33 (Figure 2E and 2F). Colistin killed $\geq 99.9\%$ of bacteria in the colistin-susceptible *P. aeruginosa* isolate after 2 hours of exposure to a concentration ≥ 1 mg/L (Figure 2G). In the colistin-resistant *P. aeruginosa* isolate, colistin concentration-dependent killing was observed in the first 2 hours of exposure, followed by bacterial re-growth up to the level of non-exposed bacteria after 24 hours, at all the colistin concentrations tested (Figure 2H).

We also showed that exposure to SET-M33 sterilized colistin-susceptible *K. pneumoniae* and *P. aeruginosa* populations already at one-fold (16 mg/L) (Figure 2A) and four-fold (64 mg/L) (Figure 2E) the MICs, respectively. In contrast, after exposure to colistin, sterilization only occurred at the extremely high concentration of 64 mg/L (Figure 2C and 2G), which is 128-fold and 32-fold the MICs of colistin-susceptible *K. pneumoniae* and *P. aeruginosa*, respectively. Colistin-resistant *K. pneumoniae* and *P. aeruginosa* were

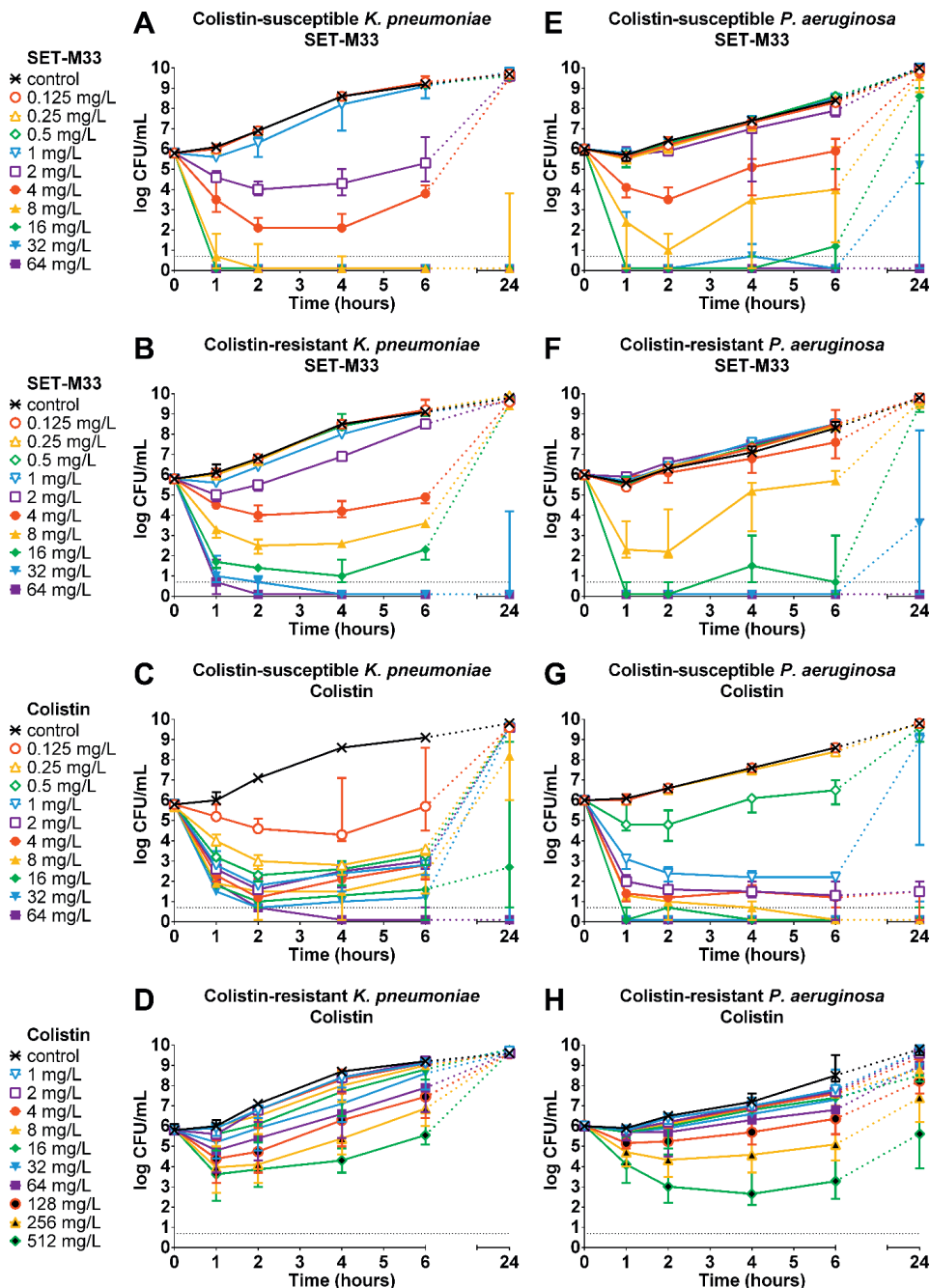


Figure 2. Concentration- and time-dependent bactericidal activity of SET-M33 and colistin against isolates of *K. pneumoniae* R-DYK 4861 (A-D) and *P. aeruginosa* B-162 (E-H). Data are medians and range of 3 experiments.

sterilized with 64 mg/L SET-M33 (Figure 2B and 2F) in both cases (four-fold the MIC) but never with colistin (Figure 2D and 2H).

SET-M33 and colistin showed concentration-dependent bactericidal activity against colistin-susceptible and colistin-resistant isolates of *K. pneumoniae* and *P. aeruginosa*. This result is similar to the action of different widely used antibiotics e.g. aminoglycosides and fluoroquinolones, as well as other AMPs³². SET-M33 retains activity against both colistin-susceptible and colistin-resistant bacteria. This result indicates that SET-M33 is impervious to the mechanisms associated with colistin resistance.

Selection of resistance

Selection of resistance was assessed in the same experiments: when re-growth was observed after 24 hours of exposure to antibiotic, bacterial susceptibilities were determined as MIC. Re-growth of colistin-susceptible strains of *K. pneumoniae* and *P. aeruginosa* after 24 hours of exposure to SET-M33 was never associated with selection of SET-M33 resistance (Table 2): in fact, MIC values did not increase more than 0.5-2 fold, whereas re-growth of *K. pneumoniae* after 24 hours of colistin exposure was associated with decreased susceptibility and a manifold increase in MIC (Table 2). Colistin was more effective against *P. aeruginosa*, although bacteria regrowing at 1 mg/L colistin showed a 6-fold increase in MIC.

Similar results were obtained with the colistin-resistant strains, although re-growth of colistin-resistant *K. pneumoniae* showed slightly lower susceptibility to SET-M33 with a 4-fold increase in MIC (Supplementary Table S2).

Gram-negative bacteria can reduce their susceptibility to AMPs by reducing their net negative surface charges, modifying capsule polysaccharides, or reducing outer membrane fluidity³³. In contrast to colistin, resistance to SET-M33 does not readily develop during 24 hours of continuous exposure. This finding provides evidence that some of the resistance mechanisms that affect colistin do not affect SET-M33 to the same extent. For example, the mutations that lead to colistin resistance may not have the same effect on the activity of SET-M33, or alternatively, exposure to SET-M33 may

Table 2. Change in *K. pneumoniae* R-DYK 4861 and *P. aeruginosa* B-162 susceptibility to SET-M33 and colistin after 24 hours exposure to antibiotic as determined by MIC assay

Antibiotic concentration (mg/L)	SET-M33 (mg/L)		Colistin (mg/L)	
	Colistin-susceptible <i>K. pneumoniae</i>	Colistin-susceptible <i>P. aeruginosa</i>	Colistin-susceptible <i>K. pneumoniae</i>	Colistin-susceptible <i>P. aeruginosa</i>
	control	16	16	0.5
0.125	16	16	>64	2
0.25	16	16	>64	2
0.5	16	16	>64	4
1	16	16	>64	12 ¹
2	16	16	>64	nd
4	32	16	>64	nd
8	nd	16	64 ¹	nd
16	nd	12 ¹	>64 ²	nd
32	nd	nd	>64 ¹	nd
64	nd	nd	nd	nd

Colistin-susceptible bacterial cultures were exposed to two-fold increasing concentrations of SET-M33 or colistin for 24 hours at 37 °C under shaking conditions. When bacteria re-grew after 24 hours exposure to antibiotic, their MIC susceptibilities (performed in triplicate) were also determined and the median value reported. nd, not determined (no regrowth in the original TKK experiment); ¹, one out of three samples did not show bacterial re-growth; ², two out of three samples did not show bacterial re-growth.

not elicit the type of resistance mutations that are selected or induced by colistin. Ways of avoiding resistance will be investigated in further studies. Importantly, the fact that resistance to SET-M33 does not appear within the 24 hours exposure period to the antibiotic provides evidence that the use of SET-M33 in the clinic may have advantages over the use of colistin. For example, colistin is currently used as an antibiotic of last resort for multidrug-resistant bacteria^{34,35}, but besides its toxic side effects, it is also becoming dangerously more often ineffective due to increasing number of resistant strains³⁶⁻³⁸.

Electron microscopy

The effect of SET-M33 treatment at MIC (8 mg/L SET-M33) for 15, 30 and 60 minutes on bacterial cell morphology was studied by SEM and TEM. SEM images (Figure 3)

showed that after 30 minutes of SET-M33 treatment, the surfaces of *K. pneumoniae* ATCC 13833 and *P. aeruginosa* PAO1 cells lost their smoothness and developed superficial blisters. After 60 minutes of SET-M33 treatment, bacterial cells appeared larger than control cells and many were empty and showed large holes, mainly at the poles.

TEM images (Figure 4) showed significant signs of alteration in most bacterial cells after 30 minutes of SET-M33 treatment: *P. aeruginosa* and *K. pneumoniae* cells appeared turgid and filamentous material appears on the external side of the outer membrane. In the first 30 minutes after incubation with SET-M33, only a few *K. pneumoniae* and *P. aeruginosa* bacterial cells (rare in the micrograph field) showed cell damage.

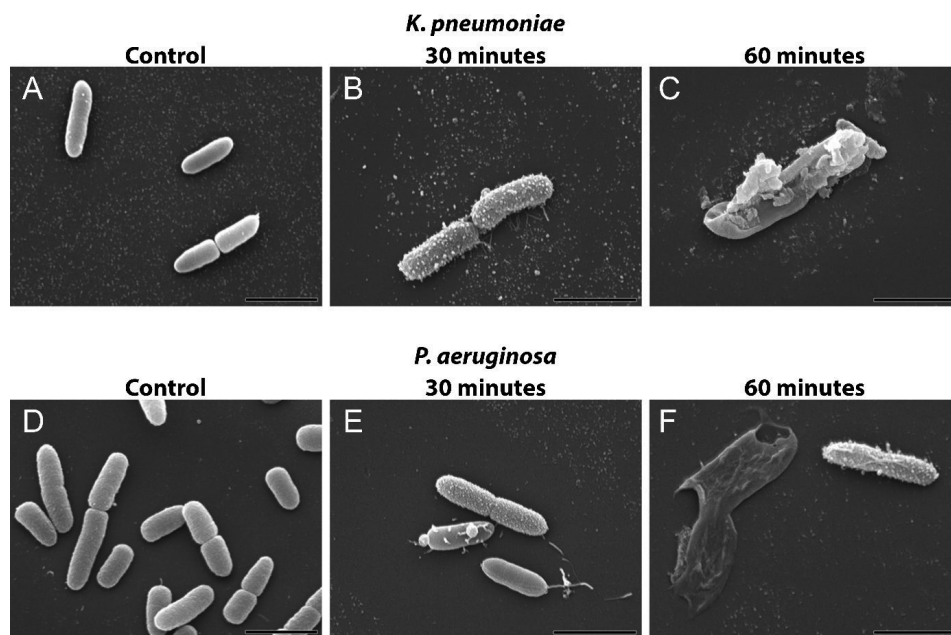


Figure 3. SEM micrographs of *K. pneumoniae* ATCC 13833 and *P. aeruginosa* PAO1. SEM micrographs of A) untreated *K. pneumoniae*; B) *K. pneumoniae* after 30 minutes incubation with SET-M33 at MIC; C) *K. pneumoniae* after 60 minutes incubation with SET-M33 at MIC; D) untreated *P. aeruginosa*; E) *P. aeruginosa* after 30 minutes incubation with SET-M33 at MIC; F) *P. aeruginosa* after 60 minutes incubation with SET-M33 at MIC. Scale bar 2 μ m.

Some linear peptides are reported to kill bacteria very quickly¹⁶, while others, such as magainin-2, kill bacteria after 15-90 minutes. SET-M33 damages bacteria in the latter time range: indeed, microscopy only showed initial signs of bacterial membrane disturbance in very few cells after 10-15 minutes of exposure. With longer exposure, the damage to bacterial membranes increased in frequency and severity.

Peptide conformation – Nuclear magnetic resonance (NMR) structure analysis and circular dichroism (CD) spectra

The supramolecular structure of peptides is important and has been extensively studied in interactions of peptides with bacterial membranes^{16,39,40}. The NMR spectra of free SET-M33 showed a chemical shift index typical of a random coiled conformation and no significant inter-residue NOEs, indicating that the peptide explores a large conformational space. On addition of SDS-d25 micelles, the NMR spectrum of SET-M33 undergoes a generalized broadening, caused by the production of slow-tumbling high-mass species, precluding further analysis. The high-mass species could be aggregates of SET-M33-SDS-d25, possibly promoted by the multimericity of SET-M33. We therefore synthesized an analogue peptide, Q-33, in linear form and capped it with an additional amino acid (Q-KKIRVRLSA) at the N-terminus in order to generate a model of SET-M33 that could be studied in the presence of SDS-d25. Q-33 has an extremely lower half life in serum and plasma than SET-M33, 2 hours versus 24 hours, and consistently it has a lower activity against Gram-negative bacteria^{41,42}. The additional Q allowed us to study the structure of all residues, including the first lysine. Q-33 did not show any stable conformation in water, but addition of SDS-d25 micelles caused a generalized dispersion of proton resonances and the emergence of NOE peaks, indicating that a stable conformer was present as a consequence of the peptide micelle interaction. In particular, NOE signals of the $H\alpha_i$ - HN_{i+3} , $H\alpha_i$ - $H\beta_{i+3}$ and HN_i - HN_{i+2} types for residue $i=1-6$ are diagnostic of α -helix conformation spanning residues 1-9 (Figure 5A). Peak integration of a total set of 32 NOEs allowed us to calculate the relative interproton distances, which were used as constraints for simulation of torsion angle dynamics and subsequent peptide structure calculations. The resulting structure showed a regular α -helix encompassing the full-length of the peptide.

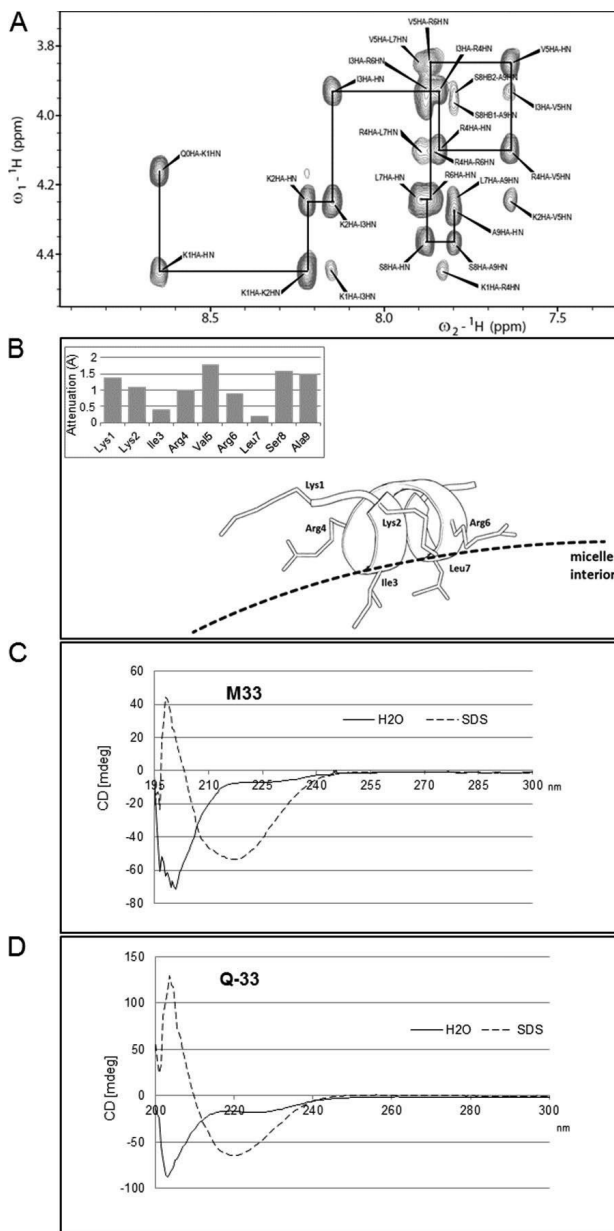


Figure 5. A) NOESY spectrum of Q-33 peptide in the presence of SDS-d25 micelles showing the Ha-HN correlation path typical of α -helices. B) Structural model of peptide conformation and interaction geometry with micelle surface (dashed line) as derived from NMR data, attenuation values A obtained by adding the soluble paramagnetic probe Gd(III)DTPA-BMA to the peptide/SDS-d25 sample are reported in the upper part. C) CD spectrum of SET-M33 100 μM in water and SDS 30 mM. D) CD spectrum of Q-33 100 μM in water and SDS 30 mM.

To assess the interaction geometry of the helix with SDS-d25 micelles, a paramagnetic solution-NMR experiment was performed. Total correlation spectroscopy (TOCSY) spectra of the peptide-micelle system were acquired in the presence and absence of increasing concentrations of the paramagnetic probe Gd(III)DTPA-BMA. The soluble probe causes nuclear spin relaxation proportional to the local surface accessibility of the molecule investigated⁴³⁻⁴⁵. Relaxation is measured by calculating the decrease in peak volumes on addition of the probe, and is summarized as a bare number, the attenuation value *A*, which ranges from 0 to 2 and can be determined for each known proton peak. Protons shielded by contact with the solvent, and therefore not accessible to the probe, show low *A* values, while exposed protons show high *A* values (Figure 5B, upper part). Attenuation analysis was carried out on the Q-33-micelle system and an accurate accessibility profile was determined. Residues I3 and L7 showed much lower accessibility of the probe to their sidechains, and this can be ascribed to shielding by close interaction with the micelle surface. Charged residue pairs K1/R4 and K2/R6, situated on the opposite side of the helix, showed a higher *A* value, while V5 and S8 showed the highest attenuation due to their high exposure to the solvent. The resulting structure was a helix lying on the micelle surface with I3/L7 sidechains inserted into the SDS-d25 assembly, and R and K sidechains arranged parallel to the surface, their charged tips interacting with the negative sulfate groups (Figure 5B). This facial amphiphilic structure has already been reported for other positively charged peptides⁴⁶, such as LL37 fragments⁴⁷ and CRAMP⁴⁸.

Finally, we wanted to assess whether SET-M33 and Q-33 had the same ability to adopt a helix conformation in a membrane mimicking environment, using CD. The technique proved to be applicable to both the tetrabranched and the linear peptide. SET-M33 and Q-33 CD spectra were recorded at room temperature in water and in SDS 30 mM. In line with the NMR experiments, SET-M33 showed a non-structured conformation in water but the CD spectrum shifted sharply to longer wavelengths in the presence of SDS micelles (Figure 5C), and the calculated helix ratio switched from 0% to 30%. A similar result was obtained with Q-33 (Figure 5D): the spectra recorded in water had a calculated helix ratio of 3.3% compared to 39% in the presence of SDS micelles. The

CD spectra of SET-M33 and Q-33, recorded with or without micelles, were very similar, confirming that Q-33 was a reliable model of SET-M33 for the NMR experiments.

Selectivity / hemolytic activity

The ability of cationic peptides to stabilize as an α -helix, and particularly as a facial amphiphilic structure, is often associated with self-aggregation and undesired peptide interactions with blood proteins due to exposed hydrophobic surfaces⁴⁶. The tendency to self-aggregate is correlated to hydrophobicity and provides an indirect estimate of the propensity for partitioning into lipid membranes with unselective detergent-like characteristics. Antimicrobial peptides need to be selective for prokaryotic membranes; a well-established method of verifying their ability to damage eukaryotic cell membranes is to measure their hemolytic activity⁴⁹. Our results showed that red blood cells incubated with increasing concentrations of SET-M33 did not show more than 26% lysis, even using a concentration of 1.8 mg/mL (320 μ M), which is more than 100-fold the MIC (Figure 6).

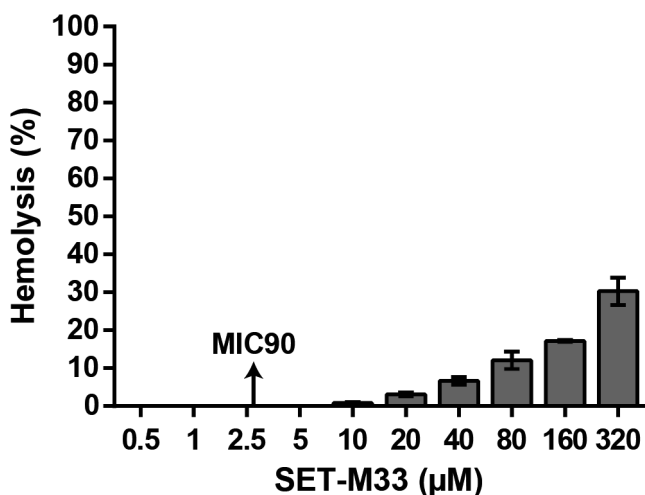


Figure 6. Hemolytic activity of SET-M33. Percentage of red blood cell hemolysis after 24 hours incubation at 37 °C. The MIC required to inhibit 90% of tested isolates (MIC90) of *K. pneumoniae* and *P. aeruginosa* is indicated at 2.7 μ M SET-M33.

In contrast with other cationic peptides⁵⁰, SET-M33 showed very little hemolytic activity against red blood cells, although it shares the ability to form a regular α -helix shape. Indeed, SET-M33 also proved not to be cytotoxic to human bronchial epithelial cells (16HBE14 and CFBE41)²³. Self-aggregation, often associated with amphiphilic structures and undesired secondary effects⁵⁰, was also studied in FPLC experiments (Supplementary Figure S1) and showed that no self-aggregation occurred when SET-M33 was dissolved in PBS. The presence of LPS promoted the formation of high-mass hetero-multimers, but not homo-multimers, in line with what we observed and described above in relation to SDS.

Conclusions

Current understanding of the mechanism of action of cationic AMPs includes a first step of electrostatic attraction between the cationic peptide and the negatively charged bacterial outer membrane. As SET-M33 is a cationic amphiphilic peptide it is attracted to the negatively charged bacterial membrane. Once close to the microbial surface, AMPs need to cross the polysaccharide cell wall barrier before interacting with the cytoplasmic membrane^{15,51,52}. In line with this, in previous studies, SET-M33 was shown, by surface plasmon resonance, to bind LPS of *K. pneumoniae* and *P. aeruginosa*⁵³ and the binding prevented tumor necrosis factor α (TNF- α) release, neutralizing endotoxin activity *in vitro* and *in vivo*^{22,42}. In the present study, NMR investigation of Q-33/SDS micelles in solution and in the presence of a paramagnetic probe showed that the α -helix arranges itself on the surface of micelles as previously described for other antimicrobial peptides⁵⁴⁻⁵⁶. Though direct measurement of the geometry of SET-M33/SDS micelle interactions was not possible, we demonstrated with CD that the structural transition observed using Q-33/SDS micelles also occurs using the original tetrabranched SET-M33 peptide. The α -helix showed to be partially buried in the lipid-bilayer. In the course of 15 to 60 minutes, the signs of membrane damages are, indeed, evident in electron microscopy. We also knew that SET-M33 is internalized in *E. coli* within 5 minutes, proving that it can cross cell wall and plasma membranes,

causing enhanced membrane permeability, as observed with fluorescent probes⁴². Bacterial death may realistically be caused by impairment of the membrane homeostasis and functionality.

Interestingly, SET-M33 is different from other α -helix antimicrobial peptides in that it shows little propensity to self-aggregate and also no hemolytic activity. Homo-aggregation, which is considered related with undesired toxicity^{49,50}, is never observed. This aspect probably contributes in preventing non-specific interactions with eukaryotic cells^{49,50} and indeed correlates with an acceptable tolerability profile obtained in toxicology studies in mice²¹.

SET-M33 does not show any cross-resistance with colistin in colistin-resistant bacteria and, differently from colistin, it appears to generate substantially no resistance within 24 hours of exposure in extensively resistant isolates of *K. pneumoniae* and *P. aeruginosa*. These observations suggest that the two peptides have a different mechanism of action. SET-M33 is attracted onto the surface of bacteria by the anionic charges of the cell wall. Being the core of the branched peptide completely flexible, we speculate that in the presence of phospholipid-bilayers, the peptide can assume a star like conformation, where hydrophobic residues are buried in the surface and hydrophilic residues point outwards. The disturbance of bi-layers integrity, produced by SET-M33's peculiar way to interact with membranes, makes it more difficult for bacteria to trigger resistance mechanisms than it is for colistin.

Finally SET-M33, in contrast to other similar antimicrobial peptides such as colistin, does not generate resistant mutants after 24 hours of exposure, and non-specific interactions or toxicity against eukaryotic cell membranes, suggesting that SET-M33 is a promising new option for the treatment of Gram-negative antibiotic-resistant infections.

Acknowledgements

We thank Silvia Scali for qualified assistance with peptide synthesis and Giacomo Landi for support with FPLC chromatography.

Funding

Setlance srl and Erasmus University Medical Center Rotterdam received funding from the European Union's Seventh Programme for Research, Technological Development and Demonstration under grant agreement No. 604434 (PneumoNP). A.P. received funding from the Italian Foundation for Cystic Fibrosis (Project FFC#17/2016).

Competing interests

Chiara Falciani, Alessandro Pini and Luisa Bracci are co-founders of Setlance srl. SET-M33 is owned by Setlance srl.

References

1. Kahlmeter G. An international survey of the antimicrobial susceptibility of pathogens from uncomplicated urinary tract infections: the ECO-SENS Project. *Journal of Antimicrobial Chemotherapy*. 2003;51(1):69-76.
2. Chalmers JD, Rother C, Salih W, Ewig S. Healthcare-associated pneumonia does not accurately identify potentially resistant pathogens: a systematic review and meta-analysis. *Clinical Infectious Diseases*. 2013;58(3):330-9.
3. Karaikos I, Giamarellou H. Multidrug-resistant and extensively drug-resistant Gram-negative pathogens: current and emerging therapeutic approaches. *Expert Opinion on Pharmacotherapy*. 2014;15(10):1351-70.
4. Fair RJ, Tor Y. Antibiotics and bacterial resistance in the 21st century. *Perspectives in Medicinal Chemistry*. 2014;6:PMC. S14459.
5. Maragakis LL, Perencevich EN, Cosgrove SE. Clinical and economic burden of antimicrobial resistance. *Expert Review of Anti-infective Therapy*. 2008;6(5):751-63.
6. Organization WH. Antimicrobial resistance: global report on surveillance: World Health Organization; 2014.
7. Hancock RE, Sahl H-G. Antimicrobial and host-defense peptides as new anti-infective therapeutic strategies. *Nature Biotechnology*. 2006;24(12):1551.
8. de la Fuente-Nunez C, Silva ON, Lu TK, Franco OL. Antimicrobial peptides: role in human disease and potential as immunotherapies. *Pharmacology & Therapeutics*. 2017;178:132-40.
9. Haney EF, Mansour SC, Hancock RE. Antimicrobial peptides: An introduction. *Antimicrobial Peptides*: Springer; 2017. p. 3-22.
10. Zhang L-j, Gallo RL. Antimicrobial peptides. *Current Biology*. 2016;26(1):R14-R9.
11. Roscia G, Falciani C, Bracci L, Pini A. The development of antimicrobial peptides as new antibacterial drugs. *Current Protein and Peptide Science*. 2013;14(8):641-9.

12. Brunetti J, Falciani C, Bracci L, Pini A. Models of in-vivo bacterial infections for the development of antimicrobial peptide-based drugs. *Current Topics in Medicinal Chemistry*. 2017;17(5):613-9.
13. Epanand RM, Vogel HJ. Diversity of antimicrobial peptides and their mechanisms of action. *Biochimica et Biophysica Acta (BBA)-Biomembranes*. 1999;1462(1-2):11-28.
14. Bechinger B, Lohner K. Detergent-like actions of linear amphipathic cationic antimicrobial peptides. *Biochimica et Biophysica Acta (BBA)-Biomembranes*. 2006;1758(9):1529-39.
15. Cushnie TT, O'Driscoll NH, Lamb AJ. Morphological and ultrastructural changes in bacterial cells as an indicator of antibacterial mechanism of action. *Cellular and Molecular Life Sciences*. 2016;73(23):4471-92.
16. Brogden KA. Antimicrobial peptides: pore formers or metabolic inhibitors in bacteria? *Nature Reviews Microbiology*. 2005;3(3):238.
17. Wilmes M, Cammue BP, Sahl H-G, Thevissen K. Antibiotic activities of host defense peptides: more to it than lipid bilayer perturbation. *Natural Product Reports*. 2011;28(8):1350-8.
18. Bierbaum G, Sahl H-G. Lantibiotics: mode of action, biosynthesis and bioengineering. *Current Pharmaceutical Biotechnology*. 2009;10(1):2-18.
19. Epanand RM, Epanand RF. Bacterial membrane lipids in the action of antimicrobial agents. *Journal of Peptide Science*. 2011;17(5):298-305.
20. Epanand RM, Epanand RF. Domains in bacterial membranes and the action of antimicrobial agents. *Molecular BioSystems*. 2009;5(6):580-7.
21. Pollini S, Brunetti J, Sennati S, Rossolini GM, Bracci L, Pini A, et al. Synergistic activity profile of an antimicrobial peptide against multidrug-resistant and extensively drug-resistant strains of Gram-negative bacterial pathogens. *Journal of Peptide Science*. 2017;23(4):329-33.
22. Brunetti J, Falciani C, Roscia G, Pollini S, Bindi S, Scali S, et al. In vitro and in vivo efficacy, toxicity, bio-distribution and resistance selection of a novel antibacterial drug candidate. *Scientific Reports*. 2016;6:26077.
23. Brunetti J, Roscia G, Lampronti I, Gambari R, Quercini L, Falciani C, et al. Immunomodulatory and anti-inflammatory activity in vitro and in vivo of a novel antimicrobial candidate. *Journal of Biological Chemistry*. 2016;291(49):25742-8.
24. Pini A, Lozzi L, Bernini A, Brunetti J, Falciani C, Scali S, et al. Efficacy and toxicity of the antimicrobial peptide M33 produced with different counter-ions. *Amino Acids*. 2012;43(1):467-73.
25. Pini A, Falciani C, Mantengoli E, Bindi S, Brunetti J, Lozzi S, et al. A novel tetrabranching antimicrobial peptide that neutralizes bacterial lipopolysaccharide and prevents septic shock in vivo. *The FASEB Journal*. 2010;24(4):1015-22.
26. Bracci L, Falciani C, Lelli B, Lozzi L, Runci Y, Pini A, et al. Synthetic peptides in the form of dendrimers become resistant to protease activity. *Journal of Biological Chemistry*. 2003;278(47):46590-5.
27. Vila-Farrés X, Ferrer-Navarro M, Callarisa AE, Martí S, Espinal P, Gupta S, et al. Loss of LPS is involved in the virulence and resistance to colistin of colistin-resistant *Acinetobacter nosocomialis* mutants selected in vitro. *Journal of Antimicrobial Chemotherapy*. 2015;70(11):2981-6.
28. Testing ECoAS, Testing ECoAS. Breakpoint tables for interpretation of MICs and zone diameters. Version 7.1, 2017. 2017.
29. de Steenwinkel JE, de Knecht GJ, ten Kate MT, van Belkum A, Verbrugh HA, Kremer K, et al. Time-kill kinetics of anti-tuberculosis drugs, and emergence of resistance, in relation to metabolic activity of *Mycobacterium tuberculosis*. *Journal of Antimicrobial Chemotherapy*. 2010;65(12):2582-9.
30. Goddard T, Kneller D. San Francisco: University of California. SPARKY.
31. Güntert P, Mumenthaler C, Wüthrich K. Torsion angle dynamics for NMR structure calculation with the new program DYANA. *Journal of Molecular Biology*. 1997;273(1):283-98.
32. Lampiris H, Maddix D. Clinical use of antimicrobial agents (chapter 51). In: Katzung B, Masters S, Trevors A, editors. *Basic and Clinical Pharmacology* 2012.

33. Campos MA, Vargas MA, Regueiro V, Llompart CM, Albertí S, Bengoechea JA. Capsule polysaccharide mediates bacterial resistance to antimicrobial peptides. *Infection and Immunity*. 2004;72(12):7107-14.
34. Li J, Nation RL, Turnidge JD, Milne RW, Coulthard K, Rayner CR, et al. Colistin: the re-emerging antibiotic for multidrug-resistant Gram-negative bacterial infections. *The Lancet Infectious Diseases*. 2006;6(9):589-601.
35. Petrosillo N, Giannella M, Antonelli M, Antonini M, Barsic B, Belancic L, et al. Clinical experience of colistin-glycopeptide combination in critically ill patients infected with Gram-negative bacteria. *Antimicrobial Agents and Chemotherapy*. 2014;58(2):851-8.
36. Ah Y-M, Kim A-J, Lee J-Y. Colistin resistance in *Klebsiella pneumoniae*. *International Journal of Antimicrobial Agents*. 2014;44(1):8-15.
37. Giske CG. Contemporary resistance trends and mechanisms for the old antibiotics colistin, temocillin, fosfomicin, mecillinam and nitrofurantoin. *Clinical Microbiology and Infection*. 2015;21(10):899-905.
38. Liu Y-Y, Wang Y, Walsh TR, Yi L-X, Zhang R, Spencer J, et al. Emergence of plasmid-mediated colistin resistance mechanism MCR-1 in animals and human beings in China: a microbiological and molecular biological study. *The Lancet Infectious Diseases*. 2016;16(2):161-8.
39. Hancock RE, Lehrer R. Cationic peptides: a new source of antibiotics. *Trends in Biotechnology*. 1998;16(2):82-8.
40. Kemayo Koumkoua P, Aisenbrey C, Salnikov E, Rifi O, Bechinger B. On the design of supramolecular assemblies made of peptides and lipid bilayers. *Journal of Peptide Science*. 2014;20(7):526-36.
41. Pini A, Giuliani A, Falciani C, Runci Y, Ricci C, Lelli B, et al. Antimicrobial activity of novel dendrimeric peptides obtained by phage display selection and rational modification. *Antimicrobial Agents and Chemotherapy*. 2005;49(7):2665-72.
42. Pini A, Giuliani A, Falciani C, Fabbrini M, Pileri S, Lelli B, et al. Characterization of the branched antimicrobial peptide M6 by analyzing its mechanism of action and in vivo toxicity. *Journal of Peptide Science: an official publication of the European Peptide Society*. 2007;13(6):393-9.
43. Bernini A, Spiga O, Venditti V, Prischi F, Botta M, Croce G, et al. The use of a ditopic Gd (III) paramagnetic probe for investigating α -bungarotoxin surface accessibility. *Journal of Inorganic Biochemistry*. 2012;112:25-31.
44. Bernini A, De Angelis LH, Morandi E, Spiga O, Santucci A, Assfalg M, et al. Searching for protein binding sites from molecular dynamics simulations and paramagnetic fragment-based NMR studies. *Biochimica et Biophysica Acta (BBA)-Proteins and Proteomics*. 2014;1844(3):561-6.
45. Bernini A, Venditti V, Spiga O, Ciutti A, Prischi F, Consonni R, et al. NMR studies on the surface accessibility of the archaeal protein Sso7d by using TEMPOL and Gd(III)(DTPA-BMA) as paramagnetic probes. *Biophysical Chemistry*. 2008;137(2):71-5.
46. Xiong M, Lee MW, Mansbach RA, Song Z, Bao Y, Peek RM, et al. Helical antimicrobial polypeptides with radial amphiphilicity. *Proceedings of the National Academy of Sciences*. 2015;112(43):13155-60.
47. Li X, Li Y, Han H, Miller DW, Wang G. Solution structures of human LL-37 fragments and NMR-based identification of a minimal membrane-targeting antimicrobial and anticancer region. *Journal of the American Chemical Society*. 2006;128(17):5776-85.
48. Yu K, Park K, Kim Y, Kang SW, Shin S, Hahn KS. Solution structure of a cathelicidin-derived antimicrobial peptide, CRAMP as determined by NMR spectroscopy. *The Journal of Peptide Research*. 2002;60(1):1-9.
49. Prenner EJ, Kiricsi M, Jelokhani-Niaraki M, Lewis RN, Hodges RS, McElhaneey RN. Structure-Activity Relationships of Diastereomeric Lysine Ring Size Analogs of the Antimicrobial Peptide Gramicidin S mechanism of action and discrimination between bacterial and animal cell membranes. *Journal of Biological Chemistry*. 2005;280(3):2002-11.

50. Jiang Z, Vasil A, Vasil M, Hodges R. "Specificity determinants" improve therapeutic indices of two antimicrobial peptides piscidin 1 and dermaseptin S4 against the gram-negative pathogens *Acinetobacter baumannii* and *Pseudomonas aeruginosa*. *Pharmaceuticals*. 2014;7(4):366-91.
51. Datta A, Bhattacharyya D, Singh S, Ghosh A, Schmidtchen A, Malmsten M, et al. Role of aromatic amino acids in lipopolysaccharide and membrane interactions of antimicrobial peptides for use in plant disease control. *Journal of Biological Chemistry*. 2016;291(25):13301-17.
52. Datta A, Ghosh A, Airoldi C, Sperandeo P, Mroue KH, Jiménez-Barbero J, et al. Antimicrobial peptides: insights into membrane permeabilization, lipopolysaccharide fragmentation and application in plant disease control. *Scientific Reports*. 2015;5:11951.
53. Falciani C, Lozzi L, Pollini S, Luca V, Carnicelli V, Brunetti J, et al. Isomerization of an antimicrobial peptide broadens antimicrobial spectrum to gram-positive bacterial pathogens. *PLOS ONE*. 2012;7(10):e46259.
54. Hartmann M, Berditsch M, Hawecker J, Ardakani MF, Gerthsen D, Ulrich AS. Damage of the bacterial cell envelope by antimicrobial peptides gramicidin S and PGLa as revealed by transmission and scanning electron microscopy. *Antimicrobial Agents and Chemotherapy*. 2010;54(8):3132-42.
55. Sato H, Feix JB. Peptide-membrane interactions and mechanisms of membrane destruction by amphipathic α -helical antimicrobial peptides. *Biochimica et Biophysica Acta (BBA)-Biomembranes*. 2006;1758(9):1245-56.
56. Bahar A, Ren D. Antimicrobial peptides. *Pharmaceuticals*. 2013;6(12):1543-75.

Supplementary Table S1. Phenotypic characterization of bacterial isolates

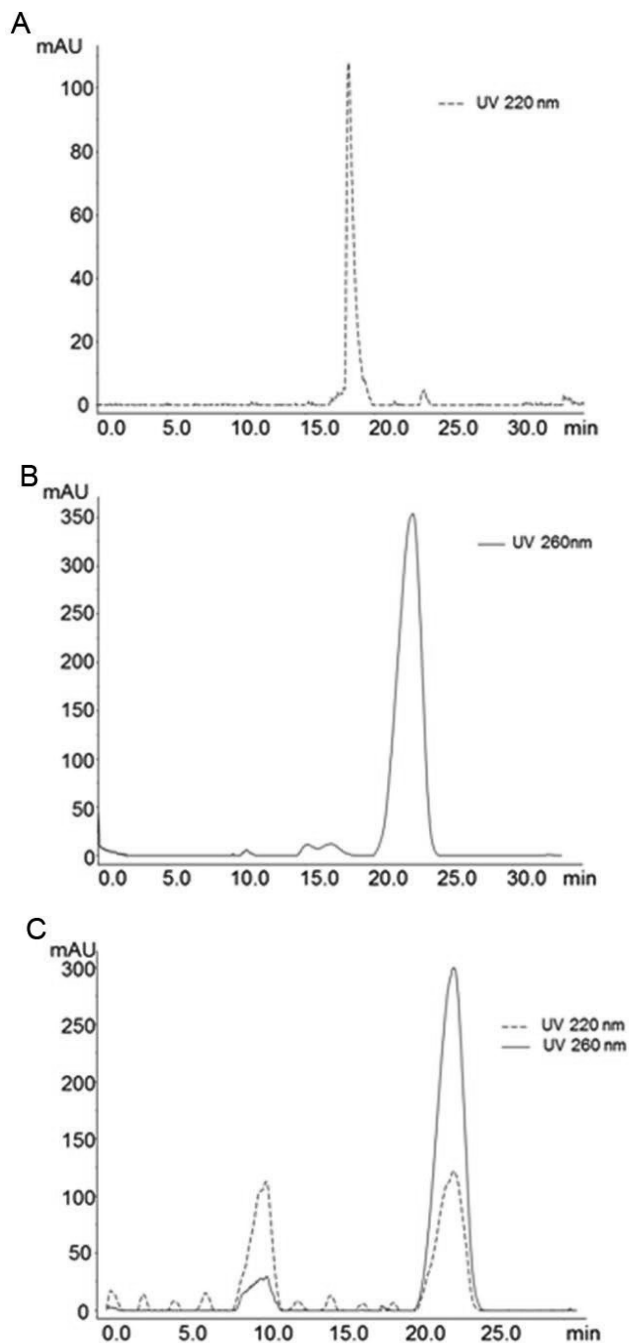
Bacterial isolate	colistin-susceptible	colistin-resistant	colistin-susceptible	colistin-resistant
	<i>K. pneumoniae</i> R-DYK 4861	<i>K. pneumoniae</i> R-DYK 4861	<i>P. aeruginosa</i> B-162	<i>P. aeruginosa</i> B-162
Ampicillin	≥32	≥32		
Amoxicillin/ Clavulanic Acid	≥32	≥32		
Piperacillin/ Tazobactam	≥128	≥128	≥128	≥128
Cefuroxime	≥64	≥64		
Cefuroxime Axetil	≥64	≥64		
Cefoxitin	≥64	≥64		
Cefotaxime	≥64	≥64		
Ceftazidime	16	16	≥64	32
Cefepime	≥64	≥64	≥64	≥64
Imipenem	≥16	≥16	≥16	≥16
Meropenem	≥16	≥16	≥16	≥16
Gentamicin	≥16	≥16	≥16	≥16
Tobramycin	≥16	≥16	≥16	≥16
Ciprofloxacin	≥4	≥4	≥4	≥4
Norfloxacin	≥16	≥16		
Trimethoprim	≥16	≥16		
Trimethoprim/ sulfamethoxazole	≥320	≥320		
Colistin	≤0.5	≥16	≤0.5	≥16

MICs (mg/L) were determined using the automated VITEK® 2 antimicrobial identification system and AST-N140 cards. Interpretation of antimicrobial susceptibility was defined by the VITEK® antimicrobial identification system as susceptible, intermediate (italic), or resistant (bold) based on EUCAST 2017 guidelines.

Supplementary Table S2. Change in colistin-resistant *K. pneumoniae* R-DYK 4861 and *P. aeruginosa* B-162 susceptibility to M33 and colistin after 24 hours exposure to antibiotic as determined by MIC assay

Antibiotic concentration (mg/L)	M33 (mg/L)		Colistin (mg/L)	
	colistin-resistant <i>K. pneumoniae</i>	colistin-resistant <i>P. aeruginosa</i>	colistin-resistant <i>K. pneumoniae</i>	colistin-resistant <i>P. aeruginosa</i>
control	16	16	>512	512
0.125	32	16		
0.25	16	16		
0.5	32	16		
1	32	16	>512	256
2	64	16	>512	256
4	64	16	>512	256
8	>64	16	>512	256
16	>64	16	>512	512
32	Nd	16 ²	>512	512
64	Nd	nd	>512	512
128			>512	512
256			>512	512 ¹
512			>512	>512 ¹

Colistin-resistant bacterial cultures were exposed to two-fold increasing concentrations of SET-M33 or colistin for 24 hours at 37 °C under shaking conditions. When bacteria re-grew after 24 hours exposure to antibiotic, their MIC susceptibilities (performed in triplicate) were also determined and the median value reported. nd, not determined (no regrowth in the original time-kill kinetics experiment); ¹, one out of three samples did not show bacterial re-growth; ², two out of three samples did not show bacterial re-growth.



Supplementary Figure S1. Fast protein liquid chromatography (FPLC). A) SET-M33; B) Lipopolysaccharide (LPS); C) LPS and SET-M33. Peak at $t_R = 9$ minutes might correspond to SET-M33-LPS hetero-multimer.

Chapter 6 Successful high-dosage monotherapy of tigecycline in a multidrug-resistant *Klebsiella pneumoniae* pneumonia-septicemia model in rats

Chapter 7 *In vitro* and *in vivo* bacterial killing activity of novel antimicrobial peptide SET-M33-nanomedicines against multidrug-resistant *Klebsiella pneumoniae*

Chapter 8 Therapeutic efficacy of novel antimicrobial peptide AA139-nanomedicines in a multidrug-resistant *Klebsiella pneumoniae* pneumonia-septicemia model in rats

The chapters in **Section III** cover the *in vivo* investigation of selected antimicrobial peptide (AMP)-nanomedicines in uninfected and infected rats.

In **Chapter 6**, we established and characterized a rat model of pneumonia-septicemia caused by multidrug-resistant *Klebsiella pneumoniae* which was validated using a high-dose treatment regimen of tigecycline, with meropenem serving as comparator drug.

Chapter 7 and **Chapter 8** cover the investigation of SET-M33-nanomedicines and AA139-nanomedicines, respectively. Nanomedicines were selected by screening of their *in vitro* antimicrobial activity. The nanomedicines were administered by endotracheal aerosolization at a single dose to determine their limiting dose in uninfected rats and to assess the bacterial killing activity in the lung of infected rats. Based on these results, the most promising AA139-nanomedicines were selected for continued investigation in **Chapter 8**. Biodistribution of nanomedicines was investigated in uninfected rats, and therapeutic efficacy studies were performed in infected rats using a 10-day treatment.



Section



IN VIVO INVESTIGATIONS

Abstract

Background: Recent scientific reports on the use of high dose tigecycline monotherapy as a 'drug of last resort' warrant further research into the use of this regimen for the treatment of severe multidrug-resistant Gram-negative bacterial infections. In the current study, the therapeutic efficacy of tigecycline monotherapy was investigated and compared to meropenem monotherapy in a newly developed rat model of fatal lobar pneumonia-septicemia.

Methods: A *Klebsiella pneumoniae* producing extended-spectrum β -lactamase (ESBL) and an isogenic variant producing *K. pneumoniae* carbapenemase (KPC) were used in the study. Both strains were tested for their *in vitro* antibiotic susceptibility and used to induce pneumonia-septicemia in rats, which was characterized using disease progression parameters. Therapy with tigecycline or meropenem was initiated at the moment that rats suffered from progressive infection and was administered 12-hourly over 10 days. The pharmacokinetics of meropenem were determined in infected rats.

Results: In rats with ESBL pneumonia-septicemia, the minimum dosage of meropenem achieving survival of all rats was 25 mg/kg/day. However, in rats with KPC pneumonia-septicemia this meropenem dosage was unsuccessful. In contrast, all rats with KPC pneumonia-septicemia were successfully cured by administration of high-dose tigecycline monotherapy of 25 mg/kg/day (i.e., the minimum tigecycline dosage achieving 100% survival of rats with ESBL pneumonia-septicemia in a previous study).

Conclusions: The current study supports recent literature recommending high-dose tigecycline as a last resort regimen for the treatment of severe multidrug-resistant bacterial infections. The use of ESBL- and KPC-producing *K. pneumoniae* strains in the current rat model of pneumonia-septicemia enables further investigation, helping provide supporting data for follow-up clinical trials in patients suffering from severe multidrug-resistant bacterial respiratory infections.



Chapter

6



SUCCESSFUL HIGH-DOSAGE MONOTHERAPY OF TIGECYCLINE IN A MULTIDRUG-RESISTANT KLEBSIELLA PNEUMONIAE PNEUMONIA- SEPTICEMIA MODEL IN RATS

*Hessel van der Weide, Marian T. ten Kate, Denise M.C. Vermeulen-de Jongh,
Aart van der Meijden, Rixt A. Wijma, Stefan A. Boers, Mireille van Westreenen,
John P. Hays, Wil H.F. Goessens, Irma A.J.M. Bakker-Woudenberg*

Introduction

Recent data from the US indicate that Gram-negative bacteria are responsible for more than 30% of hospital-acquired infections¹. A complicating factor in the treatment of infections caused by Gram-negative bacteria is the worldwide increase of antimicrobial resistance. In particular, Gram-negative bacteria resistant to carbapenem antibiotics – due to the presence of plasmid-mediated multidrug-resistance, such as with extended-spectrum β -lactamase (ESBL) or *Klebsiella pneumoniae* carbapenemase (KPC) – can no longer be effectively treated with β -lactam antibiotics and tend to be susceptible only to ‘drugs of last resort’^{2,3}.

Tigecycline (an antibiotic belonging to the class of glycylcyclines) is one such drug of last resort, although resistance to tigecycline has been reported⁴. Further, although the United States Food and Drug Administration (FDA) issued a warning in 2013 relating to an apparent increased death rate during antibiotic treatment using tigecycline (loading dose of 100 mg followed by 50 mg every 12 hours)⁵, multiple studies have suggested that using a high dose of tigecycline could actually improve outcome in comparison to conventional dosing^{6,7}. Additionally, the European Committee on Antimicrobial Susceptibility Testing (EUCAST) has recently recommended the use of high-dosage tigecycline treatment in seriously ill patients infected with multidrug-resistant bacteria⁸. As well as dosing issues, another debate about the role of tigecycline involves its use in monotherapy as opposed to combination therapy, particularly in the treatment of multidrug-resistant Gram-negative bacterial infections. This issue is complicated by the fact that comparative clinical efficacy studies into tigecycline are complex, involving differing patient characteristics, various combinations of antibiotics, and differences in the nature and severity of infections^{9,10}.

To investigate this issue further, in rats we developed a model of bilateral pneumonia-septicemia in which we were able to compare the therapeutic efficacy of individual antibiotics at similar conditions of severity, duration of infection, and host defense. This novel pneumonia-septicemia model was based on a previously established rat model of unilateral pneumonia-septicemia (in which one lung was left uninfected), which was

intended for antimicrobial pharmacokinetic and pharmacodynamic studies¹¹. Further, in order to mimic the actual clinical situation, the rat infection model is fatal if left untreated, with rat survival (based on rats reaching humane endpoints) as a treatment outcome parameter. In the present study, we established and characterized the lobar pneumonia leading to fatal septicemia, which was caused by either an ESBL-producing *K. pneumoniae* strain or its isogenic KPC-producing variant. The model was used to investigate the therapeutic efficacy of tigecycline as monotherapy as compared to meropenem monotherapy, a potent carbapenem antibiotic which serves as the conventional treatment for multidrug-resistant Gram-negative bacterial infections¹².

Materials and Methods

Bacterial strains

K. pneumoniae American Type Culture Collection (ATCC) 43816TM (capsular serotype 2) was used as a parent strain to generate the isogenic ESBL-producing variant *K. pneumoniae* ESBL EMC2003 (referred to in this study as *K. pneumoniae* ESBL) and the isogenic KPC-producing variant *K. pneumoniae* KPC EMC2014 (referred to in this study as *K. pneumoniae* KPC) via bacterial conjugation with an ESBL-producing or KPC-producing clinical isolate and subsequent selection on antibiotic agar plates. The stability of both plasmid-containing strains was assessed through five consecutive passages in Mueller-Hinton II (MH-II) broth (Becton Dickinson BV, Vianen, the Netherlands). The virulence of the bacterial strains was maintained by rat lung passage every 12 months. ATCC Quality Control strains *K. pneumoniae* ATCC 13883TM (WT), *K. pneumoniae* ATCC 700603TM (ESBL) and *K. pneumoniae* ATCC BAA1705TM (KPC) were used as reference strains.

Genotypic characterization of bacterial strains

Due to the complex relationship between antibiotic resistance and virulence factors, it is important to report the genotypic data of bacterial strains used in microbiological studies^{13,14}. Polymerase chain reaction (PCR) assays were used to verify the presence of

the following resistance genes: cefotaxime-M β -lactamase (CTX-M) groups 1, 2, 8, 9, 25¹⁵; temoniera β -lactamase (TEM)¹⁶; sulfhydryl reagent variable β -lactamase (SHV)¹⁷; oxacillinase β -lactamase (OXA)-1-like¹⁸; OXA-48-like¹⁹; KPC²⁰; and New Delhi metallo- β -lactamase (NDM)-1²¹. Multilocus sequence typing (MLST) was used to investigate genetic relatedness. For this, partial deoxyribonucleic acid (DNA) sequences of the seven housekeeping genes *gapA*, *infB*, *mdh*, *pgi*, *phoE*, *rpoB* and *tonB* were generated and compared using a published high-throughput MLST (HiMLST) strategy²² that had been adapted for *K. pneumoniae* isolates²³. To further assess the genetic relation between the strains, pulsed-field gel electrophoresis (PFGE) was used as previously described²⁴.

Antibiotics and anesthetics

The antibiotics used were amikacin hydrate, ceftazidime hydrate, ciprofloxacin hydrochloride monohydrate, colistin sulfate salt, gentamicin sulfate, meropenem trihydrate, norfloxacin, tigecycline, tobramycin sulfate salt, trimethoprim, and sulfamethoxazole (Sigma-Aldrich Chemie BV, Zwijndrecht, the Netherlands). For co-trimoxazole, the ratio trimethoprim:sulfamethoxazole was 1:19. Meropenem was combined with cilastatin sodium (Bosche Scientific LLC, New Brunswick, NJ, USA) (1:1) when used *in vivo* to inhibit the function of dehydropeptidase enzyme, which is a known catalyst of meropenem in rats²⁵.

The anesthetics used were medetomidine hydrochloride (Eurovet Animal Health BV, Bladel, the Netherlands), fentanyl citrate (Hameln Pharma Plus GmbH, Hameln, Germany) and midazolam hydrochloride (Actavis Group PTC ehf, Hafnarfjörður, Iceland), which were administered together intraperitoneally at 0.5 mg/kg, 50 μ g/kg and 5 mg/kg, respectively. Antagonists were atipamezole hydrochloride (Vetoquinol BV, 's Hertogenbosch, the Netherlands), naloxone hydrochloride dihydrate (Hameln Pharma Plus GmbH) and flumazenil (Fresenius Kabi Nederland BV, Zeist, the Netherlands), which were administered together intraperitoneally at 1.5 mg/kg, 0.7 mg/kg, and 0.3 mg/kg, respectively.

Antimicrobial susceptibility of *K. pneumoniae* strains

The antimicrobial susceptibility of bacterial strains was assessed by minimum inhibitory concentration (MIC) determination using the broth microdilution method following EUCAST guidelines²⁶, which represents the lowest antibiotic concentration needed to inhibit bacterial growth under standardized and predefined laboratory conditions. Phenotypic characterization of bacterial strains was based on antimicrobial susceptibility as determined using the VITEK®2 system and AST-N344 Gram-Negative Susceptibility Cards (bioMérieux Benelux BV, Zaltbommel, the Netherlands).

Concentration- and time-dependent bactericidal activity of antibiotics *in vitro*

The bacterial killing capacity of meropenem and tigecycline was investigated using the time-kill kinetics (TKK) assay as previously described²⁷. Two-fold increasing antibiotic concentrations were used representing $\frac{1}{16}$ -fold up to 32-fold the epidemiological cut-off value (ECOFF) of the two antibiotics as reported by EUCAST²⁸. The ECOFF of *K. pneumoniae* for meropenem is 0.125 mg/L and for tigecycline was 1 mg/L, but has recently been increased to 2 mg/L. Samples were centrifuged at $12,500 \times g$ for 5 min to avoid drug carry-over, serially 10-fold diluted and subcultured on MH-II agar plates (Becton Dickinson BV, Vianen, the Netherlands) for colony-forming units (CFU) counts after 24 hours at 37 °C. At 24 hours, changes in antibiotic susceptibility were determined via MIC assay using subsamples of 1 mL to prepare bacterial inocula.

Animals

Specified pathogen-free (SPF) male strain RP/AEur/RijHsd albino rats bred at the Laboratory Animals Center of Erasmus University Medical Center Rotterdam (Erasmus MC) were used. Rats (age, 10-18 weeks; body weight, 250-350 g) were housed individually in ventilated cages and were given food and water *ad libitum*. Rats were randomly allocated to experimental groups once they reached the appropriate age and body weight. Group sizes were based on estimates of the hazard ratio. Euthanasia was applied by CO₂ exposure when humane endpoints were reached or at termination of experiments.

Ethics

Animals were maintained and handled in accordance with the Guidelines for Accommodation and Care of Animals (European Convention for the Protection of Vertebrate Animals Used for Experimental and Other Scientific Purposes). All animal procedures were performed in accordance with the Dutch Animal Experimentation Act (BWBR0003081) which meets the requirements of the European Union Animal Directive (2010/63/EU). Experimental procedures were approved by the Institutional Animal Care and Use Committee of the Erasmus MC. The current study was designed to abide by the three Rs principles of animal research (replace, reduce, refine) wherever possible²⁹ and was written to conform to the animal research: reporting of *in vivo* experiments (ARRIVE) guidelines for reporting animal research³⁰.

Rat model of pneumonia-septicemia

Acute bilateral pneumonia-septicemia in rats (referred to in this study as ESBL pneumonia-septicemia or KPC pneumonia-septicemia) was established in groups of 11 rats using suspensions of washed bacteria in the logarithmic phase of growth. After intubation and cannulation of the trachea under anesthesia, rats were held in a vertical position and the lungs were inoculated with 60 μ L PBS containing the respective absolute lethal dose (LD¹⁰⁰) inocula: 2×10^6 *K. pneumoniae* ESBL or 6×10^7 *K. pneumoniae* KPC. An implantable programmable temperature transponder (IPTT)-300 (Plexx BV, Elst, the Netherlands) was implanted subcutaneously. Infected rats were monitored 12-hourly for 11 days to assess the disease progression as well as pre-defined humane endpoints by changes in body temperature and body weight, and by external symptoms of disease including ungroomed appearance, pallor, nose bleeding, lack of reactivity, inactivity, instability, or abnormal breathing of rats. Rat survival was based on rats reaching humane endpoints, at which point euthanasia was applied by CO₂ exposure. After dissection, bacteria isolated from lung and blood were identified by matrix-assisted laser desorption/ionization time-of-flight (MALDI-TOF) mass spectrometer (Bruker Daltonics, Bremen, Germany) to rule out co-infection – a pre-established exclusion criterium.

Characterization of pneumonia-septicemia model

The early phase of infection was characterized at 24 hours and 48 hours after initiation of infection by viable counts of *K. pneumoniae* in lungs and blood taken from 6 rats per time point. Blood obtained by cardiac puncture was collected from euthanized rats in lithium-heparin tubes (Sarstedt BV, Etten-Leur, the Netherlands). The five lung lobes were collected separately, each in 2 mL PBS and homogenized using the gentleMACS™ Octo Dissociator (Milteny Biotec BV, Leiden, the Netherlands). Blood and lung homogenates undiluted and in 10-fold dilutions were subcultured on MH-II agar plates (Sigma-Aldrich Chemie BV, Zwijndrecht, the Netherlands) for CFU counts after 24 hours at 37 °C. In blood plasma samples the alanine aminotransferase (ALAT) and aspartate aminotransferase (ASAT) levels were assessed for hepatic function, and the creatinine and blood urea nitrogen (BUN) levels for renal function at the Department of Clinical Chemistry, Erasmus MC. Histopathological examination of the infected lungs at 24 hours after infection was performed in 2 rats with ESBL pneumonia-septicemia and 2 rats with KPC pneumonia-septicemia. In sacrificed rats, *in situ* lungs were fixated with 10% formalin under constant pressure to re-expand the lungs. Segments of the left lung were dehydrated in ethanol and toluol, and finally embedded in paraffin. Paraffin-embedded tissues were cut into 4 µm sections from which one in every 15 cuts was used for hematoxylin-eosin (HE) staining and one for Gram-staining.

Antimicrobial treatment of pneumonia-septicemia

The therapeutic response to meropenem was determined in rats with ESBL pneumonia-septicemia and rats with KPC pneumonia-septicemia. The response to tigecycline was only investigated in rats with KPC pneumonia-septicemia, as this had already been investigated in a previous unilateral pneumonia-septicemia rat model caused by the identical *K. pneumoniae* ESBL strain¹¹. Treatment groups consisted of 11 rats. Antibiotics were always administered intraperitoneally in a volume of 2.5 mL/kg 12-hourly for 10 days, started at 24 hours after initiation of infection. Meropenem in doses ranging from 6.25 to 25 mg/kg/day were administered by 2-fold increases until a minimum effective dose (MED) of meropenem was reached at which all rats survived.

Tigecycline was administered at 25 mg/kg/day i.e. the MED necessary for survival of all rats with ESBL pneumonia-septicemia from a previous study¹¹. Disease progression was monitored 12-hourly. Rats reaching humane endpoints were euthanized and dissected to rule out co-infection.

Pharmacokinetics of meropenem

Meropenem plasma concentrations were determined in 3 rats with ESBL pneumonia-septicemia. Rats received 3 doses of 25 mg/kg/day meropenem 12-hourly, starting at 24 hours after initiation of infection. Blood obtained by tail vein puncture was collected in ethylenediaminetetraacetic acid (EDTA)-coated tubes (Sigma-Aldrich Chemie BV, Zwijndrecht, the Netherlands). Meropenem concentrations were determined by high-performance liquid chromatography-mass spectrometry (HPLC-MS)³¹. The lower limit of quantification of meropenem was 0.20 mg/L. The calibration line was linear from 0.20 to 40.0 mg/L with a determination coefficient of at least 0.995. Rat samples were prepared together with calibration standards and quality control samples at three levels. The values of the volume of distribution (V), the clearance (CL) and the concentration half-life time ($t_{1/2}$) of the meropenem elimination process were calculated using a PKSolver 2.0 one-compartment model of extravascular administration with time delay to account for absorption³². V and CL were presented as a fraction of the absorbed dose (bioavailability, F). The protein binding of meropenem in rats has been reported as 22.4%³³. As only the unbound fraction of the drug is responsible for its antimicrobial effect, the values of: 1) the cumulative percentage of a 12-hour period that the unbound fraction of drug exceeded the MIC ($fT > MIC$) and 2) the highest unbound drug concentration reached in blood plasma (fC_{max}), were calculated based on unbound meropenem concentrations.

Statistical analysis

Kaplan-Meier rat survival curves were generated, and statistical differences in rat survival rates were calculated using the log rank test using Prism 5.01 (Graphpad Inc., San Diego, CA, USA).

Results

Bacterial strains

The results from HiMLST (Supplementary Table S1) and PFGE (data not shown) assays confirmed the isogenicity of the *K. pneumoniae* ESBL and *K. pneumoniae* KPC strains. ESBL and KPC resistance genes were detected via PCR as expected in the respective strains (Supplementary Table S1).

Antimicrobial susceptibility of *K. pneumoniae* strains

The antimicrobial susceptibility of *K. pneumoniae* ESBL and *K. pneumoniae* KPC for clinically relevant antibiotics was assessed by MIC determination and compared with the MIC values of 3 ATCC Quality Control reference strains. The *K. pneumoniae* ESBL strain was resistant to ceftazidime and tobramycin, and susceptible to meropenem based on MIC values (Table 1). The isogenic *K. pneumoniae* KPC strain was resistant to ceftazidime, tobramycin and meropenem. According to the EUCAST 2020 guidelines,

Table 1. MIC values of clinically relevant antibiotics for *K. pneumoniae* strains

Strain	ATCC 43816	EMC 2003	EMC 2014	ATCC 13883	ATCC 700603	ATCC BAA1705
Phenotype	WT Parent	ESBL	KPC	WT	ESBL	KPC
CAZ	0.5	256	256	0.5	64	128
MEM	0.063	0.063	16	0.063	0.063	32
AMK	2	2	2	1	1	32
TOB	0.5	>64	>64	0.5	8	32
CIP	0.031	0.125	0.063	0.125	0.5	>32
NOR	0.125	0.25	0.25	0.25	2	512
SXT	0.5	1	2	0.5	4	>64
CST	0.5	1	0.5	2	1	0.5
TGC	1	1	2	1	16	4

MIC assays were performed in triplicate, median values are displayed. MIC values are interpreted as susceptible, intermediate (italic), or resistant (bold) according to EUCAST 2019 guidelines. CAZ, ceftazidime; MEM, meropenem; AMK, amikacin; TOB, tobramycin; CIP, ciprofloxacin; NOR, norfloxacin; SXT, trimethoprim/sulfamethoxazole expressed as the trimethoprim concentration; CST, colistin; TGC, tigecycline; WT, wildtype.

both *K. pneumoniae* isolates are resistant to tigecycline, as are all the reference strains used in this study²⁶. However, both *K. pneumoniae* isolates still fell within the antimicrobial wild-type distribution of *K. pneumoniae* based on the ECOFF value of tigecycline for *K. pneumoniae* (2 mg/L), and can be considered representative of the tigecycline susceptibility of wild-type *K. pneumoniae* populations – albeit on the high-end of the wild-type distribution²⁸.

VITEK®2 data (Supplementary Table S2) showed that *K. pneumoniae* ESBL and *K. pneumoniae* KPC were both resistant to a wide range of β -lactam antibiotics and aminoglycoside antibiotics.

Concentration- and time-dependent bactericidal activity of antibiotics *in vitro*

The *in vitro* killing capacity of meropenem and tigecycline against *K. pneumoniae* ESBL or *K. pneumoniae* KPC during 24 hours was determined using TKK assays. In the absence of antibiotics, the bacterial populations rapidly increased within 24 hours of incubation (Figure 1). Meropenem showed time-dependent killing against *K. pneumoniae* ESBL. A concentration of ≥ 0.125 mg/L meropenem resulted in a 100-fold reduction in bacterial numbers after 2 hours and complete bacterial elimination after 24 hours. At 0.03 mg/L meropenem, bacteria were initially killed, although after 24 hours, bacterial re-growth occurred up to the level of non-exposed bacterial growth after 24 hours. However, this finding was not associated with changes in susceptibility to meropenem. Concentrations of ≤ 0.015 mg/L meropenem had no effect on *in vitro* bacterial growth. For *K. pneumoniae* KPC, initial killing by meropenem was observed at concentrations ≥ 0.5 mg/L during the first 2 hours exposure, but bacterial re-growth was observed at all concentrations up to the level of non-exposed bacteria after 24 hours.

The mode of action of tigecycline was observed to be bacteriostatic and the antibiotic was equally effective against *K. pneumoniae* ESBL and *K. pneumoniae* KPC, indicating that the 2-fold difference in MIC values to tigecycline for the two strains represents essential agreement in susceptibility to this antibiotic. Inhibition of bacterial growth after 24 hours of exposure was only observed above 2 mg/L tigecycline. Concentrations

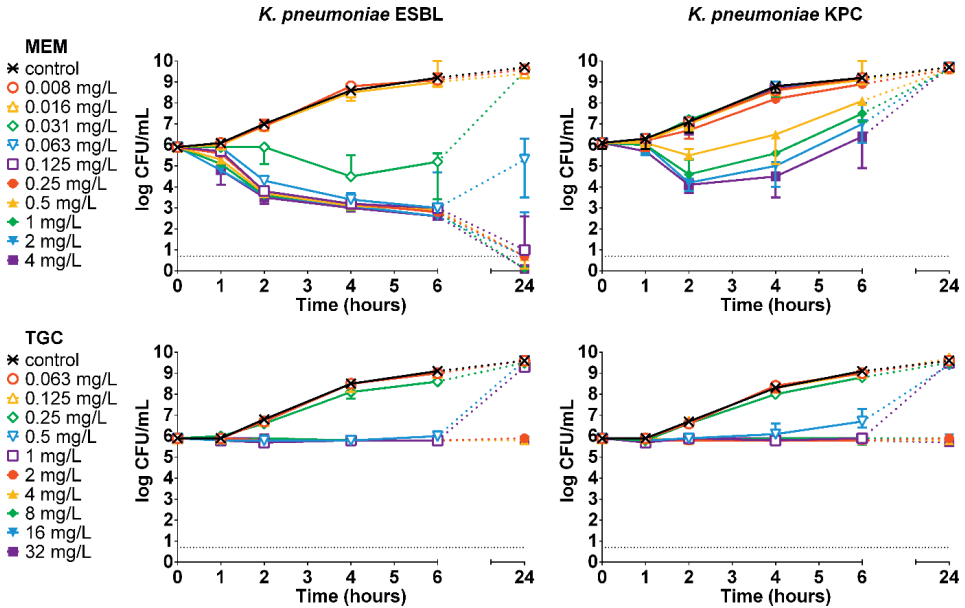


Figure 1. Concentration- and time-dependent bactericidal activity of meropenem (MEM) and tigecycline (TGC) against *K. pneumoniae* strains. Bacterial cultures of *K. pneumoniae* ESBL or *K. pneumoniae* KPC were exposed to two-fold increasing concentrations of antibiotic for 24 hours. Shown are the median \pm range of in triplo experiments. The dashed grey line indicates the lower limit of quantification of log 0.7

below 2 mg/L resulted in growth inhibition during 4 hours of exposure, but bacterial re-growth occurred after 24 hours, which was never associated with changes in bacterial susceptibility to tigecycline. Concentrations ≤ 0.25 mg/L had no effect.

Characterization of pneumonia-septicemia model

Rats were inoculated with *K. pneumoniae* ESBL or *K. pneumoniae* KPC and developed acute bilateral pneumonia with septicemia. Bacterial numbers increased rapidly in all lung lobes, with the relatively large lobes containing the most bacteria (Figure 2). As a consequence of a higher inoculum used to induce KPC pneumonia-septicemia, higher counts of *K. pneumoniae* were found at 24 hours in the lungs of rats with KPC pneumonia-septicemia compared to rats with ESBL pneumonia-septicemia. By 48 hours, differences in *K. pneumoniae* counts in the lungs in both models were minor.

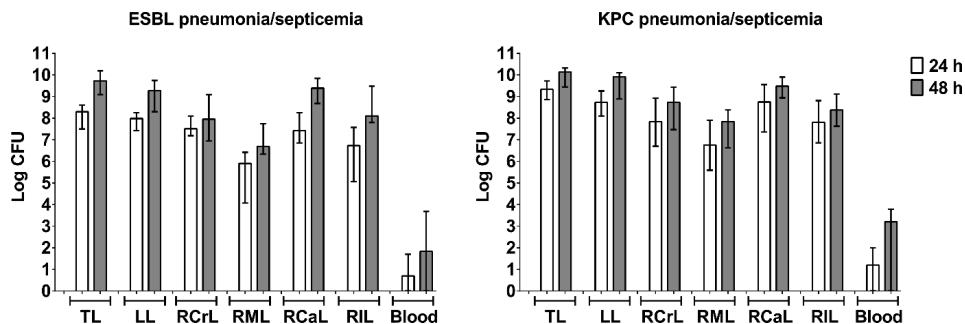


Figure 2. Bacterial load of *K. pneumoniae* in lungs and blood of rats with *K. pneumoniae* pneumonia-septicemia in the early phase of infection. Bacterial load of *K. pneumoniae* was determined for total lungs and individual lung lobes and blood (per mL) of rats with *K. pneumoniae* ESBL pneumonia-septicemia and rats with *K. pneumoniae* KPC pneumonia-septicemia at 24 hours and 48 hours after initiation of infection. TL, total lungs; LL, left lobe; RCrL, right cranial lobe; RML, right middle lobe; RCaL, right caudal lobe; RIL, right intermediate lobules. Groups of 6 rats per time point. Bacterial load is expressed as log CFU (median \pm range).

After 24 hours, bacteremia was present in 4/6 (66%) of rats with ESBL pneumonia-septicemia and in 4/6 (66%) of rats with KPC pneumonia-septicemia. Changes in liver and kidney function in terms of ALAT, ASAT, creatinine, and BUN were never found (data not shown). Histopathological examination of the infected lungs at 24 hours after initiation of infection revealed distinctive alveolar pathology, as shown for KPC pneumonia-septicemia (Supplementary Figure S1). Similar histopathological characteristics were observed in rats with ESBL pneumonia-septicemia (data not shown).

The disease progression over time in terms of rat survival rate (Figure 3A) was similar for either infecting *K. pneumoniae* strain ($p=0.4662$). In both cases, the body temperatures (Figure 3B) initially showed some fluctuation, but decreased over time to below the lower limit (36.1 °C) of normal values. Rat body weight decreased over time (Figure 3C). A control experiment revealed that the technique of intubation and inoculation itself did not influence body temperature or body weight.

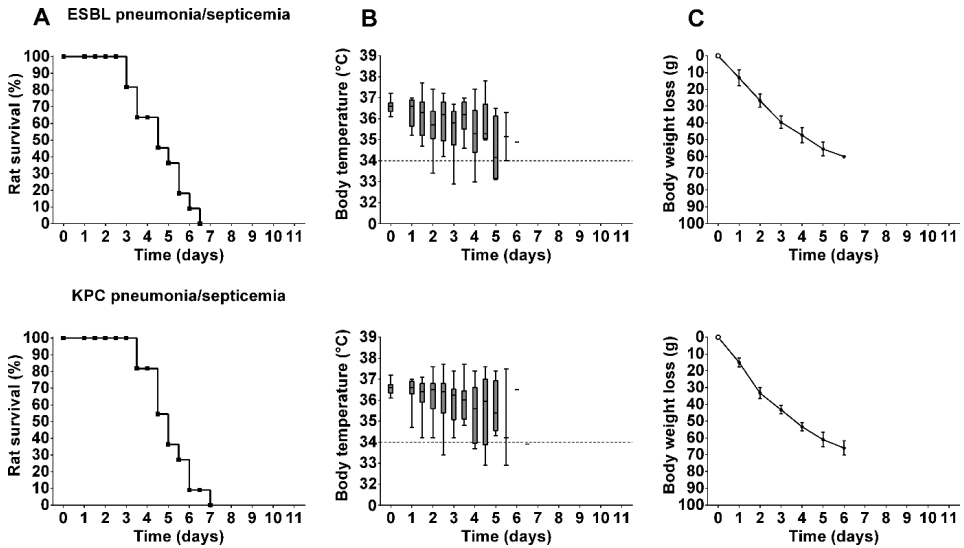


Figure 3. Disease progression in rats with *K. pneumoniae* pneumonia-septicemia. Groups of 11 rats were used for each experiment. A) Rat survival (Kaplan-Meier curves) of rats reaching humane endpoints. B) Box plots of pooled body temperatures showing the range of the data; the dashed line at 34 °C represents the humane endpoint. C) Body weight loss from the onset of the infection (mean \pm standard deviation).

Therapeutic efficacy of meropenem in rats with ESBL pneumonia-septicemia

Treatment was started at 24 hours after infection, when bacterial numbers in the lung had increased 100-fold and most rats had developed early bacteremia. Increasing doses of meropenem were investigated ranging from 6.25 – 25 mg/kg/day administered 12-hourly until a MED of meropenem was reached at which all rats survived. Meropenem showed a dose-dependent therapeutic activity, and effected survival of all rats at 25 mg/kg/day – the MED (Figure 4). Rat body temperatures initially showed some fluctuation, but stabilized around normal values after 3 days and from that time onward showed the normal circadian rhythm. Body weight values initially decreased but remained stable after 3 days. The lungs of the surviving rats sacrificed at termination of the experiment were sterile.

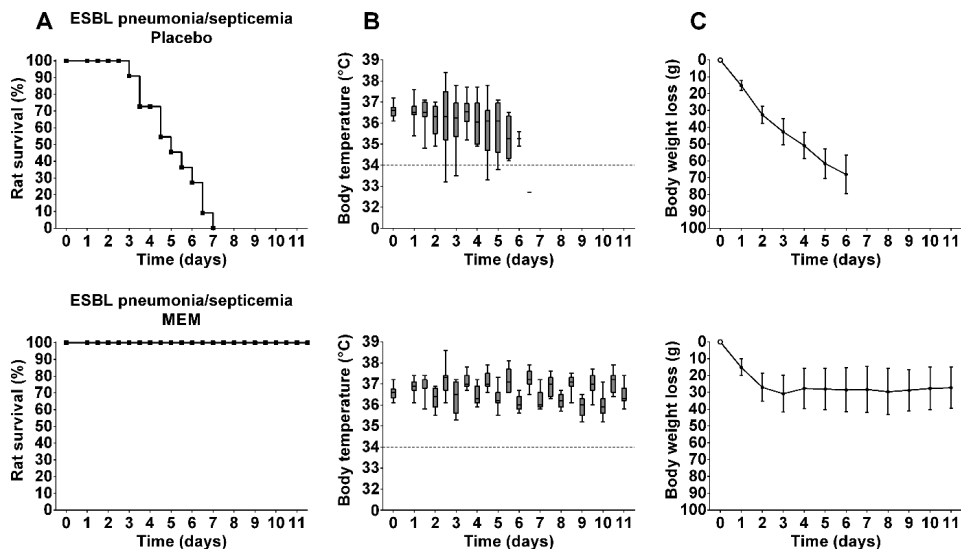


Figure 4. Therapeutic efficacy of meropenem (MEM) in rats with ESBL pneumonia-septicemia. Groups of 11 rats were treated 12-hourly for 10 days with Placebo (physiological saline) or 25 mg/kg/day meropenem, started at 24 hours after initiation of infection. A) Rat survival (Kaplan-Meier curves) of rats reaching humane endpoints. B) Box plots of pooled body temperatures showing the range of the data; the dashed line at 34 °C represents the humane endpoint. C) Body weight loss from the onset of infection (mean \pm standard deviation).

Pharmacokinetics of meropenem in rats with ESBL pneumonia-septicemia

Meropenem plasma concentrations were determined to investigate the steady-state pharmacokinetic profile of meropenem at MED in rats with ESBL pneumonia-septicemia. The plasma concentration-time curve indicated a one-compartment deposition (Figure 5). The corresponding estimated pharmacokinetic parameters are displayed in Table 2. The $fT > MIC$ for *K. pneumoniae* ESBL was 5.18 hours, which was 43.17% of the twice-daily dosing interval. For *K. pneumoniae* KPC, the fC_{max} (13.37 mg/L) did not reach the respective meropenem MIC (16 mg/L), resulting in a $fT > MIC$ of 0 hours.

ESBL pneumonia/septicemia

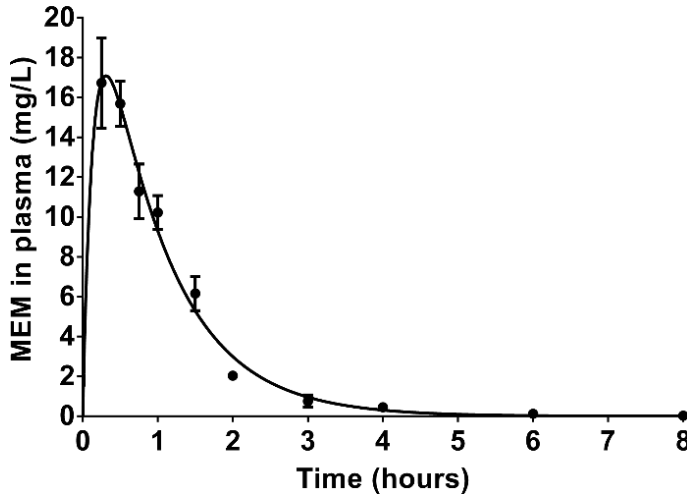


Figure 5. Plasma concentrations of total (bound and unbound) meropenem (MEM) in rats with ESBL pneumonia-septicemia. Rats were treated 12-hourly with 3 consecutive doses of 25 mg/kg/day meropenem, started at 24 hours after initiation of infection. The concentration-time curve predicted by a one-compartment model of extravascular administration was imposed over the observed concentrations at each time point in 3 rats (mean \pm standard error).

6

Table 2. Pharmacokinetic parameters of meropenem in rats with ESBL pneumonia-septicemia

Pharmacokinetic parameters	V/F	CL/F	$t_{1/2}$	fC_{max}	$fT > MIC$			
					0.063 mg/L	16 mg/L		
Units	L/kg	L/kg/h	h	mg/L	h	%	h	%
Estimate	1.03	1.17	0.61	13.37	5.18	43.17	0.00	0.00
SEM	0.07	0.06	0.03	1.43	0.24	2.00	0.00	0.00

Plasma concentrations of meropenem in rats with ESBL pneumonia-septicemia treated 12-hourly with 3 consecutive doses of 25 mg/kg meropenem, started at 24 hours after initiation of infection. The $fT > MIC$ was calculated based on unbound meropenem concentrations using the MIC of *K. pneumoniae* ESBL (0.063 mg/L) and the MIC of *K. pneumoniae* KPC (16 mg/L) and is shown in hours (h) as well as percentage of the 12-hour dosing interval (%). SEM, standard error of the mean; V, volume of distribution; F, bioavailability; CL, clearance; $t_{1/2}$, elimination half-life time; fC_{max} , highest unbound drug concentration reached in blood plasma; $fT > MIC$, cumulative percentage of a 12-hour period that the unbound fraction of drug exceeds the MIC.

Therapeutic efficacy of meropenem and tigecycline in rats with KPC pneumonia-septicemia

Rats with KPC pneumonia-septicemia were treated with 25 mg/kg/day meropenem 12-hourly for 10 days, which correlates to a $fT>MIC$ of 0 hours. This treatment resulted in survival of only 1/12 rats with KPC pneumonia-septicemia (Figure 6), which was not significantly different compared to the placebo-treated rats ($p=0.5728$). The failure of meropenem was also reflected in the body temperatures and the body weight values.

Next, the therapeutic response to tigecycline treatment of 25 mg/kg/day 12-hourly for 10 days was investigated in rats with KPC pneumonia-septicemia. This dosage was the MED of tigecycline found in a previous unilateral pneumonia-septicemia rat model caused by an identical *K. pneumoniae* ESBL strain¹¹. The 25 mg/kg/day tigecycline dosage resulted in survival of all rats with bilateral KPC pneumonia-septicemia. Body temperatures remained stable, but body weights decreased slowly over time (Figure 6). Low bacterial numbers were present in the lungs of the surviving rats, with a median of 2.6×10^3 *K. pneumoniae* and an upper limit of 1.9×10^4 *K. pneumoniae*. None of the isolated bacteria showed a change in susceptibility to tigecycline.

Discussion

Antimicrobial resistance continues to spread worldwide and is often encountered in clinically relevant organisms such as *K. pneumoniae*. This bacterial species is becoming increasingly resistant to currently available antibiotics^{3,34}, with many isolates only susceptible to a limited number of 'last-resort' antibiotics such as colistin and tigecycline. However, much debate still exists on the clinical efficacy of tigecycline in relation to the dose administered. Freire *et al.* in 2010 showed a lower therapeutic response for tigecycline than imipenem (using a dosing regimen of initial 100 mg followed by 50 mg every 12 hours in a group of ventilated patients), a study often referenced as showing the limited efficacy of tigecycline in this situation³⁵. Additionally,

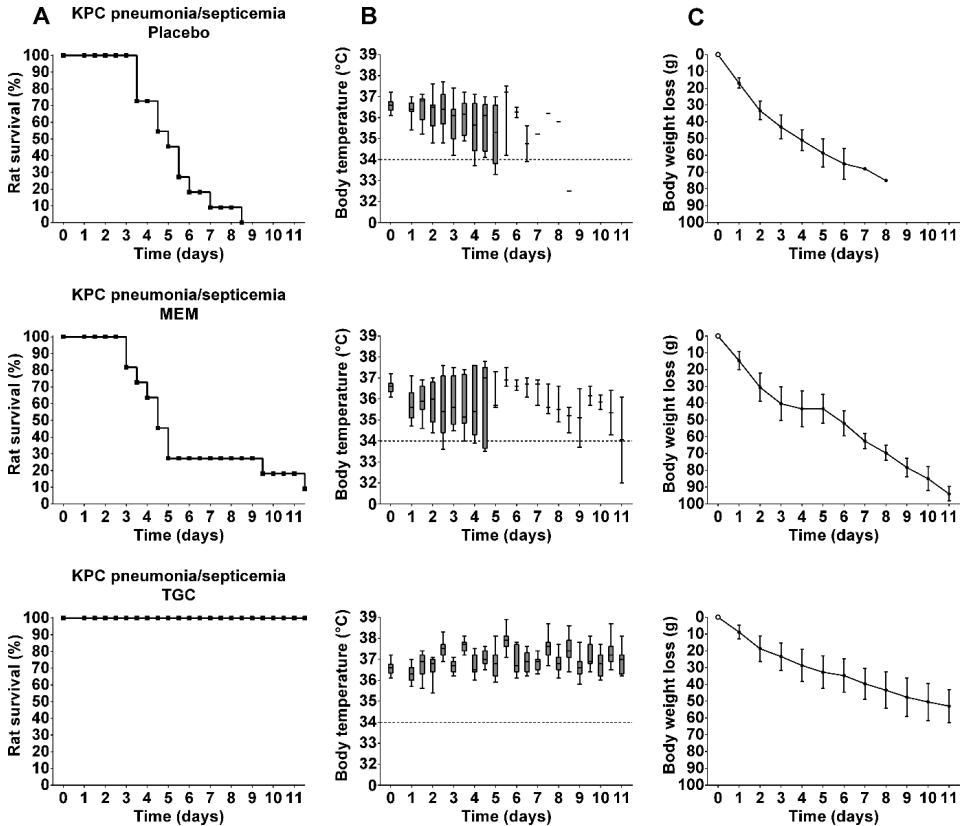


Figure 6. Therapeutic efficacy of meropenem (MEM) or tigecycline (TGC) in rats with KPC pneumonia-septicemia. Groups of 11 rats were treated 12-hourly for 10 days with Placebo (physiological saline) or 25 mg/kg/day meropenem or 25 mg/kg/day tigecycline, started at 24 hours after initiation of infection. A) Rat survival (Kaplan-Meier curves) of rats reaching humane endpoints. B) Box plots of pooled body temperatures showing the range of the data; the dashed line at 34 °C represents the humane endpoint. C) Body weight loss from the onset of infection (mean \pm standard deviation).

the administration of tigecycline treatment has been associated with an increased death rate⁵, and a number of case reports have indicated serious complications in patients as a consequence of tigecycline treatment³⁶⁻⁴⁰. On the other hand, a meta-analysis by Falagas *et al.* in 2014, concluded that high-dose tigecycline regimens may be effective for the treatment of severe bacterial infections⁹ and a meta-analysis by Gong *et al.*

concluded that high-dose tigecycline regimens did not elevate the risk of toxic side effects⁴¹. Further, pharmacokinetic and pharmacodynamic studies have indicated that higher dosages of tigecycline can be administered to humans, resulting in improved therapeutic efficacy^{6,42,43}. This has been corroborated by more recent studies which have shown that administration of high-dose tigecycline regimens are tolerated and result in improved therapeutic efficacy in infected patients compared to conventional tigecycline dosing⁴³⁻⁴⁷. Cunha *et al.*, reported clinical efficacy using once-daily high-dose tigecycline monotherapy in the treatment of multidrug-resistant Gram-negative bacilli and published recommendations for high-dose regimens^{7,42}. These studies are also supported by the *in vitro* modeling studies of Tsala *et al.*, suggesting that higher doses of tigecycline are required to achieve therapeutic efficacy⁴⁸ and by a Monte Carlo simulation analysis of standard and high-dose tigecycline against carbapenemase-producing *K. pneumoniae*, showing that the cumulative fractional response rate of >90% was only achievable with the high-dose tigecycline regimen⁴⁹. Taken together, these studies suggest that current clinical guidelines on the antibiotic prescribing of tigecycline may need to be revised upwards in order to reach a clinically effective dose. In this respect, EUCAST has recently published a new “Guidance Document on Tigecycline Dosing by the EUCAST”, recommending the use of high-dosage tigecycline treatment in seriously ill patients infected with multidrug-resistant bacteria⁸.

Complicating this debate is the fact that tigecycline is frequently applied in the treatment of infections caused by multidrug-resistant bacteria as part of combination therapy rather than monotherapy¹⁰. Based on these limitations, and on accompanying discussions relating to the efficacy of tigecycline administration, a study was established into the efficacy of high-dose tigecycline monotherapy using a newly established rat model of fatal acute pneumonia-septicemia caused by ESBL- or KPC-producing *K. pneumoniae* with meropenem as a comparator drug. This model is representative of a particularly severe multidrug-resistant infection in human patients⁵⁰⁻⁵² and allows for research comparing the therapeutic efficacy of individual antibiotics at similar conditions of severity, duration of infection, and host defense, which is not possible with most comparative clinical efficacy studies on tigecycline treatment^{9,10}.

Treatment with tigecycline at 25 mg/kg/day 12-hourly for 10 days resulted in 100% survival of rats with KPC pneumonia-septicemia and normalization of body temperature. In our previous study using the *K. pneumoniae* ESBL unilateral pneumonia-septicemia model, this tigecycline dosage was the successful MED, generating 100% survival of rats and normalization of body temperature. In the same study, the efficacy of tigecycline was found to be dose-dependent and was correlated to the ratio of the area under the plasma concentration-time curve (AUC) to the MIC (AUC/MIC). The AUC during a 24 hour period (AUC_{0-24h}) for this tigecycline dosage in rats with was similar to the AUC_{0-24h} of high-dose tigecycline treatments in human patients (a loading dose of 300 mg tigecycline followed by 150 mg tigecycline every 12 hours)⁵³. For pneumonia-septicemia caused by *K. pneumoniae* ESBL with a tigecycline MIC of 1 mg/L, the AUC/MIC was 34.29 mg·h/L at a tigecycline dosage of 25 mg/kg/day which was the MED of tigecycline for survival of all rats. As the tigecycline MIC of *K. pneumoniae* KPC is 2 mg/L, the extrapolated AUC/MIC ratio for KPC pneumonia-septicemia at a tigecycline dosage of 25 mg/kg/day is calculated to be 17.15 mg·h/L. Despite this MED having a lower AUC/MIC ratio in rats with bilateral KPC pneumonia-septicemia, the tigecycline treatment at 25 mg/kg/day 12-hourly for 10 days remained successful. Unlike the meropenem treatment, this treatment did not result in normalization of body weight, which might be explained by either the persistence of low bacterial numbers in the lungs of the rats at the end of treatment, or by potential gastro-intestinal side effects of tigecycline.

Treatment with meropenem in rats with ESBL pneumonia-septicemia showed a clear dose-response relationship. At the MED of 25 mg/kg/day, meropenem resulted in 100% rat survival, in stabilization of body weights, in body temperatures returning to the circadian rhythm, and effected bacterial elimination from the lung tissue at the end of treatment. Meropenem concentrations in rat plasma remained above the MIC of *K. pneumoniae* ESBL for >5 hours, achieving the bactericidal target of carbapenem regimens in human patients, which is a $fT > MIC$ of approximately 40% of the dosing interval⁵⁴. In terms of total dosage, meropenem at 25 mg/kg/day 12-hourly for 10 days

in rats is similar to the current clinical treatment of ESBL pneumonia-septicemia, although in patients, an 8-hourly meropenem schedule is more common⁵⁵.

The MED of meropenem in rats with ESBL pneumonia-septicemia was not successful in rats with KPC pneumonia-septicemia which is in line with the difference in susceptibility of *K. pneumoniae* ESBL and *K. pneumoniae* KPC. This difference in susceptibility resulted in different $fT>MIC$ values for the two strains, with unbound meropenem concentrations in rat plasma remaining above the MIC of *K. pneumoniae* ESBL for >5 hours, whereas the fC_{max} (<14 mg/L) did not reach the meropenem MIC of *K. pneumoniae* KPC (16 mg/L), resulting in a $fT>MIC$ of 0 hours. The respective therapeutic success or failure of this meropenem dose in both infection models can be explained as a consequence of the time-dependent bactericidal activity of meropenem, which was shown in the *in vitro* TKK data in the present study, as well as in other *in vivo* pharmacokinetic/pharmacodynamic studies⁵⁶.

The pneumonia-septicemia model established in the present study is representative of a particularly severe human infection with *K. pneumoniae* bacteria resulting in rapid mortality when left untreated⁵⁰⁻⁵². Further, although the tigecycline MIC of *K. pneumoniae* ESBL (1 mg/L) and *K. pneumoniae* KPC (2 mg/L) are considered resistant, these MICs remain within the wild-type distribution of tigecycline MICs for *K. pneumoniae*^{26,28}. In view of these factors, the successful treatment of this animal model necessitated the use of a high-dose tigecycline regimen, as the AUC of the tigecycline monotherapy MED administered to rats with ESBL pneumonia-septicemia exceeds the AUC of the tigecycline dosage which is conventionally administered to infected patients (50 mg tigecycline every 12 hours)⁵⁷, demonstrating the effectiveness of high-dosage tigecycline regimens in the treatment of severe multidrug-resistant bacterial infections. The scope of the current research was limited to investigating the efficacy of a high-dosage tigecycline regimen in a model of pneumonia-septicemia caused by two isogenic multidrug-resistant *K. pneumoniae* strains. Future research can improve on the generalizability of these results by investigating high-dosage tigecycline regimens in the treatment of infection models caused by other *K. pneumoniae* strains or different Gram-negative bacterial species. Another interesting avenue for further research with the

current pneumonia-septicemia model would be the investigation of high-dose meropenem regimens⁵⁸ or high-dose meropenem and high-dose tigecycline combination regimens⁵⁹.

Conclusions

The data obtained in the current study provide evidence that high-dosage tigecycline monotherapy is effective in a rat model representative of human pneumonia-septicemia caused by multidrug-resistant *K. pneumoniae*. Based on the therapeutic tigecycline dose observed in this publication, the limited susceptibility to tigecycline of both strains, and current clinical guidelines, the *in vivo* data reported in the present study further supports recent literature on the applicability of high-dosage tigecycline as a treatment of 'last resort' in patients with severe multidrug-resistant *K. pneumoniae* infections. The present work involves a clinically relevant animal model for multidrug-resistant *K. pneumoniae* infections that facilitates the future investigation of antibiotics and novel therapeutic approaches to pneumonia-septicemia.

Acknowledgements

We are grateful to the Clinical Pharmacological and Toxicological Laboratory as well as the Pathology Research Trial Service at the Erasmus University Medical Center, Rotterdam, the Netherlands, for the pharmacokinetic analysis of blood samples and the preparation of histopathological samples, respectively. We would also like to express our appreciation to D. Horst-Kreft and J. den Boer for their technical support and to H. I. Bax and J. W. Mouton for providing expert perspectives, all from the Department of Medical Microbiology and Infectious Diseases, Erasmus University Medical Center, Rotterdam, the Netherlands.

Funding

This work was financially supported by the European Union's Seventh Program for Research, Technological Development and Demonstration under grant agreement No. 604434 PneumoNP.

Competing interests

The authors declare no competing or financial interests.

References

1. Peleg AY, Hooper DC. Hospital-acquired infections due to gram-negative bacteria. *New England Journal of Medicine*. 2010;362(19):1804-13.
2. Girlich D, Poirer L, Nordmann P. CTX-M expression and selection of ertapenem resistance in *Klebsiella pneumoniae* and *Escherichia coli*. *Antimicrobial Agents and Chemotherapy*. 2009;53(2):832-4.
3. Tzouveleki LS, Markogiannakis A, Psychogiou M, Tassios PT, Daikos GL. Carbapenemases in *Klebsiella pneumoniae* and other Enterobacteriaceae: an evolving crisis of global dimensions. *Clinical Microbiology Reviews*. 2012;25(4):682-707.
4. Duin D, Cober ED, Richter SS, Perez F, Cline M, Kaye KS, et al. Tigecycline therapy for carbapenem-resistant *Klebsiella pneumoniae* (CRKP) bacteriuria leads to tigecycline resistance. *Clinical Microbiology and Infection*. 2014;20(12).
5. Temkin E, Adler A, Lerner A, Carmeli Y. Carbapenem-resistant Enterobacteriaceae: biology, epidemiology, and management. *Annals of the New York Academy of Sciences*. 2014;1323(1):22-42.
6. Burkhardt O, Rauch K, Kaefer V, Hadem J, Kielstein JT, Welte T. Tigecycline possibly underdosed for the treatment of pneumonia: a pharmacokinetic viewpoint. *International Journal of Antimicrobial Agents*. 2009;34(1):101-2.

7. Cunha BA, Baron J, Cunha CB. Monotherapy with High-Dose Once-Daily Tigecycline is Highly Effective Against *Acinetobacter baumannii* and other Multidrug-Resistant (MDR) Gram-Negative Bacilli (GNB). *International Journal of Antimicrobial Agents*. 2018;52(1):119.
8. The European Committee on Antimicrobial Susceptibility Testing. Guidance Document on Tigecycline Dosing in association with Revision of Breakpoints for Enterobacterales and other species with an "Intermediate" category (2018). Available on <http://www.eucast.org>: Accessed on 2 March 2020.
9. Falagas ME, Vardakas KZ, Tsiveriotis KP, Triarides NA, Tansarli GS. Effectiveness and safety of high-dose tigecycline-containing regimens for the treatment of severe bacterial infections. *International Journal of Antimicrobial Agents*. 2014;44(1):1-7.
10. Heizmann W, Löschmann P-A, Eckmann C, Von Eiff C, Bodmann K-F, Petrik C. Clinical efficacy of tigecycline used as monotherapy or in combination regimens for complicated infections with documented involvement of multiresistant bacteria. *Infection*. 2015;43(1):37-43.
11. Goessens WHF, Mouton JW, Marian T, Sörgel F, Kinzig M, Bakker-Woudenberg IAJM. The therapeutic effect of tigecycline, unlike that of ceftazidime, is not influenced by whether the *Klebsiella pneumoniae* strain produces extended-spectrum β -lactamases in experimental pneumonia in rats. *Antimicrobial Agents and Chemotherapy*. 2013;57(1):643-6.
12. Bassetti M, Welte T, Wunderink RG. Treatment of Gram-negative pneumonia in the critical care setting: is the beta-lactam antibiotic backbone broken beyond repair? *Critical Care*. 2015;20(1):19.
13. Fasciana T, Gentile B, Aquilina M, Ciammaruconi A, Mascarella C, Anselmo A, et al. Co-existence of virulence factors and antibiotic resistance in new *Klebsiella pneumoniae* clones emerging in south of Italy. *BMC Infectious Diseases*. 2019;19(1):928.
14. Hennequin C, Robin F. Correlation between antimicrobial resistance and virulence in *Klebsiella pneumoniae*. *European Journal of Clinical Microbiology & Infectious Diseases*. 2016;35(3):333-41.
15. Woodford N, Fagan EJ, Ellington MJ. Multiplex PCR for rapid detection of genes encoding CTX-M extended-spectrum β -lactamases. *Journal of Antimicrobial Chemotherapy*. 2005;57(1):154-5.
16. Mabilat C, Goussard S. PCR detection and identification of genes for extended-spectrum β -lactamases. *Diagnostic Molecular Microbiology: Principles and Applications: American Society for Microbiology*; 1993. p. 553-9.
17. Nüesch-Inderbinen MT, Hächler H, Kayser FH. Detection of genes coding for extended-spectrum SHV beta-lactamases in clinical isolates by a molecular genetic method, and comparison with the E test. *European Journal of Clinical Microbiology & Infectious Diseases*. 1996;15(5):398-402.
18. Karisik E, Ellington MJ, Pike R, Warren RE, Livermore DM, Woodford N. Molecular characterization of plasmids encoding CTX-M-15 β -lactamases from *Escherichia coli* strains in the United Kingdom. *Journal of Antimicrobial Chemotherapy*. 2006;58(3):665-8.
19. Dallenne C, Da Costa A, Decré D, Favier C, Arlet G. Development of a set of multiplex PCR assays for the detection of genes encoding important β -lactamases in Enterobacteriaceae. *Journal of Antimicrobial Chemotherapy*. 2010;65(3):490-5.
20. Bradford PA, Bratu S, Urban C, Visalli M, Mariano N, Landman D, et al. Emergence of carbapenem-resistant *Klebsiella* species possessing the class A carbapenem-hydrolyzing KPC-2 and inhibitor-resistant TEM-30 β -lactamases in New York City. *Clinical Infectious Diseases*. 2004;39(1):55-60.
21. Islam MA, Talukdar PK, Hoque A, Huq M, Nabi A, Ahmed D, et al. Emergence of multidrug-resistant NDM-1-producing Gram-negative bacteria in Bangladesh. *European Journal of Clinical Microbiology & Infectious Diseases*. 2012;31(10):2593-600.
22. Boers SA, Van der Reijden WA, Jansen R. High-throughput multilocus sequence typing: bringing molecular typing to the next level. *PLOS ONE*. 2012;7(7):e39630.
23. Souverein D, Boers SA, Veenendaal D, Euser SM, Kluytmans J, Den Boer JW. Polyclonal Spread and Outbreaks with ESBL Positive Gentamicin Resistant *Klebsiella* spp. in the Region Kennemerland, The Netherlands. *PLOS ONE*. 2014;9(6):e101212.

24. Gruteke P, Goessens W, Van Gils J, Peerbooms P, Lemmens-den Toom N, van Santen-Verheuevel M, et al. Patterns of resistance associated with integrons, the extended-spectrum β -lactamase SHV-5 gene, and a multidrug efflux pump of *Klebsiella pneumoniae* causing a nosocomial outbreak. *Journal of Clinical Microbiology*. 2003;41(3):1161-6.
25. Padilla E, Alonso D, Doménech-Sánchez A, Gomez C, Pérez JL, Albertí S, et al. Effect of porins and plasmid-mediated AmpC β -lactamases on the efficacy of β -lactams in rat pneumonia caused by *Klebsiella pneumoniae*. *Antimicrobial Agents and Chemotherapy*. 2006;50(6):2258-60.
26. The European Committee on Antimicrobial Susceptibility Testing. Breakpoint tables for interpretation of MICs and zone diameters, Version 10.0 (2020). Available on <http://www.eucast.org>: Accessed on 2 March 2020.
27. de Steenwinkel JEM, de Knecht GJ, ten Kate MT, van Belkum A, Verbrugh HA, Kremer K, et al. Time–kill kinetics of anti-tuberculosis drugs, and emergence of resistance, in relation to metabolic activity of *Mycobacterium tuberculosis*. *Journal of Antimicrobial Chemotherapy*. 2010;65(12):2582-9.
28. The European Committee on Antimicrobial Susceptibility Testing. Antimicrobial wild type distributions of microorganisms, version 5.26 (2020). Available on <http://mic.eucast.org/Eucast2>: Accessed on 2 March 2020.
29. Balls M, Goldberg AM, Fentem JH, Broadhead CL, Burch RL, Festing MF, et al. The three Rs: the way forward: the report and recommendations of ECVAM Workshop 11. *Alternative to Laboratory Animals*. 1995;23(6):838.
30. Kilkenny C, Browne WJ, Cuthill IC, Emerson M, Altman DG. Improving bioscience research reporting: the ARRIVE guidelines for reporting animal research. *PLOS Biology*. 2010;8(6).
31. Abdulla A, Bahmany S, Wijma RA, van der Nagel BCH, Koch BCP. Simultaneous determination of nine β -lactam antibiotics in human plasma by an ultrafast hydrophilic-interaction chromatography–tandem mass spectrometry. *Journal of Chromatography B*. 2017.
32. Zhang Y, Huo M, Zhou J, Xie S. PKSolver: An add-in program for pharmacokinetic and pharmacodynamic data analysis in Microsoft Excel. *Computer Methods and Programs in Biomedicine*. 2010;99(3):306-14.
33. Hori T, Nakano M, Kimura Y, Murakami K. Pharmacokinetics and tissue penetration of a new carbapenem, doripenem, intravenously administered to laboratory animals. *In Vivo*. 2006;20(1):91-6.
34. Bradford PA. Extended-spectrum β -lactamases in the 21st century: characterization, epidemiology, and detection of this important resistance threat. *Clinical Microbiology Reviews*. 2001;14(4):933-51.
35. Freire AT, Melnyk V, Kim MJ, Datsenko O, Dzyublik O, Glumcher F, et al. Comparison of tigecycline with imipenem/cilastatin for the treatment of hospital-acquired pneumonia. *Diagnostic Microbiology and Infectious Disease*. 2010;68(2):140-51.
36. Duran FY, Yildirim H, Şen EM. A Lesser Known Side Effect of Tigecycline: Hypofibrinogenemia. *Turkish Journal of Hematology*. 2018;35(1):83.
37. Pieringer H, Schmekal B, Biesenbach G, Pohanka E. Severe coagulation disorder with hypofibrinogenemia associated with the use of tigecycline. *Annals of Hematology*. 2010;89(10):1063-4.
38. Zhang Q, Zhou S, Zhou J. Tigecycline treatment causes a decrease in fibrinogen levels. *Antimicrobial Agents and Chemotherapy*. 2015;59(3):1650-5.
39. Routsis C, Kokkoris S, Douka E, Ekonomidou F, Karaikos I, Giamarellou H. High-dose tigecycline-associated alterations in coagulation parameters in critically ill patients with severe infections. *International Journal of Antimicrobial Agents*. 2015;45(1):90-3.
40. Wu X, Zhao P, Dong L, Zhang X. A case report of patient with severe acute cholangitis with tigecycline treatment causing coagulopathy and hypofibrinogenemia. *Medicine*. 2017;96(49).
41. Gong J, Su D, Shang J, Yu H, Du G, Lin Y, et al. Efficacy and safety of high-dose tigecycline for the treatment of infectious diseases: A meta-analysis. *Medicine*. 2019;98(38).

42. Cunha BA, Baron J, Cunha CB. Once daily high dose tigecycline-pharmacokinetic/pharmacodynamic based dosing for optimal clinical effectiveness: dosing matters, revisited. *Expert Review of Anti-infective Therapy*. 2017;15(3):257-67.
43. Baron J, Cai S, Klein N, Cunha B. Once Daily High Dose Tigecycline Is Optimal: Tigecycline PK/PD Parameters Predict Clinical Effectiveness. *Journal of Clinical Medicine*. 2018;7(3):49.
44. De Pascale G, Montini L, Pennisi MA, Bernini V, Maviglia R, Bello G, et al. High dose tigecycline in critically ill patients with severe infections due to multidrug-resistant bacteria. *Critical Care*. 2014;18(3):R90.
45. Geng T-T, Xu X, Huang M. High-dose tigecycline for the treatment of nosocomial carbapenem-resistant *Klebsiella pneumoniae* bloodstream infections: A retrospective cohort study. *Medicine*. 2018;97(8).
46. Chen Z, Shi X. Adverse events of high-dose tigecycline in the treatment of ventilator-associated pneumonia due to multidrug-resistant pathogens. *Medicine*. 2018;97(38).
47. Gao H, Yao Z, Li Y, Huang S, Liu J, Jing Y. Safety and Effectiveness of High Dose Tigecycline for Treating Patients with Acute Leukemia after Ineffectiveness of Carbapenems Chemotherapy Combining with Febrile Neutropenia: Retrospective study [Article in Chinese; spelling errors present in PubMed reference]. *Zhongguo Shi Yan Xue Ye Xue Za Zhi*. 2018;26(3):684-90.
48. Tsala M, Vourli S, Daikos GL, Tsakris A, Zerva L, Mouton JW, et al. Impact of bacterial load on pharmacodynamics and susceptibility breakpoints for tigecycline and *Klebsiella pneumoniae*. *Journal of Antimicrobial Chemotherapy*. 2016;72(1):172-80.
49. Ni W, Li G, Zhao J, Cui J, Wang R, Gao Z, et al. Use of Monte Carlo simulation to evaluate the efficacy of tigecycline and minocycline for the treatment of pneumonia due to carbapenemase-producing *Klebsiella pneumoniae*. *Infectious Diseases*. 2018;50(7):507-13.
50. Lin Y-T, Jeng Y-Y, Chen T-L, Fung C-P. Bacteremic community-acquired pneumonia due to *Klebsiella pneumoniae*: clinical and microbiological characteristics in Taiwan, 2001-2008. *BMC Infectious Diseases*. 2010;10(1):307.
51. Lin Y-T, Wang Y-P, Wang F-D, Fung C-P. Community-onset *Klebsiella pneumoniae* pneumonia in Taiwan: clinical features of the disease and associated microbiological characteristics of isolates from pneumonia and nasopharynx. *Frontiers in Microbiology*. 2015;6:122.
52. Qureshi ZA, Paterson DL, Potoski BA, Kilayko MC, Sandovsky G, Sordillo E, et al. Treatment outcome of bacteremia due to KPC-producing *Klebsiella pneumoniae*: superiority of combination antimicrobial regimens. *Antimicrobial Agents and Chemotherapy*. 2012;AAC. 06268-11.
53. Xie J, Roberts JA, Alobaid AS, Roger C, Wang Y, Yang Q, et al. Population pharmacokinetics of tigecycline in critically ill patients with severe infections. *Antimicrobial Agents and Chemotherapy*. 2017;61(8):e00345-17.
54. Nicolau DP. Pharmacokinetic and pharmacodynamic properties of meropenem. *Clinical Infectious Diseases*. 2008;47(Supplement_1):S32-S40.
55. Gilbert DN, Chambers HF, Eliopoulos GM, Saag MS, Pavia AT. The Sanford guide to antimicrobial therapy, 47th edition. Sperryville, VA, USA: Antimicrobial Therapy, Inc.; 2017.
56. Mouton JW, Touw DJ, Horrevorts AM, Vinks AA. Comparative pharmacokinetics of the carbapenems. *Clinical Pharmacokinetics*. 2000;39(3):185-201.
57. Muralidharan G, Micalizzi M, Speth J, Raible D, Troy S. Pharmacokinetics of tigecycline after single and multiple doses in healthy subjects. *Antimicrobial Agents and Chemotherapy*. 2005;49(1):220-9.
58. Ghazi IM, Crandon JL, Lesho EP, McGann P, Nicolau DP. Efficacy of humanized high-dose meropenem, cefepime, and levofloxacin against Enterobacteriaceae isolates producing Verona integron-encoded metallo- β -lactamase (VIM) in a murine thigh infection model. *Antimicrobial Agents and Chemotherapy*. 2015;59(11):7145-7.

59. Giannella M, Treccarichi EM, Giacobbe DR, De Rosa FG, Bassetti M, Bartoloni A, et al. Effect of combination therapy containing a high-dose carbapenem on mortality in patients with carbapenem-resistant *Klebsiella pneumoniae* bloodstream infection. *International Journal of Antimicrobial Agents*. 2018;51(2):244-8.

Supplementary Table S1. Genotypic characterization of *K. pneumoniae* strains

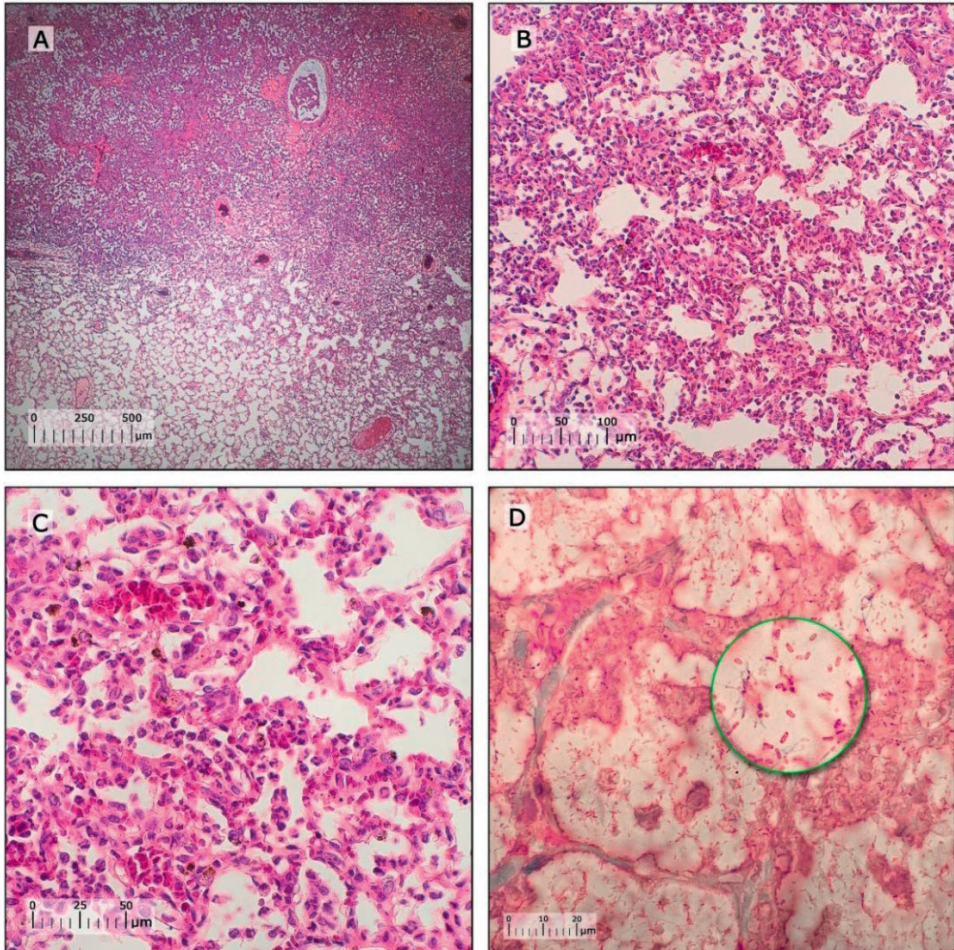
Strain	ATCC 43816™	EMC 2003	EMC 2014	ATCC 13883™	ATCC 700603™	ATCC BAA1705™
Antibiotic profile	WT Parent	ESBL	KPC	WT	ESBL	KPC
Sequence type	493	493	493	3	489	258
1	negative	negative	negative	negative	negative	negative
2	negative	negative	negative	negative	negative	negative
CTX-M 8	negative	negative	negative	negative	negative	negative
9	negative	negative	negative	negative	negative	negative
25	negative	negative	negative	negative	negative	negative
TEM	negative	negative	positive	negative	negative	positive
SHV	positive	positive	positive	positive	positive	positive
OXA 1	negative	negative	negative	negative	negative	negative
48	negative	negative	negative	negative	negative	negative
KPC	negative	negative	positive	negative	negative	positive
NDM-1	negative	negative	negative	negative	negative	negative

Sequence types were determined by HiMLST and the presence of plasmid-mediated resistance genes was determined using PCR assays for the *K. pneumoniae* strains used in this study and relevant *K. pneumoniae* ATCC reference strains. *K. pneumoniae* ESBL and *K. pneumoniae* KPC both contained an SHV-5 gene, and the *K. pneumoniae* KPC strain had gained an additional KPC gene. Both *K. pneumoniae* strains belonged to the same sequence type (ST 493) compared to the WT parent strain, but were genetically different compared to the three ATCC reference strains, which each belonged to a different sequence type indicating the genetic diversity among these strains.

Supplementary Table S2. Phenotypic characterization of *K. pneumoniae* strains

Strain	ATCC 43816™	EMC 2003	EMC 2014	ATCC 13883™	ATCC 700603™	ATCC BAA1705™
Antibiotic profile	WT Parent	ESBL	KPC	WT	ESBL	KPC
Ampicillin	16	≥32	≥32	≥32	≥32	≥32
Amoxicillin/ Clavulanic Acid	≤2	4	≥32	≤2	16	≥32
Piperacillin/ Tazobactam	≤4	≤4	≥128	≤2	32	≥128
Cefuroxime	2	16	≥64	4	≥64	≥64
Cefuroxime Axetil	2	16	≥64	4	≥64	≥64
Cefoxitin	≤4	≤4	≤4	≤4	≥64	≥64
Cefotaxime	≤1	2	8	≤1	8	8
Ceftazidime	≤1	≥64	≥64	≤1	32	16
Cefepime	≤1	≤1	2	≤1	≤1	2
Imipenem	≤0.25	≤0.25	≥16	0.5	≤0.25	≥16
Meropenem	≤0.25	≤0.25	≥16	≤0.25	≤0.25	≥16
Gentamicin	≤1	≥16	≥16	≤1	≥16	4
Tobramycin	≤1	≥16	≥16	≤1	8	≥16
Ciprofloxacin	≤0.25	≤0.25	≤0.25	≤0.25	0.5	≥4
Norfloxacin	≤0.5	≤0.5	≤0.5	≤0.5	2	≥16
Trimethoprim	≤0.5	≤0.5	≤0.5	≤0.5	2	≥16
Trimethoprim/ sulfamethoxazole	≤1	≤1	≤1	≤1	≤1	≥16
Colistin	≤0.5	≤0.5	≤0.5	≤0.5	≤0.5	≤0.5

MICs (mg/L) were determined using the automated VITEK®2 antimicrobial identification system for the *K. pneumoniae* strains used in this study and relevant *K. pneumoniae* ATCC reference strains. Trimethoprim/sulfamethoxazole was expressed as the trimethoprim concentration. Interpretation of antimicrobial susceptibility was defined by the VITEK® antimicrobial identification system as susceptible, intermediate (italic), or resistant (bold) based on EUCAST 2014 guidelines. *K. pneumoniae* ESBL EMC2003 and *K. pneumoniae* KPC EMC2014 had few major differences in susceptibility profile compared to ATCC reference strains.



Supplementary Figure S1. Representative lung histopathology in lung tissue from rats with *K. pneumoniae* KPC pneumonia/septicaemia at 24 hours after initiation of infection. (A-C) Sections stained with HE at different magnifications. (D) Section stained with Gram stain. An outer hemorrhagic zone of the lesion was observed (in areas next to uninfected tissue) in which the alveoli were filled with mucoid exudates dominated by edema fluid and a light cellular infiltrate. More extensive areas of pneumonia were observed towards the center of the lesion i.e. in the zone of early consolidation. In these areas alveoli were packed with predominantly polymorphonuclear leukocytes and alveolar walls were necrotic. Numerous encapsulated Gram-negative bacilli were freely present in the exudates within the hemorrhagic zone of the lesions. KPC, *K. pneumoniae* carbapenemase producing.

Abstract

Introduction: Antimicrobial peptides (AMPs) have seen limited clinical use as antimicrobial agents, largely due to issues relating to toxicity, short biological half-life, and lack of efficacy against Gram-negative bacteria. However, the development of novel AMP-nanomedicines, i.e. AMPs entrapped in nanoparticles, has the potential to ameliorate these clinical problems. The authors investigated two novel nanomedicines based on AAI39, an AMP currently in development for the treatment of multidrug-resistant Gram-negative infections.

Methods: AAI39 was entrapped in polymeric nanoparticles (PNP) or lipid-core micelles (MCL). The antimicrobial activity of AAI39-PNP and AAI39-MCL was determined *in vitro*. The biodistribution and limiting doses of AAI39-nanomedicines were determined in uninfected rats via endotracheal aerosolization. The early bacterial killing activity of the AAI39-nanomedicines in infected lungs was assessed in a rat model of pneumonia-septicemia caused by an extended-spectrum β -lactamase-producing *Klebsiella pneumoniae*. In this model, the therapeutic efficacy was determined by once-daily (q24h) administration over 10 days.

Results: Both AAI39-nanomedicines showed equivalent *in vitro* antimicrobial activities (similar to free AAI39) and in uninfected rats they exhibited longer residence times in the lungs compared to free AAI39 (~20% longer for AAI39-PNP and ~80% longer for AAI39-MCL), as well as reduced toxicity enabling a higher limiting dose. In rats with pneumonia-septicemia, both AAI39-nanomedicines showed significantly improved therapeutic efficacy in terms of an extended rat survival time, although survival of all rats was not achieved.

Conclusion: These results demonstrate potential advantages that can be achieved using AMP-nanoformulations. AAI39-PNP and AAI39-MCL may be promising novel therapeutic agents for the treatment of patients suffering from multidrug-resistant Gram-negative pneumonia-septicemia.



Chapter

8

THERAPEUTIC EFFICACY OF NOVEL ANTIMICROBIAL PEPTIDE AA139-NANOMEDICINES IN A MULTIDRUG-RESISTANT KLEBSIELLA PNEUMONIAE PNEUMONIA- SEPTICEMIA MODEL IN RATS

*Hessel van der Weide, Unai Cossío, Raquel Gracia,
Yvonne M. te Welscher, Marian T. ten Kate, Aart van der Meijden,
Marco Marradi, Jeffrey A.S. Ritsema,
Denise M.C. Vermeulen-de Jongh, Gert Storm,
Wil H.F. Goessens, Iraidia Loinaz, Cornelus F. van Nostrum,
Jordi Lloel, John P. Hays, Irma A.J.M. Bakker-Woudenberg*

Introduction

Pneumonia is responsible for over 230,000 deaths and €10 billion in economic costs across the European Union (EU) every year^{1,2}, with Gram-negative bacteria being the primary causative pathogens in ~70% of healthcare-associated pneumonia cases³. Therefore, the availability of effective antimicrobial drugs is crucial if clinicians are to adequately treat patients suffering from Gram-negative bacterial pneumonia⁴. Unfortunately, the current crisis of growing antimicrobial resistance and fewer antimicrobials reaching the market has resulted in a lack of new antimicrobials that are effective against multidrug-resistant Gram-negative bacteria^{5,6}. In response to this growing healthcare crisis, researchers have focused on the development and improvement of known but underutilized antibiotic classes to generate new approaches for treating bacterial pneumonia.

One class of antibiotics under investigation is the antimicrobial peptides (AMPs), a broad family of antibiotics that are produced in nature by organisms as a natural defense against microbes⁷. Although AMPs have been known since the 1950's, this family of antibiotics has seen only limited use for the treatment of pneumonia, largely due to a number of hurdles that have limited their clinical use, including toxic side-effects⁸, short biological half-life due to degradation by proteases^{8,9}, and limited efficacy against Gram-negative bacteria¹⁰.

Some of these issues may be offset by the concurrent development of new AMPs and new delivery systems for these antimicrobials. For example, entrapment of AMPs into nanoparticles to produce nanomedicines may generate several solutions to the hurdles traditionally associated with the clinical utility of AMPs in the treatment of multidrug-resistant infections^{11,12}. Notably, nanomedicine formulations could potentially reduce toxic side-effects and extend the biological half-life of AMPs¹³. Further, the direct delivery of antibiotics to the site of infection represents an additional therapeutic improvement¹⁴, which could facilitate increased antibiotic activity at the actual site of infection^{15,16} and lead to reduced systemic toxicity and 'collateral damage' to patients^{17,18}.

As such, the direct delivery of AMP nanomedicines to the lungs is a promising research strategy at a time when traditional antibiotics and treatment for respiratory tract infections are becoming ineffective^{19,20}. In this respect, the 7th Framework Programme of the EU provided funding to the PneumoNP research consortium, with the goal of developing and investigating novel AMP nanomedicines in the treatment of pneumonia²¹.

One of the AMPs investigated in the PneumoNP project was AA139, an AMP originally isolated from the marine lugworm *Arenicola marina* as ‘Arenicin-3’ and subsequently further developed to decrease the original AMP’s plasma protein binding properties, cytotoxicity, and hemolytic activity^{22,23}. AA139 is a cationic AMP with a 21-residue amphipathic hairpin structure that appears to have a dual mode of action involving direct binding of the AMP to membrane phospholipids and interruption of phospholipid transportation pathways, resulting in membrane dysregulation and bacterial cell death^{22,24}. AA139 has previously demonstrated potent *in vitro* and *in vivo* activity against multidrug-resistant Gram-negative bacteria^{25,26} and is not readily absorbed into systemic circulation from the lungs following inhalation in mice²⁷.

With respect to the development of nanomedicines, PneumoNP utilized several different nanomedicine formulations including polymeric nanoparticles (PNP) and lipid-core micelles (MCL). PNP are hydrophilic dextran-based single-chain polymer nanoparticles to which cationic drugs like AA139 can be attached by electrostatic interaction for increased drug delivery²⁸. MCL are self-assembling colloidal nanoparticles with a hydrophilic surface and a hydrophobic core in which drugs like AA139 can be entrapped for drug delivery²⁹. Both PNP³⁰ and MCL³¹ are suitable for nanomedicine formulation due to their favorable biocompatibility, non-toxicity, biodistribution, and ease of modification. PNP and MCL are promising nanocarriers for pulmonary drug delivery, as the relatively small size of PNP (1–20 nm) may allow for improved penetration of the respiratory mucus³², and MCL have been shown to facilitate sustained drug release in the lungs³³.

In the present study, two novel AA139 nanomedicines were developed using either PNP or MCL: AA139-PNP, in which AA139 has been attached to PNP by electrostatic interactions; and AA139-MCL, in which AA139 has been enclosed in the hydrophobic core of MCL. Their antimicrobial activity was assessed first via *in vitro* concentration- and time-dependent bactericidal activity studies against extended-spectrum β -lactamase (ESBL)-producing *Klebsiella pneumoniae*. *In vivo* studies were then performed involving the administration of the nanomedicines by endotracheal aerosolization as a means of direct delivery to the lungs, the primary site of infection in pneumonia. First, the biodistribution and residence time in the lungs of the nanomedicines was determined and the maximum tolerated dose (MTD) was assessed in uninfected rats. Next, the early bacterial killing activity of the nanomedicines was assessed in a rat model of pneumonia-septicemia caused by ESBL-producing *K. pneumoniae*. Finally, the therapeutic efficacy of the nanomedicines was determined in the pneumonia-septicemia rat model by once-daily (q24h) administration over 10 days.

Materials and methods

Peptide, nanocarriers, chemical agents, and solvents

AA139 in Ringer's acetate solution was obtained from Adenium Biotech ApS (Copenhagen, Denmark). PNP were produced at CIDETEC (Donostia-San Sebastián, Spain). MCL were produced at Utrecht University (Utrecht, the Netherlands). Polyethylene glycosylated distearyl phosphatidyl ethanolamine (DSPE-PEG2000) Na-salt was purchased from Lipoid GmbH, Ludwigshafen, Germany. Ultrapure water (18M Ω cm) was generated using a Milli-Q® system (MilliporeSigma, Bedford, MA, USA). Dextran, glycidyl methacrylate (GMA), dimethyl sulfoxide (DMSO), 3-mercaptopropionic acid (3-MPA) and 2,2'-(ethylenedioxy)diethanethiol were of analytical grade and purchased from Sigma-Aldrich Corporation (St. Louis, MO, USA). Phosphate-buffered saline (PBS) was purchased from Scharlab SL (Barcelona, Spain).

Preparation of AA139 nanomedicines

AA139 was entrapped in the two different nanoparticles PNP or MCL to prepare two distinct AA139 nanomedicines: PNP were used to prepare polymeric nanoparticulate AA139 nanomedicines (AA139-PNP) and MCL were used to prepare lipid-core micellar AA139 nanomedicines (AA139-MCL).

Preparation of AA139-PNP: Dextran-based PNPs functionalized with 3-MPA were obtained as previously described in the literature²⁸. To prepare AA139-PNP, loading of AA139 to PNP was carried out by non-covalent interaction with an AA139-to-PNP mass ratio of 10%. In brief, 100 mg AA139 was incubated with 1 g PNP in 25 mL of saline solution at pH = 7.2 for 15 hours at room temperature. This was the maximum amount of AA139 that could be used, as proportions of AA139 greater than 10% resulted in aggregation as larger particles sizes were observed by dynamic light scattering (DLS). The crude complex was then purified by membrane ultrafiltration using Vivaspin® 500 10 kDa molecular weight cutoff (MWCO) polyethersulphone (PES) centrifugal concentrators (GE Healthcare, Chicago, USA) and aqueous saline solution at pH = 7.2 to eliminate any unbound AA139. The maximum loading, established as the maximum concentration of peptide at which no peptide was collected in the filtrate, was 0.1 mg AA139/1 mg PNP. The AA139-PNP particle dispersions (corresponding to 5 mg/mL AA139 and 50 mg/mL PNP) in normal saline solution (NSS) of 0.9 wt. % NaCl had a mean size of 20 nm as determined by DLS and were negatively charged. High-performance liquid chromatography (HPLC) studies demonstrated that the nanomedicines were stable for at least 1 year when frozen at -20°C. Size measurement of AA139-PNP after freeze-thaw conditions demonstrated that the diameter of the nanomedicines was not affected by these storage conditions. Further dilution of this pristine dispersion of AA139-PNP in NSS for use in *in vitro* and *in vivo* experiments did not show any sign of instability.

Preparation of AA139-MCL: Entrapment of AA139 in MCL was carried out during the formation of MCL, which were prepared by using a thin lipid film hydration method.

In brief, a thin lipid film of DSPE-PEG2000 was prepared by dissolving the lipid in MeOH in a glass round-bottom flask and evaporation of the organic solvent under reduced pressure. Residual solvent was removed under a nitrogen flow. The lipid film was hydrated at 30 °C in PBS containing the AA139 peptide at a 1:3 molar ratio of the peptide to DSPE-PEG2000. This was the maximum amount of AA139 that could be used, as higher proportions of AA139 resulted in aggregation as determined by DLS. The eluted product was collected in 100 μ L fractions. AA139-MCL have a size of 15.4 (\pm 1.5) nm according to DLS measurement and a near neutral zeta-potential of -2.1 (\pm 2.2) mV as was measured from MCL prepared in 10 mM HEPES buffered saline (HBS) buffer. The loading was between 10–13 mg/mL AA139 in 11–14 mM DSPE-PEG2000 with a loading efficiency of 100% (\pm 4%). Further dilution of this pristine dispersion of AA139-MCL in NSS for use in *in vitro* and *in vivo* experiments did not show any sign of instability.

The preparation of unloaded PNP and MCL for control experiments was identical to the preparation process of their respective AA139-nanomedicines. The concentration of unloaded PNP and MCL was adjusted with NSS after the preparation process to ensure that the administered concentration of unloaded PNP and MCL was identical to the administered concentration of nanoparticles in the nanomedicine formulations.

All nanomedicine preparations were transported to partner locations in insulated thermal boxes with cooling elements frozen at -20 °C to ensure that sample temperatures did not exceed -5 °C. A selection of samples were sent back to the original partner faculties (CIDETEC or Utrecht University) for re-analysis to confirm stability under these transportation conditions.

Bacterial strains

The ESBL-positive strain *K. pneumoniae* ESBL EMC2003 (referred to in this publication as *K. pneumoniae* ESBL) used in this study has previously been characterized in terms of genotype and antimicrobial susceptibility profile and was used to establish pneumonia-septicemia in rats³⁴. The stability of the plasmid-containing *K. pneumoniae* ESBL strain was confirmed through five consecutive passages in Mueller Hinton II (MH-II) broth

(Becton Dickinson BV, Vianen, The Netherlands). The virulence of the bacterial strain was maintained by rat lung passage every 12 months.

Concentration- and time-dependent antimicrobial activity of AA139, AA139-PNP, and AA139-MCL *in vitro*

The antimicrobial activity of AA139, AA139-PNP, and AA139-MCL was compared using the time-kill kinetics (TKK) assay as previously described³⁵. Three two-fold increasing antibiotic concentrations were used, representing: 1) the lowest concentration at which AA139 showed bacterial growth inhibition; 2) the minimum inhibitory concentration (MIC) of AA139; and 3) the lowest concentration at which AA139 led to complete bacterial killing after 24 hours of antibiotic exposure. These AA139 concentrations were respectively: 2 mg/L, 4 mg/L, 8 mg/L. AA139-PNP (corresponding to 20 mg/L, 40 mg/L, 80 mg/L of PNP) and AA139-MCL (corresponding to 2.2 μ M, 4.5 μ M, 9 μ M of MCL) were tested at the same AA139 concentrations based on the AA139 content of the nanomedicines. Samples were serially 10-fold diluted and sub-cultured on MH-II agar plates (Becton Dickinson BV) for CFU counts after 24 hours at 37 °C.

Animals

Female Sprague Dawley rats bred at Janvier Labs (Le Genest-Saint-Isle, France) were used for the *in vivo* imaging studies (age, 6-8 weeks). Specified pathogen-free (SPF) male strain RP/AEur/RijHsd albino rats bred at the Laboratory Animals Center of Erasmus University Medical Center Rotterdam (Erasmus MC) were used for the *in vivo* tolerability and infection studies. Rats (age, 10-18 weeks; body weight, 250-350 g) were housed individually in ventilated cages with food and water *ad libitum*. Rats were randomly allocated to experimental groups once they reached the appropriate age and body weight. Group sizes were based on estimates of the hazard ratio. Euthanasia was applied by CO₂ exposure when humane endpoints were reached or at termination of experiments.

Infected rats were monitored 12-hourly for 11 days to assess the disease progression and signs of acute toxicity as well as pre-defined humane endpoints by changes in body

temperature and body weight, and by external symptoms of disease including ungroomed appearance, pallor, nose bleeding, lack of reactivity, inactivity, instability, or abnormal breathing of rats. Rat survival was based on rats reaching humane endpoints, at which point euthanasia was applied by CO₂ exposure. The rat survival parameter thus reflects rats reaching humane endpoints. After dissection, bacteria isolated from lung and blood were identified by matrix-assisted laser desorption/ionization time-of-flight (MALDI-TOF) mass spectrometry (Bruker Daltonics, Bremen, Germany) to rule out co-infection as a pre-established exclusion criterium.

Ethics

Animals were maintained and handled in accordance with the Guidelines for Accommodation and Care of Animals (European Convention for the Protection of Vertebrate Animals Used for Experimental and Other Scientific Purposes). All animal procedures were performed in accordance with either the Dutch Animal Experimentation Act (BWBR0003081) or the Spanish policy for animal protection (RD53/2013), both of which meet the requirements of the European Union Animal Directive (2010/63/EU). Experimental procedures were approved by either the Ethical Committee of the Asociación Centro de Investigación Cooperativa en Biomateriales (CIC biomaGUNE) or by the Institutional Animal Care and Use Committee of the Erasmus MC. The current study was designed to abide by the three Rs principles of animal research (replace, reduce, refine) wherever possible³⁶ and was written to conform to the animal research: reporting of *in vivo* experiments (ARRIVE) guidelines for reporting animal research³⁷.

Endotracheal aerosolization of AA139, AA139-PNP, and AA139-MCL in rats

Rats were anesthetized with 3–5% isoflurane (IsoFlo®, Abbott Laboratories, Lake Bluff, IL, USA) in pure O₂ for 5 minutes to ensure deep sedation. Animals were placed on a rodent workstand (Hallowell EMC, Pittsfield, MA, USA) in supine position inclined at a 45° angle. Endotracheal aerosolization was performed using a MicroSprayer®-Syringe Assembly for Rat (Penn-Century, Inc., Wyndmoor, PA, USA).

A small animal laryngoscope (Penn-Century, Inc.) was used for visualization of the epiglottis, ensuring correct positioning of the tip just above the carina. A pre-defined volume of nanomedicine suspension was administered by endotracheal aerosolization, and rats remained in place for 10 seconds after administration to allow for inhalation.

Radiolabelling of AA139, AA139-PNP, and AA139-MCL for imaging studies

The radio-iodination of AA139 was carried out by electrophilic aromatic substitution on the tyrosine residues. For that purpose, 1 mg/mL AA139 solution was incubated with [¹²⁴I]NaI (Perkin Elmer, Inc., Waltham, MA, USA) in 0.2 M sodium acetate buffer solution (50 µL, pH 5.5) for 2 hours at 25 °C in the presence of Iodo-beads® (Thermo Fisher Scientific, Waltham, MA, USA). The crude reaction mixture was purified by retention in a Sep-Pak® C18 Plus Light cartridge (Waters Corporation, Milford, MA, USA) and subsequent elution using 1 mL of 0.1% aqueous trifluoroacetic acid (TFA) solution/ethanol 20/80. The solvent was evaporated and the residue reconstituted with 0.2 M sodium acetate buffer solution (300 µL, pH 5.5). Chemical and radiochemical purity were determined by HPLC with radioactive detection (radio-HPLC), using a *Mediterranea*TM Sea 18 (5 µm, 15 x 0.46 cm) column (Teknokroma Analítica SA, Barcelona, Spain) as the stationary phase and 0.1% solution of TFA in water (A) and 0.1% solution of TFA in acetonitrile (B) as mobile phase, using the following gradient: initial, A-90% B-10%; 4 min, A-85% B-15%; 6 min, A-75% B-25%; 10 min, A-75% B-25%; 16 min, A-5% B-95%; 18 min, A-5% B-95%; 20 min, A-90% B-10%, 22 min, A-90% B-10%. Overall decay-corrected radiochemical yield was 62±2% and the molar activity was within the range of 0.5-1.5 GBq/µmol at the end of the synthesis.

Radiochemical stability of the ¹²⁴I-labelled AA139 was assessed by incubation in different media at 37 °C, including moderately acidic conditions (sodium acetate buffer, pH=5.5). At different time points, samples were withdrawn and analyzed by radio-HPLC using the experimental conditions described above. Radiochemical stability was directly calculated from chromatographic profiles. [¹²⁴I]AA139 was stable in moderately acidic conditions similar to the infected lung environment for 48 hours and did not lead to detachment of ¹²⁴I from AA139 (Supplementary Figure S1).

Labelled [^{124}I]AA139-PNP and [^{124}I]AA139-MCL nanomedicines were prepared as described above using [^{124}I]AA139. For the preparation of [^{124}I]AA139-MCL nanomedicines, Illustra™ Nap™-5 Columns pre-packaged with Sephadex™ G-25 DNA grade (GE Healthcare, Chicago, IL, USA) were preconditioned with a sodium acetate buffer solution (10 mL, 0.02 M, pH=5.5) and then used for final purification by size exclusion chromatography, using PBS (10 mM, 0.8% NaCl, pH=7.4) as the mobile phase.

The radiochemical yields of labelled [^{124}I]AA139-PNP and [^{124}I]AA139-MCL were calculated as the ratio between the amount of radioactivity present in [^{124}I]AA139 nanomedicines and the starting amount of [^{124}I]AA139. When the [^{124}I]AA139-to-PNP mass ratio was set to 1/10, quantitative attachment of AA139 to PNP was achieved and radiochemical yields close to 60% were achieved after purification of [^{124}I]AA139-PNP. [^{124}I]AA139 was efficiently attached to PNP as well as efficiently incorporated within MCL. Incorporation of [^{124}I]AA139 into MCL resulted in >95% radiochemical yields in the initial fractions of [^{124}I]AA139-MCL.

Imaging studies of AA139, AA139-PNP, and AA139-MCL in uninfected rats

Rats were administered 50 μL (ca. 1.85 MBq) of [^{124}I]AA139, [^{124}I]AA139-PNP, or [^{124}I]AA139-MCL by endotracheal aerosolization in groups of 4 rats. One group of 2 rats was administered with an equivalent amount of [^{124}I]NaI in saline solution as the control. Immediately after endotracheal aerosolization animals were positioned in an eXploreVista computerized tomography (CT) and positron emission tomography (PET) small animal preclinical imaging system (GE Healthcare). A PET scan was acquired over 40 minutes, while anesthesia was maintained using 1–2% isoflurane in pure O_2 and body temperature was maintained with a homeothermic blanket control unit (Bruker BioSpin GmbH, Karlsruhe, Germany) to prevent hypothermia. Animals were then allowed to recover from anesthesia and returned to their cages. Imaging sessions were repeated at 3, 6, 9, 15, and 24 hours after administration.

After each PET acquisition, a CT scan (X-Ray energy: 40 kV, intensity: 140 μA) was performed for a later attenuation correction application in the image reconstruction, as

well as for unambiguous localization of the radioactive signal. Random and scatter corrections were also applied to the reconstructed image (filtered back projection reconstruction algorithm), generating a $175 \times 175 \times 220$ voxel image, with a 2 mm axial full width at half maximum (FWHM) spatial resolution in the center of the Field Of View (FOV). After reconstruction, images were analyzed using π MOD analysis software (version 3.4, PMOD Technologies Ltd., Zürich, Switzerland). Volumes of interest (VOIs) were manually delineated in the whole lungs, and the concentration of radioactivity in the lungs was determined for each compound and time point.

Deposition of AA139 in lungs and blood of uninfected rats

Deposition of AA139 in lungs and distribution to blood plasma was determined in 6 rats which were sacrificed immediately after endotracheal aerosolization of 1 mg AA139 in 100 μ L. The five lung lobes were collected separately, weighed, and homogenized in 2 mL NSS using the gentleMACS™ Octo Dissociator (Milteny Biotec BV, Leiden, The Netherlands). Blood plasma was obtained from whole blood collected via cardiac puncture in lithium-heparin tubes (Sarstedt BV, Etten-Leur, The Netherlands) and total rat blood plasma volume was estimated based on body weight³⁸. AA139 concentrations were determined at Covance Laboratories (Harrogate, UK) using a liquid chromatography with tandem mass spectrometric detection (LC-MS/MS) bioanalytical assay.

Limiting dose of AA139, AA139-PNP, and AA139-MCL in uninfected rats

To determine the maximum tolerated dose (MTD) or maximum feasible dose (MFD), rats were administered 100 μ L of AA139, AA139-PNP, or AA139-MCL by endotracheal aerosolization in groups of 11 rats, starting at a low dose of 0.125 mg AA139 based on the AA139 content of the nanomedicines (corresponding to 1.25 mg/mL AA139; 12.5 mg/mL PNP; 0.14 mM MCL). 100 μ L of normal saline solution (NSS) was used as control treatment. After administration, animals were placed on an electric heating pad to emerge from anesthesia before being placed back in cages.

Rats were then regularly checked for signs of acute toxicity over 24 hours. After 24 hours, rats were sacrificed and blood plasma was obtained from whole blood

collected via cardiac puncture in lithium-heparin tubes to assess blood biomarkers for acute toxicity: alanine aminotransferase (ALAT), aspartate aminotransferase (ASAT), creatinine, and blood urea nitrogen (BUN) at the Department of Clinical Chemistry, Erasmus MC. When no acute toxicity was observed, the dose was increased two-fold, either until acute toxicity was observed (in which case the lower dose was determined as the MTD), or until the dose could not be further increased due to technical limitations, thereby reaching the MFD.

Rat model of pneumonia-septicemia

Bilateral *K. pneumoniae* ESBL pneumonia-septicemia was induced as described previously³⁴. In short, suspensions of washed bacteria in the logarithmic phase of growth were used to prepare inocula. After intubation and cannulation of the trachea under anesthesia, rats were held in a vertical position. Rat lungs were inoculated with 60 μ L PBS containing 2×10^6 *K. pneumoniae* ESBL followed by inhalation.

Early bacterial killing activity of AA139, AA139-PNP, and AA139-MCL in infected rats

K. pneumoniae ESBL pneumonia-septicemia was induced in groups of 6 rats. At 24 hours after initiation of infection, rats were administered 100 μ L of AA139, AA139-PNP, or AA139-MCL by endotracheal aerosolization administered at the same dose which was the MTD of free A139. Rats were administered 100 μ L of unloaded PNP, unloaded MCL, or NSS as control treatment. Rats were sacrificed at 0 hours (before start of treatment) and at 2, 6 and 24 hours after start of treatment, 2 rats per timepoint per treatment group. Lungs were homogenized in 5 mL NSS using the gentleMACS™ Octo Dissociator (Milteny Biotec BV). Lung homogenates were diluted and sub-cultured on MH-II agar plates for CFU count after 20 hours incubation of plates at 37 °C. Blood plasma was obtained for determination of blood biomarkers of acute toxicity as described above.

Therapeutic efficacy of AA139, AA139-PNP, and AA139-MCL in infected rats

K. pneumoniae ESBL pneumonia-septicemia was induced in groups of 12 rats. At 24 hours after initiation of infection, rats were administered 100 μ L of AA139, AA139-PNP, or AA139-MCL once-daily (q24h) by endotracheal aerosolization. The treatments were all administered at their respective limiting dose, as well as at the MTD of free AA139. Rats were administered 100 μ L of unloaded PNP, unloaded MCL, or NSS as control treatments. The disease progression was monitored twice-daily (q12h) for 10 days. Rats having reached humane endpoints were euthanized and dissected to check for the presence of *K. pneumoniae* ESBL in lungs and blood.

Statistics

Statistical significance of bacterial growth inhibition was determined by interpolating four-parameter sigmoidal growth curves and performing extra-sum-of-squares *F*-tests for the slope in Prism 5.01 (Graphpad Inc., San Diego, CA, USA). Kaplan-Meier rat survival curves were generated and statistical differences in rat survival rates were calculated using the log rank test in Prism 5.01.

Results

Concentration- and time-dependent antimicrobial activity of AA139, AA139-PNP, and AA139-MCL *in vitro*

TKK assays were used to determine the antimicrobial activity of free AA139, AA139-PNP, and AA139-MCL against *K. pneumoniae* ESBL over 24 hours. The bacterial populations rapidly increased in the absence of antibiotics within 24 hours of incubation (Figure 1). Free AA139 showed bactericidal activity resulting in bacterial growth inhibition at 2 mg/L AA139, a 100-fold reduction in bacterial numbers within 2 hours at 4 mg/L AA139, and near-complete bacterial killing after 24 hours at 8 mg/L AA139. AA139-PNP and AA139-MCL both showed similar bactericidal activity compared to free AA139, but the bacterial growth inhibition observed at 2 mg/L AA139 ($p = 0.0461$)

was not observed for 2 mg/L AA139-PNP and 2 mg/L AA139-MCL. Unlike free AA139 and AA139-MCL, AA139-PNP did not lead to complete bacterial killing after 24 hours at 8 mg/L AA139-PNP. Unlike free AA139 and AA139-PNP, AA139-MCL did not result in a 100-fold reduction in bacterial numbers within 2 hours at 4 mg/L AA139-MCL, but at 8 mg/L AA139-MCL. The rebound after 24 hours observed for 4 mg/L AA139-PNP and 4 mg/L AA139-MCL is likely the result of degradation of AA139^{25,39}. Unloaded PNP and unloaded MCL did not show any antimicrobial activity.

Biodistribution of AA139, AA139-PNP, and AA139-MCL in uninfected rats

PET-CT image sequences were obtained for [¹²⁴I]NaI (control), [¹²⁴I]AA139, [¹²⁴I]AA139-PNP, and [¹²⁴I]AA139-MCL (Figure 2) in groups of 4 rats. The images reveal that the biodistribution patterns of [¹²⁴I]AA139, [¹²⁴I]AA139-PNP and [¹²⁴I]AA139-MCL significantly differ from the control. When [¹²⁴I]NaI was administered, it was rapidly cleared from the lungs and almost no signal was observed in this organ after three hours. On the contrary, a significant fraction of [¹²⁴I]AA139 and both [¹²⁴I]AA139 nanomedicines were still visible within the lungs at the same time point. Of note, the images reveal that the residence time of [¹²⁴I]AA139-PNP and [¹²⁴I]AA139-MCL is longer than residence time of free [¹²⁴I]AA139, since for the first two a clear signal within the lungs is still visible at 9, 15 and 24 hours after administration. The elimination pathways of the different species suggest excretion via urine and the gastrointestinal tract.

The deposition of free AA139 among the five lung lobes and distribution to blood plasma in uninfected rats immediately after endotracheal aerosolization was determined by LC-MS/MS bioanalysis (Supplementary Figure S2). Total deposition in the lungs (ca. ~88% of delivered dose) was high but showed considerable variation between the lung lobes, with most AA139 found in the relatively large left lobe and least AA139 found in the small right middle lobe. Total distribution to blood plasma (ca. ~2% of delivered dose) was low. These findings matched our *in vivo* imaging results, as well as the findings from an earlier study in which the deposition of 2-deoxy-2-[¹⁸F]fluoro-D-glucose (a clinically used radiotracer) using the same administration method was studied⁴⁰.

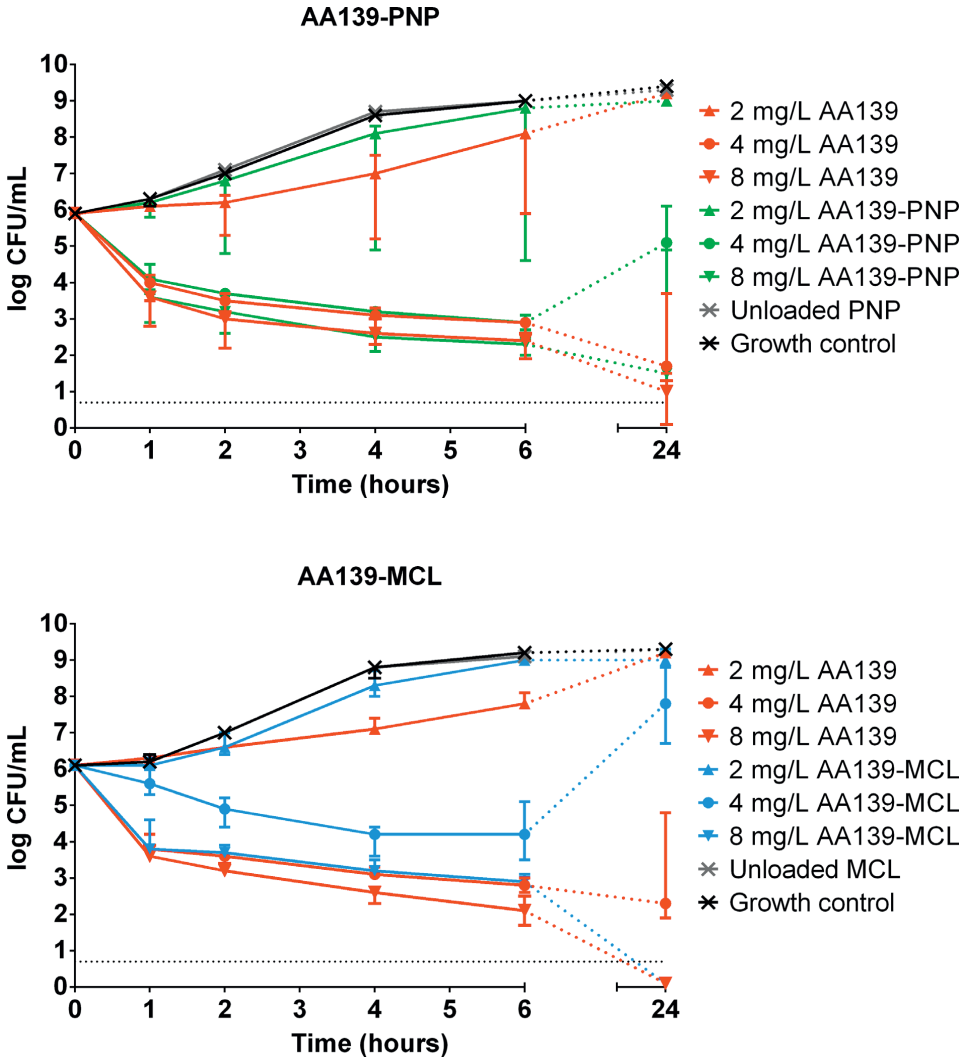


Figure 1. Concentration- and time-dependent antimicrobial activity of AA139, AA139-PNP or AA139-MCL against *K. pneumoniae* ESBL. Bacterial cultures of *K. pneumoniae* ESBL were exposed to two-fold increasing concentrations of free AA139, AA139-PNP, or AA139-MCL for 24 hours at 37 °C under shaking conditions. Shown are the median ± range of triplicate experiments. The dashed grey line indicates the lower limit of quantification being log 0.7.

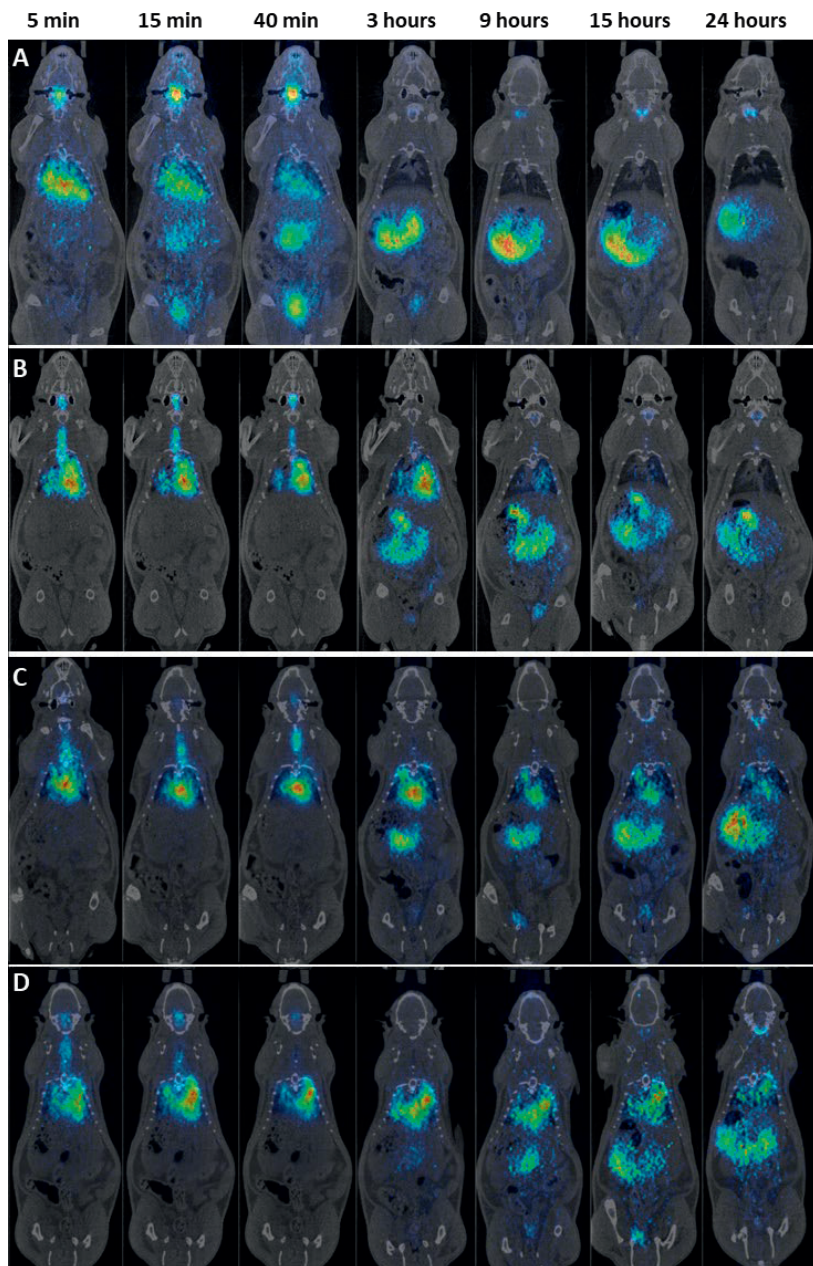


Figure 2. PET-CT coronal images showing biodistribution of radiolabelled compounds after endotracheal aerosolization in uninfected rats. Shown are PET-CT images obtained at different timepoints of A) [^{124}I]NaI (control), B) [^{124}I]AA139, C) [^{124}I]AA139-PNP and D) [^{124}I]AA139-MCL. PET images have been overlaid with CT images of the same animals for accurate location of the radioactive signal.

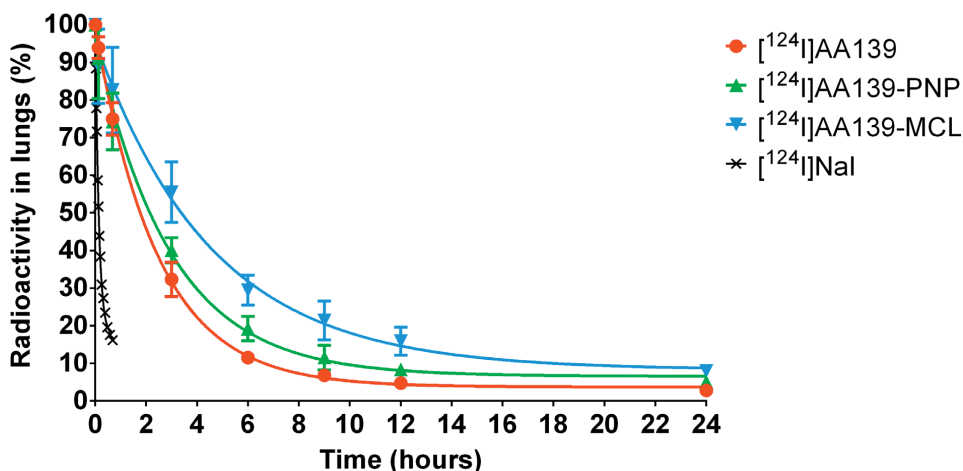


Figure 3. Time-dependent concentration of radioactivity in rat lungs after endotracheal aerosolization of radiolabelled compounds. Shown are the mean \pm standard deviation of four experiments as well as mono-exponential curves fitted to the experimental data.

Residence time of AA139, AA139-PNP, and AA139-MCL in lungs of uninfected rats

Quantification of the radioactivity in the lungs confirmed the trends observed in these *in vivo* sequences. To determine the biological half-life ($t_{1/2}$) of the radiolabelled compounds in the rat lungs, the concentration of radioactivity in the lungs at different time-points were fitted to a mono-exponential decay equation (Figure 3). The residence time in lungs of free [¹²⁴I]AA139 ($t_{1/2} = 1.71$ h) was longer by 21.6% when administered as [¹²⁴I]AA139-PNP ($t_{1/2} = 2.08$ h) and longer by 82.4% when administered as [¹²⁴I]AA139-MCL ($t_{1/2} = 3.12$ h). The residence time of the control [¹²⁴I]NaI in lungs was very short ($t_{1/2} = 0.09$ h).

Limiting dose of AA139, AA139-PNP and AA139-MCL in uninfected rats

Rats were administered two-fold increasing doses of free AA139, AA139-PNP, AA139-MCL, or NSS by endotracheal aerosolization in groups of 11 rats. As shown in Table 1, administration of NSS did not lead to any signs of acute toxicity or discomfort.

Table 1. Limiting dose of AA139, AA139-PNP, or AA139-MCL

Treatment	Limiting dose	Dose-limiting toxicity
AA139	MTD = 0.25 mg/rat ~1 mg/kg	Acute toxicity (abnormal breathing) observed at 0.5 mg/rat
AA139-PNP	MFD = 0.5 mg/rat ~2 mg/kg	Maximum feasible dose due to technical limitations
AA139-MCL	MTD = 0.5 mg/rat ~2 mg/kg	Acute toxicity (abnormal breathing) observed at 1 mg/rat
NSS		Well tolerated at this volume

Treatment was administered to groups of 11 rats via endotracheal aerosolization of 100 μ L suspension. Rats were regularly checked for signs of acute toxicity over 24 hours. When no acute toxicity was observed, the dose was increased two-fold, until acute toxicity was observed or until the dose could not be further increased due to technical limitations.

Free AA139 was not tolerated when administered at doses above the MTD of 0.25 mg/rat (~1 mg/kg) which induced acute toxicity in terms of abnormal breathing. AA139-PNP could be safely administered at the MFD of 0.5 mg/rat (~2 mg/kg), which was the highest possible dose that could be given due to technical limitations. AA139-MCL could be safely administered at the MTD of 0.5 mg/rat (~2 mg/kg), but induced acute toxicity in terms of abnormal breathing at higher doses. Analysis of blood biomarkers showed no indications of acute toxicity at limiting doses (Supplementary Figure S3).

Early bacterial killing activity of AA139, AA139-PNP, and AA139-MCL in infected rats

At 24 hours after initiation of infection, rats in groups of 6 were treated with a single dose of free AA139, AA139-PNP, or AA139-MCL at the MTD of free AA139 (0.25 mg/rat; ~1 mg/kg) by endotracheal aerosolization. Rats were sacrificed at 2, 6, and 24 hours after administration to determine bacterial counts in the rat lungs, and blood biomarkers (Figure 4). In rats treated with NSS as placebo, bacterial numbers increased almost 100-fold within 24 hours. Following treatment with free AA139, bacterial counts exhibited a robust decrease by 6 hours after administration, but had rebounded at 24 hours to bacterial counts similar to placebo. Administration of

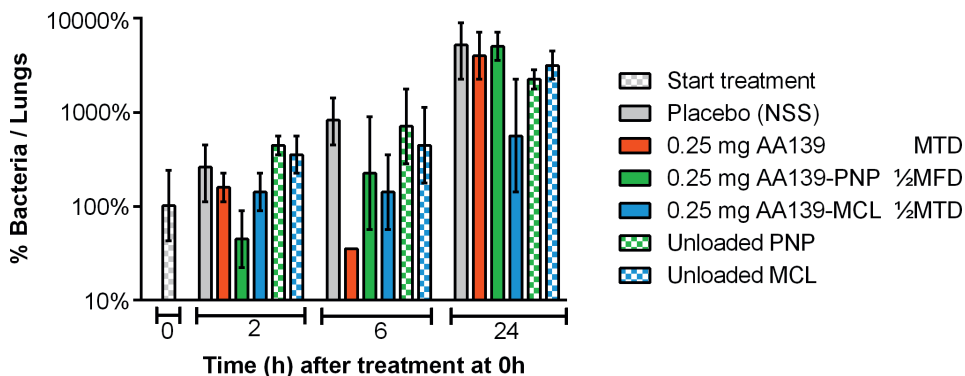


Figure 4. Early bacterial killing activity of AA139, AA139-PNP or AA139-MCL in rats with ESBL pneumonia-septicemia. At 24 hours after initiation of infection, rats were treated with a single dose of free AA139, AA139-PNP, or AA139-MCL at 0.25 mg (ca. ~1 mg/kg). Rats were sacrificed at 2, 6, and 24 hours after administration and dissected. Shown are the mean \pm range of 2 rats per timepoint per treatment group.

AA139-PNP resulted in a rapid decrease of bacterial counts within 2 hours after administration, but began to rebound at 6 hours post-dose, generating similar bacterial counts to placebo by 24 hours bacterial decrease which persisted for at least 24 hours. Rats treated with unloaded PNP or unloaded MCL had bacterial counts similar to placebo, showing no bacterial decrease during treatment. Analysis of blood biomarkers showed no indications of acute toxicity of any treatment (Supplementary Figure S4). Early *in vivo* bacterial killing activity experiments were performed to screen those potential nanomedicine candidates that had showed promising *in vitro* bactericidal activity. However, only a limited number of rats were used in these screening experiments³⁶, and consequently, statistical evaluation of these results could not be performed.

Therapeutic efficacy of AA139, AA139-PNP and AA139-MCL, in infected rats

At 24 hours after initiation of infection, rats in groups of 12 were treated with free AA139, AA139-PNP, or AA139-MCL once-daily (q24h) for 10 days. Placebo-treated

rats reached humane endpoints within 7 days after start of treatment (Figure 5). The treatment outcomes were statistically evaluated and compared; all *p*-values can be found in Table 2. Infected rats were monitored 12-hourly for the entire duration of the experiment. No signs of acute toxicity were observed following administration of compounds at the limiting dose once-daily (q24h) for 10 days. Rats treated with free AA139 at MTD (0.25 mg/rat; ~1 mg/kg), unloaded PNP, or unloaded MCL did not show an improvement in survival compared to placebo-treated rats. Rats treated with AA139-PNP at MFD (0.5 mg/rat; ~2 mg/kg) showed significantly improved survival compared to rats treated with free AA139 at MTD, unloaded PNP, or placebo. Rats treated with AA139-PNP at ½MFD did not show significantly improved survival. Rats treated with AA139-MCL at MTD (0.5 mg/rat; ~2 mg/kg) or at ½MTD showed significantly improved survival compared to rats treated with free AA139 at MTD, unloaded MCL, or placebo. No significant differences in therapeutic efficacy were found between AA139-PNP and AA139-MCL.

Table 2. Statistical evaluation of rat survival after treatment with AA139, AA139-PNP, or AA139-MCL

p-values Log-rank test Mantel-Cox	Placebo (NSS)	Unloaded		Free	AA139			
		PNP	MCL		PNP	MCL		
				0.25mg	0.25mg	0.5mg	0.25mg	0.5mg
Placebo (NSS)								
Unloaded-PNP	0.9329							
Unloaded-MCL	0.9689	0.9778						
AA139 0.25mg	0.9772	0.9879	0.9747					
AA139 0.25mg -PNP 0.5mg	0.0911	0.1218	0.1680	0.1208				
AA139 0.25mg -MCL 0.5mg	0.0131	0.0156	0.0161	0.0079	0.5966			
	0.0043	0.0074	0.0061	0.0069	0.1140	0.7208		
	0.0055	0.0068	0.0085	0.0056	0.0997	0.5966	0.7635	

Statistical evaluation using the Log-rank (Mantel-Cox) test of rat survival after once-daily (q24h) administration of free AA139, AA139-PNP, or AA139-MCL over 10 days. Significant *p*-values (*p* < 0.05) are indicated in bold.

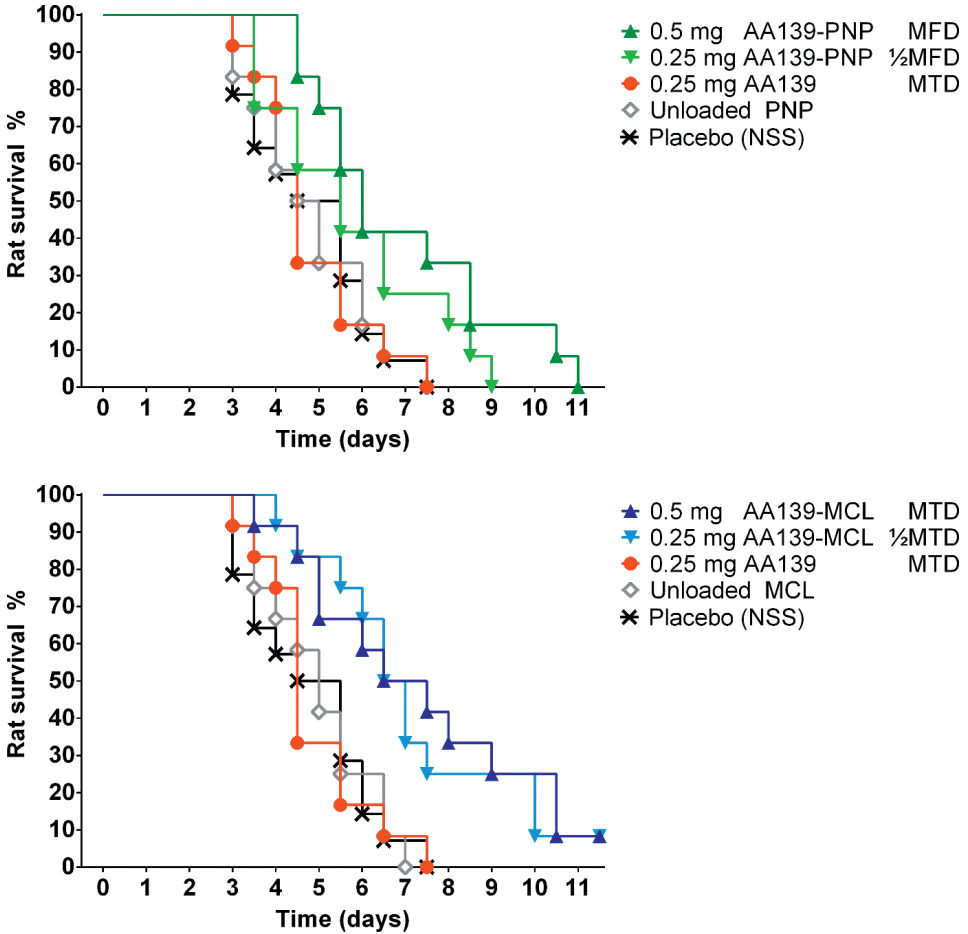


Figure 5. Therapeutic efficacy of AA139, AA139-PNP, or AA139-MCL in rats with ESBL pneumonia-septicemia. At 24 hours after initiation of infection, groups of 12 rats were treated once-daily (q24h) for 10 days with free AA139, AA139-PNP or AA139-MCL. Shown are the survival curves (Kaplan-Meier) representing rats reaching humane endpoints.

Discussion

The clinical utility of many AMPs is currently limited by several implementation barriers, such as toxic side-effects⁸ and short biological half-lives due to susceptibility to proteases^{8,9}. However, these implementation barriers could potentially be off-set by the development of nanomedicine formulations based on AMPs^{13,19}. Additionally, the

direct delivery of antibiotic-nanomedicines to the lungs may provide therapeutic advantages when compared to conventional administration methods^{19,20}. To investigate this hypothesis, the novel AMP AA139 was successfully entrapped in two nanocarriers (PNP or MCL) to generate two novel nanomedicines (AA139-PNP and AA139-MCL). The *in vitro* antimicrobial activity of both nanomedicines was found to be comparable to free AA139 at multiple concentrations, suggesting that AA139 retained its bactericidal activity despite formulation in PNP or MCL nanocarriers, a promising characteristic for further *in vivo* studies. Further studies into the mechanisms of entrapment and subsequent release of AA139 from the nanomedicines were barred as we did not succeed in the successful labelling of AA139 for NMR studies.

In uninfected rats, biodistribution studies showed that the residence time in the lungs of both AA139-PNP and AA139-MCL was longer than that observed with free AA139. Specifically, AA139-PNP exhibited ca. ~20% longer residence time in the lung as compared to free AA139. The residence time of AA139-MCL in the rat lung was observed to be even longer (at ca. ~80%) when compared to free AA139. As discussed by Kumari *et al.*, many types of PNP-based drug delivery systems exhibit controlled release mechanisms, although this depends on the particular type of PNP utilized⁴¹. Further, Gill *et al.* previously reported that entrapping drugs in MCLs facilitates sustained drug release in the lung³³. Regarding the limiting dose, both nanomedicines could be safely administered at twice the dose of free AA139. Although not a particularly high increase, this finding does demonstrate that nanomedicine formulations can result in reduced toxic side effects, consequently allowing the administration of higher doses of AMPs during treatment. Other investigators have previously discussed the reduction of toxic side effects as benefits of drug nanoformulation, which has been reported for both PNP⁴² and MCL³¹.

The early bacterial killing activity of the nanomedicines by single-dose administration was investigated in rats with fatal pneumonia-septicemia caused by multidrug-resistant *K. pneumoniae*. AA139-PNP showed a rapid but short-lasting bacterial killing effect whereas AA139-MCL showed a slow but sustained bacterial killing effect, reflecting the difference in biological half-lives between AA139-PNP and AA139-MCL as observed

in our biodistribution studies. Taken together, similar doses (0.25 mg/rat; ~1 mg/kg) of free AA139, AA139-PNP and AA139-MCL showed comparable bacterial killing activity over the first 6 hours post-dose; although bactericidal activity persisted through 24 hours only for AA139-MCL, while bacterial counts following the other two treatments had rebounded to placebo levels by 24 hours post-dose. As these studies were used for early assessment of *in vivo* bacterial killing activity in the development pipeline, only a limited number of rats were used to reduce and refine the use of experimental animals³⁶. As a consequence, evaluation of the early bacterial killing results with statistical significance calculations could not be performed. However, these experiments have been included to: 1) provide a preliminary look at the effect of AA139-nanomedicines on the bacterial load in the lungs over time, 2) to further support conclusions that can be drawn from the TKK assays and biodistribution studies, 3) to showcase how the early development pipeline of novel nanomedicines is structured, and 4) because the dissemination of animal experimental results should be a professional standard for ethical animal research⁴³.

Further studies assessed the therapeutic efficacy of the nanomedicines by once-daily (q24h) administration for 10 days at the limiting dose of both nanomedicines (0.5 mg/rat; ~2 mg/kg), or at the MTD of free AA139 (0.25 mg/rat; ~1 mg/kg). Both nanomedicines exhibited a statistically significant improvement in therapeutic efficacy when dosed at their limiting dose compared to free AA139 dosed at its MTD. While not particularly high, the two-fold increase in limiting dose was sufficient to demonstrate a potential advantage of nanomedicine formulations in minimizing potential toxic side-effects which may be associated with particular AMPs when treating patients. In addition, AA139-MCL showed significantly improved therapeutic efficacy at 1/2MTD as well, suggesting that the superior residence time of AA139-MCL in the lung resulted in further improved therapeutic efficacy in a daily dosing schedule. The lung residence time as well as the early bacterial killing activity of AA139-nanomedicines in the lung indicate that more frequent administration could have resulted in improved therapeutic efficacy. In our first pilot therapeutic efficacy experiment twice-daily (q12h) administration of AA139-nanomedicines was used, however this schedule was found

to show acute toxicity (abnormal breathing of rats) after several days which lead to termination the pilot experiment. The once-daily (q24h) dosing schedule was well tolerated and was therefore chosen to perform the therapeutic efficacy studies.

Future pharmacokinetic studies of the two AA139-nanomedicines may reveal more appropriate dosing schedules which could lead to improvement of their therapeutic efficacy. The present study shows that although both nanomedicines resulted in significantly improved therapeutic efficacy in terms of increased rat survival time compared to free AA139, survival of all infected rats was not achieved. In relation to this, it should be noted that the pneumonia-septicemia rat model used in this study is representative of multidrug-resistant bacterial infections that are associated with very high mortality rates in patients and are particularly challenging to treat successfully³⁴. Further, there is published evidence that rats may be more sensitive to the innate immune activation known to be caused by AMPs, including histamine release⁴⁴⁻⁴⁶. This makes the rat a good model for evaluating potential AMP toxicity decreases using nanomedicine formulation, as the tolerability of AMPs in rats is generally low. Of note, single and repeated AA139 aerosol administrations of up to 20 mg/kg/day have been well-tolerated in uninfected mice²⁷.

A practical limitation in the experimental set-up was the maximum volume of compounds (100 μ L) that could be administered to the rats by endotracheal aerosolization in order to avoid reflux of compound after administration. This meant that only restricted doses could be administered to the rats, in this way preventing the demonstration of a more optimal therapeutic effect. In addition, the animals must be under anesthesia for the administration which results in a low respiratory rate and therefore a low efficiency of drug delivery, restricting the dose that can be administered. In patients, inhalation of antibiotics would be the preferred route of administration, as inhalation allows higher doses of antibiotic to be delivered to the lungs over a longer period of time⁴⁷. In an attempt to improve aerogenic treatment in rats, we previously tested two aerosol inhalation systems for their capacity to administer the described nanomedicines to uninfected rats⁴⁰. Although an improved uniform distribution of compound in the lungs was achieved, the results also indicated that only <0.1% of

compound was deposited in the lungs, compared to ~85% deposition using endotracheal aerosolization⁴⁰. Based on these results, a decision was made to utilize the more efficient endotracheal aerosolization in our efficacy studies in rats.

Free AA139 has been shown to be potent in *in vivo* efficacy in studies using different infection models, including a murine pneumonia model^{26,27}. In the present study, both AA139-nanomedicines showed significantly improved therapeutic efficacy in terms of an extended rat survival time. While these results are promising, survival of all infected rats was not obtained. Various factors could explain the lack of survival of infected rats receiving free AA139 or nanomedicine, including: 1) a suboptimal administration frequency, 2) the severity of the present infection model in rats, 3) the general sensitivity of rats to AMP toxicity, or 4) the limitations of endotracheal aerosolization as an administration method. Due to these factors, a maximum therapeutic effect (in terms of survival of all infected rats) could unfortunately not be achieved. Importantly, it is clear that the choice of animal model and study protocol are of significant importance for the success of preclinical studies involving AMPs and should be taken into consideration during the drug development process. In addition, future studies on AA139-nanomedicines should further refine these antimicrobial candidates for the treatment of bacterial infections to show more clinically significant improvements over free AA139 in different experimental set-ups.

Conclusions

The present study demonstrates that AMP nanomedicines may reduce some of the main barriers to the clinical use of underutilized AMP antibiotics, primarily by ameliorating potential toxic side-effects and prolonging the biological half-life of AMP at the site of infection, while maintaining the AMP antimicrobial activity. Our results support the further evaluation of AA139-based nanomedicines as potential 'second-generation' novel therapeutic agents for the treatment of multidrug-resistant Gram-negative pulmonary infections.

Acknowledgements

Analysis of blood plasma was performed by the Clinical Pharmacology and Toxicology Laboratory at the Erasmus University Medical Center, Rotterdam, The Netherlands. The LC-MS/MS bioanalytical procedure was performed by Covance Laboratories, Harrogate, United Kingdom.

Funding

This work was financially supported by the European Union's Seventh Program for Research, Technological Development and Demonstration under grant agreement No. 604434 PncumoNP.

Competing interests

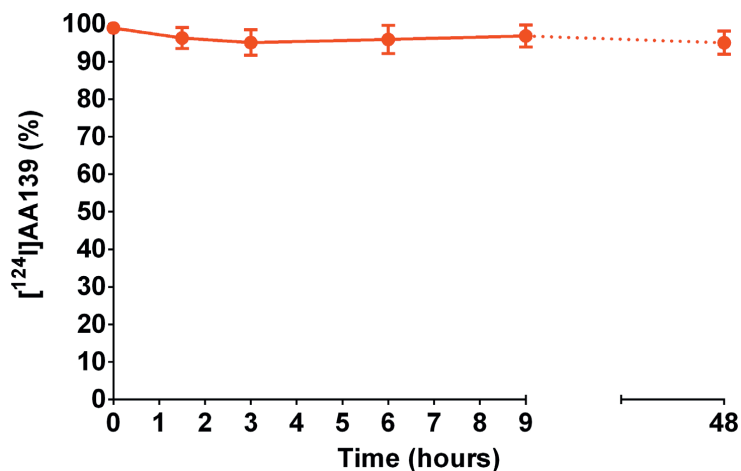
This study was performed in collaboration with CIDETEC, who are the patent holders of AA139-PNP. It was approved for publication by all consortium members of the PncumoNP project, including Adenium Biotech ApS, who are the patent holders of AA139.

References

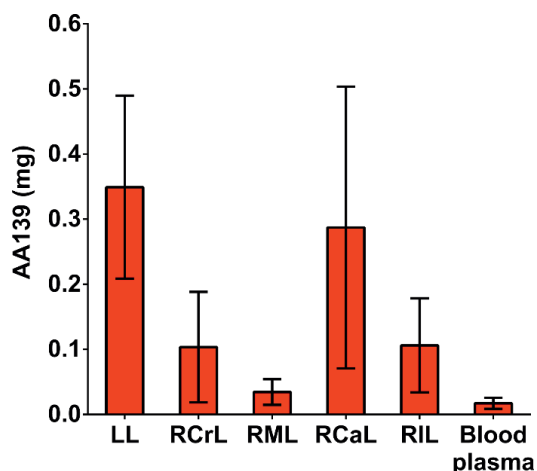
1. Marshall DC, Goodson RJ, Xu Y, Komorowski M, Shalhoub J, Maruthappu M, et al. Trends in mortality from pneumonia in the Europe union: a temporal analysis of the European detailed mortality database between 2001 and 2014. *Respiratory Research*. 2018;19(1):81.
2. Welte T, Torres A, Nathwani D. Clinical and economic burden of community-acquired pneumonia among adults in Europe. *Thorax*. 2012;67(1):71-9.
3. Sader HS, Farrell DJ, Flamm RK, Jones RN. Antimicrobial susceptibility of Gram-negative organisms isolated from patients hospitalised with pneumonia in US and European hospitals: results from the SENTRY Antimicrobial Surveillance Program, 2009–2012. *International Journal of Antimicrobial Agents*. 2014;43(4):328-34.
4. Bassetti M, Welte T, Wunderink RG. Treatment of Gram-negative pneumonia in the critical care setting: is the beta-lactam antibiotic backbone broken beyond repair? *Critical Care*. 2015;20(1):19.
5. Butler MS, Blaskovich MA, Cooper MA. Antibiotics in the clinical pipeline at the end of 2015. *The Journal of Antibiotics*. 2017;70(1):3.
6. Lewis K. Platforms for antibiotic discovery. *Nature Reviews Drug Discovery*. 2013;12(5):371-87.
7. Hancock RE, Sahl H-G. Antimicrobial and host-defense peptides as new anti-infective therapeutic strategies. *Nature Biotechnology*. 2006;24(12):1551.

8. Marr AK, Gooderham WJ, Hancock RE. Antibacterial peptides for therapeutic use: obstacles and realistic outlook. *Current Opinion in Pharmacology*. 2006;6(5):468-72.
9. Pini A, Falciani C, Bracci L. Branched peptides as therapeutics. *Current Protein and Peptide Science*. 2008;9(5):468-77.
10. Fox JL. Antimicrobial peptides stage a comeback. Nature Publishing Group; 2013.
11. Zazo H, Colino CI, Lanao JM. Current applications of nanoparticles in infectious diseases. *Journal of Controlled Release*. 2016;224:86-102.
12. Biswaro LS, da Costa Sousa MG, Rezende T, Dias SC, Franco OL. Antimicrobial peptides and nanotechnology, recent advances and challenges. *Frontiers in Microbiology*. 2018;9:855.
13. Huh AJ, Kwon YJ. "Nanoantibiotics": a new paradigm for treating infectious diseases using nanomaterials in the antibiotics resistant era. *Journal of Controlled Release*. 2011;156(2):128-45.
14. Wenzler E, Fraidenburg DR, Scardina T, Danziger LH. Inhaled antibiotics for Gram-negative respiratory infections. *Clinical Microbiology Reviews*. 2016;29(3):581-632.
15. Yang W, Peters JI, Williams III RO. Inhaled nanoparticles—a current review. *International Journal of Pharmaceutics*. 2008;356(1-2):239-47.
16. Patton JS, Byron PR. Inhaling medicines: delivering drugs to the body through the lungs. *Nature Reviews Drug Discovery*. 2007;6(1):67.
17. Sung JC, Pulliam BL, Edwards DA. Nanoparticles for drug delivery to the lungs. *Trends in Biotechnology*. 2007;25(12):563-70.
18. Bailey MM, Berkland CJ. Nanoparticle formulations in pulmonary drug delivery. *Medicinal Research Reviews*. 2009;29(1):196-212.
19. Ritsema JA, van der Weide H, Te Welscher YM, Goessens WH, Van Nostrum CF, Storm G, et al. Antibiotic-nanomedicines: facing the challenge of effective treatment of antibiotic-resistant respiratory tract infections. *Future Microbiology*. 2018;13(15):1683-92.
20. Andrade F, Rafael D, Videira M, Ferreira D, Sosnik A, Sarmiento B. Nanotechnology and pulmonary delivery to overcome resistance in infectious diseases. *Advanced Drug Delivery Reviews*. 2013;65(13-14):1816-27.
21. Frima HJ, Gabellieri C, Nilsson M-I. Drug delivery research in the European Union's Seventh Framework Programme for Research. *Journal of Controlled Release*. 2012;161(2):409-15.
22. Huang JX, Neve S, Elliot AG, Cain AK, Boinett CJ, Zuegg J, et al. Novel Arenicin-3 peptide antibiotics with broad-spectrum activity against MDR Gram-negative bacterial act via dual mode of actions. 54th International Conference of Antimicrobial Agents and Chemotherapy (ICAAC) and Infectious Diseases Society of America (IDSA) Joint Meeting: <https://adeniumBiotech.com/publications/>; 2014.
23. Neve S, Lociuo S, Morrissey I, Hawser S, Nordkild P. The arenicin-3 derived clinical candidate AA139 shows potent activity against Gram-negative pathogens, Poster F-261. 54th ICAAC Meeting; 5-9 September 2014; Washington, DC2014.
24. Cain AK, Boinett CJ, Barquist L, Neve S, Huang JX, Elliot AG, et al. Transposon directed insertion-site sequencing (TraDIS) to elucidate the mode of action of the antimicrobial Arenicin-3 (Arn-3). 54th International Conference of Antimicrobial Agents and Chemotherapy (ICAAC) and Infectious Diseases Society of America (IDSA) Joint Meeting: <https://adeniumBiotech.com/publications/>; 2014.
25. van der Weide H, Vermeulen-de Jongh DM, van der Meijden A, Boers SA, Kreft D, Marian T, et al. Antimicrobial activity of two novel antimicrobial peptides AA139 and SET-M33 against clinically and genotypically diverse *Klebsiella pneumoniae* isolates with differing antibiotic resistance profiles. *International Journal of Antimicrobial Agents*. 2019;54(2):159-66.
26. Lociuo S. Oral presentation: Arenicin antimicrobial peptides (novel AMPs with a novel mode of action). 54th International Conference of Antimicrobial Agents and Chemotherapy (ICAAC) and Infectious Diseases Society of America (IDSA) Joint Meeting: <https://adeniumBiotech.com/publications/>; 2014.
27. Adenium Biotech ApS. Personal communication on confidential experimental data obtained from mice. 2019.

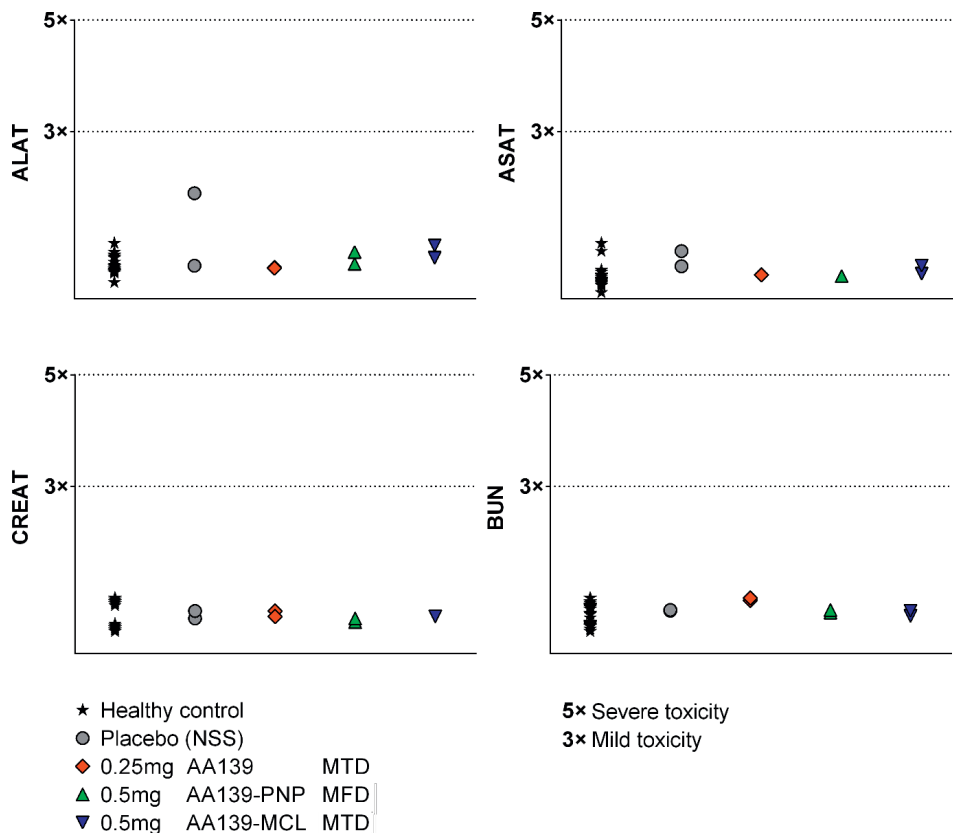
28. Gracia R, Marradi M, Cossío U, Benito A, Pérez-San Vicente A, Gómez-Vallejo V, et al. Synthesis and functionalization of dextran-based single-chain nanoparticles in aqueous media. *Journal of Materials Chemistry B*. 2017;5(6):1143-7.
29. Torchilin VP. Structure and design of polymeric surfactant-based drug delivery systems. *Journal of Controlled Release*. 2001;73(2-3):137-72.
30. Kröger APP, Paulusse JM. Single-chain polymer nanoparticles in controlled drug delivery and targeted imaging. *Journal of Controlled Release*. 2018;286:326-47.
31. Sawant RR, Torchilin VP. Multifunctionality of lipid-core micelles for drug delivery and tumour targeting. *Molecular Membrane Biology*. 2010;27(7):232-46.
32. Murgia X, Pawelzyk P, Schaefer UF, Wagner C, Willenbacher N, Lehr C-M. Size-limited penetration of nanoparticles into porcine respiratory mucus after aerosol deposition. *Biomacromolecules*. 2016;17(4):1536-42.
33. Gill KK, Nazzal S, Kaddoumi A. Paclitaxel loaded PEG5000–DSPE micelles as pulmonary delivery platform: Formulation characterization, tissue distribution, plasma pharmacokinetics, and toxicological evaluation. *European Journal of Pharmaceutics and Biopharmaceutics*. 2011;79(2):276-84.
34. van der Weide H, ten Kate MT, Vermeulen-de Jongh DMC, van der Meijden A, Wijma RA, Boers SA, et al. Successful High-Dosage Monotherapy of Tigecycline in a Multidrug-Resistant *Klebsiella pneumoniae* Pneumonia–Septicemia Model in Rats. *Antibiotics*. 2020;9(3):109.
35. van der Weide H, Vermeulen-de Jongh DM, van der Meijden A, Boers SA, Kreft D, Marian T, et al. Antimicrobial activity of two novel antimicrobial peptides AA139 and SET-M33 against clinically and genotypically diverse *Klebsiella pneumoniae* isolates with differing antibiotic resistance profiles. *International Journal of Antimicrobial Agents*. 2019.
36. Balls M, Goldberg AM, Fentem JH, Broadhead CL, Burch RL, Festing MF, et al. The three Rs: the way forward: the report and recommendations of ECVAM Workshop 11. *Alternative to Laboratory Animals*. 1995;23(6):838.
37. Kilkenny C, Browne WJ, Cuthill IC, Emerson M, Altman DG. Improving bioscience research reporting: the ARRIVE guidelines for reporting animal research. *PLOS Biology*. 2010;8(6).
38. Lee H, Blaufox M. Blood volume in the rat. *Journal of Nuclear Medicine*. 1985;26(1):72-6.
39. Adenium Biotech ApS. Personal communication on confidential experimental data obtained on AA139 degradation. 2015.
40. Cossío U, Gómez-Vallejo V, Flores M, Gañán-Calvo B, Jurado G, Llop J. Preclinical evaluation of aerosol administration systems using Positron Emission Tomography. *European Journal of Pharmaceutics and Biopharmaceutics*. 2018;130:59-65.
41. Kumari A, Yadav SK, Yadav SC. Biodegradable polymeric nanoparticles based drug delivery systems. *Colloids and Surfaces B: Biointerfaces*. 2010;75(1):1-18.
42. Jain AK, Swarnakar NK, Godugu C, Singh RP, Jain S. The effect of the oral administration of polymeric nanoparticles on the efficacy and toxicity of tamoxifen. *Biomaterials*. 2011;32(2):503-15.
43. Wieschowski S, Biernot S, Deutsch S, Glage S, Bleich A, Tolba R, et al. Publication rates in animal research. Extent and characteristics of published and non-published animal studies followed up at two German university medical centres. *PLOS ONE*. 2019;14(11).
44. Brzezińska-Błaszczak E, Czuwaj M, Kuna P. Histamine release from mast cells of various species induced by histamine releasing factor from human lymphocytes. *Agents and Actions*. 1987;21(1-2):26-31.
45. Decorti G, Klugmann FB, Candussio L, Furlani A, Scarcia V, Baldini L. Uptake of adriamycin by rat and mouse mast cells and correlation with histamine release. *Cancer research*. 1989;49(8):1921-6.
46. Brown KL, Hancock RE. Cationic host defense (antimicrobial) peptides. *Current Opinion in Immunology*. 2006;18(1):24-30.
47. Brain JD, Knudson DE, Sorokin SP, Davis MA. Pulmonary distribution of particles given by intratracheal instillation or by aerosol inhalation. *Environmental Research*. 1976;11(1):13-33.



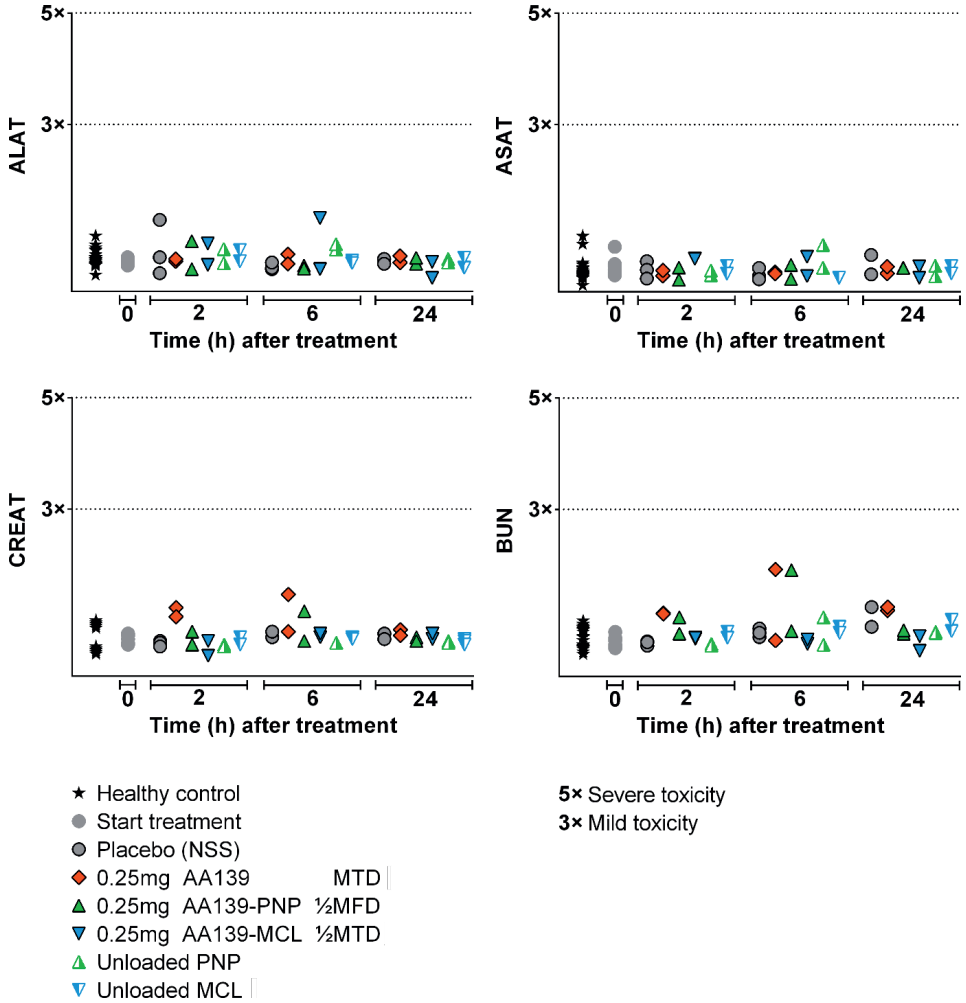
Supplementary Figure S1. Stability of radiolabelled AA139. [¹²⁴I]AA139 was incubated in moderately acidic conditions (sodium acetate buffer at pH = 5.5) and the percentage of unchanged [¹²⁴I]AA139 was determined by radio-HPLC. Experiments were performed in triplicate (mean ± standard deviation).



Supplementary Figure S2. AA139 deposition in lungs and distribution to blood plasma of uninfected rats immediately after endotracheal aerosolization. 1 mg AA139 was administered to 6 rats which were immediately sacrificed after dosing. AA139 was measured in lung lobes and blood plasma by LC-MS/MS bioanalytical assay. Shown are the mean ± standard deviation of total AA139 in rat lung lobes and total blood plasma volume (estimation based on body weight). LL, left lobe; RCrL, right cranial lobe; RML, right middle lobe; RCaL, right caudal lobe; RIL, right intermediate lobe.



Supplementary Figure S3. Biomarkers of acute toxicity in blood plasma of uninfected rats treated with a single dose of free AA139, AA139-PNP, or AA139-MCL. Each compound was administered at its limiting dose in 100 μ L by endotracheal aerosolization. Groups of 2 rats were sacrificed at 24 hours after administration.



Supplementary Figure S4. Biomarkers of acute toxicity in blood plasma of rats with ESBL-producing *K. pneumoniae* pneumonia-septicemia treated with a single dose of free AA139, AA139-PNP, or AA139-MCL. Each compound was administered at 0.25 mg in 100 μ L by endotracheal aerosolization. Groups of 2 rats were sacrificed at 2 hours, 6 hours and 24 hours after administration, which was 24 hours after initiation of infection.

Chapter 9 Summarizing discussion and future perspectives

Chapter 10 Glossary

Chapter 11 Nederlandse samenvatting



Section

IV

FINAL ASSESSMENT



Chapter

9

SUMMARIZING DISCUSSION
AND FUTURE PERSPECTIVES

Summarizing discussion

Gram-negative pneumonia and antimicrobial resistance

Pneumonia is responsible for over 230,000 deaths and €10 billion in economic costs across the European Union (EU) every year^{1,2}, with Gram-negative bacteria being the primary causative pathogens in ~70% of healthcare-associated pneumonia cases³. This group of bacteria is at the forefront of the current antibiotic crisis^{4,5}, capable of rapidly developing and disseminating resistance against novel antibiotics⁶. Further, the general lack of development of new antibiotic classes^{7,8} means that novel therapeutic approaches must be investigated to combat this emerging healthcare crisis⁹.

Novel therapeutic approaches

Among these novel approaches are the development of underutilized classes of antibiotics such as antimicrobial peptides (AMPs)^{10,11}; advanced drug delivery systems such as nanomedicine formulation¹², and more efficient and safe delivery of antibiotics to the site of infection¹³. **Chapter 2** is a review of the current state of antibiotic-nanomedicines research aimed at the treatment of antibiotic-resistant respiratory tract infections, including multidrug-resistant Gram-negative pneumonia. It provides an overview of the current state of research, the development of different nanocarriers, and the potential value and clinical status of inhalable antibiotic-nanomedicines. Research focused on combining these three therapeutic approaches is described in **Chapters 4 – 8**, helping establish an extensive pre-clinical developmental pipeline for novel antibiotic-nanomedicines. The key feature of this pipeline is the development and testing of novel nanomedicine combinations comprising novel AMPs with various nanocarriers, including investigations into their antimicrobial activity and therapeutic efficacy for the treatment of multidrug-resistant Gram-negative pneumonia (Figure 1). This research was supported via an EU FP7 grant (PneumoNP).

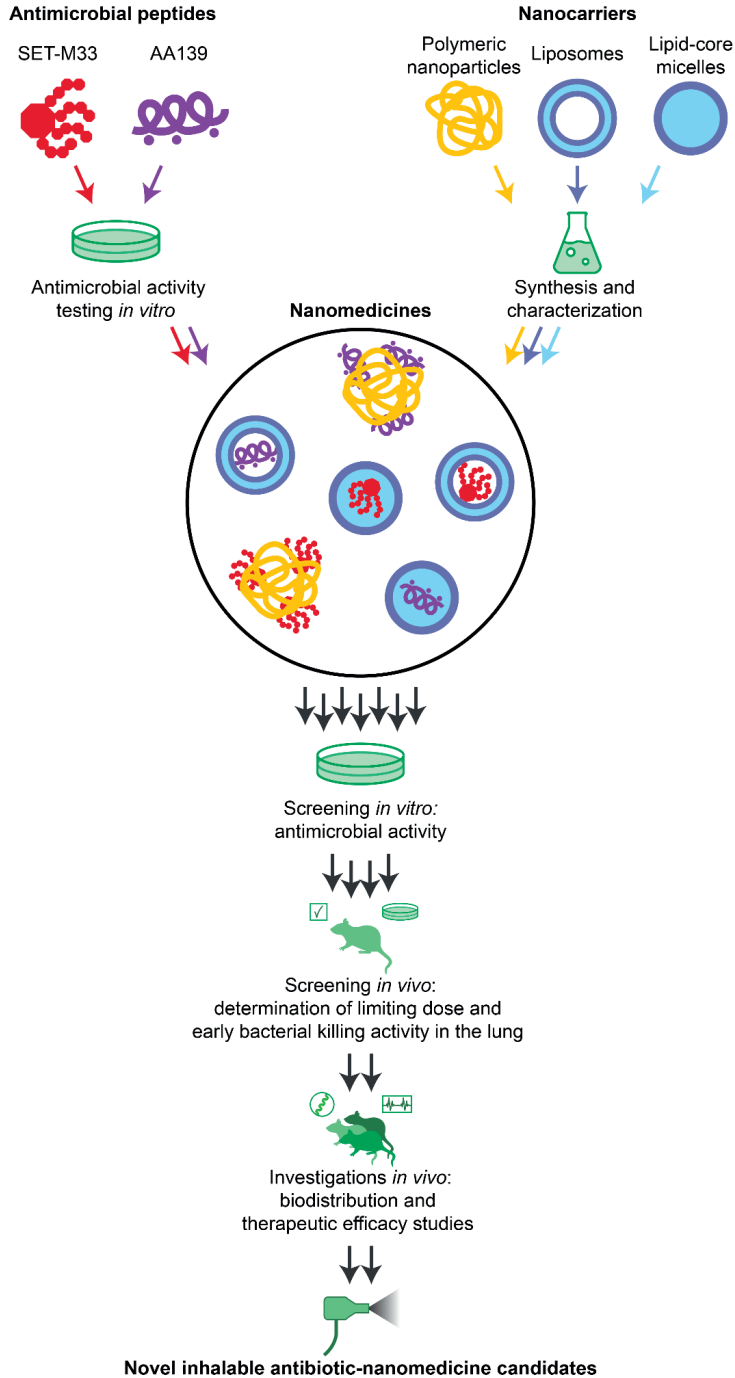


Figure 1. Diagram of the research in the PneumoNP pre-clinical development pipeline to develop novel AMP-nanomedicine candidates which is included in this thesis.

Novel antimicrobial peptides

One promising class of novel antibiotics currently undergoing increased investigation is the antimicrobial peptides (AMPs), a broad family of antibiotics that are produced in nature by organisms as a natural defense against microbes¹⁴. Although AMPs have been known since the 1950's, this family of antibiotics has seen only limited use for the treatment of pneumonia, largely due to a number of hurdles that have limited their clinical use, including toxic side-effects¹⁵, short biological half-life due to degradation by proteases^{15,16} and limited efficacy against Gram-negative bacteria¹⁷. However, novel AMPs are continually being discovered and developed¹⁷⁻¹⁹, and new delivery systems are being investigated in order to overcome these challenges. For example, entrapment of AMPs into nanoparticles to produce nanomedicines may generate several solutions to the hurdles traditionally associated with the clinical utility of AMPs in the treatment of multidrug-resistant infections^{20,21}. Notably, nanomedicine formulations could potentially reduce toxic side-effects and extend the biological half-life of AMPs¹². Further, the direct delivery of antibiotics to the site of infection represents an additional therapeutic improvement¹³, which could facilitate increased antibiotic activity at the actual site of infection^{22,23} and lead to reduced systemic toxicity and 'collateral damage' to patients^{24,25}.

In **Chapter 4** and **Chapter 5**, the *in vitro* antimicrobial activity of two novel AMPs (AA139 and SET-M33) against Gram-negative *Klebsiella pneumoniae* and *Pseudomonas aeruginosa* bacteria was investigated. In **Chapter 4**, we examined the antimicrobial activity of AA139 and SET-M33 against a collection of clinically relevant *K. pneumoniae* isolates recovered from a variety of different clinical samples from individual patients. This collection was characterized genotypically and phenotypically to confirm that it represented a variety of unrelated clinical isolates that could be encountered in the clinic, and represented a variety of 5 distinct antibiotic resistance profiles, from susceptible to extensively multidrug-resistant phenotypes. The antimicrobial activity of both AMPs remained similar despite the various antibiotic resistance profiles present in this *K. pneumoniae* collection, including for colistin-susceptible and colistin-resistant

phenotypes. Indeed, neither AA139 nor SET-M33 was affected by resistance to colistin (an AMP currently used in the clinic as an antibiotic of ‘last resort’). This is an important finding in view of the emergence and spread of colistin-resistant bacteria^{26,27}, as well as the ‘self-promoted uptake’ mechanism shared by colistin and the cationic AMPs AA139 and SET-M33. In this mechanism, the antibiotics first bind and inhibit LPS in the bacterial outer membrane, which is then followed by insertion of the antibiotic into the cell envelope, resulting in outer membrane permeabilization, disruption of the cytoplasmic membrane, and bacterial cell death²⁸.

The concentration- and time-dependent antimicrobial activity of AA139 and SET-M33 in comparison to colistin was investigated in a panel of extensively antibiotic-resistant *K. pneumoniae* isolates, including an isolate carrying plasmidal colistin resistance. Both AA139 and SET-M33 showed a concentration-dependent bactericidal effect irrespective of the susceptibility of the isolates to colistin, although a limited decrease in activity was observed in the colistin-resistant isolates. At the end of 24 hours of exposure to AA139 or SET-M33, only small changes in susceptibility of the *K. pneumoniae* isolates to the AMPs were observed, and only after exposure to their respective minimum inhibitory concentrations (MICs). In contrast, exposure of the same *K. pneumoniae* isolates to colistin resulted in large changes in colistin susceptibility in both colistin-susceptible and colistin-resistant isolates. The ease with which colistin is able to select resistance in these strains is likely to be the result of rather high mutation rates for colistin resistance²⁹ or pre-existing colistin-resistant sub-populations in otherwise colistin-susceptible bacterial populations (colistin heteroresistance)³⁰. This is a worrying observation, as it means that colistin-resistance is easily selected upon long-term exposure to the antibiotic and therefore could easily be spread in bacterial populations treated with colistin. Our results show that AA139 and SET-M33 will not readily select for resistance, which is important in view of the potential longevity of these novel AMPs for clinical use. Notably, this observation remained true for colistin-resistant strains as well, showing that AMPs will remain viable candidates for treatment even in the case of colistin-resistant strains.

In conclusion, the findings in **Chapter 4** showed that both AA139 and SET-M33 may be suitable alternatives to colistin and viable candidates for the treatment of multidrug-resistant *K. pneumoniae* infections, including infections associated with colistin-resistant bacteria. Both novel AMPs retain their antimicrobial activity regardless of antibiotic-resistance profile or colistin-resistance, and do not readily generate AMP-resistance in bacterial isolates upon exposure. An important inclusion in this study was the MCR-producing *K. pneumoniae* strain. Since its first discovery in 2015²⁶, various variants of plasmidal colistin-resistance have been found across the world³¹, meaning that it is likely that MCR-producing strains will become more prevalent in the coming decades³², and due to the partially shared ‘self-promoted uptake’ mechanism it is important to verify that the AMPs remain effective against isolates carrying these plasmids.

Chapter 5 is an in-depth investigation of the *in vitro* bactericidal activity of SET-M33, as insights into its mechanism of bacterial killing could inform rational development to optimize the clinical utility of SET-M33. For these studies, extensively antibiotic-resistant but colistin-susceptible clinical isolates of *K. pneumoniae* and *P. aeruginosa* were selected. Both strains were also used to generate isogenic colistin-resistant mutants. SET-M33 showed concentration-dependent bactericidal activity against isogenic colistin-susceptible and colistin-resistant isolates of *K. pneumoniae* and *P. aeruginosa*. Changes in susceptibility of the bacterial strains after 24 hours of exposure to SET-M33 were only minor. Electron microscopic studies clearly revealed the cellular damage to the cell envelope of bacteria exposed to SET-M33. These studies also demonstrated that while SET-M33 is internalized within 5 minutes by bacteria³³, this rapid internalization does not lead to an immediate bacterial killing effect as seen for some other cationic AMPs³⁴.

Next, a linear analogue peptide of SET-M33 was synthesized (Q-33) for supramolecular structure investigations of SET-M33 which could not be performed with the original AMP due to its tetrabranch structure. Q-33 showed a similar ability as SET-M33 to adopt a helix conformation, confirming it as a reliable model for structural investigations of SET-M33. Similar to other cationic peptides^{35,36}, Q-33 was shown to adopt an α -helix structure partially buried in the membrane in a bacterial membrane-

mimicking environment. In contrast, it has been shown that colistin adopts a structure with random coiling and β -sheet features in lipid membrane models³⁷, further supporting the hypothesis that there are differences in the ‘self-promoted uptake’ mechanism between SET-M33 and colistin.

One commonly reported issue with cationic AMPs which share similar structural characteristics to SET-M33 is their tendency for self-aggregation and undesired peptide interactions with blood proteins³⁸. Further investigations showed that SET-M33 exhibited no self-aggregation, no cytotoxicity against human bronchial epithelial cells and only limited hemolytic activity against red blood cells. These findings indicate that SET-M33 does not have the disadvantageous biological characteristics reported for structurally similar AMPs, which is supported by previous studies where the *in vivo* administration of SET-M33 was well-tolerated³⁹.

In conclusion, the data obtained in **Chapter 5** further corroborate the findings presented in **Chapter 4** that SET-M33 remains a viable candidate for the treatment of multidrug-resistant Gram-negative pneumonia, even after prior exposure to colistin (potentially resulting in colistin resistance of the causative pathogen).

Animal disease model

Prior to continuing with *in vivo* studies, a suitable animal model of disease was developed, characterized and validated in rats as described in **Chapter 6**. In rats, we established a novel model of acute lobar pneumonia leading to fatal septicemia caused by an extended-spectrum β -lactamase (ESBL)-producing *K. pneumoniae* strain (referred to as *K. pneumoniae* ESBL) or an isogenic *K. pneumoniae* carbapenemase (KPC)-producing *K. pneumoniae* strain (referred to as *K. pneumoniae* KPC). This model is representative of a particularly severe multidrug-resistant infection in human patients⁴⁰⁻⁴² and allows for research comparing the therapeutic efficacy of individual antibiotics at similar conditions of severity, duration of infection, and host defense, which is not possible with most comparative clinical efficacy studies on tigecycline treatment^{43,44}. The course of infection in the disease model was characterized by a disease progression including complications of the pulmonary infection such as pleuritis or pericarditis, defined by



continuous body weight loss and fluctuating body temperatures eventually leading to hypothermia in the final stage, necessitating euthanasia of rats.

The translational value of the above disease model was demonstrated in terms of the therapeutic response of infected rats to the antibiotics meropenem and tigecycline, administered in clinically relevant therapeutic schedules started when rats suffered from progressive pulmonary infection and had developed septicemia. Carbapenem antibiotics such as meropenem are the antibiotic of choice in the case of antibiotic-resistant infections, but increasing numbers of carbapenem-resistant bacterial isolates such as *K. pneumoniae* KPC have further complicated the successful treatment of multidrug-resistant Gram-negative bacterial infections⁴⁵. As a result, alternative drugs of last resort like tigecycline have therefore seen increased use in patients suffering from such infections, although the appropriate dosing of tigecycline has been the subject of debate⁴⁶. We demonstrated that the *in vivo* response to a 12-hourly treatment of meropenem or tigecycline during 10 days reflected the *in vitro* susceptibility of the causative *K. pneumoniae* strain, with meropenem being successful in the treatment of pneumonia-septicemia caused by *K. pneumoniae* ESBL, but being unsuccessful in the treatment of pneumonia-septicemia caused by *K. pneumoniae* KPC. To confirm that pneumonia-septicemia caused by *K. pneumoniae* KPC could be effectively treated using appropriate antibiotic therapy, a high-dose regimen of tigecycline was successful in treating pneumonia-septicemia caused by *K. pneumoniae* KPC. The findings in our study in **Chapter 6** support recent literature^{47,48} recommending the use of high-dose tigecycline treatment as a last resort option for the treatment of patients with severe infections (such as pneumonia) caused by carbapenem-resistant Gram-negative bacteria.

Targeted delivery of AMP-nanomedicines

Moving forward in the PneumoNP developmental pipeline, we followed two novel approaches in the *in vivo* efficacy studies using SET-M33 and AA139. In **Chapter 7** and **Chapter 8**, we developed novel AMP-nanomedicines by entrapment of SET-M33 and AA139 in nanocarriers¹², and we administered the nanomedicines via endotracheal

aerosolization to achieve more efficient and safe delivery of the nanomedicines to the site of infection¹³. The AMP-nanomedicines were developed by combining AA139 and SET-M33 with three distinct forms of nanocarriers: polymeric nanoparticles (PNP)⁴⁹, liposomes (LIP)^{50,51}, or lipid-core micelles (MCL)⁵².

Multiple iterations and adjustments of the various nanomedicines were developed and refined based on initial *in vitro* antimicrobial activity screening experiments, until four final nanomedicines were selected for more extensive *in vitro* and *in vivo* testing. Four final AMP-nanomedicines were selected: SET-M33-PNP, SET-M33-LIP, AA139-PNP, and AA139-MCL. These four AMP-nanomedicines were compared to their respective AMPs in the 'free form' (free AMPs) and were examined by *in vitro* testing of bactericidal activity against *K. pneumoniae* ESBL and *in vivo* studies in the rat model of pneumonia-septicemia caused by *K. pneumoniae* ESBL. **Chapter 7** covers the examination of SET-M33-PNP and SET-M33-LIP, and **Chapter 8** covers the investigation of AA139-PNP and AA139-MCL.

In **Chapter 7**, we observed that SET-M33-PNP showed *in vitro* similar rapid bactericidal activity leading to complete bacterial killing at the same concentrations as free SET-M33, whereas SET-M33-LIP exhibited a delayed bactericidal effect compared to free SET-M33. In uninfected rats, determination of the limiting dose showed that the maximum feasible dose (MFD) of both SET-M33-nanomedicines was equal to the maximum tolerable dose (MTD) of free SET-M33; unfortunately, the SET-M33-nanomedicines could not be administered at higher dosages due to technical limitations related to SET-M33 nanoformulation and to the attainable dosage using endotracheal aerosolization in rats under anesthesia. In rats with *K. pneumoniae* pneumonia-septicemia after a single dose treatment, the early bacterial killing activity in the lungs of SET-M33-PNP was similar to free SET-M33. The activity of SET-M33-LIP was slow, but sustained over time compared to free SET-M33. At this point, it should be noted that the studies described above were performed as pilot experiments, with the goal of providing preliminary data on the *in vivo* effects of the different AMP-nanomedicines via our PneumoNP developmental pipeline. This meant that only a limited number of rats were used following recommendations from our animal ethics committee⁵³.

Although no firm conclusions could be drawn from these experiments, the results obtained were essential in the selection of AMP-nanomedicines and the design of further *in vivo* therapeutic efficacy experiments.

Summarizing, the data obtained in **Chapter 7** suggests that SET-M33-PNP retains its rapid bactericidal activity *in vitro* and *in vivo* against *K. pneumoniae* ESBL equal to free SET-M33 despite formulation in PNP nanocarriers, whereas SET-M33-LIP shows slow but sustained release of SET-M33 from the liposomes, which could have potential advantages compared to free SET-M33. Unfortunately, administration of higher dosages of SET-M33-nanomedicines could not be performed due to technical limitations. Further studies with a different experimental set-up could show further potential therapeutic advantages of SET-M33-PNP and SET-M33-LIP.

In **Chapter 8**, we showed that AA139-PNP showed relatively slow bactericidal activity *in vitro* – leading to near-complete bacterial killing at the same concentrations as free AA139. It was concluded that AA139 retained its relatively slow bactericidal activity despite formulation in PNP nanocarriers, whereas AA139-MCL exhibited a delayed bactericidal effect compared to free AA139. In uninfected rats, both AA139-nanomedicines were better tolerated than free AA139, demonstrating that nanoformulation resulted in reduced toxic side effects. Both AA139-nanomedicines also exhibited a longer residence time in the lungs compared to free AA139 in biodistribution studies. With respect to the early bacterial killing activity in the lungs of rats with pneumonia-septicemia after single dose administration, the killing activity of AA139-PNP appeared to be more rapid compared to free AA139, however, the activity of both AA139-PNP and free AA139 was of short duration. The killing activity of AA139-MCL initially appeared less compared to free AA139, however resulted in sustained bacterial killing activity over time. Our conclusion, drawn with caution, was that both AMP-nanomedicines showed a longer residence time in the lungs and decreased toxic side effects, but that nanoformulation of AA139 in PNP appears to facilitate rapid bactericidal activity, while nanoformulation of AA139 in MCL appears to show delayed release of AA139, both of which could have potential therapeutic advantages. In a final series of therapeutic efficacy studies, rats with pneumonia-

septicemia treated with AA139-PNP or AA139-MCL once-daily over a 10-day treatment period showed statistically significant improved therapeutic efficacy compared to free AA139.

Summarizing, the data obtained in **Chapter 8** suggest that PNP formulation of AA139 facilitates faster killing of *K. pneumoniae* ESBL in the lung compared to free AA139, however of short duration. MCL nanoformulation of AA139 resulted in slower bacterial killing in the lung, however, of longer duration. Both AA139-nanomedicines could be safely administered at double the dosage of free AA139, indicating that nanoformulation improves the tolerability of AA139 allowing higher dosages to be administered without toxic side effects²⁰. This is in contrast to the limiting dose of both SET-M33-PNP and SET-M33-LIP which was equivalent to the MTD of free SET-M33. Nanoformulation of AA139 also resulted in increased residence time in the lungs. Finally, the improved therapeutic efficacy obtained resulting from PNP- or MCL-nanoformulation of AA139 demonstrates their potential as novel nanomedicine candidates against multidrug-resistant Gram-negative pneumonia.

Conclusions

Overall, the results presented in this thesis demonstrate the positive effects of the entrapment of novel promising AMP antibiotics within nanocarriers for treating multidrug-resistant Gram-negative pneumonia. The findings also support the concept that aerosol-delivered nanomedicine formulations can be useful in the design of a new generation of antibiotic-based medicines for the treatment of multidrug-resistant pneumonia, including the treatment of infections that are resistant to antibiotics of 'last resort' e.g. colistin. The future use of our nanomedicine developmental and assessment pipeline is a promising pre-clinical research tool at a time when traditional antibiotics are failing and the treatment of antibiotic-resistant respiratory tract infections are of global importance. We are still far from having a novel treatment approach ready for clinical trials, but we have generated knowledge on the road to better treatment. Future studies with a different experimental set-up may show the further potential therapeutic advantages of AMP-nanomedicines administered via the aerogenic route.

Future perspectives

The studies described in this thesis were performed as part of the PneumoNP nanomedicine developmental pipeline and are directed at the increasing global threat of antibiotic-resistant respiratory tract infections⁵⁴. Essentially, in order to prevent a dreaded ‘post-antibiotic era’, novel therapeutic strategies (such as novel nanomedicines) must be efficiently developed and assessed if they are to be effectively employed in the treatment of such devastating infections. The *in vitro* and *in vivo* studies described aim for therapeutic improvement by combining three new approaches:

1. Novel antibiotic compounds

The two novel AMPs AA139^{18,55} and SET-M33¹⁹ developed by PneumoNP partners and members of an underutilized antibiotic class of AMPs appear to be promising antibiotic candidates to combat multidrug-resistant Gram-negative bacteria. They showed rapid bactericidal activity irrespective of the antibiotic resistance profile of bacteria, including colistin-resistant bacteria. In addition, exposure to AA139 and SET-M33 did not readily generate resistant mutants. This is in contrast to colistin, an AMP that is currently used as a last-resort antibiotic in the clinic which easily provokes resistance^{29,30}. Finally, it was observed that SET-M33 adopts a partially buried α -helix structure in the bacterial membrane, but unlike other AMPs which adopt this structure, we demonstrated that SET-M33 does not have disadvantageous biological characteristics such as cytotoxicity, hemolysis, and self-aggregation.

Taken together, our studies showed that cationic AMPs like AA139 and SET-M33 are promising candidate antibiotics for the treatment of multidrug-resistant Gram-negative bacterial infections, including infections associated with colistin resistance. The discovery of new antibiotics is only the first step in a long process towards marketability, with many potential hurdles lying in the path of drug commercialization in the antibiotic space⁵⁶. One clear example of this problem is the antibiotic AA139 (as we learned in November 2019), when PneumoNP partner Adenium Biotech ApS went into voluntary liquidation. It appears that AA139 ran into difficulties in the late pre-clinical phase. The experience communicated from our partner Adenium Biotech ApS was that it is

essential to take advantage of any new initiatives and funding opportunities available in the field. SET-M33 on the other hand is currently at the end of its preclinical development phase and ready to enter clinical trials for the treatment of lung infections in cystic fibrosis (CF) patients. SET-M33 is also being investigated for the treatment of urinary tract infections and bacterial septicemia.

In light of the currently unfolding antibiotic resistance crisis, studies on cationic AMPs should include investigations into their efficacy against pathogens with various forms of multidrug resistance. In this respect, colistin resistance is a particularly important subject for investigation, as some cationic AMPs have shown colistin cross-resistance due to similarities in the mechanism⁵⁷⁻⁵⁹. The precise mechanisms by which colistin and other cationic AMPs exert their antimicrobial killing activity and how resistance is generated towards these antibiotics is a complex and poorly understood matter⁶⁰, and continued mechanistic investigations will be essential in understanding if exposure to AMPs is likely to generate resistance and if there is the potential for colistin cross-resistance.

2. Nanomedicine formulation of antibiotics

Although AMPs are potent antibiotics, their clinical use is limited due to toxic side effects¹⁵ and short biological half-life resulting from degradation by proteases^{15,16}. Nanomedicine formulations could potentially reduce toxic side effects and extend the biological half-life of the antibiotics¹². The nanoformulation of AA139 and SET-M33 was successfully achieved using three distinct forms of nanocarriers: polymeric nanoparticles (PNP)⁴⁹, liposomes (LIP)^{50,51}, or lipid-core micelles (MCL)⁵².

The AMP-nanomedicines were stable and antibiotic leakage was never observed during storage. The bacterial killing activity of AA139 and SET-M33 after nanoformulation was retained *in vitro* and *in vivo*, with PNP appearing to facilitate rapid bactericidal activity, whereas LIP and MCL appeared to facilitate sustained bactericidal activity. Regarding toxic side effects, the nanomedicine formulation of AA139 in PNP⁶¹ and MCL⁶² resulted in decreased toxicity, allowing for the administration of higher doses. For SET-M33-nanomedicines, these advantages could not be confirmed due to

technical limitations which prevented the administration of higher doses of SET-nanomedicines. For this reason, AA139-nanomedicines were selected for continued *in vivo* investigations. Regarding biodistribution, the residence time of AA139 in the lungs was prolonged by nanoformulation, particularly for AA139-MCL. Therapeutic efficacy studies using once-daily administration of AA139-nanomedicines over 10 days to treat fatal multidrug-resistant *K. pneumoniae* pneumonia-septicemia in rats resulted in significantly increased rat survival compared to free AA139. AA139-PNP showed improved therapeutic efficacy when administered at a higher dose than the MTD of free AA139 which could be attributed to the decreased toxic side effects thanks to nanoformulation. AA139-MCL showed improved therapeutic efficacy at an equal dose to the MTD of free AA139, which could be explained by the significantly prolonged residence time and sustained bacterial killing activity in the lung.

From our *in vitro* and *in vivo* studies, it is clear that the characteristics of the nanocarrier strongly influence the therapeutic effects of nanoformulation. The versatility of nanocarriers among which the size, the charge, the fluidity/rigidity, and the surface characteristics offers many options for different applications of distinct antibiotic-nanomedicines²⁰, which may allow novel or underutilized antibiotics that would otherwise go unexploited to be optimized for clinical use. This means that for future development of antibiotic-nanomedicines, the characteristics of the nanocarrier must be carefully considered in view of the class of antibiotic, the type of pathogen, and the type of infection in order to achieve optimal therapeutic improvement. For example, the therapeutic efficacy of antibiotics with time-dependent antimicrobial activity can be improved by delayed antibiotic release from nanocarriers⁶³, antibiotics targeted at intracellular pathogens can benefit from intracellular delivery by nanocarriers⁶⁴, and controlled-release nanocarriers can improve the use of topical application of antibiotics⁶⁵.

3. Direct delivery of antibiotic-nanomedicines

More efficient and safe delivery of the antibiotic-nanomedicines to the actual site of infection could facilitate increased local antibiotic activity^{22,23}, while reducing systemic

toxicity and ‘collateral damage’ to the healthy microbiome in patients^{24,25}. To investigate direct delivery to the lungs, we developed and validated a rat disease model of pneumonia leading to septicemia caused by multidrug-resistant *K. pneumoniae*. This model was fatal if left untreated and representative of a severe multidrug-resistant Gram-negative pneumonia in human patients. Endotracheal aerosolization was the most efficient and quantitative method of antibiotic administration for this animal model to achieve direct delivery of AMP-nanomedicines to the lung, the primary site of infection.

The nanocarriers used to generate AMP-nanomedicines were chosen for their promising characteristics for pulmonary drug delivery: PNP may allow for improved drug penetration of the respiratory mucus⁶⁶, inhaled LIP is well tolerated and has the potential to reduce systemic drug toxicity⁶⁷⁻⁷⁰, and MCL has been shown to facilitate sustained drug release in the lungs⁷¹. For SET-M33-nanomedicines, the advantages of nanoformulation were not evident due to the low concentration of SET-M33 in the nanomedicines combined with the limited volume which could be administered by endotracheal aerosolization. For AA139-nanomedicines, we demonstrated the therapeutic improvement of nanoformulation compared to the free AMP, especially in terms of the achieved decrease in toxicity and the prolonged residence time in the lung, which are important improvements over conventional systemic administration of free AA139.

Important to mention here is that several factors prevented us from achieving a maximum therapeutic effect using the AMP-nanomedicines in our rat model of infection. The reason for this is the choice of aerogenic administration in small animals which presents some significant barriers to achieving the maximum delivery of compound. First, the animals must be under anesthesia for the administration, which results in a low respiratory rate and therefore a low efficiency of drug delivery, restricting the dose that can be administered⁷². Second, only a limited volume of drug can be administered in order to avoid reflux after administration, which in the case of antibiotic-nanomedicines with an upper limit on the antibiotic concentration in the nanomedicines restricts the dose that can be administered. In human patients,

inhalation of antibiotics would of course be the preferred route of aerogenic administration⁷³. In an attempt to improve aerogenic treatment in rats, two aerosol inhalation systems were tested for their capacity to administer the nanomedicines to uninfected rats⁷². Unfortunately, neither of these systems resulted in an improved deposition over endotracheal aerosolization.

It is clear that the choice of animal model, infection type, administration method, experimental set-up and the envisioned therapeutic improvements need to be important considerations in future studies. For the future development of AMP-nanomedicines, it will be pertinent to demonstrate the maximum therapeutic effect which could be accomplished by investigating routes of administration that allow for relatively large volumes to be administered so that higher doses can be applied, and by using an animal model which is less susceptible to AMP toxicity than rats⁷⁴⁻⁷⁶.

The work of the Erasmus MC PhD candidate outlined in this thesis was funded and performed as part of the European Union's Seventh Programme for Research, Technological Development and Demonstration under grant agreement No. 604434 (PneumoNP).

References

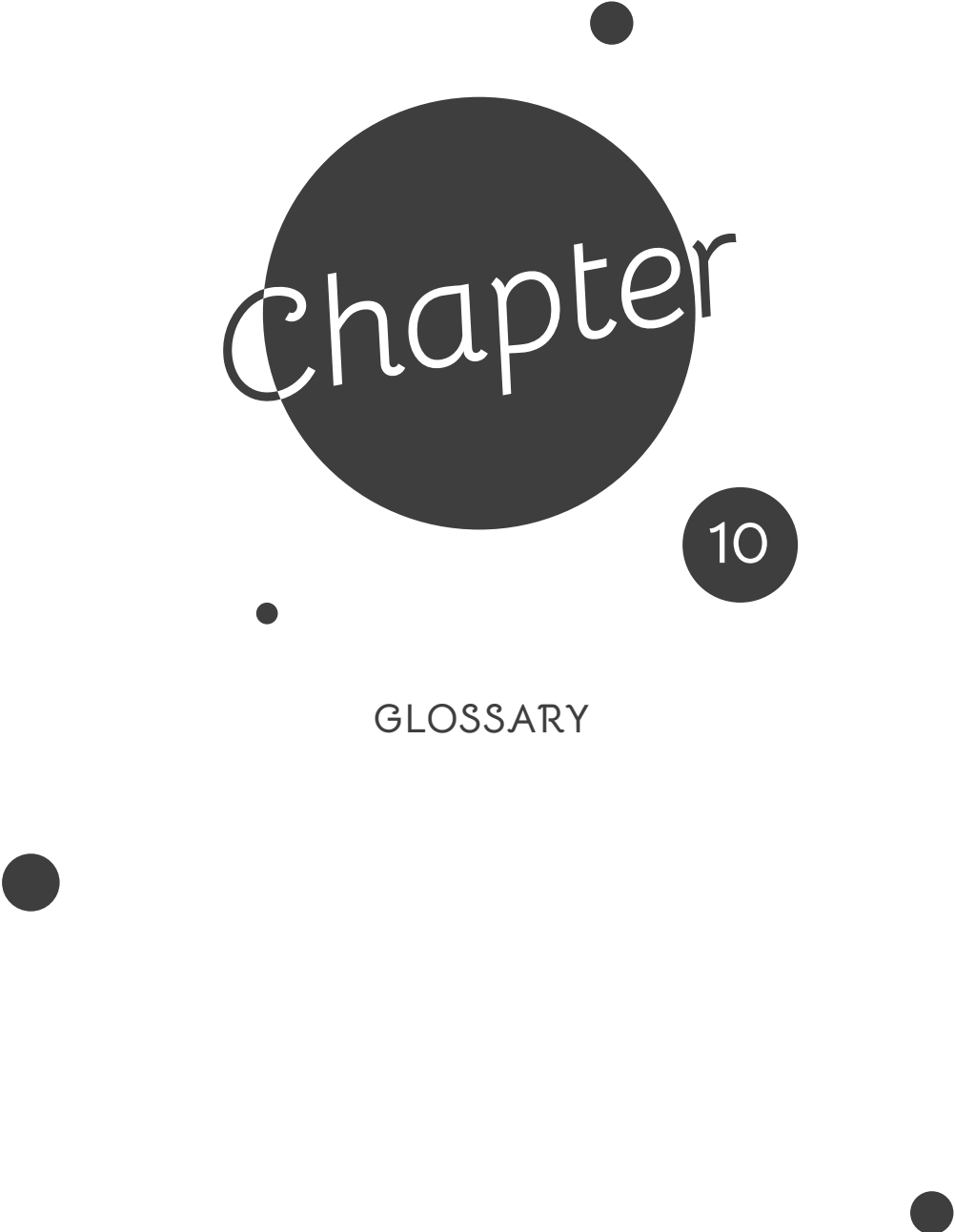
1. Marshall DC, Goodson RJ, Xu Y, Komorowski M, Shalhoub J, Maruthappu M, et al. Trends in mortality from pneumonia in the Europe union: a temporal analysis of the European detailed mortality database between 2001 and 2014. *Respiratory Research*. 2018;19(1):81.
2. Welte T, Torres A, Nathwani D. Clinical and economic burden of community-acquired pneumonia among adults in Europe. *Thorax*. 2012;67(1):71-9.
3. Sader HS, Farrell DJ, Flamm RK, Jones RN. Antimicrobial susceptibility of Gram-negative organisms isolated from patients hospitalised with pneumonia in US and European hospitals: results from the SENTRY Antimicrobial Surveillance Program, 2009–2012. *International Journal of Antimicrobial Agents*. 2014;43(4):328-34.
4. O'Neill J. Antimicrobial resistance: tackling a crisis for the health and wealth of nations. *The Review on Antimicrobial Resistance*. 2014;20.
5. Ventola CL. The antibiotic resistance crisis: part 1: causes and threats. *Pharmacy and Therapeutics*. 2015;40(4):277.
6. Blair JM, Webber MA, Baylay AJ, Ogbolu DO, Piddock LJ. Molecular mechanisms of antibiotic resistance. *Nature Reviews Microbiology*. 2015;13(1):42.
7. Butler MS, Blaskovich MA, Cooper MA. Antibiotics in the clinical pipeline at the end of 2015. *The Journal of Antibiotics*. 2017;70(1):3.
8. Lewis K. Platforms for antibiotic discovery. *Nature Reviews Drug Discovery*. 2013;12(5):371-87.
9. Hauser AR, Meccas J, Moir DT. Beyond antibiotics: new therapeutic approaches for bacterial infections. *Clinical Infectious Diseases*. 2016;63(1):89-95.
10. Gordon YJ, Romanowski EG, McDermott AM. A review of antimicrobial peptides and their therapeutic potential as anti-infective drugs. *Current Eye Research*. 2005;30(7):505-15.
11. Novak R, Shlaes DM. The pleuromutilin antibiotics: a new class for human use. *Current Opinion in Investigational Drugs*. 2010;11(2):182-91.
12. Huh AJ, Kwon YJ. "Nanoantibiotics": a new paradigm for treating infectious diseases using nanomaterials in the antibiotics resistant era. *Journal of Controlled Release*. 2011;156(2):128-45.
13. Wenzler E, Fraidenburg DR, Scardina T, Danziger LH. Inhaled antibiotics for Gram-negative respiratory infections. *Clinical Microbiology Reviews*. 2016;29(3):581-632.
14. Hancock RE, Sahl H-G. Antimicrobial and host-defense peptides as new anti-infective therapeutic strategies. *Nature Biotechnology*. 2006;24(12):1551.
15. Marr AK, Gooderham WJ, Hancock RE. Antibacterial peptides for therapeutic use: obstacles and realistic outlook. *Current Opinion in Pharmacology*. 2006;6(5):468-72.
16. Pini A, Falciani C, Bracci L. Branched peptides as therapeutics. *Current Protein and Peptide Science*. 2008;9(5):468-77.
17. Fox JL. Antimicrobial peptides stage a comeback. *Nature Publishing Group*; 2013.

18. Huang JX, Neve S, Elliot AG, Cain AK, Boinett CJ, Zuegg J, et al. Novel Arenicin-3 peptide antibiotics with broad-spectrum activity against MDR Gram-negative bacterial act via dual mode of actions. 54th International Conference of Antimicrobial Agents and Chemotherapy (ICAAC) and Infectious Diseases Society of America (IDSA) Joint Meeting: <https://adeniumBiotech.com/publications/>; 2014.
19. Pini A, Falciani C, Mantengoli E, Bindi S, Brunetti J, Iozzi S, et al. A novel tetrabrached antimicrobial peptide that neutralizes bacterial lipopolysaccharide and prevents septic shock in vivo. *The FASEB Journal*. 2010;24(4):1015-22.
20. Zazo H, Colino CI, Lanao JM. Current applications of nanoparticles in infectious diseases. *Journal of Controlled Release*. 2016;224:86-102.
21. Biswaro LS, da Costa Sousa MG, Rezende T, Dias SC, Franco OL. Antimicrobial peptides and nanotechnology, recent advances and challenges. *Frontiers in Microbiology*. 2018;9:855.
22. Yang W, Peters JI, Williams III RO. Inhaled nanoparticles—a current review. *International Journal of Pharmaceutics*. 2008;356(1-2):239-47.
23. Patton JS, Byron PR. Inhaling medicines: delivering drugs to the body through the lungs. *Nature Reviews Drug Discovery*. 2007;6(1):67.
24. Sung JC, Pulliam BL, Edwards DA. Nanoparticles for drug delivery to the lungs. *Trends in Biotechnology*. 2007;25(12):563-70.
25. Bailey MM, Berkland CJ. Nanoparticle formulations in pulmonary drug delivery. *Medicinal Research Reviews*. 2009;29(1):196-212.
26. Liu Y-Y, Wang Y, Walsh TR, Yi L-X, Zhang R, Spencer J, et al. Emergence of plasmid-mediated colistin resistance mechanism MCR-1 in animals and human beings in China: a microbiological and molecular biological study. *The Lancet Infectious Diseases*. 2016;16(2):161-8.
27. Arcilla MS, van Hattem JM, Matamoros S, Melles DC, Penders J, de Jong MD, et al. Dissemination of the mcr-1 colistin resistance gene. *The Lancet Infectious Diseases*. 2016;16(2):147-9.
28. Velkov T, Roberts KD, Nation RL, Thompson PE, Li J. Pharmacology of polymyxins: new insights into an 'old' class of antibiotics. *Future Microbiology*. 2013;8(6):711-24.
29. Hindler JA, Humphries RM. Colistin MIC Variability by Method for Contemporary Clinical Isolates of Multidrug-Resistant Gram-Negative Bacilli. *Journal of Clinical Microbiology*. 2013;51(6):1678-84.
30. Meletis G, Tzampaz E, Sianou E, Tzavaras I, Sofianou D. Colistin heteroresistance in carbapenemase-producing *Klebsiella pneumoniae*. *Journal of Antimicrobial Chemotherapy*. 2011;66(4):946-7.
31. Partridge SR, Di Pilato V, Doi Y, Feldgarden M, Haft DH, Klimke W, et al. Proposal for assignment of allele numbers for mobile colistin resistance (mcr) genes. *Journal of Antimicrobial Chemotherapy*. 2018;73(10):2625-30.
32. Nang SC, Li J, Velkov T. The rise and spread of mcr plasmid-mediated polymyxin resistance. *Critical Reviews in Microbiology*. 2019;45(2):131-61.
33. Pini A, Giuliani A, Falciani C, Fabbri M, Pileri S, Lelli B, et al. Characterization of the branched antimicrobial peptide M6 by analyzing its mechanism of action and in vivo toxicity. *Journal of Peptide Science: an official publication of the European Peptide Society*. 2007;13(6):393-9.
34. Brogden KA. Antimicrobial peptides: pore formers or metabolic inhibitors in bacteria? *Nature Reviews Microbiology*. 2005;3(3):238.
35. Li X, Li Y, Han H, Miller DW, Wang G. Solution structures of human LL-37 fragments and NMR-based identification of a minimal membrane-targeting antimicrobial and anticancer region. *Journal of the American Chemical Society*. 2006;128(17):5776-85.
36. Yu K, Park K, Kim Y, Kang SW, Shin S, Hahn KS. Solution structure of a cathelicidin-derived antimicrobial peptide, CRAMP as determined by NMR spectroscopy. *The Journal of Peptide Research*. 2002;60(1):1-9.

37. Dupuy FG, Pagano I, Andenoro K, Peralta MF, Elhady Y, Heinrich F, et al. Selective interaction of Colistin with lipid model membranes. *Biophysical Journal*. 2018;114(4):919-28.
38. Xiong M, Lee MW, Mansbach RA, Song Z, Bao Y, Peek RM, et al. Helical antimicrobial polypeptides with radial amphiphilicity. *Proceedings of the National Academy of Sciences*. 2015;112(43):13155-60.
39. Brunetti J, Falciani C, Roscia G, Pollini S, Bindi S, Scali S, et al. In vitro and in vivo efficacy, toxicity, bio-distribution and resistance selection of a novel antibacterial drug candidate. *Scientific Reports*. 2016;6:26077.
40. Lin Y-T, Jeng Y-Y, Chen T-L, Fung C-P. Bacteremic community-acquired pneumonia due to *Klebsiella pneumoniae*: clinical and microbiological characteristics in Taiwan, 2001-2008. *BMC Infectious Diseases*. 2010;10(1):307.
41. Lin Y-T, Wang Y-P, Wang F-D, Fung C-P. Community-onset *Klebsiella pneumoniae* pneumonia in Taiwan: clinical features of the disease and associated microbiological characteristics of isolates from pneumonia and nasopharynx. *Frontiers in Microbiology*. 2015;6:122.
42. Qureshi ZA, Paterson DL, Potoski BA, Kilayko MC, Sandovsky G, Sordillo E, et al. Treatment outcome of bacteremia due to KPC-producing *Klebsiella pneumoniae*: superiority of combination antimicrobial regimens. *Antimicrobial Agents and Chemotherapy*. 2012;AAC. 06268-11.
43. Falagas ME, Vardakas KZ, Tsiveriotis KP, Triarides NA, Tansarli GS. Effectiveness and safety of high-dose tigecycline-containing regimens for the treatment of severe bacterial infections. *International Journal of Antimicrobial Agents*. 2014;44(1):1-7.
44. Heizmann W, Löschmann P-A, Eckmann C, Von Eiff C, Bodmann K-F, Petrik C. Clinical efficacy of tigecycline used as monotherapy or in combination regimens for complicated infections with documented involvement of multiresistant bacteria. *Infection*. 2015;43(1):37-43.
45. Tzouveleakis LS, Markogiannakis A, Psychogiou M, Tassios PT, Daikos GL. Carbapenemases in *Klebsiella pneumoniae* and other Enterobacteriaceae: an evolving crisis of global dimensions. *Clinical Microbiology Reviews*. 2012;25(4):682-707.
46. Temkin E, Adler A, Lerner A, Carmeli Y. Carbapenem-resistant Enterobacteriaceae: biology, epidemiology, and management. *Annals of the New York Academy of Sciences*. 2014;1323(1):22-42.
47. Burkhardt O, Rauch K, Kaefer V, Hadem J, Kielstein JT, Welte T. Tigecycline possibly underdosed for the treatment of pneumonia: a pharmacokinetic viewpoint. *International Journal of Antimicrobial Agents*. 2009;34(1):101-2.
48. Cunha BA, Baron J, Cunha CB. Monotherapy with High-Dose Once-Daily Tigecycline is Highly Effective Against *Acinetobacter baumannii* and other Multidrug-Resistant (MDR) Gram-Negative Bacilli (GNB). *International Journal of Antimicrobial Agents*. 2018;52(1):119.
49. Gracia R, Marradi M, Cossío U, Benito A, Pérez-San Vicente A, Gómez-Vallejo V, et al. Synthesis and functionalization of dextran-based single-chain nanoparticles in aqueous media. *Journal of Materials Chemistry B*. 2017;5(6):1143-7.
50. Bozzuto G, Molinari A. Liposomes as nanomedical devices. *International Journal of Nanomedicine*. 2015;10:975-99.
51. Fendler JH, Romero A. Liposomes as drug carriers. *Life Sciences*. 1977;20(7):1109-20.
52. Torchilin VP. Structure and design of polymeric surfactant-based drug delivery systems. *Journal of Controlled Release*. 2001;73(2-3):137-72.
53. Russell WMS, Burch RL, Hume CW. *The principles of humane experimental technique*: Methuen London; 1959.
54. Bassetti M, Welte T, Wunderink RG. Treatment of Gram-negative pneumonia in the critical care setting: is the beta-lactam antibiotic backbone broken beyond repair? *Critical Care*. 2015;20(1):19.
55. Neve S, Lociuo S, Morrissey I, Hawser S, Nordkild P. The arenicin-3 derived clinical candidate AA139 shows potent activity against Gram-negative pathogens, Poster F-261. 54th ICAAC Meeting; 5-9 September 2014; Washington, DC2014.

56. Årdal C, Balasegaram M, Laxminarayan R, McAdams D, Outtersson K, Rex JH, et al. Antibiotic development—economic, regulatory and societal challenges. *Nature Reviews Microbiology*. 2019;1-8.
57. Napier BA, Burd EM, Satola SW, Cagle SM, Ray SM, McGann P, et al. Clinical use of colistin induces cross-resistance to host antimicrobials in *Acinetobacter baumannii*. *mBio*. 2013;4(3):e00021-13.
58. Pránting M, Andersson DI. Mechanisms and physiological effects of protamine resistance in *Salmonella enterica* serovar Typhimurium LT2. *Journal of Antimicrobial Chemotherapy*. 2010;65(5):876-87.
59. Hashemi MM, Rovig J, Weber S, Hilton B, Forouzan MM, Savage PB. Susceptibility of colistin-resistant, Gram-negative bacteria to antimicrobial peptides and ceragenins. *Antimicrobial Agents and Chemotherapy*. 2017;61(8):e00292-17.
60. Li Z, Velkov T. Polymyxins: Mode of Action. *Polymyxin Antibiotics: From Laboratory Bench to Bedside*; Springer; 2019. p. 37-54.
61. Jain AK, Swarnakar NK, Godugu C, Singh RP, Jain S. The effect of the oral administration of polymeric nanoparticles on the efficacy and toxicity of tamoxifen. *Biomaterials*. 2011;32(2):503-15.
62. Sawant RR, Torchilin VP. Multifunctionality of lipid-core micelles for drug delivery and tumour targeting. *Molecular Membrane Biology*. 2010;27(7):232-46.
63. Gao P, Nie X, Zou M, Shi Y, Cheng G. Recent advances in materials for extended-release antibiotic delivery system. *The Journal of Antibiotics*. 2011;64(9):625.
64. Agarwal R, Roy K. Intracellular delivery of polymeric nanocarriers: a matter of size, shape, charge, elasticity and surface composition. *Therapeutic Delivery*. 2013;4(6):705-23.
65. Tammaro L, Costantino U, Bolognese A, Sammartino G, Marenzi G, Calignano A, et al. Nanohybrids for controlled antibiotic release in topical applications. *International Journal of Antimicrobial Agents*. 2007;29(4):417-23.
66. Murgia X, Pawelczyk P, Schaefer UF, Wagner C, Willenbacher N, Lehr C-M. Size-limited penetration of nanoparticles into porcine respiratory mucus after aerosol deposition. *Biomacromolecules*. 2016;17(4):1536-42.
67. Cipolla D, Gonda I, Chan H-K. Liposomal formulations for inhalation. *Therapeutic Delivery*. 2013;4(8):1047-72.
68. Waldrep JC, Gilbert BE, Knight CM, Black MB, Scherer PW, Knight V, et al. Pulmonary delivery of beclomethasone liposome aerosol in volunteers: tolerance and safety. *Chest*. 1997;111(2):316-23.
69. Gilbert BE, Knight C, Alvarez FG, Waldrep JC, Rodarte JR, Knight V, et al. Tolerance of Volunteers to Cyclosporine A-dilauroylphosphatidylcholine Liposome Aerosol. *American Journal of Respiratory and Critical Care Medicine*. 1997;156(6):1789-93.
70. Monforte V, Ussetti P, Gavalda J, Bravo C, Laporta R, Len O, et al. Feasibility, tolerability, and outcomes of nebulized liposomal amphotericin B for *Aspergillus* infection prevention in lung transplantation. *The Journal of Heart and Lung Transplantation*. 2010;29(5):523-30.
71. Gill KK, Nazzal S, Kaddoumi A. Paclitaxel loaded PEG5000–DSPE micelles as pulmonary delivery platform: Formulation characterization, tissue distribution, plasma pharmacokinetics, and toxicological evaluation. *European Journal of Pharmaceutics and Biopharmaceutics*. 2011;79(2):276-84.
72. Cossío U, Gómez-Vallejo V, Flores M, Gañán-Calvo B, Jurado G, Llop J. Preclinical evaluation of aerosol administration systems using Positron Emission Tomography. *European Journal of Pharmaceutics and Biopharmaceutics*. 2018;130:59-65.
73. Brain JD, Knudson DE, Sorokin SP, Davis MA. Pulmonary distribution of particles given by intratracheal instillation or by aerosol inhalation. *Environmental Research*. 1976;11(1):13-33.
74. Brzezińska-Błaszczyk E, Czuwaj M, Kuna P. Histamine release from mast cells of various species induced by histamine releasing factor from human lymphocytes. *Agents and Actions*. 1987;21(1-2):26-31.

75. Decorti G, Klugmann FB, Candussio L, Furlani A, Scarcia V, Baldini L. Uptake of adriamycin by rat and mouse mast cells and correlation with histamine release. *Cancer Research*. 1989;49(8):1921-6.
76. Brown KL, Hancock RE. Cationic host defense (antimicrobial) peptides. *Current Opinion in Immunology*. 2006;18(1):24-30.



Chapter

10

GLOSSARY

Glossary of acronyms and abbreviations

ALAT	Alanine transaminase
AMK	Amikacin
AMP	Antimicrobial peptide
ARRIVE	Animal research: reporting of <i>in vivo</i> experiments
ASAT	Aspartate aminotransferase
ATCC	American Type Culture Collection
AUC	Area under the plasma concentration-time curve
AUC _{0-24h}	Area under the plasma concentration-time curve during a 24 hour period
AUC/MIC	Ratio of the area under the plasma concentration-time curve to the minimum inhibitory concentration
BUN	Blood urea nitrogen
CAZ	Ceftazidime
CD	Circular dichroism
CIP	Ciprofloxacin
CF	Cystic fibrosis
CFU	Colony-forming units
CL	Clearance
CREAT	Creatinine
CST	Colistin
CT	Computerized tomography
CTX-M	Cefotaxime-M β -lactamase
DLS	Dynamic light scattering
DMPC:Chol	1,2-dimyristoyl- <i>sn</i> -glycero-3-phosphocholine-cholesterol
DMSO	Dimethyl sulfoxide
DNA	Deoxyribonucleic acid
DPPC:Chol	Dipalmitoylphosphatidylcholine-cholesterol
DSPC:Chol	1,2-distearoyl- <i>sn</i> -glycero-3-phosphocholine-cholesterol
DSPE-PEG2000	Polyethylene glycosylated distearyl phosphatidyl ethanolamine
ECDC	European Centre for Disease Prevention and Control
ECOFF	Epidemiological cut-off value
ECTS	European Credit Transfer and Accumulation System
EDTA	Ethylenediaminetetraacetic acid
EEA	European Economic Area
EMA	European Medicines Agency
EPC	Egg phosphatidylcholine
EPG	Egg phosphatidylglycerol

Erasmus MC	Erasmus University Medical Center Rotterdam
ESBL	Extended-spectrum β -lactamase
ESBL pneumonia -septicemia	Acute lobar pneumonia leading to fatal septicemia in rats caused by <i>Klebsiella pneumoniae</i> strain ESBL EMC2003
EU	European Union
EUCAST	European Committee on Antimicrobial Susceptibility Testing
<i>E. coli</i>	<i>Escherichia coli</i>
F	Bioavailability
FDA	United States Food and Drug Administration
FID	Free induction decay
FOV	Field of view
FPLC	Fast protein liquid chromatography
FWHM	Full width at half maximum
Gd(III)DTPA-BMA	Gadolinium-(III)-diethylenetriaminepentaacetic acid-bisamide
GMA	Glycidyl methacrylate
HBS	4-(2-hydroxyethyl)-1-piperazineethanesulfonic acid buffered saline
HE	Hematoxylin-eosin
HEPES	4-(2-hydroxyethyl)-1-piperazineethanesulfonic acid
HiMLST	High-throughput multilocus sequence typing
HPLC	High-performance liquid chromatography
HPLC-MS	High-performance liquid chromatography mass spectrometry
IPTT	Implantable programmable temperature transponder
ISO	International Organization for Standardization
KPC	<i>Klebsiella pneumoniae</i> carbapenemase
KPC pneumonia -septicemia	Acute lobar pneumonia leading to fatal septicemia in rats caused by <i>Klebsiella pneumoniae</i> strain ESBL EMC2003
<i>K. pneumoniae</i>	<i>Klebsiella pneumoniae</i>
<i>K. pneumoniae</i> ESBL	Extended-spectrum β -lactamase-producing <i>Klebsiella pneumoniae</i> strain ESBL EMC2003
<i>K. pneumoniae</i> KPC	<i>Klebsiella pneumoniae</i> carbapenemase producing <i>Klebsiella pneumoniae</i> strain KPC EMC2014
LC-MS/MS	Liquid chromatography with tandem mass spectrometric detection
LD ₁₀₀	Absolute lethal dose
LPS	Lipopolysaccharide

LUV	Large unilamellar vesicle
MAC	<i>Mycobacterium avium</i> complex
MALDI	Matrix-assisted laser desorption/ionization
MALDI-TOF	Matrix-assisted laser desorption/ionization time-of-flight
MCR	Mobilized colistin resistance
MED	Minimum effective dose
MEM	Meropenem
MFD	Maximum feasible dose
MGE	Mobile genetic elements
MH-II	Mueller Hinton II
MIC	Minimum inhibitory concentration
MIC90	Minimum inhibitory concentration required to inhibit 90% of tested isolates
MLST	Multilocus sequence typing
MS	Mass spectrometry
MTD	Maximum tolerated dose
MWCO	Molecular weight cutoff
<i>M. tuberculosis</i>	<i>Mycobacterium tuberculosis</i>
NDA	New Drug Application
NDM	New Delhi metallo- β -lactamase
NMR	Nuclear magnetic resonance
NOE	Nuclear Overhauser effect
NOESY	Nuclear Overhauser effect spectroscopy
NOR	Norfloxacin
NP	Nanoparticle
NSS	Normal saline solution
NTM	Nontuberculous mycobacteria
OXA	Oxacillinase β -lactamase
PB	Phosphate buffer
PBCA	Poly(butylcyanoacrylate)
PBS	Phosphate-buffered saline
PC:Chol	Phosphatidylcholine-cholesterol
PCR	Polymerase chain reaction
PDI	Polydispersity index
PEG	Polyethylene glycol
PES	Polyethersulphone
PET	Positron emission tomography
PFGE	Pulsed-field gel electrophoresis

PLG	Poly(DL-lactide- <i>co</i> -glycolide)
PLGA	Poly(lactic- <i>co</i> -glycolic acid)
PVA	Polyvinyl alcohol
<i>P. aeruginosa</i>	<i>Pseudomonas aeruginosa</i>
QRDR	Quinolone-resistance determining region
Radio-HPLC	High-performance liquid chromatography with radioactive detection
RTI	Respiratory tract infection
R&D	Research and development
SDS	Sodium dodecyl sulfate
SDS-d25	Fully deuterated sodium dodecyl sulfate
SEM	Scanning electron microscopy
SHV	Sulphydryl reagent variable β -lactamase
SPF	Specified pathogen-free
ST	Sequence type
SXT	Trimethoprim/sulfamethoxazole
TEM	Temoniera β -lactamase (Chapters 4 & 6)
TEM	Transmission electron microscopy (Chapter 5)
TFA	Trifluoroacetic acid
TGC	Tigecycline
TKK	Time-kill kinetics
TNF- α	Tumor necrosis factor α
TOB	Tobramycin
TOCSY	Total correlation spectroscopy
$t_{1/2}$	Half-life time
UN	United Nations
UPLC	Ultra-performance liquid chromatography
UV	Ultraviolet
V	Volume of distribution
VOI	Volume of interest
WHO	World Health Organization
WT	Wildtype
3-MPA	3-mercaptpropionic acid
fC_{max}	Highest unbound drug concentration reached in blood plasma
$fT > MIC$	Cumulative percentage of a 12-hour period that the unbound fraction of drug exceeds the minimum inhibitory concentration



Chapter

11

NEDERLANDSE SAMENVATTING

Longinfecties zijn jaarlijks verantwoordelijk voor meer dan 230.000 sterfgevallen en 10 miljard euro aan economische kosten over de gehele Europese Unie. In bijna driekwart van de gevallen van longinfecties in de gezondheidszorg zijn Gram-negatieve bacteriën de primaire ziekteverwekkers. Zulke Gram-negatieve bacteriën zijn tevens koplopers in de huidige antibioticacrisis en snel in staat om resistentie tegen nieuwe antibiotica te ontwikkelen en verspreiden. Dit heeft in combinatie met een gebrek aan nieuwe antibiotica gezorgd voor een opkomende crisis in de gezondheidszorg. Om deze crisis het hoofd te kunnen bieden is er wereldwijd aandacht voor het ontdekken en ontwikkelen van o.a. nieuwe klassen van antibiotica, verbeterde handhaving van infectiepreventieve maatregelen en snellere diagnostiek. Maar minstens zo belangrijk in het voorkómen van een ‘post-antibiotisch tijdperk’ is de ontwikkeling van nieuwe therapeutische benaderingen, waaronder: de optimalisatie van onderbenutte antibioticaklassen, zoals de antimicrobiële peptiden (AMPs); de ontwikkeling van geavanceerde systemen voor antibioticatoediening, zoals het insluiten van antibiotica in zeer kleine nanodeeltjes (nanoformulering); en een meer gerichte en veilige afgifte van antibiotica aan de infectiehaard, zoals directe toediening naar de longen via inademing in de behandeling van longinfecties.

In het kader van de hierboven beschreven klinische problematiek zijn de drie hierboven genoemde therapeutische benaderingen gecombineerd in het door de EU gefinancierde ‘PneumoNP’ onderzoeksproject (EU-FP7 onderzoeksbeurs). Het PneumoNP project heeft tot doel om nieuwe inhaleerbare antibiotica-nanogeneesmiddelen te ontwikkelen voor de behandeling van longinfecties veroorzaakt door antibioticaresistente *Klebsiella pneumoniae* – een Gram-negatieve bacterie. Het gebruik van nanogeneesmiddelen zou therapeutische voordelen kunnen hebben die enkele van de nadelen geassocieerd met de klinische toepassing van AMPs kunnen overwinnen, met name toxische bijwerkingen en een korte biologische halfwaardetijd. In het PneumoNP project waren de inhaleerbare antibiotica-nanogeneesmiddelen gebaseerd op twee nieuwe antibiotica; de ‘cationische AMPs’ SET-M33 en AA139, welke werden ingesloten in verschillende nanodeeltjes; polymere nanodeeltjes (PNP), liposomen (LIP), of micellen (MCL). De nanodeeltjes PNP, LIP en MCL werden voor nanoformulering gekozen vanwege hun

gunstige biocompatibiliteit, lage toxiciteit, potentiële goede biodistributie, en mogelijkheden ter aanpassing gebaseerd op toedieningsroute. Vervolgens werden in een unieke PneumoNP onderzoekspijlijn waaraan elf Europese onderzoeksgroepen deelnamen meerdere nanogeneesmiddelen ontwikkeld. In samenwerking met deze onderzoekspartners hebben wij de twee nieuwe AMPs en een aantal geselecteerde AMP-nanogeneesmiddelen getest *in vitro* op hun vermogen om antibiotica-resistente bacteriën afkomstig van patiënten te doden. Vervolgens onderzochten wij de meest veelbelovende kandidaten in een proefdiermodel op hun effectiviteit in de behandeling van een ernstige long-/bloedinfectie veroorzaakt door een multidrug-resistente bacterie, een type infectie met een hoge mortaliteit bij patiënten in het ziekenhuis. Alle dierexperimenten hadden de goedkeuring binnen de Europese richtlijn voor dierproeven.

Deel I van dit proefschrift bevat de inleidende hoofdstukken. **Hoofdstuk 1** beschrijft de aard van multidrug-resistente Gram-negatieve bacteriën, de problematiek in de behandeling van infecties veroorzaakt door deze bacteriën, en verschillende nieuwe therapeutische benaderingen. Daarbij wordt de nadruk gelegd op AMPs en directe toediening aan de infectiehaard. **Hoofdstuk 2** is een overzichtartikel met de huidige staat van antibiotica-nanogeneesmiddelonderzoek gericht op de behandeling van antibiotica-resistente luchtweginfecties. Hierin wordt uitgebreid ingegaan op de huidige onderzoekslijnen in dit veld, de ontwikkeling van verschillende nanodeeltjes en de potentiële waarde en klinische status van inhaleerbare antibiotica-nanogeneesmiddelen. **Hoofdstuk 3** bespreekt het doel van het PneumoNP project en benoemt kort de onderzoeksactiviteiten door andere projectpartners die niet beschreven worden in dit proefschrift.

De hierna volgende hoofdstukken beschrijven het onderzoek uitgevoerd binnen de afdeling Medische Microbiologie & Infectieziekten (MMIZ) van het Erasmus Universitair Medisch Centrum Rotterdam (Erasmus MC) als onderdeel van een preklinische ontwikkelingspijlijn betreffende het bereiden en testen van nieuwe AMP nanogeneesmiddelen.

De **Hoofdstukken 4 – 5** van **Deel II** behandelen het *in vitro* onderzoek naar de antimicrobiële activiteit van de nieuwe AMPs SET-M33 en AA139 tegen Gram-negatieve *K. pneumoniae* and *Pseudomonas aeruginosa* bacteriën. Zowel SET-M33 als AA139 hebben meerdere werkwijzen en lijken o.a. de ‘zelfgestimuleerde opname’ te delen met andere cationische AMPs zoals colistine – dat in de kliniek één van de laatste toevluchtsantibiotica tegen antibiotica-resistente Gram-negatieve bacteriën is.

Hoofdstuk 4 beschrijft de antimicrobiële activiteit van SET-M33 en AA139 met colistine als vergelijkingsantibioticum tegen een collectie van genotypisch verschillende *K. pneumoniae* isolaten afkomstig van 50 individuele patiënten en diverse klinische monsters. Deze collectie isolaten vertegenwoordigt vijf verschillende antibiotica-resistentieprofielen, van gevoelige tot multidrug-resistente fenotypen, en bevat ook colistine-resistente isolaten. Daarnaast worden de resultaten besproken van de concentratie- en tijdsafhankelijke antimicrobiële activiteit van SET-M33 en AA139 in vergelijking met colistine onderzocht in een selectie van multidrug-resistente *K. pneumoniae* isolaten, waaronder een isolaat met plasmidale colistine resistentie. Aangevoerd werd dat SET-M33 en AA139 beiden een snelwerkende bacteriedodende werking hebben ongeacht het antibiotica-resistentieprofiel of de colistine-resistentie van de Gram-negatieve bacterie, en dat blootstelling aan SET-M33 en AA139 niet snel leidt tot de ontwikkeling van resistente mutanten, terwijl we dit wel zien na blootstelling aan colistine. Hieruit kunnen wij concluderen dat zowel SET-M33 als AA139 geschikte alternatieven zijn voor colistine en daardoor veelbelovend voor de behandeling van multidrug-resistente *K. pneumoniae* infecties, inclusief infecties veroorzaakt door colistine-resistente bacteriën.

Hoofdstuk 5 beschrijft een diepgaand onderzoek naar de precieze werkwijze van SET-M33. Aangevoerd werd de bacteriedodende activiteit van SET-M33 ten opzichte van isogene *K. pneumoniae* en *P. aeruginosa* isolaten die enkel verschillen in hun gevoeligheid voor colistine, waarbij slechts zeer geringe verandering in gevoeligheid van de bacteriën na 24 uur blootstelling aan SET-M33 werd gezien. Middels elektronenmicroscopie werd de beschadiging aan de bacteriële celenvlop door SET-M33 onderzocht. Studies met gebruikmaking van lipide membraanmodellen lieten

zien dat SET-M33 waarschijnlijk een α -helix-structuur aanneemt en deels verscholen ligt in de bacteriële celmembraan, in tegenstelling tot colistine dat een geheel andere structuur laat zien na opname in de celmembraan. De resultaten ondersteunen de hypothese dat SET-M33 en colistine essentieel verschillen in opnamemechanismen door de bacteriële celmembraan. Verder onderzoek liet zien dat SET-M33 geen zelf-aggregatie vertoont, noch cytotoxiciteit tegen menselijke bronchiale epitheelcellen, en slechts beperkte hemolytische activiteit tegen menselijke rode bloedcellen. Deze bevindingen tonen aan dat SET-M33 niet de nadelige biologische eigenschappen heeft die geassocieerd zijn met structureel soortgelijke AMPs, hetgeen wordt ondersteund door eerdere *in vivo* studies waar SET-M33 na toediening in een muisinfectiemodel goed getolereerd werd.

Bij elkaar genomen laat het onderzoek uit deze twee hoofdstukken zien dat SET-M33 en AA139 veelbelovende antibioticakandidaten zijn voor de behandeling van multidrug-resistente Gram-negatieve bacteriële infecties en mogelijk als alternatief voor colistine gebruikt kunnen worden in de kliniek. Daarmee zijn beide antibiotica geschikte kandidaten voor de ontwikkeling van AMP-nanogeneesmiddelen.

De **Hoofdstukken 6 – 8** van **Deel III** behandelen het *in vivo* onderzoek naar de therapeutische effectiviteit van de ontwikkelde AMP-nanogeneesmiddelen in vergelijking tot die van de AMPs in de vrije vorm ('vrije AMPs'). Daartoe werd eerst een dierexperimenteel infectiemodel ontwikkeld omdat dieronderzoek een essentiële en vereiste schakel is tussen preklinisch *in vitro* onderzoek en klinisch onderzoek in patiënten.

Hoofdstuk 6 beschrijft een nieuw diermodel in de rat van acute lobaire longinfectie, waarbij ook het bloed geïnfecteerd raakt, veroorzaakt door een multidrug-resistente ESBL-producerende of KPC-producerende *K. pneumoniae*, welke infectie zonder behandeling fataal verloopt. Dit diermodel beoogt in zekere mate representatief te zijn voor ernstige multidrug-resistente longinfecties bij patiënten die heel moeilijk te behandelen zijn in het ziekenhuis en niet zelden een fataal verloop hebben. Een diermodel van een infectieziekte maakt het mogelijk de therapeutische effectiviteit van

antibiotica te vergelijken onder gelijke omstandigheden van ernst en duur van infectie en gastheerafweer, hetgeen niet mogelijk is in de meeste vergelijkende klinische effectiviteitsstudies van antibiotica. De translationele waarde van het diermodel werd aangetoond door beide infecties – op het moment dat de dieren erg ziek waren – te behandelen met antibiotica toegediend in klinisch relevante schema's. Daarbij werd een hoge dosering van tigecycline (een laatste toevluchtsantibioticum voor multidrug-resistente infecties) gebruikt en vergeleken met het carbapenem-antibioticum meropenem. Aangetoond werd dat de *K. pneumoniae* ESBL long-/bloedinfectie succesvol kon worden behandeld met meropenem of tigecycline, en dit komt overeen met de *in vitro* gevoeligheid van de bacterie voor beide antibiotica. In de multidrug-resistente *K. pneumoniae* KPC long-/bloedinfectie was meropenem niet effectief, zoals te verwachten gezien de resistentie van de bacterie voor meropenem. Tigecycline in een hoge dosering was daarentegen wel succesvol. De resultaten van dit onderzoek ondersteunen recente studies die het gebruik van tigecycline in hoge dosering aanbevelen in de behandeling van patiënten met ernstige infecties (zoals long-/bloed infecties) veroorzaakt door carbapenem-resistente Gram-negatieve bacteriën.

Hoofdstuk 7 en **Hoofdstuk 8** beschrijven het onderzoek naar de therapeutische effectiviteit van de SET-M33-nanogeneesmiddelen en AA139-nanogeneesmiddelen. Deze werden bereid door SET-M33 en AA139 in te sluiten in drie verschillende nanodeeltjes: PNP, LIP, of MCL. Meerdere nanogeneesmiddelen werden ontwikkeld en verfijnd op basis van *in vitro* screeningsexperimenten, waarin ze werden vergeleken met de vrije AMPs op hun *in vitro* antimicrobiële activiteit. Op deze wijze werden de beste vier nanogeneesmiddelen geselecteerd: SET-M33-PNP, SET-M33-LIP, AA139-PNP en AA139-MCL. Deze bleken allen stabiel en lekkage van antibiotica tijdens opslag werd nooit waargenomen. De vier geselecteerde nanogeneesmiddelen werden vergeleken met de respectievelijke vrije AMPs *in vitro* en *in vivo* in het ratmodel van long-/bloedinfectie veroorzaakt door *K. pneumoniae* ESBL. **Hoofdstuk 7** bespreekt het onderzoek van SET-M33-PNP en SET-M33-LIP, en **Hoofdstuk 8** bespreekt het onderzoek van AA139-PNP en AA139-MCL.

De eerste studies betroffen de concentratie- en tijdsafhankelijke antimicrobiële activiteit *in vitro*. Daaruit bleek dat, ondanks insluiting in nanodeeltjes, de bacteriedodende werking van SET-M33 en AA139 grotendeels behouden bleef. Insluiting in PNP leek een snellere werking van het AMP te faciliteren, terwijl insluiting in LIP of MCL een langzamere doch langer durende werking van het AMP mogelijk maakte.

In alle *in vivo* studies werden de AMP-nanogeneesmiddelen direct toegediend naar de longen via endotracheale insufflatie met als doel dat dit zou leiden tot versterking van de bacteriedodende werking in de geïnfecteerde long en vermindering van systemische gevolgen – zoals toxische bijwerkingen en nevenschade aan het microbioom (de beschermende gastheer-geassocieerde bacteriën).

In de eerste serie *in vivo* experimenten verricht in niet-geïnfecteerde ratten werd na een éénmalige dosering van het nanogeneesmiddel de limiterende dosis bepaald, met als doel de vervolgstudies in de geïnfecteerde ratten volledig binnen de dier-ethische normen te kunnen uitvoeren. De limiterende dosis die maximaal kan worden toegediend zonder toxische bijwerkingen van beide SET-M33-nanogeneesmiddelen bleek niet hoger dan de limiterende dosis van vrij SET-M33; medebepalend hierbij waren helaas technische beperkingen die de toediening van hogere doseringen SET-M33-nanogeneesmiddelen onmogelijk maakten. AA139-PNP en AA139-MCL daarentegen lieten wel een hogere limiterende dosis zien; ze konden bij een dubbele dosering veilig worden toegediend in vergelijking tot vrij AA139.

In een tweede serie *in vivo* studies werd in de geïnfecteerde ratten de ‘vroeg bacteriedodende activiteit’ van de AMP-nanogeneesmiddelen na een enkelvoudige dosis bepaald. Deze resultaten ondersteunden de eerdere *in vitro* resultaten die aantoonde dat de AMPs ondanks insluiting in nanodeeltjes grotendeels de bacteriedodende werking behouden; en dat insluiting in PNP een snellere doch kortdurende werking in de long leek te faciliteren, terwijl insluiting in LIP of MCL een langzamere doch langer durende werking van het AMP mogelijk maakten.

Omdat de AA139-nanogeneesmiddelen hoger gedoseerd konden worden dan vrij AA139 (in tegenstelling tot de SET-M33-nanogeneesmiddelen en vrij SET-M33)

werden de AA139-nanogeneesmiddelen geselecteerd voor de vervolgstudies naar de therapeutische effectiviteit in geïnfecteerde ratten na meerdere doses over langere tijd. Dit neemt niet weg dat SET-M33 als nanogeneesmiddel of in vrije vorm nog steeds zeer interessante antibioticakandidaten zijn voor verder onderzoek in een andere experimentele set-up.

Zoals beschreven in **Hoofdstuk 8** lieten uitgebreide biodistributiestudies met beide AA139-nanogeneesmiddelen in niet-geïnfecteerde ratten zien dat nanoformulering van AA139 resulteert in een verlengde verblijfsduur van het antibioticum in de longen. Dit gold met name voor AA139-MCL. Vervolgens werd de therapeutische effectiviteit van de AA139-nanogeneesmiddelen bepaald in geïnfecteerde ratten na een eenmaaldaagse dosering toegediend gedurende een periode van 10 dagen. Ook in dit langdurig doseringsschema konden zowel AA139-PNP als AA139-MCL veilig worden toegediend bij een dubbele dosering vergeleken met vrij AA139. Dit geeft opnieuw aan dat nanoformulering de verdraagbaarheid van AA139 verbetert hetgeen hoger doseren zonder toxische bijwerkingen over langere periode mogelijk maakt. Dankzij de hogere dosering bleek de behandeling met AA139-nanogeneesmiddelen te resulteren in een verhoogde therapeutische effectiviteit in termen van een significant verbeterde overleving van de geïnfecteerde ratten.

Samenvattend zijn onze resultaten veelbelovend voor de verdere ontwikkeling van deze AMP-nanogeneesmiddelen ten behoeve van de behandeling van multidrug-resistente Gram-negatieve longinfecties. Toekomstig onderzoek naar nanoformulering van SET-M33 zou zich kunnen richten op het verkrijgen van hogere concentraties SET-M33 binnen aangepaste nanodeeltjes om toediening van hogere doseringen van het nanogeneesmiddel mogelijk te maken. Wat betreft de toepassing van AA139-nanogeneesmiddelen is een therapeutische verbetering dankzij nanoformulering van AA139 in ons onderzoek aangetoond. Weliswaar werd een volledige therapeutische effectiviteit (complete overleving van de geïnfecteerde ratten) niet bereikt. Verschillende factoren binnen de dierexperimentele onderzoeksopzet dragen hieraan bij. Zo is er de keuze van de rat als proefdier, bij welke dieren het geneesmiddel slechts in een beperkt volume via endotracheale insufflatie kan worden toegediend. Ook heeft

het dier onder narcose tijdens de endotracheale insufflatie een lage ademhalingsfrequentie met als gevolg een lage efficiëntie van inhalatie van het geneesmiddel. Beide beperkingen zijn er niet in geval van de toediening van geneesmiddelen per inhalatie bij patiënten. Om de aerogene behandeling in de ratten te verbeteren hebben we twee andere aerosol inhalatie systemen getest in onze dieren. Beide methoden bleken helaas niet te leiden tot verbetering van de door ons reeds toegepaste methode.

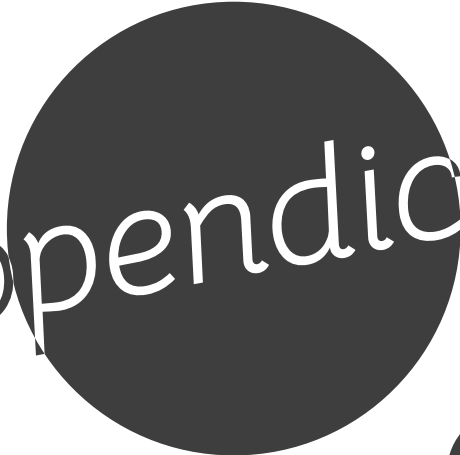
De resultaten beschreven in dit proefschrift laten het potentieel van nieuwe cationische AMPs als veelbelovende antibioticakandidaten zien. Ook zijn de mogelijke verbeteringen van AMP-nanogeneesmiddelen ten opzichte van vrije AMPs voor de behandeling van multidrug-resistente Gram-negatieve longinfecties aangetoond. Tijdens het onderzoek is een unieke PneumoNP nanogeneesmiddelen-onderzoekspijplijn opgezet die aangepast kan worden voor het testen van nieuwe toekomstige (combinaties van) antibiotica als nanogeneesmiddelen. Ten slotte ondersteunt het onderzoek in dit proefschrift het concept dat het gebruik van nanogeneesmiddelen toegediend middels inhalatie een interessante onderzoeksrichting is in de verbetering van de behandeling van antibiotica-resistente longinfecties.

Dankwoord

Curriculum Vitae

List of publications

PhD portfolio



Appendices



A

Dankwoord

Zoals bij de meeste mijlpalen in het leven was dit proefschrift nooit tot stand gekomen zonder de hulp en steun van vele mensen in mijn persoonlijke en professionele omgeving. Ik wil in dit hoofdstuk graag iedereen bedanken die mij in de afgelopen jaren met raad of daad heeft bijgestaan, of dat nou in de vorm was van een goed gesprek in een gezellig café of met het uitplaten van een luttele honderdtal bacteriemonsters! Ik wil de volgende mensen graag in het bijzonder bedanken:

Beste Irma, het was een eer om je laatste promovendus te mogen zijn. Ik heb veel bewondering voor je oog voor detail en je bereidheid om altijd in de bres te springen voor grondig uitgevoerd onderzoek. Ook heb ik veel waarde gehecht aan de gezonde balans van gezellige gesprekken en constructieve kritiek tijdens onze besprekingen. Na zo'n illustere carrière zal het moeilijk zijn om helemaal van het onderzoek weg te stappen, maar je kan nu zeker welverdiend genieten van je pensioen, de (klein)kinderen, en nog vele fijne weekenden te Terschelling.

Beste John, je hebt me begeleid van een groene masterstudent tot een ervaren doctoraalstudent. Met name tijdens de laatste zware loodjes van het schrijven van dit proefschrift was jouw steun onmisbaar. Jouw nieuwsgierigheid en passie voor de wetenschap zijn een inspiratie, meer dan enig ander ben jij altijd in staat om een nieuw perspectief te bieden en heb je altijd interesse in nieuwe onderzoekslijnen. Bedankt voor de vele jaren van prettige en productieve samenwerking!

Beste Annelies, ik ben je zeer dankbaar dat je bereid was om de positie van promotor op je te nemen in de laatste fase van mijn promotie na de verdrietige gebeurtenis van het vroegtijdig overlijden van Johan Mouton. Hoewel niemand gewent had dat dit nodig zou zijn, heb jij deze rol uitgevoerd met de karakteristieke professionaliteit en persoonlijke noot waarmee je de afdeling de afgelopen jaren ook hebt begeleid.

Geachte leden van de promotiecommissie, ik wil u allen vriendelijk danken voor de tijd die u heeft genomen om mijn proefschrift te lezen en kritisch te beoordelen.

Aan alle collega's van de MMIZ, na een veelbewogen jaar van quarantaines en social distancing zal het velen verbazen om te horen dat wij microbiologen toch nog best sociale mensen zijn! Ik wil jullie graag allemaal bedanken voor de vele helpende handen en de altijd gemoedelijke werksfeer. Ook buiten kantooruren heb ik genoten van de vele gezellige koffiepauzes, dinertjes, borrels, afdelingsuitjes, en kerstfeesten!

Wil, hoewel jij officieel niet één van mijn co-promotoren was, leek dat af en toe wel zo. Bedankt dat je deur altijd open stond voor een snelle vraag of een lange bespreking, het was een plezier om nieuwe onderzoeksresultaten met je door te nemen en te brainstormen over de voortzetting van nieuwe onderzoekslijnen.

Marian, met jouw jarenlange ervaring in het uitvoeren van wetenschappelijk onderzoek was jij de drijvende motor achter de vele pittige experimenten die we uitgevoerd hebben. Ik heb enorm veel geleerd van jouw discipline en organisatie tijdens mijn promotietraject, eigenschappen waar ik zelf als eeuwig warhoofd juist mee worstel! Bedankt voor al je steun en geduld tijdens mijn promotieonderzoek.

Aart, bedankt voor je inzet tijdens de laatste fase van het onderzoeksproject, jouw steun en ervaring waren tijdens deze periode onmisbaar. Zelfs tijdens experimenten waar we 's avonds laat in het weekend terug voor moesten komen kwam jij wonder boven wonder met een goed humeur voor de dag!

Denise, ik wil je bedanken voor al het labwerk en je altijd aanwezige gevoel voor humor, het lab zou niet hetzelfde zijn geweest zonder je vele sarcastische (maar altijd goedbedoelde) grappen. En de heerlijke zelfgebakken traktaties die je regelmatig meebracht naar de koffiepauzes zal ik ook niet rap vergeten!

Heleen, Maarten, ondanks de lange dagen die we allemaal moesten maken voor onze experimenten hebben we toch nog ergens de tijd gevonden voor collegiaal borrelen, late bordspelavonden, en zelfs flink festivalvieren. Bedankt voor de leuke tijden samen!

Anne, Gerjo, Sanne, tijdens de eerste jaren van mijn aanstelling was ons kantooireiland een rots in de branding om de wilde wateren van mijn promotietraject te trotseren (tot zover deze vergezochte metafoor). Bedankt voor de prettige kantoorfeer!

Agnes, Astrid, Bas, Carmine, Jasper, Michiel, Mirjam, Rogier, Stefan, Silvie, Suzanne, Wendy, elke kakelverse promovendus heeft een goede voorbereiding nodig op wat hem of haar tijdens zijn promotietraject te wachten staat – bedankt voor jullie oh zo wijze levenslessen als de ervarener promovendi en postdocs van de afdeling!

Anja, Bertrand, Chinmoy, Elise, Gerdie, Hassna, Iain, Janette, Joell, Manon, Rixt, Rofyan, Tanmoy, Valérie, Wilson, I really appreciate that we could always count on the solidarity of our fellow PhD students at the department! I had a great time in the office and at the lab with you (including our sillier activities, like training for the trappenloop) and enjoyed the opportunity to get to know all of you better after hours.

Carla, Corné, Deborah, Elke, Mehri, Mickey, Nicole, Susan, Wendy, als promovendus heb ik vele lange dagen moeten doorbrengen met het uitvoeren van experimenten, daarom wil ik jullie graag allemaal bedanken voor de behulpzaamheid en de immer gezellige sfeer op het lab (en tijdens de koffiepauzes natuurlijk)!

Chiara, thank you for all the hard work during your internship! I hope you fondly think back on your time in Rotterdam and wish you good luck with your own doctoral studies.

To the partners of the PneumoNP consortium, I would like to thank you all for the years of productive collaboration! Our half-yearly meetings were always full of invigorating research discussions as well as enjoyable dinner conversations. It was a pleasure to work together with all of you across different scientific disciplines towards a single scientific goal, and I hope our paths cross in the future!

Antoinette, Marco, Jeffrey, Raquel, Rene, Sabine, Unai, Yvonne, I would like to thank you in particular for our close cooperation during the PneumoNP research project. I really enjoyed working together with all of you on the different moving parts involved in the project and had a great time visiting your cities and faculties!

Alessandro, Chiara, Magnus, thank you for the pleasant collaboration – there is a careful balance between the interests of private biotech companies with those of academic institutions, but it was one that I think we managed well during the project.

Aan al mijn vrienden, to all my friends, the study of microbiology isn't just limited to the laboratory of course – as it turns out, a lot can be learned from having one (or multiple) fermented beverages in good company! Thank you for all the good times we've had together and giving me the opportunity to clear my head after long workdays.

Elmer, Jasper, Thomas, het is geweldig dat we elkaar nog steeds met enige (on)regelmaat weten op te zoeken sinds de dagen dat we na school gingen spelen in het bos of op skateboards het dorp onveilig maakten. Jasper en ik hebben uitgerekend dat we inmiddels ons porseleinen jubileum al hebben behaald; we hoeven het nog maar een paar decennia vol te houden om op een dag ons ivoren jubileum te kunnen beklinken!

Cynthia, Mart, Randy, Ronald, Roeland, Tim, Yannick, een belangrijk onderdeel van elke academische carrière is natuurlijk het studentenleven dat wij uitbundig in Groningen hebben gevierd! Inmiddels zijn we na ons afstuderen allemaal een stuk wijzer en verstandiger geworden (nou ja, relatief gezien uiteraard...) maar weten we gelukkig net zoals vroegâh nog steeds af en toe lekker van het padje te gaan dankzij tradities als de Eurovisie-bingo en het jaarlijkse kerstdiner (en natuurlijk... de Fireman)!

Bich, Elise, Miriam, sinds we elkaar hebben leren kennen in Groningen hebben wij ons steeds verder verspreid maar gelukkig over de jaren nog steeds contact gehouden – voornamelijk voor het organiseren van leuke technofeestjes! Bedankt voor de vele leuke herinneringen die we samen hebben gemaakt en hopelijk nog gaan maken.

Amar, Christina, Gabriel, Hugo, Judith, Kadri, Lina, Pierre, we all learned a lot during our time as exchange students in Sweden – and probably most of it outside of the university lecture halls! Most importantly, we learned we had to stay close together during those harsh cold winter months, and we took that to heart and after all this time we still manage to meet up once every while. Jag hoppas att vi ses snart igen!

Johannes, Sahar, Sandrine, Serdar, there is no better way to relax after a long day of performing experiments than founding a new student union together or playing an intensely competitive card game to find out who has the best bluff. Thanks for all the good times in Rotterdam and our railway journey to play Carcassonne in Carcassonne!

Bram & Celine, bedankt dat Lucie en ik altijd welkom waren in jullie heerlijke huisje! Uiteraard is er altijd een goed excuus te verzinnen om langs te komen knuffelen met konijnen, katten en puppy's... en hè, dat we jullie dan toevallig weer even zien komt dan ook goed uit. Het is ook leuk dat we de rest van jullie vrienden hebben leren kennen in de afgelopen jaren en ik kijk uit naar nog vele vieringen van verjaardagen en nieuwjaarsdagen samen!

Emoji Spammers, who could wish for a better moral support system than a bunch of guys being dudes who never stop posting? Although I'm not really sure if you guys were morale boosters or simply a never-ending distraction, I wouldn't have had it any other way. Thanks for all the good laughs and remember... keep yourself safe!

Rik, Waly, bedankt voor de vele gezellige avonturen die we samen beleefd hebben, dat er nog vele mogen volgen! Rik, het is altijd fijn om te weten dat er in ieder geval één persoon is met wie ik een avond kan vullen met gesprekken over meerlaags-ironische memes, esthetische vaporwave, en willekeurige feitjes over geschiedenis en wetenschap. Waly, ik kijk er naar uit om met jou als gids Valencia en omstreken te ontdekken!

Fellow D&D players, thank you all for allowing me to express my creative side! Few things are more enjoyable than having weekly drinks with a great bunch of people while going on fantastical adventures together. I'm glad to have gotten to know you all over our shared hobby and look forward to many more campaigns!

Huisgenoten van de Coloniastraat, jullie waren tijdens het grootste deel van mijn promotietraject met mij en mijn rare werktijden opgezadeld, bedankt voor de gezellige sfeer in huis en natuurlijk de leuke huisavonden (wanneer we er tijd voor hadden)!

Famille et amis de Lucie, vous avez été patient avec moi et mes efforts pour comprendre la langue et la culture française. Je tiens à vous remercier tous et toutes pour votre accueil si chaleureux et bien sûr votre excellente gastronomie !

A mis nuevos amigos y colegas de Barcelona, estoy emocionado por mi nueva vida y trabajo en Barcelona, y por conocerlos a todos mucho mayor. Estoy deseando explorar y disfrutar de esta hermosa ciudad y sus vermuts con vosotros. ¡Hasta luego!

Aan mijn familie, bedankt voor jullie onvoorwaardelijke steun. De laatste jaren hebben we voor elkaar klaargestaan in zowel goede als zware tijden en hebben jullie me gesteund om mijn dromen te bereiken – en staan ons nu vele mooie jaren voor de boeg!

Lieve Mam, bedankt dat je me altijd hebt ondersteund om mijn ambities te kunnen bereiken en mijn creatievere kant hebt aangespoord, waar dit proefschrift een prachtig voorbeeld van is (en dan met name de kaft, natuurlijk)! Niets maakt mij blijer dan te zien dat je weer helemaal goed op je plek zit na een aantal uitdagende jaren. Ik hou van je en wens Herman en jou nog een gelukkig huwelijk samen tegemoet.

Lieve Pap, bedankt dat je mijn interesse in de wetenschap van jongs af aan hebt aangewakkerd met kinderboeken en later krantenartikelen waar ik geen genoeg van kon krijgen. Ik waardeer enorm dat ik door weer en wind op je steun heb mogen rekenen en hoop dat ik hetzelfde ook voor jou kan betekenen. Ik hou van je en hoop dat Manon en jij nog vele jaren samen gelukkig zijn.

Lieve Rutger, ook jij hebt geen gemakkelijke jaren achter de rug, maar tegelijkertijd heb je de juiste stappen vooruit gezet en ga je een hele mooie toekomst tegemoet, daar ben ik van overtuigd! Als broers blijven we natuurlijk altijd ervaringsdeskundigen in elkaar op de kast jagen, maar ik wil dat je weet dat ik van je hou en je alle geluk toewens.

Lieve Opa & Oma, bedankt voor jullie goede zorgen voor de oudste kleinzoon. Het is natuurlijk vervelend als die steeds verder van je af gaat wonen, maar gelukkig zijn jullie nog steeds bereid om te reizen naar verre oorden om de familie op te zoeken – en ben ik evengoed van plan om regelmatig langs te komen in het Noorden!

Lieve Mireille, Jan, Tijn, jullie zijn een onmisbare bron van steun en behulpzaamheid geweest in de afgelopen jaren, bedankt voor alles wat jullie gedaan hebben voor de familie. Ik kijk er naar uit om regelmatig op bezoek te kunnen komen in jullie vakantiehuis te Spanje (niet in het minst voor het zwembad natuurlijk)!

Lieve familie van der Weide, bedankt voor de gezelligheid tijdens de jaarlijkse voorjaarsbrunches. Het is fijn om te weten dat er nu goed voor Oma van der Weide wordt gezorgd en iedereen goed op weg is naar een leuke toekomst!

Beste paranimfen, Aart & Rutger, bedankt voor jullie steun tijdens mijn promotie. Aart, naast je vele bijdragen aan het onderzoeksproject heb ik je ook buiten werk leren kennen als een goede vriend die altijd wel zin heeft in een laatste borrel, ook al zit het qua tijd niet altijd mee! Rutger, als mijn broer heb ik niemand liever aan mijn zijde tijdens de verdediging van mijn proefschrift – hoewel onze gezamenlijke videogame-talenten ditmaal niet zo bruikbaar zullen zijn! Ik ben heel dankbaar dat jullie beiden mij zullen bijstaan in mijn verdediging.

Chère Lucie, je suis tellement heureuse de tous les moments que nous avons partagés pendant mes études. Merci pour tous les rires pendant les bons moments, et merci d'avoir été mon roc solide pendant les moments difficiles – je n'aurais pas pu le faire sans ton amour et ton soutien. Je me réjouis de toutes les aventures que nous allons vivre ensemble dans les nombreuses années à venir.

Curriculum Vitae

Hessel van der Weide was born on the 17th of June 1989 in Groningen, the Netherlands. He received his preparatory scientific schooling (atheneum) at the Dr. Nassau College Quintus in Assen with a Nature & Health profile. He went on to study Life Sciences at the University of Groningen, the Netherlands, where he majored in Molecular Life Sciences and studied at the Uppsala University in Sweden for one year as part of the Erasmus Exchange program. During this period, he was an editor of the 'Lifeline' magazine for the biology student union GLV Idun. After an internship at the department of Molecular Microbiology on nanodisc technology in membrane protein research, Hessel graduated from the University of Groningen in 2012 with a Bachelor of Science. Next, he enrolled in the Infection & Immunity program at the Erasmus University Medical Center Rotterdam (Erasmus MC), the Netherlands. For his first internship, he set up a pilot study on the mucosal adaptive immune response to the human microbiome at the department of Immunology and the department of Medical Microbiology & Infectious Diseases. During this period, he also founded and presided over SURE, a student union for research master students intended to promote more collaboration and collegiality. After his final internship on the evasion of the innate immune response by the human metapneumovirus at the department of Viroscience, he graduated in 2014 with a Research Master of Science.

Hessel accepted a PhD candidacy at the department of Medical Microbiology & Infectious Diseases at the Erasmus MC in 2014, where he performed research as part of a multi-national consortium in the European Union FP7-funded project 'PneumoNP', with the goal to develop a novel theragnostic approach using nanomedicines based on antimicrobial peptides in the treatment of Gram-negative pneumonia. His main role was as lead researcher for the *in vitro* and *in vivo* investigations into the antimicrobial activity and therapeutic efficacy of the antimicrobial peptides and nanomedicines. After writing this thesis, Hessel started a fellowship at Ysios Capital in Barcelona, Spain on venture capital in the field of biotechnology and drug development.

List of publications

H van der Weide, U Cossío, R Gracia, YM te Welscher, MT ten Kate, A van der Meijden, M Marradi, JAS Ritsema, DMC Vermeulen-de Jongh, G Storm, WHF Goessens, I Loinaz, CF van Nostrum, J Llop, JP Hays, IAJM Bakker-Woudenberg. Therapeutic efficacy of novel antimicrobial peptide AA139-nanomedicines in a multidrug-resistant *Klebsiella pneumoniae* pneumonia-septicemia model in rats. *Antimicrob Agents Chemother*. 2020 Jun; accepted for publication.

H van der Weide, MT ten Kate, DMC Vermeulen-de Jongh, A van der Meijden, RA Wijma, SA Boers, M van Westreenen, JP Hays, WHF Goessens, IAJM Bakker-Woudenberg. Successful high-dosage monotherapy of tigecycline in a multidrug-resistant *Klebsiella pneumoniae* pneumonia-septicemia model in rats. *Antibiotics*. 2020 Mar;9(3):109.

H van der Weide, DMC Vermeulen-de Jongh, A van der Meijden, SA Boers, D Kreft, MT ten Kate, C Falciani, A Pini, M Strandh, IAJM Bakker-Woudenberg, JP Hays, WHF Goessens. Antimicrobial activity of two novel antimicrobial peptides AA139 and SET-M33 against antibiotic-resistant *Klebsiella pneumoniae* clinical isolates. *Int J Antimicrob Agents*. 2019 Aug;54(2):159-166.

C Grosserichter-Wagener, D Radjabzadeh, **H van der Weide**, KN Smit, R Kraaij, JP Hays, MC van Zelm. Differences in systemic IgA reactivity and circulating Th subsets in healthy volunteers with specific microbiota enterotypes. *Front Immunol*. 2019 Mar 7;10:341.

JAS Ritsema[&], **H van der Weide**[&], YM te Welscher, WHF Goessens, CF van Nostrum, G Storm, IAJM Bakker-Woudenberg, JP Hays. Antibiotic-nanomedicines: facing the challenge of antibiotic-resistant respiratory tract infections. *Future Microbiol*. 2018 Nov;13:1683-1692.

H van der Weide[&], J Brunetti[&], A Pini, L Bracci, C Ambrosini, P Lupetti, E Paccagnini, M Gentile, A Bernini, N Niccolai, DMC Vermeulen-de Jongh, IAJM Bakker-Woudenberg, WHF Goessens, JP Hays, C Falciani. Investigations into the killing activity of an antimicrobial peptide active against extensively antibiotic-resistant *K. pneumoniae* and *P. aeruginosa*. *Biochim Biophys Acta Biomembr*. 2017 Oct;1859(10):1796-1804.

[&]The two first authors contributed equally.

PhD portfolio

Name:	Hessel van der Weide
Institute:	Erasmus University Medical Center Rotterdam (Erasmus MC)
Department:	Medical Microbiology & Infectious Diseases
PhD period:	2014 – 2020
Promotor:	Prof. dr. A. Verbon
Copromotoren:	Dr. J.P. Hays Dr. I.A.J.M. Bakker-Woudenberg

Scientific meetings	Year	Workload (ECTS)
Research meetings & Journal clubs		
➤ Department of Medical Microbiology & Infectious Diseases Erasmus MC, Rotterdam, the Netherlands	2014 - 2018	2.0
Progress meetings & Review meetings		
➤ PneumoNP Consortium Various locations and organizations	2014 - 2017	3.0

Teaching	Year	Workload (ECTS)
Supervision of 2 nd year medical students		
➤ "VO Infectieziekten" Erasmus MC, Rotterdam, the Netherlands	2015 - 2018	3.0
Supervision of 1 st year research master students		
➤ "Lab rotations Infection & Immunity" Erasmus MC, Rotterdam, the Netherlands	2017	1.0
Supervision of master student		
➤ 3-month internship of Chiara Ambrosini University of Siena, Siena, Italy	2015	2.0

Courses and workshops	Year	Workload (ECTS)
Attendance		
➤ 2 nd International Molecular Imaging Workshop CIC biomaGUNE, Donostia-San Sebastián, Spain	2017	1.2
Oral presentation		
➤ NAREB Workshop: Nanomedicine & antibiotic resistance NAREB project, Madrid, Spain	2017	1.3
Poster presentation		
➤ Course on Translational Research & Medicine Development C-COMEND, Manchester, United Kingdom	2016	2.8
Oral presentation		
➤ Novel approaches to fight bacteria Workshop Jacobs University, Bremen, Germany	2016	2.2
Attendance		
➤ Scientific integrity Erasmus MC, Rotterdam, the Netherlands	2015	0.3
Attendance		
➤ Translational Imaging Workshop: From mouse to man Erasmus MC, Rotterdam, the Netherlands	2014	1.3

National and international conferences	Year	Workload (ECTS)
Attendance		
➤ 28 th ECCMID ESCMID, Madrid, Spain	2018	1.5
Attendance		
➤ Scientific Spring Meeting KNVM & NVMM KNVM & NVMM, Papendal, the Netherlands	2018	0.6
Oral presentation		
➤ Irma Bakker-Woudenberg Symposium Erasmus MC, Rotterdam, the Netherlands	2018	1.3
Oral presentation		
➤ MMIZ Science Day Erasmus MC, Rotterdam, the Netherlands	2017	1.3
Poster presentation		
➤ Scientific Spring Meeting KNVM & NVMM 2017 KNVM & NVMM, Papendal, the Netherlands	2017	1.1
Oral presentation		
➤ FIGON Dutch Medicines Days FIGON, Ede, the Netherlands	2016	1.3
Oral presentation		
➤ 26 th ECCMID ESCMID, Amsterdam, the Netherlands	2016	2.5
Oral presentation		
➤ Scientific Spring Meeting KNVM & NVMM KNVM & NVMM, Papendal, the Netherlands	2016	1.3
Attendance		
➤ Scientific Spring Meeting KNVM & NVMM KNVM & NVMM, Papendal, the Netherlands	2015	0.6

